

Bacterial acid phosphatase and its application to waste remediation and metal recovery

By

Claire Mennan

**A thesis submitted to the University of Birmingham
For the degree of
DOCTOR OF PHILOSOPHY**

School of Biosciences
The University of Birmingham
February 2010

UNIVERSITY OF
BIRMINGHAM

University of Birmingham Research Archive

e-theses repository

This unpublished thesis/dissertation is copyright of the author and/or third parties. The intellectual property rights of the author or third parties in respect of this work are as defined by The Copyright Designs and Patents Act 1988 or as modified by any successor legislation.

Any use made of information contained in this thesis/dissertation must be in accordance with that legislation and must be properly acknowledged. Further distribution or reproduction in any format is prohibited without the permission of the copyright holder.

For my parents...

Abstract

PhoN-type acid phosphatase from an atypical *Serratia* sp. was applied to the removal of radionuclides from aqueous flows. In the presence of metal ions the phosphatase produces metal phosphate at the cell surface via the liberation of inorganic phosphate from a phosphate donor (glycerol-2-phosphate). Previous studies using biogenic hydrogen uranyl phosphate (HUP) on *Serratia* sp. removed ^{60}Co , ^{137}Cs and ^{90}Sr via intercalative ion exchange into the HUP crystal lattice. Due to their non toxic and non radioactive nature, zirconium phosphates offer an alternative to HUP for the decontamination of potable water. Zirconium was successfully biomineralised by *Serratia* sp. forming gel-like deposits with little or no crystalline phases, as shown by XRD. This biogenic zirconium phosphate removed 100 % Co^{2+} and Sr^{2+} from solutions. Increased capacity can be achieved by co-crystallisation with Zr(IV) supplement assuming phosphatase radioresistance.

The *Serratia* sp. phosphatase exists in two distinct isoforms (SP1 (radioresistant) and SP2 (radiosensitive)) which were purified and further characterised in this study. Both isoforms were found to have redox capability and were able to potentiate free radical damage to deoxyribose in a Fenton-type reaction. Analysis using highly sensitive Micro-Proton Induced X-ray Emission (PIXE) analysis found no metallic components in SP1 or SP2. Database interrogation using partial sequences of the phosphatase and the Basic Local Alignment Search Tool (BLAST) confirmed homology with PhoC and PhoN of several pathogenic bacterial species and also similarities with the vanadium haloperoxidases, indicating these phosphatases and peroxidases could have a common ancestor. The relatedness of the *Serratia* sp. PhoN to pathogenic species producing PhoN is discussed along with the possible role of phosphatase as both a scavenger of phosphate and in providing a defense mechanism for the pathogenic bacterial cell against the free radical-mediated immune response of the host.

STATEMENT

I declare that this thesis contains no material which has been accepted for the award of any other degree or diploma in any University and that, to the best of my knowledge, this thesis contains no materials written by any person except where due reference is given in the text.

Claire Mennan

Contents:

1	Chapter 1 Introduction to the thesis and rationale for the study	1
1.1	General overview and rationale	1
1.1.1	<i>Serratia</i> sp. mechanism of action	2
1.1.2	Metal removal using <i>Serratia</i> sp.	2
1.1.3	Importance of a biogenic system for the possible clean up of heavy metals	3
1.1.4	Project aims	4
1.2	Layout of the thesis	4
1.3	Introduction and general overview	6
1.3.1	Problems of radionuclide contamination and potential radioterrorist threat	6
1.4	Application of microorganisms to heavy metal and radionuclide clean up	8
1.4.1	Biosorption a passive method of metal removal	9
1.4.2	Bioaccumulation and Enzymatically-mediated Biomineralisation	10
1.5	Biomineralisation using <i>Serratia</i> sp. and how this can be applied to radionuclide remediation	11
1.5.1	<i>Serratia</i> sp.	11
1.6	Biofilm formation	13
1.7	Extracellular polymeric substances	15
1.8	Biomineralisation of metals that do not readily form insoluble metal phosphate on <i>Serratia</i> biofilm; a new approach	16
1.9	Inspiration from solid state chemistry: bio-zirconium phosphate as a potential ion exchanger for radionuclide decontamination	18
1.10	Ion exchange and co-crystallisation comparison of approaches	20
1.11	Bacterial acid phosphatase	22
1.12	Mammalian purple acid phosphatase	23
1.13	Virulence and acid phosphatase	27
1.14	PhoN and virulence	29
1.15	Study of <i>Serratia</i> sp. <i>phoN</i> phosphatase to date	31
1.16	Isoenzymes	34
1.17	Peroxidases	36
1.18	Vanadium peroxidases and phosphatases: dual functionalities?	37
1.19	The nature of the redox active group	38
1.19.1	Redox active cysteine	38
1.20	Objectives of the work	39
2	Chapter 2 Materials and Methods	41
2.1	General Methods	41
2.1.1	Organism	41
2.1.2	Chemicals	41
2.1.3	Media	42
2.1.4	Protein measurement	42
2.1.5	Assay of phosphatase activity	42
2.1.6	Polyacrylamide gel electrophoresis	43
2.2	Phosphatase purification	44
2.3	Effects of various compounds on <i>Serratia</i> sp. phosphatase	45
2.4	Deoxyribose method for assessment of free radical damage	45
2.5	Matrix assisted laser desorption ionisation-time of flight (MALDI- ToF) mass spectrometry of <i>Serratia</i> sp. phosphatase	47
2.5.1	Analysis of SP1 and SP2 by mass spectrometry	47

2.5.2	Destaining, digestion, peptide extraction and data dependent analysis (DDA)	47
2.5.3	Peptide separation by in-line liquid chromatography and electrospray ionisation mass spectrometry (detection of phosphorylated peptides)	48
2.6	Elemental analysis of acid phosphatase by micro PIXE analysis	49
2.7	Spectrophotometric analysis of metals and phosphate	50
2.7.1	Spectrophotometric analysis of zirconium	50
2.7.2	Spectrophotometric analyses of cobalt and strontium.	50
2.7.3	Spectrophotometric analysis of phosphate	51
2.8	Biom mineralisation experiments	51
2.8.1	2.5 L reactor growth of <i>Serratia</i> sp. biofilm	51
2.8.2	Biom mineralisation of zirconium by <i>Serratia</i> sp. continuous process	55
2.8.3	Biom mineralisation experiments with Zr (continuous process)	56
2.8.4	Biom mineralisation of zirconium by <i>Serratia</i> sp. (batch process)	56
2.8.5	Chemical production of α -Zr(HPO ₄) ₂ reference material	58
2.9	X-ray diffraction analysis	58
2.9.1	X-ray powder diffraction (XRD) analysis of biogenic ZrP on biofilm	59
3	Chapter 3 Accumulation of zirconium phosphate by <i>Serratia</i> sp.: A benign system for the removal of radionuclides from aqueous flows	60
4	Chapter 4 Purification and partial characterisation of the phosphatases SP1 and SP2 from <i>Serratia</i> sp.	82
4.1	Chapter summary	82
4.2	Introduction	83
4.3	Results and Discussion	83
4.3.1	Purification of SP1 and SP2 using the method of Jeong (1992)	83
4.3.2	Phosphatase purification flowsheet taken from Jeong (1992)	87
4.3.3	Phosphatase purification flowsheet for this study	88
4.3.4	Purification of SP1 and SP2 using two step ion exchange and gel filtration	90
4.4	Summary of the Results	103
5	Chapter 5 Characterisation of <i>Serratia</i> sp. phosphatase SP1 and SP2: metal content and possible function of the enzyme	104
5.1	Chapter summary	105
5.2	Introduction	105
5.3	Results and discussion	106
5.3.1	Polyacrylamide Gel Electrophoresis and MALDI-ToF mass spectrometry of <i>Serratia</i> sp. phosphatase SP1 and SP2.	106
5.3.2	Analysis of <i>Serratia</i> phosphatase by mass spectrometry and identification of the protein by database interrogation	109
5.3.3	Examination of transition metal associations with <i>Serrratia</i> phosphatase by micro PIXE analysis	114
5.3.4	Effect of various compounds on <i>Serratia</i> sp. phosphatase	118
5.3.5	Phosphatase as a potentiator of free radical damage	122
5.4	Summary of the results	126
6	Chapter 6 Crystallisation of <i>Serratia</i> sp. phosphatase SP2	127
6.1	Chapter summary	128
6.2	Introduction	128
6.3	Methods	129
6.3.1	Set up of initial crystal screens to establish crystal growing conditions	129
6.3.2	Set up of secondary crystal screens	130
6.3.3	Preparation of buffer stock solutions	131
6.3.4	Preparation and set up of optimisation screens (Index, screen 2 (SW2) and screen (SW3))	131
6.4	Results and discussion	133
6.4.1	Initial screens using Index, screens SW2 and SW3	133

6.4.2	Optimisation Screen 4	138
6.4.3	Optimisation screen 5	142
6.4.4	Optimisation screen 6 - addition of glycerol to promote stability	148
6.4.5	Optimisation screen 7 - addition of glycerol-2-phosphate to promote crystallisation.....	148
6.5	Discussion	150
6.6	Summary of the results.....	153
7	Chapter 7 Discussion	154
7.1	Hypothesis and future work	154
7.1.1	Zr work, biomineralisation and possible roles of <i>Serratia</i> phosphatase.....	154
7.2	Further work	163
8	References	167
9	Appendices	183

List of illustrations

Chapter 1 Introduction

Figure 1: <i>Serratia</i> biofilm on polyurethane foam viewed under cryo-scanning electron microscope	14
Figure 2: Extracellular polymeric substances on hydrated <i>Serratia</i> biofilm	15
Figure 3: Hydrogen uranyl phosphate on <i>Serratia</i> biofilm viewed under ESEM	17
Figure 4: Idealised structure of zirconium phosphate	19
Figure 5: Fenton reaction involving tartrate resistant acid phosphatase	26
Figure 6: Localisation of phosphatase on and around <i>Serratia</i> cells shown by immunogold labelling	31

Chapter 2 Materials and Methods

Figure 7: Polyurethane foam cube and disc without <i>Serratia</i> biofilm	53
Figure 8: Air lift fermenter in operation and view of foam cubes and discs	53
Figure 9: Set up of reactors containing <i>Serratia</i> sp. biofilm for biomineralisation and formation of metal phosphates	54
Figure 10: Erlenmeyer flask containing biofilm coated polyurethane foam discs and biogenic ZrP gel	57
Figure 11: Hydrothermal bomb	57

Chapter 3 Accumulation of zirconium phosphate by a *Serratia* sp.: A benign system for the removal of radionuclides from aqueous flows

Figure 1: Break through curves for the sorption of Co^{2+} and Sr^{2+} on ZrP biogel supported into <i>Serratia</i> sp. biofilm immobilised onto polyurethane foam discs	81
--	----

Chapter 4 Purification and partial characterisation of the phosphatases SP1 and SP2 from *Serratia* sp.

Figure 12.a: Phosphatase purification flowsheet taken from Jeong (1992)	87
Figure 12.b: Successful phosphatase purification flowsheet for this study	88
Figure 13: HiTrap Q (anion exchange chromatography) of ammonium sulphate fractionated <i>Serratia</i> phosphatases	94
Figure 14: SDS-PAGE of the <i>Serratia</i> proteins at various stages of phosphatase purification	96
Figure 15.a: Superdex 200 gel filtration of SP2	98
Figure 16.a: Superdex 200 gel filtration of SP1	99
Figure 17.a: Showing 35 % and 60 % ammonium sulphate fractionated proteins prior to de-salting and concentrating	100
Figure 17.b: Showing pigment present in pooled fractions containing SP2 after elution	100
Figure 17.c: Fraction collector after HiTrap Q chromatography of ammonium sulphate Fractions (35 % and 60 %) showing pigmentation	100
Figure 18: SDS-PAGE of <i>Serratia</i> sp. phosphatases SP1 and SP2 after superdex 200 gel filtration	101

Chapter 5 Characterisation of *Serratia* sp. phosphatase SP1 and SP2: metal content and possible function of the enzyme

Figure 19.a: SDS-PAGE of SP1 and SP2 after purification	108
Figure 19.b: MALDI-ToF MS analysis of SP2	108
Figure 19.c: MALDI-ToF MS analysis of SP1	108
Figure 20: Screenshots from MS analysis (peptide mass fingerprints) of SP1 and SP2	112
Figure 21.a: The protein drying ring prior to PIXE analysis	115
Figure 21.b: PIXE map of SP1	115
Figure 21.c: PIXE map of SP2	115
Figure 22: The effect of phosphatase (SP1 and SP2), denatured phosphatase and ethanol on the free radical damage to deoxyribose	123

Chapter 6 Crystallisation of *Serratia* phosphatase SP2

Figure 23: Pictures of <i>Serratia</i> phosphatase SP2 crystals from selection of buffer conditions taken from optimisation screen 4	140
Figure 24: Crystal pictures from optimisation screen 5	145
Figure 25: Enlarged images of phosphatase crystals showing pigmentation	147

List of Tables

Chapter 1 Introduction

Table 1: The differences between reduced and oxidised forms of purple acid phosphatase	25
Table 2: Differences between <i>Serratia</i> sp. phosphatase SP1 and SP2	33

Chapter 3 Accumulation of zirconium phosphate by a *Serratia* sp.: A benign system for the removal of radionuclides from aqueous flows

Table 1: Comparison between HUP biomaterial and some commercial inorganic material	78
Table 2: Comparison of bioreactor systems, packed with <i>Serratia</i> sp. biofilm immobilised onto polyurethane foam with different formats, for the uptake of Zr from aqueous solutions, with and without citrate	79
Table 3: Comparison of two bioreactor systems, packed with ZrP supported on <i>Serratia</i> sp. biofilm immobilised onto polyurethane foam discs, for the uptake of Co^{2+} and Sr^{2+} from aqueous solutions	80

Chapter 4 Purification and partial characterisation of the phosphatases SP1 and SP2 from *Serratia* sp.

Table 3.a: Showing the composition of different buffers used during the purification of SP1 and SP2 used in Jeong's (1992) study	89
Table 3.b: Showing the composition of different buffers used during the purification of SP1 and SP2 in this study	89
Table 4: Relative amounts of SP1 and SP2 obtained from Jeong's (1992) study and in this study	97
Table 5: Purification of acid phosphatase (SP1 and SP2) from <i>Serratia</i> sp.	102

Chapter 5 Characterisation of *Serratia* sp. phosphatase SP1 and SP2: metal content and possible function of the enzyme

Table 6: A new database search (using BLAST) of the amino acid sequences of two peptide fragments of <i>Serratia</i> phosphatase	113
Table 7.a: Trace metal content of <i>Serratia</i> phosphatase SP1 and SP2	116
Table 7.b: Metal concentration (ppm) over its detection limit at that point for the lowest concentration found in each test	116
Table 8: The effect of different chemicals on the enzyme activity of SP1 and SP2	121

Abbreviations:

BCIP:	5-bromo-4-chloro-3-indolyl phosphate
BLAST:	Basic Local Allignment Search Tool
CPI:	<i>Citrobacter</i> Phosphatase I
CPII:	<i>Citrobacter</i> Phosphatase II
DDA:	Data Dependent Aquisition
EDTA:	Ethylenediaminetetraacetic Acid
EPR:	Electron Paramagnetic Resonance
EPS:	Extracellular Polymeric Substances
ESI-MS:	Electrospray Ionisation-Mass Spectrometry
G2P:	Glycerol-2-phosphate
HUP:	Hydrogen Uranyl Phosphate
LPS:	Lipopolysaccharide
MALDI-ToF:	Matrix Assisted Laser Desorption/Ionisation-Time of Flight
MS:	Mass Spectroscopy
MOPS:	3-(N-morpholino) propanesulfonic acid
NMR:	Nuclear Magnetic Resonance
NR:	(data) Not Recorded
PAP:	Purple Acid Phosphatase
PIXE:	Proton Induced X-ray Emission
PKL:	Peak List File
pNPP:	p-Nitrophenol Phosphate
Q-ToF:	Quadrupole-Time of Flight
ROS:	Reactive Oxygen Species
SP1:	<i>Serratia</i> Phosphatase 1
SP2:	<i>Serratia</i> Phosphatase 2
SOD:	Superoxide Dismutase
TRIS:	Tris(hydroxymethyl)aminomethane
XRD:	X-ray powder Diffraction
ZrP:	Zirconium Phosphate

1 Chapter 1 Introduction to the thesis and rationale for the study

1.1 General overview and rationale

This thesis focuses on applications of biotechnology for the remediation of radionuclide contamination. Due to the revival of nuclear power and its envisaged extensive useage in the future, efficient and cost effective biotechnology for the clean up of radionuclides released into the environment needs to be available. At the same time society needs a scaleable, ‘needy-response’ remediation technology for decontamination of wash waters following a radioterrorist incident. The polonium poisoning incident in London (2006) and the radio caesium contamination event in Goiânia, Brazil (1987) illustrate the large problems of such clean up operations. Previous work into biogenic methods of radionuclide and heavy metal removal have shown great promise (see below). One pioneering approach used a biological system to make hydrogen uranyl phosphate (HUP) which acted as a host mineral matrix to capture and retain metals such as ^{60}Co , ^{95}Sr and ^{137}Cs through intercalative ion exchange (Paterson-Beedle *et al.* 2006), these metals were also co-crystallised along with Uranium. This biogenic HUP system is formed and made using a *Serratia* sp. via the activity of an acid phosphatase enzyme (discussed in more detail below). HUP is a remarkable ion exchanger (Paterson-Beedle *et al.* 2006), however, where non-toxicity is a pre-requisite e.g. for the treatment of water ways and potable water, the HUP system would be unsuitable. The initial aim of this thesis is to focus on the practical use of an alternative system to HUP using zirconium phosphate, an inert, non toxic metal which has similar ion exchange properties to HUP. In addition to ion exchange studies using zirconium phosphate as a replacement to the HUP system and with a view to co-crystallisation of radionuclides with Zr in a highly radioactive system. The mediating phosphatase is usually found in soil species such as *Serratia* and *Citrobacter* but more usually found in pathogenic enterobacterial strains. The second

aim is to understand a rationale for the production of a radioresistant enzyme in the context of free radical reactions known to be characteristic with the host response. The mediating phosphatase produced by the *Serratia* sp. is also studied with the aim of enzyme characterisation to maximise production and activity of a radioresistant isoenzyme.

1.1.1 *Serratia* sp. mechanism of action

A *Serratia* sp. originally isolated from metal polluted soil (Macaskie & Dean, 1982) atypically overproduces a PhoN acid type phosphatase, which exists in two distinct isoforms (SP1 and SP2; Jeong, 1992; Jeong *et al.* 1998). SP1 and SP2 are very similar and have very few differences. SP2 has a comparatively high enzyme activity and lower radioresistance compared to SP1, however, both isoforms are yet to be fully characterised. In the presence of heavy metals the phosphatase enzyme liberates inorganic phosphate ligand (HPO_4^{2-}) from a phosphate donor glycerol-2-phosphate (G2P) and deposits metal (M) as polycrystalline cell bound MHPO_4 (Macaskie *et al.* 1992).

1.1.2 Metal removal using *Serratia* sp.

This *Serratia* sp. (NCIMB 40259) has been used for the removal of metals such as uranyl ion, lead, copper, cadmium, lanthanum, strontium, manganese, thorium, americium and plutonium (Macaskie & Dean, 1984; Macaskie & Dean, 1985; Tolley *et al.*, 1991; Macaskie, 1992; Macaskie *et al.* 1994; Yong *et al.* 1998; Forster & Wase, 2003; Paterson-Beedle *et al.* 2004). In order to achieve metal removal from solution, *Serratia* cells are immobilised on a support such as polyurethane foam and incorporated into a flow through column. Metal precipitation and crystallisation is via the production of locally high concentrations of phosphate ligand, which exceeds the solubility product of the metal phosphate in juxtaposition to nucleation sites on the cell surface (Bonthrone *et al.* 1996; Macaskie *et al.* 1994). All heavy metals having insoluble

phosphates should be amenable to bioremediation in this way; however Ni has been shown to be problematic (Bon throne *et al.* 1996).

The *Serratia* sp. has been shown to tolerate loads of ~9 g of accumulated uranium per gram of biomass (900 % of the dry weight) (See Yong & Macaskie, 1995). This comprises hydrogen uranyl phosphate (HUP) (HUO_2PO_4), which is indistinguishable from crystalline $\text{HUO}_2\text{PO}_4 \cdot 4\text{H}_2\text{O}$ prepared chemically (Yong & Macaskie, 1995). This HUP crystal lattice can then be used for the removal of nickel by intercalative ion exchange (Bon throne *et al.* 1996). HUP is a remarkable ion exchanger as it exchanges very easily its H_3O^+ with Na^+ , NH_4^+ , K^+ and some divalent cations. The fission products ^{137}Cs , ^{90}Sr and the activation product ^{60}Co have been removed from solution in this way by intercalative ion exchange within biogenic HUP (Paterson-Beedle *et al.* 2006) and by co-crystallisation with HUP (M.Paterson-Beedle, unpublished).

1.1.3 Importance of a biogenic system for the possible clean up of heavy metals

The problems of nuclear waste decontamination and treatment have been of high importance for many years and present real problems affecting the uses and future acceptability of nuclear power. In addition the threat of radioterrorism requires that a portable ‘ready response’ remediation system is developed. The development of a novel-bioinorganic ion exchanger such as the *Serratia* HUP system presents a viable alternative to costly and time consuming methods of heavy metal removal from aqueous flows from nuclear waste and also acid mine drainage. However the HUP system is not attractive for potable water treatment due to the toxicity and radioactivity of uranium. Inert and non toxic metals such as zirconium, known to make phosphate lattices with ion exchange capability, for example, a *Serratia* zirconium phosphate system could allow the bioremediation of aqueous flows where non toxicity is a pre-requisite. However, ion exchange columns have a finite capacity. By incorporating Zr(IV) and glycerol-2-phosphate a non-saturating co-crystallisation method was developed (M.Paterson-Beedle, unpublished). In this

biomineralising system using a co-crystallisation approach it is important to note that the *Serratia* phosphatase enzyme needs to be kept active and therefore needs to be resistant to the radioactivity of the accumulating radionuclides which are held in close proximity. In contrast, intercalative ion exchange into pre-formed metal phosphate does not require sustained enzyme activity.

1.1.4 Project aims

The initial part of this study aims to show proof of principle of such a system in which a zirconium phosphate can be utilised in the same way as the HUP system and used successfully for removal of radionuclide surrogates. The second part of the study aims to characterise the isoenzymes SP1 and SP2 with the overall goal to achieve conversion of the radiosensitive isoenzyme into the radiotolerant isoenzyme since preliminary evidence has suggested that the two forms are interconvertible. Continued enzyme activity under radiostress would permit application of co-crystallisation as well as ion exchange approaches, the former being potentially more attractive since it is not constrained by the column saturation which limits the capacity of ion exchange.

1.2 Layout of the thesis

Following an Introduction incorporating an overview of relevant literature and Materials and Methods section the first results chapter comprising a published paper (Biotechnology Letters) (chapter 3) shows the feasibility of using the biogenic zirconium phosphate system for removal of surrogate radionuclides by ion exchange. The second results chapter (chapter 4) details the development of a method of purification of isoenzymes SP1 and SP2 with the aim to obtain enough pure enzyme for characterisation and crystallisation studies. The third results chapter (chapter 5) investigates and compare properties of SP1 and SP2 with the aim to study their responses and effects in free radical-mediated reactions, since radiation damage is mediated via

free radicals of water radiolysis. The fourth results chapter (chapter 6) aims to crystallise the purified phosphatase. The final aim is to understand the differences in the context of a radionuclide bioremediation system and also to reveal a possible role for this enzyme in the pathogenicity of related organisms which, unlike normal *Serratia* species, express PhoN. The final discussion (chapter 7) progresses these concepts and also suggests directions for future work. Chapter 3 is presented as a self contained paper for publication as detailed on the front page of the chapter.

1.3 Introduction and general overview

1.3.1 Problems of radionuclide contamination and potential radioterrorist threat

Nuclear power is enjoying a resurgence, since its widespread use may help reduce atmospheric release of ‘greenhouse gases’; however, public embracement of nuclear technology is still limited by the need for effective waste treatment and worries over the perceived risks of environmental contamination through improper storage, accidental release or the threat of terrorism (‘dirty bomb’). Hence the need for suitable biotechnology which would provide efficient and cost effective clean up of radionuclides in the event of their release into the environment.

The list of accidents involving release of radioactive substances does not inspire historical confidence and has highlighted the enormous problems of decontamination of contaminated buildings and land. Some of the most notable disasters in history are: The Windscale fire (1957), the Mayak disaster (1957), Three Mile Island accident (1979), Soviet submarine K-431 accident (1985), Chernobyl disaster (Ukraine) (1986) and the Goiânia accident (Brazil) (1987), to name but a few. The Chernobyl and Mayak (Kyshtym) disasters released substantial ^{137}Cs and ^{90}Sr into the environment (Karavaeva *et al.* 2007), and in the case of Chernobyl, spread this as particulate and gaseous debris carried by winds across international borders leaving large areas contaminated. Other disasters such as Goiânia involved the release of ^{137}Cs due to the scavenging of a radiation source from radiotherapy equipment from an abandoned hospital and resulted in the radiation poisoning of over 200 people (da Cruz *et al.* 2008). Furthermore, large tonnages of contaminated building materials and rubble had to be disposed of with burial the only option. The windscale fire in Cumbria was responsible for releasing ^{131}I and ^{137}Cs (Garland & Wakeford, 2007). The cost of such accidents in terms of clean up is huge and often leaves areas uninhabitable (for example, in the case of Chernobyl).

The development of relatively cheap biological-based waste treatments could be advantageous in such disasters where the clean up process would inevitably become uneconomic. Many

methods are employed for the clean up of heavy metals, toxic chemicals and nuclear waste from their normal use, however, most processes leave residual contamination and in the nuclear industry this 'low level waste' is often discharged into the sea despite containing residual radioactive species some of which may become immobilised in sediments (Choppin & Wong, 1998). Such immobilisation can solve short-term problems but radioactive decay may result in the formation of daughter elements of higher mobility.

^{60}Co , ^{137}Cs and ^{90}Sr are mobile radionuclides that are of particular concern in terms of release into the environment and subsequent contamination. ^{137}Cs and ^{90}Sr are β -emitters which both have a half life of ~30 years, whereas ^{60}Co has a relatively short half life ~5 years, however its emission of potentiating gamma radiation make it particularly dangerous. ^{137}Cs has accounted for 65 % of all isotopes in low level waste from the reprocessing plant at Sellafield, which released large quantities into the Irish Sea (Lovley, 2000).

Ion exchange methodology used in the chemical, nuclear and waste water treatment industries is highly efficient when compared to equivalent chemical technologies but is expensive (Stylianou *et al.* 2007). Also, ion exchange plants are not portable and cannot be implemented in problem areas rapidly for example, the material used in the 'SIXEP' plant at Sellafield (a zeolite) was sourced from overseas. Biological-based processes could present a viable and scalable alternative; however, any bioremediation system would need to be robust enough to prevent remobilisation of entrapped radionuclides over time.

Biological techniques for the clean up of some nuclear wastes are an important consideration, within the context of threat of accidents, leaks, terrorism and the increasingly strict legislative requirements governing discharge of all types of nuclear/industrial waste as well as the expense of treatments. Estimates show that trillions of gallons of groundwater are contaminated with radionuclides along with millions of cubic metres of soil and debris and the cost of cleaning up

these sites is estimated to be over a trillion dollars in the US and over 50 billion pounds in the UK (Lloyd & Renshaw, 2005).

Biological approaches or biogenic ion exchangers could also be used alongside or as an adjunct to conventional treatments as a final ‘polishing’ step (where low level waste contains low levels of radioactivity per mass/volume) to ensure all radioactive species are removed from wastes before discharge, thereby adhering to future legislations which may not permit the liberation of radioactive waste into the environment. A biological approach could also be cheaper than conventional methods, which would make it an attractive alternative where the cost of decontamination by other methods becomes uneconomic. Biogenic inorganic ion exchangers would be advantageous over biomass *per se* due to their high portability and ease of deployment in the event of radioactive contamination; unlike biomass, inorganic materials are stable against spoilage and hence have a long shelf life. Also, although many microorganisms such as bacteria, fungi and yeasts have been used successfully for the removal of heavy metals (living and dead cells have been used) they could present a viable method of heavy metal and radionuclide removal and clean up. However the capacity of microbial systems *per se* for metals is usually only a few percent and maximally about 20 % of the biomass dry weight.

1.4 Application of microorganisms to heavy metal and radionuclide clean up

Microorganisms encounter various metals in the environment and it is therefore not surprising that they have evolved and developed many ways of dealing with toxic metals and radionuclides to aid their own survival as has been reviewed extensively elsewhere (Lovley, 2003; Gadd, 2009).

Many different microorganisms can accumulate relatively high quantities of radionuclides and heavy metals from the environment; bacteria, fungi and yeasts have all been used successfully for the remediation of heavy metals (Macaskie *et al.* 1992; Lovley & Coates, 1997; Lovley, 2003; Gadd, 2009). Both living and dead cells can be used for metal uptake from solution, therefore metal accumulative mechanisms range from processes dependent on cell metabolism

(biomineralisation and bioaccumulation) to chemical interactions with the cell surface or surface polymers such as biosorption. For the remediation of uranium for example, organisms such as *Saccharomyces cerevisiae*, *Penicillium* sp. and *Aspergillus* sp. have been used successfully. The advantage of these types of biomass are that they are waste biomass from the brewery and food industries, food and drug industry, meaning that they do not have to be grown and cultured specially for remediation. In these organisms metal is accumulated by biosorption and therefore the cells do not need to be kept alive or fed with nutrients to ensure good levels of metal removal. Microorganisms are able to remove or accumulate metals from their environment using a variety of different methods. For example, many organisms are able to leach metals using metabolic products such as acids (leaching of nickel using citric acid from *Aspergillus* and *Penicillium* sp.) (Castro *et al.* 2000). Other organisms use enzymatic detoxification of harmful metals to convert a toxic metal species to a non toxic or less toxic form by enzymatic oxidation or reduction (*Pseudomonas fluorescens* is involved in the reduction of CrO_4^{2-} to $\text{Cr}(\text{OH})_3$) (Pattanapitpaisal *et al.* 2002). However for the purposes of this study biosorption, bioaccumulation and biomineralisation will be discussed

1.4.1 Biosorption a passive method of metal removal

Biosorption is the ability of living or dead biomass to passively accumulate, bind or concentrate metals and has been extensively reviewed (Volesky & Holan, 1995; Lovley & Coates, 1997; Gadd, 2009). Biosorption is a physico-chemical process and includes such mechanisms as absorption, adsorption, ion exchange, surface complexation and precipitation (Gadd, 2009). Biosorption is difficult to define exactly as it is highly dependent on the type and state of biomass (living or dead), substance sorbed and many environmental factors (Gadd, 2009). The bacterial cell surface contains amine, hydroxyl, carboxyl (the main binding site in Gram-positive species),

phosphate and sulphydryl groups which are responsible for binding and or sorbing metal ions at appreciable quantities (Lloyd, 2002; Gadd, 2009). Bacterial extracellular polymeric substances (EPS), phosphoryl groups in the core lipid-A of LPS and proteinaceous S-layers also bind significant quantities of metal (Macaskie *et al.* 2000; Barkay & Schaefer. 2001; Gadd, 2009).

1.4.2 Bioaccumulation and Enzymatically-mediated Biomineralisation

In terms of microbial metal removal, bioaccumulation and biomineralisation can be described as metabolism dependent accumulation of metals. Bioaccumulation, in a broader context, is a process through which a bio-system retains and accumulates any substance in excess as a result of a greater rate of absorption than excretion of this substance. Biomineralisation is the next step in many species, when the absorbed substance undergoes a chemical transformation and turns into 'a mineral'. These two processes often happen in parallel in a system such as the *Serratia* HUP system (see earlier and below). Unlike biosorption, in which inactive or dead cells can be used, biomineralisation often requires enzymatic activity (if not active cell metabolism) and hence it is subject to constraints where metal toxicity, radioactivity and other environmental factors adversely affect the metabolic function of the cell; therefore the efficacy of biomineralisation may be reduced and limited to practical applications in which low levels of toxicity and radioactivity are involved. The exception is when biomineralisation is mediated by a robust enzyme which does not require continued cell viability for operation.

One such relevant example of biomineralisation is the *Serratia* hydrogen uranyl phosphate (HUP) system. *Serratia* cells accumulate UO_2^{2+} as HUP; this biomineralisation process relies upon the liberation of inorganic phosphate at a high concentration at the surface of the *Serratia* sp. cells via the activity of an acid type phosphatase which is responsible for the cleavage of a phosphate donor molecule e.g. glycerol-2-phosphate (Paterson-Beedle *et al.* 2006). Initially UO_2^{2+} coordinates onto phosphate groups within the lipid A component of the lipopolysaccharide

component of the extracellular polymeric substances (EPS) (which act as the initial nucleation point) near to the enzyme. The *Serratia* sp. phosphatase (tethered to the EPS) then liberates HPO_4^{2-} (from a phosphate donor, G2P) to make a layer of HUP around the cells. It is thought that this trapping of metal compartmentalises it away from the cell, allowing the enzyme and sites of substrate access to remain free. However in the case of radionuclides the close proximity of the metal deposit means that the mediating enzymes may be subject to radiotoxicity. Previous work using a ^{60}Co gamma source established the intrinsic radiotolerance of the *Serratia* phosphatase (Jeong, 1992).

1.5 Biomineralisation using *Serratia* sp. and how this can be applied to radionuclide remediation

1.5.1 *Serratia* sp.

Serratia is a genus of Gram negative, non spore forming, enteric bacilli belonging to the family *Enterobacteriaceae*. Other related enterobacteria are well known pathogens such as *Salmonella* spp., *Morganella* spp., *Klebsiella* spp., *Shigella* spp., and *Providencia* spp. *Serratia* is ubiquitous, found mainly in water and soil and although considered as being mostly harmless to humans, *Serratia* can be an opportunistic organism, causing nosocomial infections, e.g. colonising respiratory and urinary tracts and infecting open wounds.

In the context of this study *Serratia* sp. (NCIMB 40259) was originally isolated from metal polluted soil (Macaskie & Dean, 1982) and was originally assigned within the genus *Citrobacter* on the basis of biochemical testing at the NCIMB facility. However more recent molecular methods revealed that the organism was a *Serratia* sp. Attempts to classify the organism further in the laboratory (Macaskie, unpublished) and commercially (NCIMB: Torry research station, Aberdeen, UK) and by molecular methods failed to resolve the strain identity to beyond genus level. The *Serratia* sp. used in this study has been reported previously (Macaskie *et al.* 1994: Jeong *et al.* 1997) to accumulate heavy metals as cell bound heavy metal phosphates via the

activity of an acid type phosphatase. *Serratia* sp. NCIMB 40259 produces this acid type phosphatase in two distinct isoforms designated SP1 and SP2 (previously called CPI and CPII; Jeong, 1992). Early work looking at the amino acid sequence of fragments of this phosphatase enzyme found that it had significant homology to the PhoN phosphatase product of some other pathogenic enterobacterial species (Macaskie *et al.* 1994) (see later). *Serratia* spp. also produce extracellular polymeric substances (EPS), which are thought to not only form a protective barrier for the cell against toxic metals in the environment (Macaskie *et al.* 2000) but also to aid in their aggregation to surfaces and each other in the formation of biofilms. The role of cell surface polymers in metal phosphate nucleation using *Serratia* sp. was shown by Macaskie *et al.* (2000). Metal phosphate was shown initially to nucleate via the phosphate groups of the lipid A component of lipopolysaccharide as concluded using ^{31}P NMR, prior to more extensive metal phosphate nucleation brought about by the activity of the phosphatase shown to be localised in the periplasm and exocellularly by immunogold labelling (Jeong *et al.* 1998). Macaskie *et al.* (2000) suggested a bifunctional role for the cell surface polymers and EPS, firstly in the enzymatic removal of metal from solution via the nucleation of metal phosphate and secondly as a vehicle for immobilisation and protection (from toxic metals) of the acid phosphatase (Macaskie *et al.* 2000). Attachment of phosphatase-containing bacteria to a solid surface (biofilm formation) allows the development of continuous filtration systems and hence formation of a highly cohesive biofilm that retains both phosphatase activity and accumulated metals is very important. Early studies compared cells adhered naturally and via chemical coupling to supports, finding them identical in terms of ability to remove metals.

1.6 Biofilm formation

For continuous metal removal initial tests used polyacrylamide gel-immobilised cells but later studies used biofilm reactors (Tolley *et al.* 1991; Macaskie *et al.* 1995; Paterson-Beedle *et al.* 2006). Microbial biofilms (Fig. 1) are desirable in the remediation of wastewaters and treatment of drinking water as they confer many advantages over planktonic cells. Natural biofilms (as opposed to artificially immobilised cells) have a large, irregular and highly convoluted surface area and very high biomass, which allows shorter culturing times and the use of smaller reactors (Janning *et al.* 1995), therefore reducing cost. According to Mittleman (1985) development of a mature biofilm may take several hours to several weeks. Vanhaecke (1990) found that *Pseudomonas* cells adhere to stainless steel (even to electropolished surfaces) within thirty seconds of exposure. The process of biofilm formation (which is still poorly understood) aids in the flow of fluid and nutrients to the entire population through naturally occurring pores and channels (increasing the surface area available for reaction even further). The production of extracellular polymeric substances (EPS) around individual bacterial cells making up the biofilm aids in their adhesion and attachment to the surface. It is also thought that pili and flagella aid in attachment and directly interact with organic molecules on the surface (Korber *et al.* 1995). The natural biofilm environment shows great variation in terms of species composition, structure, distribution, cell activity and cell density. In most cases, the base of the biofilm is composed of an exudate layer approximately 5-10 μm thick, 100-200 μm upwards are colonies of bacteria shaped like mushrooms or cones and above this exists more of the exudate produced by the organisms (Costerton *et al.* 1995). Through these colonies a network of pores and channels carries bulk fluid throughout the biofilm, thus acting as a primitive circulatory system comparable with that of a higher organism (Costerton *et al.* 2000). Through this circulatory system flows water, bacterial waste, nutrients, enzymes, metabolites and oxygen (Kaiser and Losick. 1993).

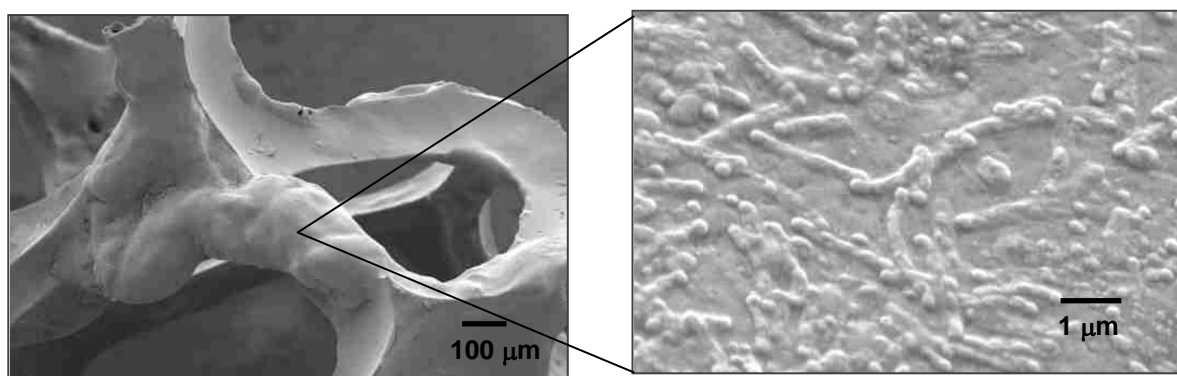


Fig. 1. *Serratia* sp. biofilm on polyurethane foam viewed under cryo-scanning electron microscope (taken from Paterson-Beedle *et al.* 2006) (maximum thickness of biofilm ~ 430 µm) (Allan *et al.* 2002).

Nutrient limitation is known to directly affect the composition and physiology of the cell (Harder & Dijkhuizen, 1983), while culturing the biofilm under-carbon limiting conditions has been shown to promote the adhesion of cells to the growth surface (Ellwood *et al.* 1982) because the limitation of carbon may directly affect the EPS. Growth of *Serratia* sp. under carbon limitation also promotes production of pili (as well as acid phosphatase over-production: see later) (Allan *et al.* 2002) which are used to anchor the cells more permanently to the surface (Kaplon *et al.* 2003). However, production of EPS is very energy and carbon-expensive to the cell (Chakrabarty, 1996). Paradoxically, during carbon limiting conditions the cell diverts available carbon into production of EPS (Tempest & Wouters, 1981). It is not yet known why the cell produces such a carbon-expensive product under carbon limitation; one hypothesis (Ellwood *et al.* 1982) is that its production helps the adherence to surfaces. In the current context uranium was shown to bind to, and crosslink the EPS following nucleation onto lipid A phosphate groups of cells grown under carbon, but not nitrogen limitation (Bonthrone *et al.* 2000). Hence EPS of cells pre-grown under carbon-restriction is integral in metal deposition by the *Serratia* sp.

1.7 Extracellular polymeric substances

The EPS produced by carbon-restricted *Serratia* sp. forms a cohesive (hydrated) matrix over the bacterial cells (Fig. 2). As well as keeping the cells hydrated and protected, the EPS is also important for aggregation of the biofilm. EPS are composed of proteins, polysaccharides, nucleic acids, lipids and other biological macromolecules, although their composition and useful properties are thought to vary with nutrient availability and bacterial species (Costerton *et al.* 1995). The EPS also provides protection to the bacterial cell against many dangers such as; predation from protozoans, biocides, toxins and desiccation. It is also responsible for defining the morphology and architecture of the biofilm itself, forming the space between biofilm cells, as well as helping adhesion and cohesion. The EPS controls convectional and diffusional mass transport because it occurs in various densities and including void spaces such as pores and channels. This forms different types of physico-chemical gradients, providing habitats in which anaerobic and aerobic organisms can coexist in close proximity and largely independent of the conditions in the water phase (Costerton *et al.* 1995).

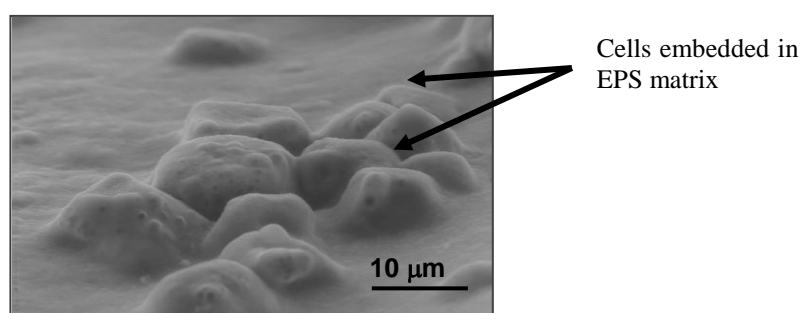


Fig 2. Extracellular polymeric substances on hydrated *Serratia* biofilm. Viewed using ESEM (from Nott *et al.* 2005).

The extracellular matrix also allows extracellular enzymes (in this case acid phosphatase: section 1.16) to be localised (tethered or enmeshed) around the cells externally. EPS has been noted before as an immobilising agent for bacterial exoenzymes (Frolund *et al.* 1995) and has been

visualised to tether the phosphatase by immunogold labelling (section 1.16, Fig. 6). In the case of this *Serratia* sp. this would be advantageous as metal deposition on the outside of the cell (on the EPS with metal phosphate deposition catalysed enzymatically; Macaskie *et al.* 2000) prevents the toxic metal ions reaching the cell in sufficient quantity to have a detrimental effect. The role of bacterial exopolymer in metal resistance generally has been described previously (Britton & Friehofer, 1978).

1.8 Biomineralisation of metals that do not readily form insoluble metal phosphate on *Serratia* biofilm; a new approach

The nuclear, mining and metallurgical industries produce waste waters contaminated with heavy metals such as nickel, uranium, lead, cadmium, copper, lanthanum, strontium, manganese, thorium, americium, and plutonium (Mishra & Tiwari, 2002). A low cost non toxic method of removing heavy metals from waste water is highly desirable and could also be used in other industries for the bioremediation of waste water where a non toxic method is a pre-requisite. The ‘new’ focus of radio-terrorism lends urgency to the problems of wash water decontamination.

Some of the metals mentioned above (e.g. nickel e.g. ^{57}Ni) are not removable by metal phosphate biogenesis per se and can only be removed by ion exchange within a host crystal lattice (Basnakova *et al.* 2001). For example: when challenged with uranium, *Serratia* sp. accumulates uranyl ion (UO_2^{2+}) as $\text{HUO}_2\text{PO}_4 \cdot n\text{H}_2\text{O}$ (Hydrogen Uranyl Phosphate: HUP) in a crystalline form using inorganic phosphate generated from the acid phosphatase enzyme (Fig. 3). The HUP then acts as the “host” lattice for the removal of nickel via intercalative ion exchange with protons or H_3O^+ groups with the crystal lattice (Basnakova *et al.* 1998; Bonthron *et al.* 1996). This has also been shown to be an efficient process for removal of ^{60}Co , ^{85}Sr and ^{137}Cs (Paterson-Beedle *et al.* 2006).

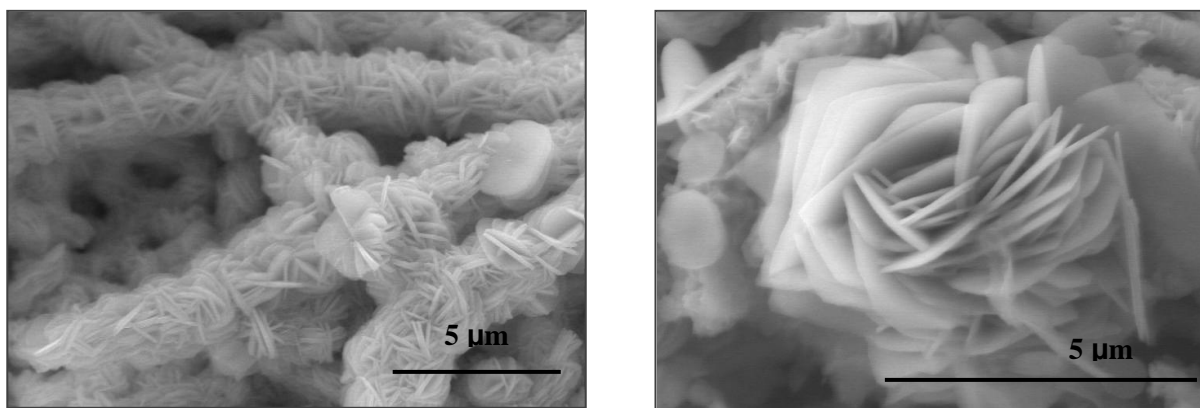


Fig 3. Hydrogen uranyl phosphate on *Serratia* biofilm viewed under environmental scanning electron microscope (ESEM) (Paterson-Beedle *et al.* 2006).

However, other metals with a good host crystal lattice (suitable for ion exchange), that are not toxic or radioactive, must be sought so that this process can be used for the remediation of potable water i.e. contaminated by a radio-terrorist attack. Zirconium is a good candidate (Clearfield & Smith, 1969) as a proton conductor. Almost all proton conductors are good ion exchangers and both HUP and ZrP fit this description (Clearfield, 1988), also the use of Zr in water purification would be completely acceptable because Zr is non-toxic and has been passed for human exposure, e.g. as an ingredient of toothpastes and suncreams. Therefore, the overall aim of this project is to move away from uranium as the host lattice for co-incorporation of target metals, and towards benign metals which can form similar host lattices such as Zr, with a view to recovery of potable water from radio-contaminated supplies. Zr based biocrystals will be generated for ion exchange and co-crystallisation removal of Cs, Sr and Co. Its efficacy in bioaccumulation of these elements on *Serratia* sp. biofilm and the ion exchange process will be evaluated.

1.9 Inspiration from solid state chemistry: bio-zirconium phosphate as a potential ion exchanger for radionuclide decontamination

Zirconium is a transition metal that resembles titanium with widespread use in the chemical and nuclear industries. Zirconium is commonly used in products such as toothpastes, suncreams and as an ion exchanger in kidney dialysis (and hence has been concluded as safe for human exposure); it also has many applications in the nuclear industry such as cladding fuel elements and creating zirconium alloy tubing for use in reactors. Commercial nuclear power generation now accounts for the use of more than 90 % of zirconium metal produced (Dyer *et al.* 1997). Zirconium is exceptionally resistant to corrosion by many common acids, alkalis, sea water and other agents; therefore it is widely used in the chemical industry where corrosive agents are employed. Examples of its broad application are: use as alloying agents in steel, in surgical appliances, photoflash bulbs and lamp filaments etc. Superconductive magnets are also made from zirconium as the metal has superconductive properties at low temperatures, offering the possibility of large-scale generation of electric power.

It was found that metal phosphates of the IV group of the periodic table generally confer good ion-exchange properties (Clearfield, 1988) and lower toxicity when compared to uranium phosphate.

α -Zirconium phosphates (α -ZrP) are synthesised chemically by reacting concentrated phosphoric acid (H_3PO_4) with an aqueous solution of a Zr salt such as ZrOCl_2 . A gelatinous amorphous precipitate is readily obtained, slow crystallisation then occurs when the precipitate is heated ($\sim 90^\circ\text{C}$) under reflux in its mother liquor and after two weeks crystallites of ca. 1 μm in diameter are obtained (Benhamza *et al.* 1991). This is a lengthy, time consuming and expensive process and biomineralisation has the potential to make ZrP in a shorter time and with considerably less expense.

α -ZrP is a very good ion exchanger and can exhibit crystalline as well as amorphous properties. The structure of α -ZrP as well as its ion exchange properties has been extensively studied by Clearfield & Smith (1969). α -ZrP crystals have a layered structure in which metal atoms lie nearly in a plane, bridged by phosphate groups. Three phosphate oxygens bond to metal atoms so that the remaining phosphate oxygen, which is bonded to a proton, points into the interlayer space (Clearfield, 1988). The layers are staggered forming a hexagonally shaped cavity with the water molecule in the centre (Clearfield *et al.* 1998) (Fig. 4).

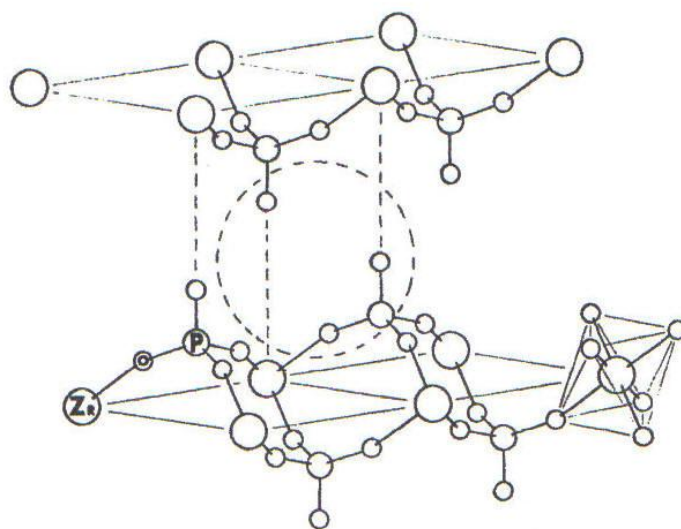


Fig. 4. Idealised structure of α -zirconium phosphate showing one of the zeolite cavities created by the arrangement of the layers (taken from Clearfield, 1988).

The layers are held together by Van der Waals forces and the inter layer distance is small. Consequently bottlenecks caused by the small interlayer distance (circled in Fig. 4) provide only enough space for an unhydrated K^+ to diffuse into the interlayer spacing (Clearfield, 1988). Therefore, the α -ZrP crystals exhibit sieving behaviour in acid solutions; ion exchange at a reasonable rate is only achieved in alkaline solutions for ions larger than K^+ (Clearfield, 1988). Under these alkaline conditions, sufficient numbers of protons are neutralised on the layers which causes layer swelling, allowing admission of larger ions. The layer expansion not only accommodates ions but also the waters of hydration (Clearfield, 1988).

Previous studies of zirconium (Zr IV) uptake by bacterial cells showed that, like Th (IV), it was biomineralised by the bacterial cells but only moderately (up to 50 % removal in the inflow solution) and in the form of gel-like deposits (Basnakova & Macaskie, 1999). ZrP in a gel-like form is not necessarily a disadvantage as α -ZrP has been prepared as a gel, as crystals and in all intermediate stages between these extremes (Clearfield *et al.* 1998). Sol-gel studies on ZrP show that the high water content of the material is responsible for its excellent ion exchange properties even though the material contained few, if any, crystalline phases when compared to α -ZrP (Bogdanov *et al.* 1997). A decrease in porosity, ion exchange capability and formation of blocks from layers occurred with a decrease in the water of the hydrogel as it dried (Bogdanov *et al.* 1997).

Zirconium has been used successfully as an inorganic ion exchanger for the removal of Cs and Sr (Dyer *et al.* 1997) in the nuclear industries; however this is expensive to produce and was most often used in a granular form, which had to be specially prepared for column use. It is expected that one of the major challenges will be the conversion of biogenic Zr (IV) phosphate (as described in this study-see later) into the ‘correct’ form for the most effective ion exchange, which is currently under study by J. Hriljac and J. Readman (School of Chemistry, University of Birmingham).

1.10 Ion exchange and co-crystallisation comparison of approaches

The identification of an alternative ‘priming metal’ to uranium for use as a host crystal from biomineralisation is a pre-requisite for widespread use in the treatment of potable and irrigation water. The most important criterion for the selection of a host crystal is the formation of layered material similar to crystalline hydrogen uranyl phosphate with good cation-exchange capacity for intercalation of the target metal(s) (Basnakova & Macaskie, 1999). It is known that metal phosphate biocrystallization *per se* does not work well for Ni, Co, Sr, Cs and Cu. These metals can only be removed appreciably by co-crystallisation i.e. crystal biogrowth along with uranium

phosphate, or by ion exchange into the HUP or ZrP host lattice of pre-formed uranyl phosphate or zirconium phosphate for example. Ion exchange of the metal works by exchanging protons from within the metal phosphate lattice; protons come out, the target metal goes in and the metal phosphate lattice stretches to accommodate the incoming ion. This was shown conclusively by intercalation of Ni^{2+} by this method, where the hydrogen uranyl phosphate lattice stretched by exactly the correct amount required to accommodate the Ni^{2+} ion (Basnakova *et al.* 1998). Radio-nuclides are taken up by ion exchange into hydrogen uranyl phosphate or indeed via co-crystallisation with UO_2^{2+} (Paterson-Beedle & Macaskie, 2004). In a real nuclear waste these would be present in addition to uranium and radionuclides, so the acid phosphatase enzyme needs to be kept active if a co-crystallisation approach is to be adopted. *Serratia* phosphatase SP1 and SP2 differ in their level of enzyme activity (SP2 has a higher enzyme activity than SP1) and in their radioresistance, SP1 is radioresistant and SP2 is radiosensitive (Jeong, 1992; section 1.15, table 2). Consequently the radioresistant isoform would be more desirable for co-crystallisation of radioactive metals (which potentially has a very high capacity) as the enzyme would need to withstand the associated metal toxicity and radioactivity whilst retaining activity to liberate inorganic phosphate. For ion exchange, the radioresistant enzyme is not needed, since the primary crystal lattice is pre-formed and metals will continue to be removed through intercalative ion exchange regardless of the presence or absence of the phosphatase.

A full characterisation of SP1 and SP2 would precede a directed conversion of the phosphatase ‘pool’ into its radioresistant form (SP1) prior to removal of radionuclides and toxic metals via co-crystallisation if this approach were to be chosen over ion-exchange e.g. ion exchange was ineffective against ^{60}Co but worked well for ^{90}Sr (Paterson-Beedle *et al.* 2006) whereas co-crystallisation removed both metals (Marion Paterson-Beedle, unpublished). In order to understand the potential roles of SP1 and SP2 in radionuclide decontamination it is useful to place these in the context of other known phosphatases.

1.11 Bacterial acid phosphatase

Phosphatases are present in many types of flora and fauna and appear in many types of plant and animal tissues as well as a wide range of microorganisms. Phosphatases are phosphoesterases which catalyse the hydrolysis of the C-O-P linkage of a variety of phosphate esters. Phosphatase removes a phosphate group from its substrate by hydrolysis of phosphoric acid monoesters into a phosphate ion and a molecule with a free hydroxyl group.

These enzymes are either called acid or alkaline phosphatases according to their optimum pH. The exact function of bacterial acid phosphatase is still poorly understood, however a historically and currently accepted role is that bacterial acid phosphatase acts as a scavenger of organic phosphate esters which are otherwise unable to pass through the cytoplasmic membrane (Uerkwitz & Beck, 1981). Many bacterial acid phosphatases are released in a soluble form or retained as membrane bound proteins. Macaskie *et al.* (2000) suggested that the acid phosphatase was excreted within membrane vesicles outside of the cell (shown previously by Nesmeyanova *et al.* 1991), and suggested a bifunctional role for the LPS and close association with the *Serratia* phosphatase and LPS, in the nucleation of metal phosphate and also as a vehicle for immobilisation and protection (from toxic and radiotoxic metals) of the *Serratia* phosphatase.

It has also been hypothesised more recently that secreted acid phosphatases function as a phosphate retrieval system in pathogenic bacteria, activated upon containment in the phagosome (the membrane lined vacuole in which ingested microorganisms are enclosed) (Felts *et al.* 2006), as well as playing an integral role in survival of the pathogen within the host's phagocytic cells (Aguirre-Garcia *et al.* 2000). Many of the intricacies of bacterial survival mechanisms remain largely unknown. However, such bacterial survival mechanisms include: inhibition of the respiratory burst (Reilly *et al.* 1996), inhibition of phagolysosome fusion and survival and or escape from within the phagolysosome (Fields *et al.* 1989). In this context it is highly relevant that the *phoN* acid phosphatase gene of *S.typhimurium* is under the control of the *phoP/phoQ*

regulon which is responsive to various stresses (such as starvation and low pH; Miller *et al.* 1989) which form part of the phagosomal response (Kinchin & Ravichandran, 2008). In addition to carbon and phosphate starvation, another 'stress' encountered in the phagolysosome is the respiratory burst brought about as part of the immune response as a mechanism for bacterial killing (Felts *et al.* 2006). The non specific acid phosphatase is thought to be produced in this system (under the control of *phoP*) as a response to environmental stimuli such as carbon, nitrogen and phosphorus starvation but not as a direct aid to virulence (Fields *et al.* 1989). To better understand and compare the many different types of phosphatases and their roles and functions, Rossolini *et al.* (1998) proposed a classification system for bacterial non specific acid phosphatases. This system divided these enzymes into subgroups, depending on their resistance to certain chemicals such as sodium tartrate, sodium molybdate and EDTA (Aguirre-Garcia *et al.* 2000) as well as their molecular weight and homotetrameric, dimeric or monomeric form. This provides a useful and direct comparison with acid phosphatases from related and unrelated microorganisms which can highlight evolutionary divergence in many different phosphatases.

1.12 Mammalian purple acid phosphatase

For a long time, acid phosphatases were not believed to be metalloenzymes because they did not seem to be inhibited by chelating agents (Hollander, 1971). In 1973 a sub class of acid metallophosphatases was identified when acid phosphatases containing iron were isolated from bovine spleen and porcine uterine fluid (Campbell *et al.* 1973). This class of enzymes was found to have a vivid purple or pink colour and became known as purple acid phosphatase. These enzymes have been isolated from a variety of mammalian, microbial and plant sources and there are substantial differences between the enzymes isolated from each. These differences refer to those associated with molecular weight, substrate specificity, subunit structure and metal contents

(Szalewicz *et al.* 1999). Enzymes from plant sources, which have been characterised in detail, are those from red kidney bean, soybean and sweet potato.

Soybean and red kidney bean acid phosphatases contain Fe (III) – Zn (II) centres in addition to small amounts of Mn, Cu and Mg in soybean acid phosphatase, whereas a similar enzyme isolated from sweet potato utilises manganese instead of zinc and contains small amounts of Zn and Cu (Schenk *et al.* 1999).

Enzymes isolated from mammalian sources have been shown to contain redox active iron centres (Schenk *et al.* 2000). The precise role(s) and function(s) of purple acid phosphatase remain unknown. However, it was hypothesised that mammalian enzymes have a role in iron transport (Nuttleman & Roberts, 1990) and high molecular weight plant enzymes have a role in phosphate acquisition (Duff *et al.* 1994). The roles of these enzymes seem to be species dependent and evidence has accumulated that links the plant enzymes (mentioned above) to a role in the acquisition of phosphate and phosphate metabolism (Hadler *et al.* 2008), whilst mammalian enzymes have been linked to bone metabolism and in the defence mechanisms of the macrophage (Kaija, 2002; Schenk *et al.* 2008). It has been shown that tartrate resistant acid phosphatase (the mammalian form of purple acid phosphatase) is found in elevated levels in activated macrophages, osteoclasts, lysosomes and lysosome-like organelles (Kaija, 2002). Mice deficient in tartrate resistant acid phosphatase develop mild osteoporosis and overexpression of this phosphatase leads to accelerated bone turnover (Ek-Rylander *et al.* 1994; 1997). Mice with a disrupted gene encoding tartrate resistant acid phosphatase were also found to have disordered inflammatory responses and reduced population of phagocytosing macrophages, implying an important role for tartrate resistant acid phosphatase in the defence mechanisms of macrophages (Kaija, 2002).

The most well known and fully characterised mammalian purple acid phosphatases have been isolated from porcine uterine fluid and bovine spleen. These enzymes have been shown to exist in

two isoforms, containing a binuclear iron centre and existing in two interconvertable states (Ek-Rylander *et al.* 1997) (Table 1).

Table 1. The differences between reduced and oxidised forms of PAP. (Kaija, 2002).

Pink: Mixed-valent Fe (II) – Fe (III) cluster	Purple: Binuclear pair Fe (III) – Fe (III)
Reduced	Oxidised
Electroparamagnetic resonance (EPR) visible	EPR silent
Enzymically active	Enzymatically inactive

Active purple acid phosphatase is also capable of generating reactive oxygen species through Fenton's reaction, where the ferrous ion reacts with H_2O_2 to produce highly destructive hydroxyl radicals (OH^\bullet ; Garret *et al.* 1990) (Fig. 5). If bacterial acid phosphatase were to contain similar iron centres, the production of destructive radical species by phosphatase could serve as a mechanism to enhance virulence in bacteria, possibly as a means of defence (e.g. by absorbing free radicals into the Fe(II)-Fe(III) iron cluster) against the immune response which itself employs macrophageal acid phosphatase for bacterial killing (Räisänen *et al.* 2005; Schenk *et al.* 2008), although the former hypothesis has yet to be proven. In other words, the Fe(II)→Fe(III) interconvertibility could be harnessed to an aggressive or a defensive role. The existence of elevated levels of tartrate resistant acid phosphatases in lysosomes, osteoclasts and macrophages may indicate that the production of free radicals made by the phosphatase may be used to break down or degrade engulfed bacteria in the phagolysosome, to degrade bone products in the osteoclast and as a mechanism for bacterial killing in the macrophage (Kaija, 2002). In *M. tuberculosis* purple acid phosphatase may assist the pathogen's survival by reducing the respiratory burst of its host and/or removing potentially lethal free radicals, as purple acid phosphatase can remove reactive oxygen species in a Fenton like reaction (Schenk *et al.* 2000). This reaction involves hydrogen peroxide (H_2O_2) and a ferrous iron catalyst (iron II salts or the

Fe(II)-Fe(III) centre of the enzyme) and the radicals formed react with many organic molecules.

The reactivity is most likely achieved via the formation of the hydroxyl radical (see below):

In the literature, generally, purple acid phosphatase is used to refer to non-mammalian acid phosphatase and the name tartrate resistant acid phosphatase for corresponding mammalian enzymes. Figure 5 shows the Fenton reaction in relation to a tartrate resistant acid phosphatase and shows two interchangeable states of this enzyme. The following reactions are important for the production of reactive oxygen species (ROS) by tartrate acid phosphatase.

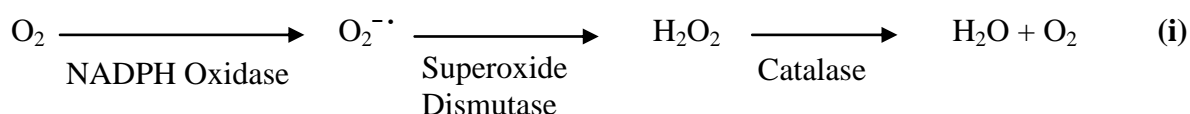


Fig. 5. Fenton reaction involving tartrate acid phosphatase (Kaija, 2002).

Superoxide is generated by the action of NADPH-oxidase on molecular oxygen. Like other metalloproteins (containing a redox-active iron), purple acid phosphatase and tartrate acid phosphatase are able to catalyse the generation of reactive oxygen species. In this example tartrate acid phosphatase absorbs single unpaired electrons from $\text{O}_2^{\cdot-}$ in reaction (ii) (potential defensive function) but can then generate electrons OH^{\cdot} (by donation of an unpaired electron) in reaction (iii) (potential aggressive function). The question can now be asked; do bacterial acid phosphatases have a similar biofunctionality, i.e. the ability to participate in redox reactions as well as in phosphate ester hydrolysis? Another consideration is a potential link between phosphatase and virulence since many pathogenic species of bacteria produce phosphatase and some use this phosphatase, for example, as an aid to gain entry to the host or attack certain cells of the human immune system. *Serratia* does not normally express PhoN phosphatase and it is therefore a possibility that *Serratia* acquired the gene for acid phosphatase production from a

pathogenic species of bacteria in which the phosphatase had a role in virulence (overviewed below).

1.13 Virulence and acid phosphatase

Many prokaryotic, pathogenic organisms have been shown to produce acid phosphatase and purple acid phosphatases, e.g. *Mycobacterium tuberculosis*, *Mycobacterium leprae*, *Salmonella* sp, *Shigella* sp, *Morganella* sp, *Providencia* sp, *Francisella tularensis* as well as the Cyanobacterium *Synechocystis* sp. (Schenk *et al.* 2000). Acid phosphatases purified from, *Legionella micdadei*, *Coxiella burnetti*, *Franciscella* sp. and from the protozoan *Leishmania donovani* have a proven link with pathogenicity (Saha *et al.* 1988; Baca *et al.* 1993; Felts *et al.* 2006; Aguirre-Garcia *et al.* 2000).

Studies have shown that the enzyme may play an integral role in the survival of these pathogens within the host's phagocytic cells (Aguirre-Garcia *et al.* 2000). One hypothesis is that acid phosphatase has a role in virulence by affecting host signaling pathways, for example, by the dephosphorylation of host proteins, inositol phosphates or phosphoinositides, which are critically important for phagosome formation within infected cells. It is also possible that acid phosphatase functions in a phosphate retrieval system that is activated upon phagosomal containment (Felts *et al.* 2006). *Entamoeba histolytica* produces two types of acid phosphatase, a membrane bound form and another form which is actively secreted into the culture medium (Aguirre-Garcia *et al.* 2000). The avirulent strain of *Entamoeba* (*E. dispar*) lacks the secreted form of acid phosphatase but contains the membrane bound form, suggesting that the exported form of the enzyme is involved in virulence and infectivity in this eukaryotic pathogen (Aguirre-Garcia *et al.* 2000). The mechanism of how the enzyme is involved in pathogenicity is still poorly understood although it is thought that this enzyme has a function in respiratory burst-inhibition. Accordingly, research using acid phosphatase purified from the bacterium *Francisella tularensis* showed that the enzyme suppressed the respiratory burst of activated human neutrophils (Reilly *et al.* 1996). There was

also a difference in optimal pH for the membrane bound and secreted acid phosphatase of *E. dispar* (5.5 and 4.5, respectively), suggesting that the secreted enzyme may need to endure the lower pH brought on by the host's immune response and resulting pH drop (Aguirre-Garcia *et al.* 2000). This has interesting connotations for the acid phosphatase produced by *Serratia* sp.; since *Serratia* is not normally pathogenic, it would give credence to the hypothesis that this *Serratia* sp. acquired the gene for acid phosphatase production (in this case via evolutionary pressure for heavy metal resistance) from another pathogen through gene transfer in the environment. Other pathogens producing PhoN acid phosphatase such as *Salmonella* sp, *Providencia* and *Morganella* sp. carry the *phoN* gene. Enterobacteria carrying *phoN* tend to be in the genera that contain pathogenic species, with *Serratia* sp. being the exception. Research into the presence of *phoN* in *Salmonella typhimurium* shows that it is likely that the organism obtained the gene for acid phosphatase through horizontal transfer from a distantly related organism attributable to the presence of DNA sequences with unusual G+C contents; *phoN* has a G+C content of 39 % whilst the overall G+C content of the *Salmonella* chromosome is 52 % (Groisman *et al.* 1992). The G+C ratio of *Serratia marcescens* is higher (59 %) than that of *Salmonella* i.e. the “*phoN*” insert in *Serratia* NCIMB 40259 can be assumed to be a “foreign” gene (Groisman *et al.* 1992) since it has the lower G+C ratio (see below).

1.14 PhoN and virulence

Non specific acid phosphatase is the product of the *phoN* gene in *Salmonella typhimurium*, which is under the transcriptional control of PhoP (a major regulator of virulence loci in *S. typhimurium*). It is interesting to note that the ability to produce acid phosphatase may be associated with virulence and infectivity and that *Serratia* sp. itself is not noted as a pathogen but like some pathogenic species of *Salmonella* and *Morganella* the organism has the enzyme denoted as PhoN (Groisman *et al.* 1993).

It is thought (see above) that *Serratia* sp. obtained the gene that enables it to accumulate metals in the environment by natural gene transfer mechanisms, as a mechanism to survive and become resistant to metal toxicity. However, this is likely to be fortuitous and the true physiological role, possibly rooted in a pathogenicity determinant remains unclear. Therefore it is important to gain an insight into how and why *phoN* is transferred in other organisms with the final aim of understanding where the gene came from and why it should have been passed to a non-pathogenic organism such as a soil *Serratia* sp.

S. typhimurium and *E. coli* have an extensive genetic similarity; however, in the 150 million years since these species diverged (Wain *et al.* 2001), both organisms have accumulated several genetic rearrangements and genetic alterations that have become fixed over this time. The genes that encode the characteristics that distinguish *E. coli* and *S. typhimurium* reside on the chromosomal loops making up these genetic alterations (Groisman *et al.* 1992). However, the ancestries of these differences are unknown. It is hypothesized that some regions unique to one species were acquired by horizontal transfer from a distantly related organism (Kier *et al.* 1979; Groisman *et al.* 1992).

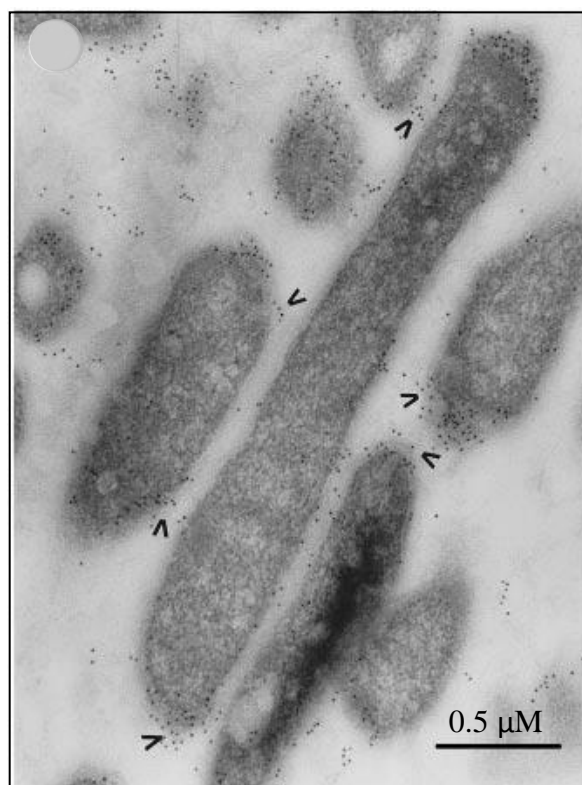
Studies on the genomes of *E.coli* and *S.typhimurium* show that they share extensive regions of homology and are almost superimposable. Pathogenicity islands (for example, inserted genes which contribute to an increase in the organism's virulence) in both organisms often have a

guanine and cytosine (G+C) content different from that of the rest of the chromosome, therefore they have almost certainly been acquired by horizontal transfer from a different bacterial genus (Wain *et al.* 2001). In support of this, Groisman *et al* (1992) noted that the *phoN* DNA from *Salmonella typhimurium* was of a G+C ratio of 39 % which is lower than the overall G+C content of the *S. typhimurium* chromosome, which averages 52 % (Groisman *et al.* 1992; Groisman, 2001). Other evidence shows that the *phoN* coding regions display codon biases which are atypical for *Salmonella* sp. Groisman *et al* (1992), showed that *phoN* preferentially uses the codons; AGA (arginine), CCA (proline), ACA (threonine) and ATA (isoleucine), which occur rarely in the genes of *Salmonella*.

Serratia sp. does not normally contain PhoN and it is possible that this *Serratia* sp. obtained the *phoN* gene (which fortuitously enables accumulation of heavy metals as a likely response to metal-stress; Macaskie & Dean, 1982)) by natural gene transfer mechanisms, (Groisman *et al.* 1992; Macaskie *et al.* 2000). This suggests natural acquisition of a ‘foreign’ gene and its maintenance under selective pressure.

1.15 Study of *Serratia* sp. *phoN* phosphatase to date

The acid phosphatase of *Serratia* sp. was assigned as PhoN on the basis of work by Macaskie *et al.* (1994) which found significant homology of partial amino acid sequences from this acid phosphatase with the PhoN phosphatase of other bacteria. *Serratia* sp. phosphatase has been shown by immunogold labelling (Jeong, 1992; Jeong *et al.* 1997) to exist both in the periplasmic space and tethered to the outside of the cell (on the EPS) (Fig. 6); these two forms are immunologically cross reactive (Jeong, 1992; Jeong *et al.* 1997).



(Macaskie *et al.* 2000)

Fig. 6. Localisation of phosphatase on and around *Serratia* cells shown by immunogold labelling of phosphatase (Jeong *et al.* 1997). The phosphatase enzyme is clearly visible in association with the outer membrane (arrowheads), and exocelluarly (from Macaskie *et al.* 2000).

It is thought that the enzyme is exported to the outside of the cell to the EPS where it cleaves phosphate esters. The enzyme was delineated into two isoforms (designated SP1 and SP2; CPI and CPII by Jeong, 1992) but it is not known if these two isoforms exist in the same location

within the cell or if one or both isoforms are exported to the EPS. Biochemical tests showed that SP1 and SP2 have different characteristics (shown in Table 2). These results show some similarities to purple acid phosphatase (Table 1). The acid phosphatase from *Serratia* sp. which is made up of four subunits (Jeong *et al.* 1998), was found to have a molecular weight of 103 kDa-108 kDa (each subunit having a molecular weight of approximately 27 kDa) and isoelectric points (pI) of approximately 8.9 and 9.1 (for SP1 and SP2, respectively) (Jeong, 1992; Jeong *et al.* 1998).

It is easy to see from Table 2, that one isoform (SP1) is more “desirable” than the other for the remediation of radioactive substances (SP1); however, SP1 has been shown to be less active than SP2. Nevertheless, studies of acid phosphatase activity observed during experiments for the remediation of radioactive metals have shown the enzyme to have a high activity which would imply that the two isoforms exist together in both the periplasmic space and tethered to the EPS, and are not present in separate locations. Alternatively this could mean that the enzyme is simply interchangeable and is produced in one particular isoform depending on the conditions of the internal and external environment of the cell. Unpublished results (H. Pflicke, M. Paterson-Beedle & L.E. Macaskie) showed that unequal amounts of SP1 and SP2 when recombined, re-fractioned into different proportions than the original composition, suggesting an interconvertability of the two forms.

Table 2. Differences between *Serratia* sp. phosphatase SP1 and SP2.

SP1	SP2
Radio-resistant (Jeong, 1992) 50% activity retained after 7.5 h exposure to ^{60}Co at ~400 Gy (Thiol addition does not increase radiostability)	Radio-sensitive (Jeong, 1992) 50% activity retained after 2.5 h exposure to ^{60}Co at ~160 Gy (Thiol addition increases radiostability)
Enzyme less active 68179 units/mg (Jeong, 1992) 33692 units/mg (this study)	Enzyme more active 71051 units/mg (Jeong, 1992) 49931 units/mg (this study)
*Higher affinity (two fold) for glycerol-1-phosphate than SP2 K_m for G1P = 190 ± 59 K_m for G2P = 1963 ± 407	*Higher affinity (two fold) for glycerol-2-phosphate than SP1 K_m for G1P = 354 ± 45 K_m for G2P = 938 ± 42
Negatively charged (retained by anion exchange column) (Jeong, 1992 and this study)	Positively charged (retained by cation exchange column) (Jeong, 1992 and this study)
Isoelectric point: 8.9	Isoelectric point: 9.1
pH optimum = 5.75	pH optimum = 6.25
Differ slightly in their amino acid composition (Appendix 3)	
Slightly more resistant to fluoride 50 % activity retained at 1.8 mM sodium fluoride	Slightly less resistant to fluoride 50 % activity retained at 1.2 mM sodium fluoride
Slightly more resistant to vanadyl sulphate 50 % activity retained at 125 μM vanadyl sulphate	Less resistant to vanadyl sulphate 50 % activity retained at 50 μM vanadyl sulphate

Unless otherwise stated, all results are taken from Jeong (1992).

* Both SP1 and SP2 had a higher affinity for glycerol-1-phosphate than glycerol-2-phosphate, results shown taken from Jeong (1992) data for SP1 and SP2 are significantly different on the basis of analysis of variance and t-test (Jeong, 1992).

The acid phosphatase appears to be up regulated under ‘stress’ (e.g. shift into anaerobiosis and carbon limitation) conditions (Jeong, 1992) similar to those found in host defense mechanisms such as transient anaerobiosis just prior to the free radical burst (Spitznagel, 1983). The low pH of the phagolysosome (due to lactic acid build up) is optimal for the function of the *Serratia* phosphatase enzyme (Table 2), therefore it is important to fully characterise the enzyme to reinforce a possible link with pathogenicity and the survival of the bacterial cell in the phagolysosome and also gain insight into the possible dual roles of AP as both a phosphomonoesterase and as a possible redox active enzyme. Previous work by Jeong (1992) has shown SP1 and SP2 to be isoenzymes of the PhoN acid phosphatase, therefore their existence as two enzymes and two interconvertible forms of each other could simply be due to the need for the fine tuning of cellular metabolism for example.

1.16 Isoenzymes

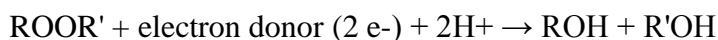
Previous work has shown SP1 and SP2 to be isoenzymes of the PhoN acid phosphatase (Jeong, 1992). “Isoenzymes” or “isozymes” are terms used to describe enzymes that catalyse the same chemical reaction but differ slightly in their amino acid compositions, regulatory properties and their kinetic parameters such as K_m values. It is thought that isoenzymes exist (i.e. multiple forms of the same enzyme in an organism or cell) to allow the fine tuning of metabolism to meet the specific needs of a cell, tissue or developmental stage.

Serratia sp. SP1 and SP2 have slightly different amino acid compositions (Appendix 3) and have different K_m values for glycerol-1-phosphate and glycerol-2-phosphate (see above table). Both isoforms show a higher affinity to glycerol-1-phosphate than to glycerol-2-phosphate, however SP1 has a higher affinity for glycerol-1-phosphate than SP2. Conversely SP2 has a higher affinity for glycerol-2-phosphate than SP1.

Isoenzymes were first described by Hunter & Markert (1957) who defined them as “*different variants of the same enzyme having identical functions and present in the same individual*”. This can mean that the isoenzymes are the product of different genes or enzymes from different alleles of the same gene (often referred to as allozymes). There are many possibilities that may explain the existence of isoenzymes (and therefore SP1 and SP2 in the same organism). Many are the result of polyploidisation or gene duplication and unless mutations occur which prevent the enzyme variant from functioning during evolution then it is likely that the enzyme may have a slightly altered pattern of gene expression or function due to small mutations. Subsequently both forms of the enzyme would be retained by natural selection and become specialised to slightly different functions. Normally isoenzymes are two forms of the same enzyme which catalyse slightly different reactions and therefore carry out slightly different functions. At the most extreme these functions can diverge leaving two separate enzymatic functions derived from a common ancestor. A striking example is phosphatase/peroxidase bifunctionality. This was mentioned earlier but has actually evolved much further. An example is that of the vanadium chloroperoxidase from the fungus *Curvularia inaequalis*, which also exhibits phosphatase activity and, *vice versa*, the vanadate-substituted recombinant acid phosphatase from *Shigella flexneri* (PhoN-Sf) and *Salmonella enteric ser. typhimurium* (PhoN-Se), which exhibit peroxidase activity (Tanaka *et al.* 2002) (overviewed below).

1.17 Peroxidases

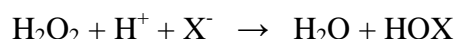
Peroxidases are a group of enzymes which typically catalyse the following reaction:



The optimal substrate for most peroxidases is hydrogen peroxide, however other peroxidases are more active with lipid peroxides or other organic hydroperoxides. From equation (i) in Figure 5 and in this context tartrate resistant acid phosphatase could equally well have apparent peroxidase activity if it removes $\text{O}_2^- \cdot$ and prevents peroxide from forming. This activity in both phosphohydrolase and free radical reactions (above) is what invites a proposed function in pathogenicity (see earlier).

Peroxidases can contain a heme cofactor in their active sites, or redox-active cysteine or selenocysteine residues (Fomenko *et al.* 2007). The heme is a prosthetic group consisting of a large heterocyclic organic ring called a porphyrin which contains an iron atom at its center, however not all porphyrins contain iron.

A class of enzymes which binds vanadate (HVO_4^{2-}) as a prosthetic group (DeBoer *et al.* 1986; Van Schijndel *et al.* 1993) are the vanadium haloperoxidases. They catalyse the oxidation of a halide by H_2O_2 to the corresponding hypohalous acids according to:



The enzymes are named after the most electronegative halide ion they are able to oxidize, therefore chloroperoxidase oxidizes Cl^- , Br^- , I^- and bromoperoxidase oxidizes Br^- and I^- (Tanaka *et al.* 2002).

Peroxidases are also known to play a role in increasing a plant's defences against pathogens, although the exact mechanisms of this remain unknown (Karthikeyan *et al.* 2005).

1.18 Vanadium peroxidases and phosphatases: dual functionalities?

The above suggests clear related functionalities between phosphatases and peroxidases. Accordingly, Hemrika *et al* (1997) showed that the amino acid residues contributing to the active sites of the vanadate-containing haloperoxidases are conserved within three families of acid phosphatases. This suggests that the active sites of these enzymes are similar and furthermore, the vanadium chloroperoxidase from the fungus *Curvularia inaequalis* exhibits phosphatase activity (Renirie *et al.* 2000). This is very interesting as the phosphatases from *Serratia* sp. (SP1 and SP2) are strongly inhibited by vanadyl sulphate (Jeong, 1992), which may suggest that the HVO_4^{2-} species may act as a 'surrogate' for the 'leaving group' HPO_4^{2-} (i.e. V(V) as compared to P(V)) but in the case of V(V) remain tightly bound. In this context it has also been shown that vanadium haloperoxidases and the bacterial class A non specific acid phosphatases have a conserved active site (Hemrika *et al.* 1997). The classification system for non specific acid phosphatases proposed by Rossolini *et al* (1998) shows that *Serratia* sp. phosphatase fits into class A, although this 'Class A' is further subdivided into A1, A2 and A3; further comparison will be facilitated by completion of further tests with the phosphatase. Vanadate-substituted recombinant acid phosphatase from *Shigella flexneri* (PhoN-Sf) and *Salmonella enterica* ser. typhimurium (PhoN-Se) have been shown to oxidise bromide to hypobromous acid in the presence of H_2O_2 , and vanadate is essential for this activity (Tanaka *et al.* 2002). The active site structure of acid phosphatase from *Escherichia blattae* also shows remarkable similarity to the vanadium-chloroperoxidase from *C. inaequalis* (Tanaka *et al.* 2002). Sulfate co-crystallises with the active site of the phosphatase in the same way as vanadium in the active site of the vanadium chloroperoxidase (Tanaka *et al.* 2002). The similarity between the enzymes from the organisms noted above indicates that the vanadium-containing haloperoxidases and this group of phosphatases may have divergently evolved from a common ancestor (Hemrika *et al.* 1997). The concept of an enzyme with a dual historic role in both hydrolytic (phosphatase) and redox (peroxidase) functions is a critical

consideration to an underlying hypothesis of this thesis where both phosphohydrolytic (phosphate-generating) and free radical (redox) effects are key to its continued function in a radiotoxic system.

1.19 The nature of the redox active group

1.19.1 Redox active cysteine

In addition to Fe(III)-Fe(II) (see above) cysteine is present in many enzymes not only to serve an important structural role but also to serve a redox function. Many enzymes contain metals to carry out redox reactions (Belle & Pierre, 2003), however redox active cysteine can be found in many different enzymes such as peroxidases in place of metal(s) (Giles *et al.* 2003). The side chain on cysteine is thiol, which often participates in enzymatic reactions, serving as a nucleophile (a reagent that forms a chemical bond to its reaction partner by the donation of both its bonding electrons). The thiol is susceptible to oxidation to give the disulfide derivative cystine, which serves an important structural role in many proteins. The thiol group on the cysteine is nucleophilic and therefore it is easily oxidised. Cysteine-based phosphatases also include the protein tyrosine phosphatases, dual-specificity phosphatases and low-molecular-weight protein tyrosine phosphatases, all of which contain a nucleophilic catalytic cysteine which enable these enzymes to dephosphorylate phosphoproteins or phospholipids (Salmeen & Barford, 2005).

In addition to enabling phosphatase activity, the nucleophilic catalytic cysteines of cysteine based phosphatases are highly susceptible to oxidation, which allows redox regulation of this enzyme family. Until now the accumulation of reactive oxygen species in cells (other than phagocytic cells) has been considered an unwanted and harmful by-product of oxidative phosphorylation, ionising radiation and lipid metabolism. However in recent years a new role for reactive species has emerged as they have been shown to be capable of changing the structure and

function of proteins in specific ways, therefore providing a way to regulate an array of cellular processes including gene expression and signal transduction pathways (Barford, 2004). The molecular mechanisms which aid the stabilisation of a reversible oxidised form of catalytic cysteine are the formation of disulfide bonds of a sulfenamide bond and formation of either of these (covalent) bonds promotes large structural rearrangements which subsequently affect signalling and enzyme regulation (Barford, 2004).

Protein structures have been elucidated by various methods such as NMR and X-ray crystallography. In the present case the precise protein structure and relationship of this to the redox state of the enzyme are of paramount importance in the light of the above discussion. Early studies showed that an actively growing culture of *Serratia* can ‘switch off’ its phosphatase activity within a few minutes (much too rapidly for dilution-out by cell growth: L.E. Macaskie, unpublished) while a highly active preparation can lose all activity spontaneously (K.M. Bonthron & L.E. Macaskie, unpublished). These observations, taken together with the above, and of the interconvertability of SP1 and SP2 (see earlier) suggest that it may be possible to ‘steer’ the enzyme into the more radioresistant form (SP1: see Table 2) since redox reactions and radiostress are united by their root in free radical associated processes. This ‘steerage’ and understanding of the mechanism by which this can be achieved, is a goal of this work. Towards this aim, this study encompassed several objectives as stated below.

1.20 Objectives of the work

The overall objective of this project is to develop a novel non toxic and portable process for the remediation of nuclear wastes, wash waters and potable water contaminated by a hypothetical radio-terrorist incident.

The first sub-objective is to gain insight into the nature of the mediating phosphatase in order to predict or steer its efficacy in solutions which may contain a high concentration of radiotoxic elements.

The second sub-objective is to show application of the remediation system against surrogates of the fission and activation products ^{90}Sr and ^{60}Co .

2 Chapter 2 Materials and Methods

2.1 General Methods

2.1.1 Organism

Serratia sp. (NCIMB 40259) isolated from metal polluted soil originally and designated as a *Citrobacter* sp. by commercial analysis (Macaskie & Dean, 1982) was used under license from Isis Innovation, Oxford, UK. Batch growth of *Serratia* sp. was carried out in the pilot plant at the University of Birmingham, school of Biochemical Engineering by previous workers. Large-scale batch cultures (600 L) were grown in a pilot plant based on an LSL Biolafitte bioreactor with a total volume of 800 L as described previously by Macaskie *et al* (1995). The culture was chilled using cold water, harvested using a continuous flow centrifuge (Sharples) and stored as blocks (0.5-1 kg) of wet biomass pellet at -70 °C. These blocks were the starting material for the preparation of enzyme described in this project.

2.1.1.1 Maintenance and storage of microorganisms

For use in the short term *Serratia* sp. was maintained on solidified nutrient agar and was sub-cultured regularly. Plates containing *Serratia* were stored at 4 °C.

2.1.2 Chemicals

General laboratory reagents were purchased from Sigma-Aldrich (UK) unless otherwise stated in the text. All resins and chromatography media used for the purification of phosphatases were purchased from GE Healthcare (UK).

2.1.3 Media

2.1.3.1 Minimal medium

Serratia sp. was grown in minimal medium as follows: Tris (12 g/l), and KCl (0.62 g/l), were added to deionised water, the pH was then lowered to 7.2 with HCl (1 M), $(\text{NH}_4)_2\text{SO}_4$ (0.96 g/l), glycerol-2-phosphate (0.67 g/L), $\text{MgSO}_4 \cdot 7\text{H}_2\text{O}$ (0.063 g/l) and $\text{FeSO}_4 \cdot 7\text{H}_2\text{O}$ (0.32 mg/l) were then added (final concentrations) and the pH was adjusted again to pH 7.2 with HCl (1 M).

For smaller cultures (1 L) the solution was made up to 980 ml (for 1 L cultures) and then sterilized at 121 °C for 20 mins. Lactose (0.6 g/l, for carbon limiting conditions) was sterilised separately at 121 °C for 20 mins and added aseptically to the minimal medium once it had cooled.

2.1.4 Protein measurement

Protein concentration was determined by the method of Bradford (1976) for soluble proteins using bovine serum albumin as the standard (Appendix 1).

2.1.5 Assay of phosphatase activity

Phosphatase activity was determined by measuring the liberation of p-nitrophenol (pNP) from p-nitrophenol-phosphate (pNPP) (disodium salt) by a modification of the method as described by Bolton and Dean (1972) (Appendix 2). One unit of enzyme activity is defined as the amount of enzyme liberating one nmole p-Nitrophenyl (pNP) per min, using a molar extinction coefficient of 17,874/cm/M for pNP (Appendix 2).

2.1.6 Polyacrylamide gel electrophoresis

Electrophoresis of proteins was performed according to the method of Laemmli (1970). All gels and chemicals were from Invitrogen (UK) unless otherwise stated. Sodium dodecyl sulphate-PAGE used pre-cast NuPAGE Novex Bis-Tris mini gels with MOPS SDS running buffer (pH 7.0) at 200 V for 50 mins. The molecular weight of the phosphatase was estimated using NOVEX Mark12 unstained molecular weight standards; gels were stained with Coomassie blue (G-250).

Protein samples for electrophoresis were heated in a heat block at 70 °C for 10 mins. Electrophoresis in the mini-gels (above) was started at 190 V. When the dye front reached the bottom of the gel, the power was turned off and the gel removed. Gels were stained with coomassie brilliant blue (G-250) (0.1 %) in water: methanol: glacial acetic acid (5:5:2 by volume respectively) at room temperature for 20 mins. Destaining was carried out with water: methanol: acetic acid (8:1:1 by volume respectively). The molecular weight of the phosphatase was estimated using NOVEX Mark12 unstained molecular weight standards, gels were stained with Coomassie blue (G-250).

2.2 Phosphatase purification

All steps were carried out at 4 °C unless otherwise stated. *Serratia* sp. cells were suspended in buffer A (Tris 20 mM, pH 8.0) to give a final concentration of 0.2 g wet weight cells/ml. The suspended cells were disrupted by two passages through a French pressure cell at 18,000 psi. Cellular debris and unbroken cells were removed by centrifugation (55,000 g, 1 h). Membrane fractions were then removed by ultracentrifugation (180,000 g, 2 h). The resulting supernatant was brought to 35 % ammonium sulphate saturation, stirred for 10 mins and allowed to stand for 20 min at room temperature. The solution was centrifuged (55,000 g, 20 min) and the resulting pellet stored at -80 °C, the supernatant was brought to 60 % ammonium sulphate saturation, stirred for 30 mins and allowed to stand for 1 h at room temperature. The supernatant was discarded and the pellet was stored at -80 °C until needed. The pellets from 35 % and 60 % ammonium sulphate fractionations were allowed to defrost and then desalted using buffer A (above) using vivaspin 20 centrifugal concentrators (Fisher Scientific) with a molecular weight cut off of 10 kDa. The desalted enzyme solution (4.5 ml) was then applied to a Hitrap Q anion exchange column (5 ml) pre-equilibrated with buffer A at a flow rate of 2.5 ml/min. SP2 was then eluted in the flow through. SP1 was eluted with a 0 M-0.3 M linear sodium chloride gradient. Active fractions of SP1 and SP2 were pooled separately and concentrated to 0.5 ml before loading onto sepharose 18/30 gel filtration column pre-equilibrated with buffer B (Tris 20 mM, NaCl 0.15 M, pH 8.0) at a flow rate 0.5 ml/min, SP2 and SP1 were loaded separately. Both SP2 and SP1 were observed as a single peaks; their purity was confirmed by SDS-PAGE. Enzymatic activity in fractions other than those showing the highest activities were considered to be contaminated and therefore were not pooled for further purification. The detailed development of this purification scheme is detailed in chapter 4.

2.3 Effects of various compounds on *Serratia* sp. phosphatase

Phosphatase activity was tested in the presence and absence of each of the indicated substances (chapter 5 and 6). All effector substances tested on the acid phosphatase were (unless otherwise stated in the text) dissolved in dH₂O prior to testing. The pH of each effector substance was tested for its effect on the pH of the assay prior to its use as an effector substance. Phosphatase was tested in the presence and absence of: L-(+)-Sodium tartrate, EDTA, H₂O₂ and β-mercaptoethanol (as described in chapters 5 and 6). All effector substances with the exception of EDTA, were incubated at 30 °C for 15 mins with *Serratia* sp. phosphatase (0.2 µg in 40mM MOPS-NaOH, pH 7.0, unless otherwise stated), prior to the addition of pNPP. EDTA was incubated with phosphatase for 24 h prior to the addition of pNPP to allow metal chelation to take place. The activity was expressed as a percentage of that observed without effector substance.

2.4 Deoxyribose method for assessment of free radical damage

The acid phosphatase was tested for its ability to ameliorate or potentiate the effect of free radical attack on deoxyribose. The assay was carried out according to the method of Halliwell *et al* (1987). The sugar deoxyribose is sensitive to attack by free radicals; under such an attack from radical species such as O₂⁻ and OH⁻, products such as malonaldehyde are formed. When warmed with thiobarbituric acid these products produce a red compound with an absorbance maximum at 532 nm. Any substance which can either inhibit the production of free radicals or de-toxify them will slow the production of these products and therefore reduce or prevent damage to deoxyribose, alternatively a potentiating agent will accelerate this damage. The reaction mixture contained: Phosphatase (variable concentration, 0-8 nM), deoxyribose (5 mM), KH₂PO₄ buffer (20 mM, pH 7.4), FeCl₃ (100 µM), EDTA (104 µM), H₂O₂ (1 mM) and ascorbate (1 µM) in a final volume of 1 ml. The reaction mixture was incubated at 37 °C for 1 h. 2-thiobarbituric acid solution 1 ml (1 %

w/v in 0.05 M NaOH) was added after the incubation time of 1 h, followed by 1 ml glacial acetic acid. The solution was then heated at 100 °C for 10 mins, cooled and the absorbance was measured at 532 nm. Controls used in the experiment were ethanol and heat denatured phosphatase. Ethanol is a known scavenger of free radicals and a rate constant has been calculated and published (Halliwell *et al.*, 1987) as $1.47 \times 10^9 \text{ M}^{-1} \text{ S}^{-1}$. As a positive control, ethanol (varying concentration, 0-20 mM) was used in the same experiment above, replacing phosphatase in the reaction mixture. Denatured phosphatase was also used as a control. Phosphatase was denatured by heating at 100 °C for 10 mins and the activity was checked to be absent by assay. The denatured enzyme was then used at a variable concentration (0-8 nM) in the experiment above in place of the active enzyme. The equation for determination of the rate constant can be seen in Appendix 4.

2.5 Matrix assisted laser desorption ionisation-time of flight (MALDI-ToF) mass spectrometry of *Serratia* sp. phosphatase

A sample of purified phosphatase (purity was confirmed by a single band on SDS-PAGE) suspended in ultra pure water at a concentration of 1 mg/ml, was subjected to MALDI-ToF to confirm molecular weight, using a Bruker biflex IV mass spectrometer. The sample (approx 10-20 pmol) was embedded in a matrix of sinapinic acid (10 mg/ml in 50:50 CH₃CN/0.1 % TFA) and irradiated at 337 nm utilising a nitrogen laser. Data acquisition and processing were done using Bruker flexControl and flexAnalysis software and carried out by Mr Peter Ashton (School of Chemistry, University of Birmingham).

2.5.1 Analysis of SP1 and SP2 by mass spectrometry

Serratia sp. phosphatase (SP1 and SP2) was loaded onto SDS-PAGE gel as above; approximately 200 µg of each isoform was separated on the gel. Phosphatase gel bands were excised using a sterile scalpel (cutting a section of gel no greater than 0.5 cm x 0.15 cm) which was then further sliced into five equally sized pieces. Extended methodology can be seen in Appendix 5.

2.5.2 Destaining, digestion, peptide extraction and data dependent analysis (DDA)

All processing of the gel plugs was done by Mrs Susan Slade at the University of Warwick (Biological Mass Spectrometry and Proteomics department) using a MassPrep robotic protein handling system (Waters Micromass) using the manufacturer's protocol, described briefly below. Extended methodology can be seen in Appendix 5.

Gel plug(s) were destained twice using acetonitrile (50 %) in ammonium bicarbonate (100 mM), rinsed with acetonitrile then allowed to dry in air for 10 mins and reduced with dithiothreitol (10 mM) in ammonium bicarbonate (100 mM) for 30 mins followed by alkylation with iodoacetamide

(55 mM) in ammonium bicarbonate (100 mM). The gel plugs were then rinsed with acetonitrile (50 %) in ammonium bicarbonate (100 mM) followed by a further three washes with acetonitrile. An aliquot of trypsin (25 μ l of 6 ng μ l⁻¹) was added to each sample and incubated at 37 °C for 4.5 h. The resulting peptides were initially extracted using an aqueous solution (30 μ l) containing acetonitrile (2 %) and formic acid (1 %). A second extraction using an aqueous solution (15 μ l) containing acetonitrile (51 %) and formic acid (0.5 %) was done and combined with the first extraction in a cooled second 96-well plate and if necessary, samples were stored at -80 °C prior to analysis by mass spectrometry.

2.5.3 Peptide separation by in-line liquid chromatography and electrospray ionisation mass spectrometry (detection of phosphorylated peptides)

Extracted tryptic peptides (section 3.5.2) were resolved using an in-line NanoAcquity LC and autosampler system. An aliquot (4.9 μ l) of each sample was loaded onto a nanoACQUITY UPLC™ trapping column (10 kpsi symmetry C18 180 μ m x 20 mm 5 μ m (Waters)) equilibrated in aqueous acetonitrile (1 %) containing formic acid (0.1 %) and the column was flushed at 15 μ l/min for 1 min to waste. The peptides were then eluted onto a nanoACQUITY UPLC BEH C18 Column (1.7 μ m, 100 μ m x 100 mm, 10 kpsi column (Waters)) at 1.2 μ l/min using the linear gradient described in Appendix 5.

The eluted peptides were analysed on a Waters Micromass Q-ToF Global Ultima mass spectrometer fitted with a nano-LC emitter (New Objective) with an applied capillary voltage of 3-4 kV. The instrument was operated in ESI-MS positive ion mode over the mass/charge (m/z) range 300-2000 using a 0.6 s⁻¹ scan time, using a neutral loss driven acquisition. On alternate MS scans the energy applied to the collision cell was either 10 eV or a stepped energy of 25 eV rising

to 35 eV 300 ms into the scan. Real time data selection was used to identify any H_3PO_4 neutral loss events during the analysis, which would then trigger an MS/MS acquisition.

A calibration was performed using a collisionally induced decomposition (CID) spectrum of the doubly charged precursor ion of [glu¹]-fibrinopeptide B. A calibration was accepted when the average error obtained on a subsequent acquisition was <10 ppm. Sensitivity was assessed by an injection of 50 fmol of a phosphorylase B tryptic digest on column giving a base peak intensity >1000 counts s⁻¹ in MS mode on the most intense peptide.

2.6 Elemental analysis of acid phosphatase by micro PIXE analysis

To identify and quantify the metals present in the phosphatase, micro PIXE analysis was used (at the Surrey ion beam centre). The phosphatase protein was concentrated to 20 mg/ml and suspended in ultrapure water. For analysis, 1 µl of each enzyme was pipetted separately onto 4 µm thick “Prolene” polypropylene film and allowed to dry. The resulting drying residues were analysed on using micro Proton Induced X-ray Emission (PIXE) and Rutherford Backscattering Spectrometry (RBS) in the Surrey Microbeam Facility at the University of Surrey.

Elemental maps were created by focussing the microbeam line (4x4µm beam, beam energy: 2.5MeV; Ion: H⁺) on a small part of the dried protein sample. The sulphur rich component of the ring was used as a marker for the protein. Three points on the sulphur rich area were analysed for each sample. Each point analysis was collected for approximately 30 mins to increase sensitivity. Prior to sample analysis a run was carried out on a Pb glass standard to determine the calibration parameters for the detector (distance and effective filter thickness) and to eliminate the possibility of detection of other contaminant metals in the detector.

Analyses were also made in areas outside the protein ring to allow quantification of background ions. Since Ca²⁺ was a ubiquitous low level contaminant and is not a known component of proteins, elemental analyses were referenced to the Ca background as an elemental ratio since

absolute elemental concentrations could not be determined since the exact sample depth at each point was not known. Raw data were converted into elemental concentrations using in-house references and software.

2.7 Spectrophotometric analysis of metals and phosphate

2.7.1 Spectrophotometric analysis of zirconium

A method was developed, similar to that described by Yong *et al.* (1996), for the determination of Zr(IV), using arsenazo III. Onishi (1989) showed that Zr can be determined with Arsenazo III in acidic conditions (9 M HCl). Zr sample or standard ($\text{ZrOCl}_2 \cdot 8\text{H}_2\text{O}$) (30 μl , 1-10 μg) was added to a cuvette (1.5 ml) followed by HCl (1.97 ml, 9 M) and finally arsenazo III (supplied by Fluka, UK) 15 % (w/v aq) (100 μl). The solution was mixed and the absorbance was measured at 665 nm.

2.7.2 Spectrophotometric analyses of cobalt and strontium.

The Co^{2+} contents were estimated using the method described by Onishi (1986), with a slight modification. The sample or standard ($\text{Co}(\text{NO}_3)_2 \cdot 6\text{H}_2\text{O}$) containing Co^{2+} (30 μl , 1-10 μg) was transferred to a test tube, citric acid solution (0.2 M, 250 μl) and phosphate-boric acid buffer (6.2 g of boric acid, 35.6 g of disodium phosphate anhydrous, and 500 ml of 1 M sodium hydroxide in a total volume of 1 l, 300 μl) were added. The pH of the solution should be close to 8.0. Nitroso-R salt (supplied by Fluka, UK) solution (0.2 %, wt/vol aq 125 μl) was added while stirring. The test tubes containing the samples were covered, transferred to a block heater at 100 °C and left for 1 min. Concentrated HNO_3 (250 μl) was added and the samples left for a further 1 min at 100 °C.

Samples were cooled in the dark and then deionised water was added (325 µl). The transmittance of the solution was measured at 420 nm.

A method was developed, similar to that described by Yong *et al.* (1996), for the determination of strontium, using arsenazo III. Michaylova & Kouleva (1974) showed that the complex formation of strontium with arsenazo III is maximum at pH 9-10. To each cuvette containing sample or standard ($\text{Sr}(\text{NO}_3)_2$) (30 µl, 1-7 µg), 1.97 ml of 0.1 M borate buffer, pH 9.0 was added. Strontium was visualised by the addition of 0.1 ml of 0.15 % (w/v) arsenazo III, with estimation of the blue-violet complex at 649 nm. The blue-violet complex develops in 25 min (Michaylova & Kouleva, 1974).

2.7.3 Spectrophotometric analysis of phosphate

Analysis of phosphate used a stock solution of stannous chloride (1.5 g in 2.5 ml HCL) diluted just before use (0.25 ml of stock solution in 100 ml HCl 1 M). Sodium molybdate solution comprised (2.5 % w/v in 1.67 M H_2SO_4). Sample containing phosphate (20 µl), deionised water (1 ml), sodium molybdate solution (0.6 ml) and stannous chloride solution (0.4 ml) were transferred to a cuvette. The solution was mixed and equilibrated for 20 mins; absorbance was measured at 720 nm.

2.8 Biomineralisation experiments

2.8.1 2.5 L reactor growth of *Serratia* sp. biofilm

Serratia sp. biofilm was grown in an air-lift fermenter containing polyurethane foam (Filtren TM30) cubes (1 cm^3) (Fig. 7.a) and discs (diameter = 2 cm and height = 0.5 cm, 1.57 cm^3) (Fig. 7.b) (supplied by Recticel, Belgium).

The biofilm was grown in a carbon-limiting continuous culture (air lift fermenter; Finlay *et al.*, 1999, Paterson-Beedle & Macaskie, 2004). Polyurethane foam cubes and foam discs were sewn into strings using cotton and hung inside the vessel (Fig. 8.a.b and c).

Minimal medium (section 2.1.3.1; containing 0.6 g/l lactose) was added, *Serratia* sp. culture (100 ml) pre-grown in the same medium, was used to inoculate the reactor and left in batch mode for 24 h (Paterson-Beedle & Macaskie, 2004). The medium was then pumped continuously for 6 days (flow rate, ca. 210 ml/h). Temperature, pH and phosphatase activity were measured daily from the fermenter outflow. Strings containing polyurethane foam with biofilm were removed from the vessel after 6 days and stored until required at 4 °C, in a cylinder (2 L) over ca. 200 ml isotonic saline (8.5 mg NaCl/L) to maintain a humid environment. For column experiments using biofilms *Serratia* sp. was initially grown on foam cubes as above, however due to channelling of solutions in the flow through biofilm reactors when foam cubes were used (as shown by magnetic resonance imaging; Graf von der Schulenberg *et al.* 2008) the system was changed to use stacked foam discs to overcome this problem (Fig. 9.c and d).

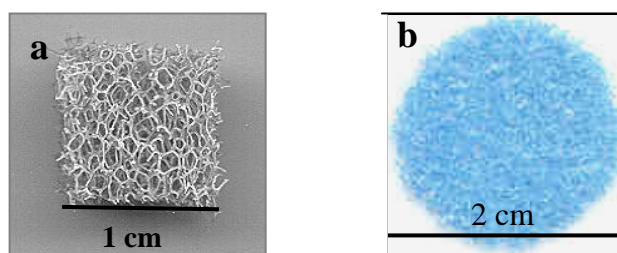


Fig. 7. Polyurethane foam cube and disc: a) foam cube without *Serratia* sp. biofilm b), foam disc, without biofilm.

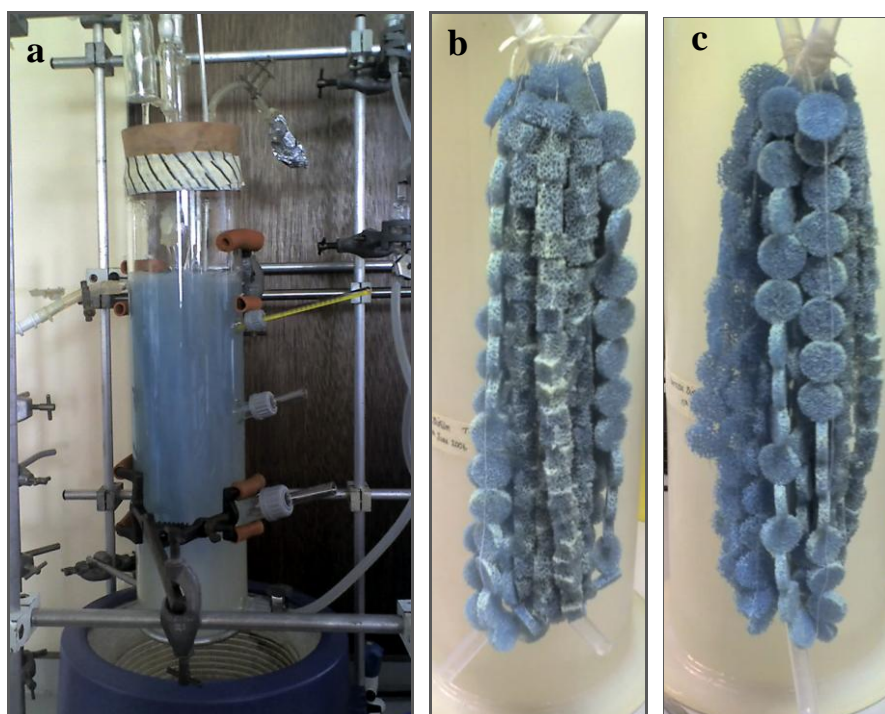


Fig 8. a) Air-lift fermenter in operation. b) View of foam discs and foam cubes after the fermentation, coated in *Serratia* sp. biofilm. c) View of foam discs with *Serratia* sp. biofilm.

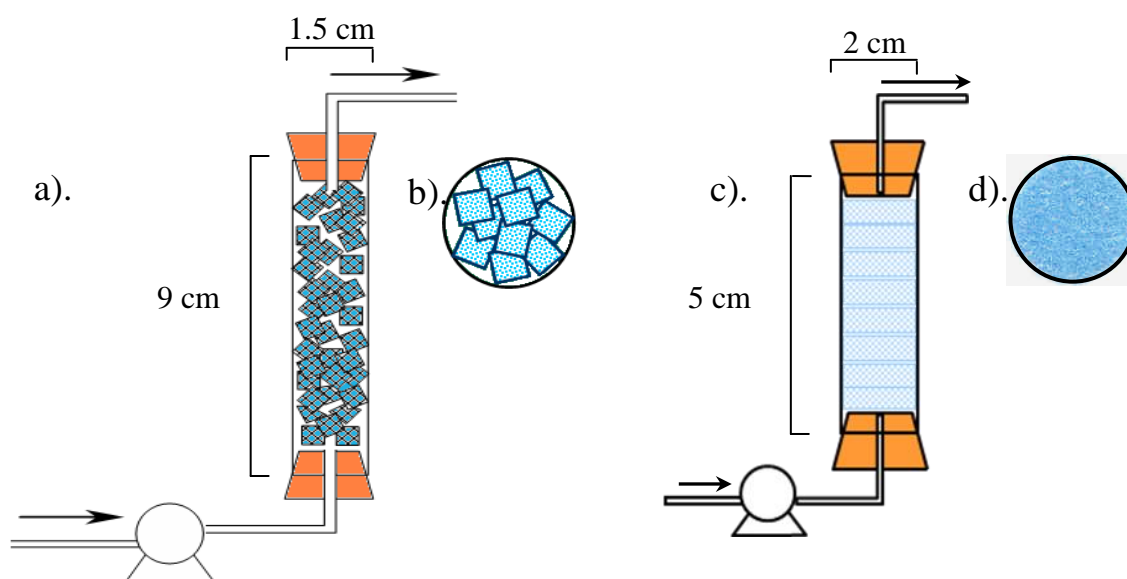


Fig. 9. Set-up of reactors containing *Serratia* sp. biofilm for biomineralisation and formation of metal phosphates. a). Reactor containing polyurethane foam cubes. b). Cross section through the reactor showing how channelling was seen to occur by MRI: Graf von der Schulenberg *et al.* 2008). c). Reactor containing polyurethane foam discs. d). Cross section through reactor showing how channelling is minimised.

2.8.2 Biomineralisation of zirconium by *Serratia* sp. continuous process

A system similar to that used for production of hydrogen uranyl phosphate (Paterson-Beedle *et al.* 2006) was used for the biomineralisation of Zr. Two packing systems were used for bioaccumulation of Zr onto biofilm immobilised onto polyurethane foam: (1) quartered cubes (88 *per* reactor, 0.125 cm³) packed in cylindrical glass columns (length 9 cm and internal diameter 1.5 cm) (Fig. 7.a, Fig. 9.a and b) and (2) discs (8 *per* reactor, 1.57 cm³) stacked in cylindrical glass columns (length 5 cm and internal diameter 2 cm) (Fig. 7.b, Fig. 9.c and d), the use of foam cubes caused channelling of solution in reactors (Fig. 9. b) and when dealing with pM amounts of radioactive material in the inflow solution, this reactor was not fully effective (M. Paterson-Beedle, unpublished). The use of foam discs eliminated this problem. In the latter system, filter paper (Whatman, qualitative, diameter ca. 2 cm) was fitted on top of the stack of foam discs to retain the precipitate formed within the reactor. Packed-bed reactors containing *Serratia* sp. biofilm immobilised onto polyurethane foam (cubes, 125 mm³, or cylinders, 1.57 cm³) were set up as seen in Fig. 9. Preliminary experiments involving the biomineralisation of Zr onto *Serratia* biofilm aimed to identify the optimum pH for maximum retention and biomineralisation of Zr. The process was tested at pH 4, 5 and 6 (see below). Results showed that the optimum pH was pH 5.0, therefore pH 5.0 was used in all further Zr experiments.

2.8.3 Biomineralisation experiments with Zr (continuous process)

Reactors with packing system (1) were exposed to a continuous upward flow (ca. 7.8 ml h⁻¹, 60 h) via an external peristaltic pump (Watson –Marlow, 323) of:

1. ZrOCl₂.8H₂O (1 mM), glycerol-2-phosphate (5 mM) and citrate (3 mM) pH 5.
2. ZrOCl₂.8H₂O (1 mM) and glycerol-2-phosphate (5 mM), pH 5.

Reactors with packing system (2) were exposed to a continuous flow (ca. 8.2 ml h⁻¹, 66 h) of:

3. ZrOCl₂.8H₂O (1 mM) G2P (5 mM) pH 5.
4. ZrOCl₂.8H₂O (1 mM) G2P (5 mM) and ethanol (5 M), pH 5 (*for 10 days).

The outflow solutions were analysed for Zr and P. Zr was analysed immediately after sampling, however, samples were stored at 4 °C prior to P analysis. Preliminary tests were carried out to measure the effect of biosorption of Zr so that any retention above this value could be attributed to biomineralisation by *Serratia* biofilm. Therefore, columns as seen in (Fig. 9.a) containing killed *Serratia* biofilm were challenged with solutions of Zr and G2P, the results of which can be seen in Appendix 7.

2.8.4 Biomineralisation of zirconium by *Serratia* sp. (batch process)

Biofilm-coated polyurethane foam (8 discs) was transferred to an Erlenmeyer flask containing ethanol (5 M). Cells were dosed daily, over 11 days, with G2P and ZrOCl₂.8H₂O in ethanol (5 M) to give a daily additional concentration of 5 mM and 1 mM respectively (pH 6) (Fig. 10). After 11 days the foam cylinders were removed and the residual contents of the flask were centrifuged for 10 mins at 2700 g to give a gel-like material. This was weighed (wet weight) and stored at 4 °C prior to use in experiments involving the removal of Co and Sr. The moisture

content of the gel-like ZrP materials were determined by drying the samples in an oven for 48 h at 60 °C.

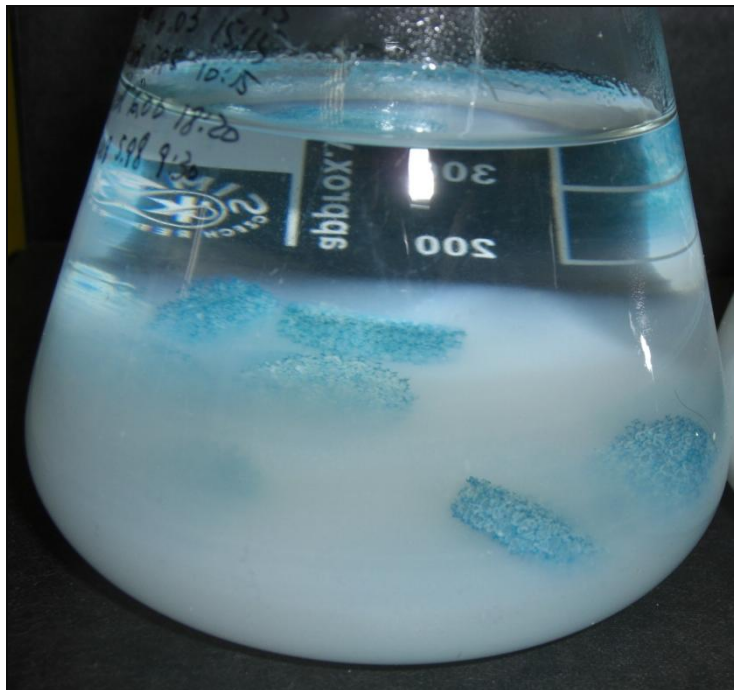


Fig. 10. Erlenmeyer flask containing biofilm coated polyurethane foam discs and biogenic ZrP gel.



Fig. 11. Hydrothermal bomb.

2.8.5 Chemical production of α -Zr(HPO₄)₂ reference material

α -ZrP was produced chemically by J.R Readman (school of Chemistry, University of Birmingham) using a method described by Trobajo *et al* (2000). Crude semi-crystalline ZrOCl₂/HCl suspension (215 ml) was added dropwise to H₃PO₄ (1.25 M, 200 ml) with stirring. The resulting precipitate was left for 24 h at room temperature without stirring and then washed with H₃PO₄ (0.3 M). This crystalline product was formed by taking crude ZrP (10 g) and H₃PO₄ (12 M, 25 ml). The mixture was placed in a hydrothermal bomb (Fig. 11) (45 ml capacity) and heated in an oven at 150 °C for 4 days. The resulting product was washed with H₃PO₄ (0.3 M), centrifuged (4,000 rpm for 10 mins) and dried at ambient temperature and its identity was checked by X-ray powder diffraction and was in agreement with the literature for α -Zr(HPO₄)₂.

2.9 X-ray diffraction analysis

X-ray diffraction analysis (XRD) of chemically synthesised and biomineralised zirconium phosphate was carried out at the school of Chemistry, University of Birmingham. (Chapter 3).

2.9.1 X-ray powder diffraction (XRD) analysis of biogenic ZrP on biofilm

Chemically synthesized α -ZrP (powder form) was analysed using XRD without further preparation. Biogenic ZrP samples for XRD analysis were prepared by removing ZrP loaded foam discs from reactors into universal bottles (25 ml) adding deionised water and squeezing the foam to remove bound ZrP. Detached ZrP material was separated, settled under gravity, washed with deionised water a further three times and left to dry at room temperature before analysis via XRD. For analysis, the ZrP was put onto magic tape and examined using a D5000 Siemens diffractometer in transmission mode.

3 Chapter 3

Accumulation of zirconium phosphate by *Serratia* sp.: A benign system for the removal of radionuclides from aqueous flows

The following chapter contains a paper which has been accepted for publication in Biotechnology Letters. The purpose of this chapter was to show the feasibility of biomineralisation of zirconium phosphate and the ability of biogenic ZrP to remove Co^{2+} and Sr^{2+} from solution.

In this paper I used biofilm material which I and Dr M. Paterson-Beedle prepared and I acquired data shown in figure 1.

I also authored the paper with input and editing by the co-authors.

The calculations and comparisons shown in Tables 1 and 2 were authored by Dr M. Paterson-Beedle. I compiled data for table 3 with Dr M. Paterson-Beedle.

Accumulation of zirconium phosphate by a *Serratia* sp.: A benign system for the removal of radionuclides from aqueous flows

Claire Mennan, Marion Paterson-Beedle and Lynne E Macaskie*

School of Biosciences, University of Birmingham, Edgbaston, Birmingham, B15 2TT, UK

*Author for correspondence Fax: +44 (0)121 414 5925; E-mail: l.e.macaskie@bham.ac.uk

Keywords Biofilm, Biomineralisation, Cobalt, *Serratia*, Strontium, Zirconium

Abstract

Metal phosphate deposited enzymatically on *Serratia* sp. has been used successfully for the removal of radionuclides from aqueous flows. Previous studies using biogenic hydrogen uranyl phosphate (HUP) on *Serratia* sp. biofilm showed removal of 100 % of ^{90}Sr , ^{137}Cs , and ^{60}Co via their intercalation into biogenic HUP crystals. Zirconium phosphates (ZrP) offer a potential non-toxic and non-radioactive alternative to HUP for water decontamination. A method was developed for biomanufacturing ZrP. Biogenic ZrP removed ca. 100 % of Sr^{2+} and Co^{2+} (0.5 mM) from solutions to a molar ratio at saturation of ca. 1:0.6 for both Zr:Sr and Zr:Co. The potential for drinking water decontamination via bio-ZrP is discussed with respect to bio-HUP and also other commercially available materials.

Introduction

Nuclear power is enjoying a resurgence since its widespread implementation would reduce atmospheric release of ‘greenhouse gases’; however, public embracement of nuclear technology is still limited by the perceived risks of environmental contamination and the need for effective waste treatment.

Radioactive wastes are of concern as they have no practical purpose and present a threat to the environment through accidental release, improper storage and potential terrorism, such as a “dirty bomb”. Ion exchange methodology used in the chemical, nuclear and waste water treatment industries is highly efficient when compared to equivalent chemical technologies but can be expensive (Stylianou et al. 2007). Biological-based processes could present a viable alternative; however, a bioremediation system should be sufficiently robust to withstand radiation damage and also minimize remobilization of entrapped radionuclides over time. A pioneering approach used a biological system to make hydrogen uranyl phosphate (HUP) which was used as a stable ‘host’ mineral matrix to capture and hold target metals such as ^{60}Co , ^{90}Sr and ^{137}Cs through intercalative ion exchange (Paterson-Beedle et al 2006).

Biogenic HUP is made using a *Serratia* sp. via the activity of a radiotolerant (Jeong, 1992) acid phosphatase enzyme. This liberates inorganic phosphate ligand (HPO_4^{2-}) from a phosphate donor to deposit (with UO_2^{2+}) polycrystalline cell bound $\text{HUO}_2\text{PO}_4 \cdot n\text{H}_2\text{O}$ (Macaskie et al. 1992). Chemically synthesized zirconium (IV) phosphates, most commonly $\alpha\text{-Zr}(\text{HPO}_4)_2 \cdot n\text{H}_2\text{O}$ ($\alpha\text{-ZrP}$) have similar ion exchange properties (Clearfield, 1988). Zirconium would be ideal for the remediation of wastes and potable water where non-toxicity is a pre-requisite. The *Serratia* metal phosphate deposition system has been demonstrated for tetravalent metals (Th(IV) , Zr(IV)) (Yong and Macaskie 1998;

Basnakova and Macaskie, 1999) although Zr(IV) was deposited poorly (Basnakova and Macaskie, 1999). Therefore the objective of this study was to develop effective biogenic ZrP deposition by the *Serratia* sp., working towards a method for use as an entrapment matrix for removal of metals such as Co^{2+} , Sr^{2+} and Cs^+ . These are convenient surrogates for the nuclides $^{60}\text{Co}^{2+}$, $^{90}\text{Sr}^{2+}$ and $^{137}\text{Cs}^+$, for which application of the HUP-based methodology to real nuclear waste was shown previously (Paterson-Beedle et al. 2006). The potential for this biogenic approach compared to some commercial materials is shown in Table 1.

The aim of this study is to show proof of concept for a portable and effective system for the removal of the radionuclide surrogates Co^{2+} and Sr^{2+} from aqueous solutions using biomanufactured ZrP, which is discussed in the context of the bio-HUP system and commercial comparators shown in Table 1.

Materials and Methods

Microorganism, support and biofilm production

Serratia sp. (NCIMB 40259) was used under license from Isis Innovation, Oxford, UK. Cells were grown as a biofilm on polyurethane reticulated foam (Filtren TM30, cubes: 1 cm^3 and discs: diameter = 2 cm and depth = 0.5 cm, 1.57 cm^3), supplied by Recticel, Belgium. The biofilm was grown in an air-lift fermenter under carbon-limiting continuous culture with the phosphatase activity of the cells from the fermenter outflow determined as described previously (Finlay et al. 1999, Macaskie et al. 2005; Paterson-Beedle and Macaskie 2004). The steady state specific activity was ~3,800 units (nmol *p*-nitrophenol released from *p*-nitrophenyl phosphate per min per mg

protein). To determine the amount of biomass (dry weight) attached to the polyurethane foam, cubes or discs (8) with and without biofilm, were dried at (60 °C; 48 h) and weighed. The amount of dry biomass was calculated by the difference of the average weights. The variations between the weights of foam and foam+biofilm samples were within 7 % and 15 %, respectively.

Preparation of reactor packed-bed systems for Zr bioaccumulation

Two packing systems were used for bioaccumulation of Zr onto biofilm immobilised onto polyurethane foam: (i) quartered cubes (88 per reactor, 0.125 cm³) were packed in cylindrical glass columns (9 cm; i.d. 1.5 cm) and (ii) discs (8 per reactor) were stacked in cylindrical glass columns (5 cm; i.d. 2 cm), the purpose of which was to reduce the channeling in the reactor, which was confirmed by magnetic resonance imaging (Graf von der Schulenburg et al. 2008).

All experiments used a standard solution of ZrOCl₂·8H₂O (1 mM) and glycerol 2-phosphate (G2P, 5 mM), pH 5 (Zr/G2P) unless otherwise stated. Reactors (6 per treatment) with packing system (a) were exposed to a continuous upward flow (ca. 7.8 ml/h, 72.6 h), via an external peristaltic pump (Watson-Marlow, 323), of Zr/G2P with and without sodium citrate buffer (3 mM, pH 5). For the determination of the background adsorption/biosorption of Zr from aqueous flows biofilm-reactors (2) were autoclaved and treated in parallel. Reactors (2) with packing system (b) were exposed to a continuous flow (ca. 8.2 ml/h, 66.6 h) of Zr/G2P alone, or identical reactors (6) were exposed to a flow of Zr/G2P at 14 ml/h for 22.5 h, then at 6.3 ml/h for a further 49.5 h. The outflow solutions of all reactors were analysed for Zr and P (see below). The variations between reactors were within 8 %.

In other experiments, reactors (6) with packing system (b) were exposed to an intermittent flow of Zr/G2P with ethanol (5 M), pH 5, with filter paper (Whatman, qualitative, diameter ca. 2 cm) fitted on top of the disc stack to retain the precipitate ('ZrP-biogel'). The reactors were filled with an upward flow (ca. 25 ml/h), as above, left statically (24 h), drained and filled with fresh solution, daily for 10 days. The outflow solutions were analysed daily for Zr and P. Deposited material on the biofilm ('ZrP-biogel') was estimated by difference. The variations between reactors were within 5 %.

Removal of Co and Sr from aqueous solutions

Bioreactor systems, containing ZrP material, were tested for the removal of Co^{2+} and Sr^{2+} from solution using methods described by Paterson-Beedle et al. (2006). All experiments were carried out twice using separate preparations and the variation between them was within 7 %. To determine the background adsorption/biosorption of metals from aqueous flows, reactors (biofilm immobilised onto polyurethane foam, without supported ZrP-biogel) were treated in parallel.

Spectrophotometric analyses of metals and phosphate

Determination of Zr was as described by Basnakova and Macaskie (1999), using xylenol orange, with a slight modification. The calibration was made from stock solution: $\text{ZrOCl}_2 \cdot 8\text{H}_2\text{O}$ made to 1 mM in a solution comprising 1 ml of conc HCl in 100 ml of deionised water. For analysis, Zr sample or standard (200 μl , 1-32 μg) was added to a cuvette (1.5 ml), followed by HCl (8 M, 200 μl), deionised water (1.4 ml) and xylenol orange (0.05 % wt/vol, 200 μl). The solution was mixed

and the absorbance was measured at 535 nm. The inorganic phosphate contents of outflows were measured as described by Yong and Macaskie (1995).

Co^{2+} was estimated using the method described by Onishi (1986), with a slight modification. To sample or standard solution ($\text{Co}(\text{NO}_3)_2 \cdot 6\text{H}_2\text{O}$) containing Co^{2+} (30 μl , 1-10 μg) was added citric acid solution (0.2 M, 250 μl) and phosphate-boric acid buffer (6.2 g of boric acid, 35.6 g of disodium phosphate dehydrated, and 500 ml of 1 M sodium hydroxide, total volume of 1 l, 300 μl), final pH ~8.0. Nitroso-R salt (Fluka, UK) solution (0.2 %, 125 μl) was added while stirring. The samples were covered, heated (100 $^\circ\text{C}$; 1 min), supplemented with HNO_3 (250 μl , 1 min), cooled in the dark, deionised water (325 μl) was then added and Co^{2+} was estimated at A_{420} by reference to the standard.

A method was developed (from Yong et al. 1996), for the determination of strontium, using arsenazo III. To samples or standard ($\text{Sr}(\text{NO}_3)_2$) (30 μl , 1-7 μg), 1.97 ml of 0.1 M borate buffer, pH 9.0 was added. Strontium was visualised by the addition of 0.1 ml of 0.15 % (w/v) arsenazo III, with estimation of the blue-violet complex (A_{649}) which develops in 25 min at pH 9-10 (Michaylova and Kouleva 1974).

X-ray powder diffraction (XRD) analysis

Biogenic ZrP samples (ZrP-biogel) were prepared by removing ZrP loaded foam discs from reactors into universal bottles (25 ml), adding deionised water and squeezing the foam to remove biomass and bound ZrP. Detached ZrP-biogel material was separated, settled under gravity, washed with deionised water a further three times and left to dry at ambient temperature. For analysis, some ZrP was put between sheets of Magic Tape and examined using a Siemens D5000 diffractometer

(transmission mode) equipped with a Ge monochromator to produce Cu $K_{\alpha 1}$ radiation, and a Braun position sensitive detector.

Results and Discussion

Bioaccumulation of Zr(IV) by *Serratia* sp. biofilm immobilised onto polyurethane foam in packed-bed reactor systems

The structure (amorphous, semicrystal or crystal) of ZrP depends on the method used for its synthesis (Bogdanov et al. 1997). However, the stoichiometric P to Zr ratio is 2 (e.g. $Zr(HPO_4)_2$), irrespective of the degree of crystallinity. α -ZrP is usually synthesized by reacting concentrated phosphoric acid with an aqueous solution of $ZrOCl_2$, e.g. Clearfield and Stynes (1964), Trobajo et al. (2000). The gelatinous amorphous precipitate initially obtained slowly crystallizes if the precipitate is heated under reflux in its mother liquor. Such harsh conditions for the synthesis of ZrP are not compatible with an enzymatically-accelerated metal phosphate biomineralization process. Other factors influencing this crystallisation process are the solubility product of the metal phosphate, the nature and concentration of the complexing ligand(s) present and the pH of the solution. Previous studies showed that, despite the low solubility products quoted in the literature, in practice tetravalent metal phosphates tend not to desolubilise readily due to the extensive hydrolysis of the tetravalent ion in solution (Yong and Macaskie, 1998, Basnakova and Macaskie, 1999).

Previous work showed that packed-bed *Serratia* sp. biofilm reactors exposed to uranyl nitrate with G2P accumulated hydrogen uranyl phosphate (Paterson-Beedle et al. 2006) with citrate buffer

present to suppress UO_2^{2+} hydrolysis. Under similar conditions (here metal:citrate ratio of 1:3, pH 5: Table 2), the Zr uptake was lower (by ~70 %) for reactors with citrate; however, the Zr:P molar ratios (1:~0.8) were similar in each case (Table 2). Since, in contrast to UO_2^{2+} , suppression of Zr(IV) hydrolysis resulted in less effective biomineral formation in this study, citrate was omitted from subsequent tests. As a control, the background adsorption/biosorption of Zr(IV) from the flow by heat-denatured biofilm was 3.4 and 4.4 % of the input concentration for systems with and without citrate, respectively, as compared to 21 % and 68 % using live-biofilm (Table 2). The Zr uptake ($\mu\text{g/h/ml}$ column volume) of reactors packed with cubes (without citrate) was similar to that of discs (40 and 41 respectively, Table 2). The space velocity (i.e. number of reactor volumes of feed treated in a unit time) was 43 % higher for the reactor packed with discs compared to that with cubes (Table 2). Importantly, the Zr:P molar ratios of ~ 1:1 indicate that α -ZrP ($\text{Zr}(\text{HPO}_4)_2$) was not the main composition of the product retained by the bioreactors (Table 2). It is known that polyvalent cations, such as Zr(VI), hydrolyse extensively in water (Baes and Mesmer 1986), and as hydroxyl groups accumulate on the cation through hydrolysis or base addition, they polymerise by olation, eventually precipitating (Clearfield, 1988). Rapid precipitation in the cold leads to amorphous or poorly crystalline products (Clearfield, 1988) and it is likely that hydrous oxides are also being accumulated in the bioreactor along with ZrP. Examination of the product by environmental scanning electron microscopy showed a gelatinous mass with no visible features, while X-ray powder diffraction analysis gave no interpretable powder pattern and no defined peaks, confirming a poorly crystalline or amorphous material (not shown). The steady state concentrations of Zr(IV) and phosphate removed from solution by reactors (without citrate) were ~0.73 mM and ~0.66 mM (~1.5 mM phosphate removal would be expected for $\text{Zr}(\text{HPO}_4)_2$) respectively, assuming

100 % hydrolysis of the G2P (see below). Hence the material is ‘enriched’ for Zr as compared to the expected ratio of Zr:P of 1:2 for $\text{Zr}(\text{HPO}_4)_2$ (Table 2).

System (ii) (discs) was chosen for further work because it produces less fluid channelling in columns compared to cubes (see Nott et al. 2005 and Graf von der Schulenburg et al. 2008) and the disc system showed higher phosphate uptake and space velocity (see Table 2).

Use of ethanol to promote ZrP formation

It has been reported that the hydration of Zr(IV) ions in solution can be reduced if oxygen-containing additives, e.g. alcohols, polyalcohols such as glycerol, or carboxylic acids, are used during the sol-gel synthesis of ZrP (Wong, 2006). The incorporation of additives in the ZrOCl_2 solution displaces water molecules that are coordinated to Zr ions and bridges Zr ions forming water soluble polymers; the additive should be selected so that it can be displaced from the Zr ions during the reaction with phosphoric acid or phosphate that forms ZrP (Wong 2006). The typical amount of additive used by Wong (2006) was 20 % by weight of ZrOCl_2 , the molar ratio of ZrOCl_2 to H_3PO_4 was ~1:3 and the concentration of H_3PO_4 used was ~4.5 M. However, the present study using 1 mM Zr(IV) showed that citrate (3 mM) and also the glycerol liberated from G2P were ineffective in the biomanufacture of crystalline ZrP detectable by XRD. Previous mass balance studies showed that at a pH of 4.5 70% of the input G2P was accountable as equimolar glycerol and liberated phosphate (M. Paterson-Beedle, unpublished) and since the phosphatase activity at pH 4 is approx. half that at neutral pH it was assumed that the glycerol concentration in the present study was 5 mM (i.e. complete hydrolysis) although this was not measured.. Ethanol was tested as an alternative additive. Preliminary tests indicated that high concentrations (2.5-5 M ethanol) were

optimal in promoting ZrP formation. A semi-continuous process was developed using the packed-bed biofilm reactor (discs) with an intermittent flow of Zr/G2P and ethanol (5 M), pH 5, for 10 days, interspersed with static 24 h periods (see Materials and Methods). Under these conditions (total ZrP loading time was 10 days including reactor refill time) the Zr uptake was increased to 95 % and the Zr:P molar ratio calculated (average of six reactors) was 1:3.4, i.e. the material was now phosphate-enriched as compared to the studies without ethanol and also with respect to the expected $\text{Zr}(\text{HPO}_4)_2$ (1:2 ratio). Subsequent tests showed that the ethanol-derived material contained a crystalline $\text{Na}_2\text{Zr}(\text{PO}_4)_2$ component by XRD analysis (M Paterson-Beedle and J E. Readman unpublished). A full characterisation of the ZrP-biogel material is outside the scope of this study and will be reported in a subsequent publication (J.E. Readman, M. Paterson-Beedle, K.W.Chapman, P.J.Chupas, L.E. Macaskie and J.A. Hriljac in preparation)

Removal of Co and Sr from aqueous solutions using packed-bed reactors containing Zr supported on *Serratia* sp. Biofilm

With deposition of ZrP successfully achieved (via ethanol treatment), two bioreactor systems, with the following Zr:P molar ratios, were tested for the removal of Co^{2+} and Sr^{2+} from solution: (i) 1:0.33 (prepared without ethanol) and (ii) 1:3.5 (prepared with ethanol). The removal of both metals was 100% (system ii shown in Fig. 1). The estimated Zr and P contents per reactor and respective uptakes of Sr^{2+} and Co^{2+} per reactor are shown in Table 3. The uptake of ions (Co^{2+} or Sr^{2+}) was similar for both systems, i.e. ~ 0.02 mmol per reactor, even though system (i) contained a \sim ten fold higher content of Zr compared to system (ii) (the phosphate contents were similar, Table 3) . The background adsorption/biosorption of Co^{2+} and Sr^{2+} ions from aqueous flows by polyurethane

foam coated with *Serratia* sp. biofilm without ZrP was ~ 0.0025 mmoles per reactor (~12 % of that containing ZrP).

According to the literature the uptake of cations for ZrO_2 , in the pH range of 5.5 to 6.0, is only 0.05 mmol/g solid; by contrast the ion exchange capacity for $\text{Zr}(\text{HPO}_4)_2 \cdot \text{H}_2\text{O}$ is ~6.64 meq/g (Clearfield, 1988). System (i) contains ten fold more Zr than system (ii), therefore, assuming the total amount of Zr in system (i) as being ZrO_2 , the estimated uptake of Co^{2+} and Sr^{2+} , would be 0.5 and 0.4 mmol/g ZrO_2 , respectively, which is ten fold higher than that reported in the literature for ZrO_2 . Therefore, these results suggest that the biogenic Zr product in system (i) is possibly a mixture of zirconium oxides and phosphates. If it is assumed that the total Zr in system (ii) is α -ZrP, the estimated ion exchange capacity for Co^{2+} and Sr^{2+} would be 4.3 and 4.2 meq/g ZrP, respectively, which is 35% lower than that described in the literature for pure α -ZrP. However, this lower experimentally-determined capacity could be due to the additional presence of Zr oxides, insufficient contact time given for the ion exchange under the dynamic conditions, as well as the pH of the metal solutions (~6.0). Greater uptake occurs at alkaline pH (Clearfield, 1988) but a slightly acidic pH was chosen to minimise the Zr(IV) hydrolysis and formation of ZrO_2 . It is known that α -ZrP exhibits sieving behaviour in acid solutions, and ions larger than K^+ are exchanged at an appreciable rate only in alkaline solution (Clearfield, 1988). Under these conditions sufficient protons on the layers are neutralised to allow swelling of the layers to admit larger ions (Clearfield, 1988).

The break through curves for the removal of Co^{2+} and Sr^{2+} on ZrP-biogel from system (ii) is shown in Figure 1. It can be seen that for Co^{2+} 1 % and 50 % breakthrough occurred after passing 20.5 ml (~2.6 column volumes) and 37.4 ml (~4.8 column volumes) of the feed solution,

respectively. Similarly, for Sr^{2+} , 1 % and 50 % breakthrough occurred after passing 24.5 ml (~3.1 column volumes) and 39.7 ml (~5.1 column volumes), respectively. Although the total ion uptake was similar for both systems, i.e. ~0.02 mmoles per reactor (Table 3), system (ii) was more efficient than system (i) in terms of quantity of reagents ($\text{ZrOCl}_2 \cdot 8\text{H}_2\text{O}$ and G2P) used to produce ZrP, i.e. ten fold less. However, the potential drawback of system (ii) was the reaction time, i.e. ~3 times longer than system (i).

Although the column breakthroughs (~4 column volumes) *per se* seem low it should be noted that Co^{2+} and Sr^{2+} were supplied at 0.5 mM. A real nuclear waste (e.g. as described by Paterson-Beedle et al. 2006) contains very low nuclide concentrations (e.g. ^{137}Cs : 1.781 Bq/ml or 4.08 pM and ^{60}Co : 0.115 Bq/ml or 0.05 pM) and hence the column capacities would not be reached until after substantial flows have passed. It could be argued that at such low concentrations the metals of interest may not be removed against an excess of other ions (e.g. Na^+). However other studies have shown that target nuclides (^{137}Cs , ^{90}Sr , ^{60}Co) are removed in co-challenge with UO_2^{2+} (i.e. co-crystallisation) at the expense of 5 mM sodium glycerol 2-phosphate (i.e. 5 mM Na^+) (M. Paterson-Beedle, unpublished) suggesting a potential selectivity that will warrant further study.

In order to calculate ‘real’ potential for waste treatment, taking bio-HUP as an example with, here, a maximum loading of 9 g of U (or 16.6 g HUP) per g of biomass (Macaskie et al. 1992) and a loading of 1.6 g HUP per g biomass (Paterson-Beedle et al. 2006), the HUP biomaterial capacity was compared to several commercially available materials (Table 1). In the present study, assuming a composition of $\text{Zr}(\text{HPO}_4)_2$, the total solid (g) per g biomass would be 0.5 % of that of the maximum load of HUP (16.6 g HUP/g biomass). The hydrous, gel-like nature of the material and its swelling in the column precluded increased loading per column.

The estimated capacity of the ZrP reactor, if a pure solution of Co^{2+} , at a concentration similar to that found in low active waste, i.e. $\sim 3.9 \times 10^{-7} \text{ mg/l}$ (see Table 1) is assumed, would be $\sim 4 \times 10^8$ bed volumes. Similarly, using a pure solution of Sr^{2+} , in a concentration range of $8.3 \times 10^{-6} - 1.4 \times 10^{-8} \text{ mg/l}$ (see Table 1), the capacity would be in the range of $\sim 2.8 \times 10^7 - \sim 1.6 \times 10^{10}$ bed volumes and the capacity (l/kg) would be $\sim 5.1 \times 10^8 - \sim 3.0 \times 10^{11}$ (dry weight). These estimated capacities obtained from ZrP reactors (from Table 3, system ii) are similar to those obtained for HUP (1.6 g per g biomass) and are in the order of ~ 2 -fold greater than for commercial materials at slightly acidic pH. This is to be expected since the commercial material for treating Sr(II) is based on titanium (IV) oxide (Table 1) and the superiority of ZrP as compared to Zr(IV) oxide is discussed above. It should also be noted that the commercial material requires a pH of > 10 for Sr^{2+} removal and between pH 4-8 for Co^{2+} removal whereas the bio-ZrP removes Sr^{2+} comparably to Co^{2+} at slightly acidic pH (Fig. 1) and also comparably to a reference $\text{Zr}(\text{HPO}_4)_2 \cdot n\text{H}_2\text{O}$ material prepared by J.E. Readman (3.9 and 3.1 mequiv Sr^{2+}/g respectively) using a batch contacting system (pH 7) to overcome the problem of gel swelling out of the column (not shown). On the basis of these projections the potential for ZrP-biogel in wastewater decontamination warrants more detailed development of the material, elucidation of its structure and better understanding of the mechanism of Sr^{2+} and Co^{2+} removal in a mixed ZrP/ ZrO_2 system.

From an economic viewpoint, large-scale manufacture of bio-ZrP at the expense of glycerol 2-phosphate is unattractive, even given that a 'rapid response' nuclear decontamination operation may be required at a future date. It is also not clear that sufficient G2P could be made available at short notice. These problems could be overcome by the use of phytic acid (inositol phosphate: 6 moles phosphate/mole as compared to 1 mole/mole for G2P). Phytic acid, a major plant phosphate storage material, is produced at large scale as a waste from biodiesel production. Its disposal is problematic

and a future use for phytic acid (see Paterson-Beedle et al. 2010) in the production of bio-Zr-based nuclear decontamination materials (and also similar materials based on bio-hydroxyapatite: L.E. Macaskie, S. Handley-Siddhu and J.C.Renshaw, unpublished) should also be explored.

Conclusions

This study shows that packed bed reactors containing *Serratia* sp. biofilm immobilised onto polyurethane reticulated foam, accumulated zirconium phosphate. The ZrP biomaterial produced without ethanol was Zr-enriched (molar ratio Zr:P of 1:1), whilst that produced with ethanol was phosphate-enriched (molar ratio Zr:P of 1:3.4), compared to the 1:2 expected for $\text{Zr}(\text{HPO}_4)_2$, indicating that $\text{Zr}(\text{HPO}_4)_2$ is not the sole composition of the product. The ethanolic biogenic material, supported on foam-immobilised biofilm, removed 100 % of Co^{2+} and Sr^{2+} until the reactor reached saturation. The estimated capacities (l/kg) obtained for the bio-ZrP reactors were similar to those obtained for bio-HUP; this, and bio-ZP are shown to be superior to commercial materials in this respect. These conclusions warrant further development of the ZrP biomaterial.

Acknowledgements

This work was supported by the EPSRC (EP/C548809/1) and an EPSRC studentship to CM. The authors thank Recticel (Belgium) for supplying the reticulated foam, Dr J. E. Readman for collecting the X-ray diffraction patterns and Drs J.E. Readman and J.A.Hriljac (School of Chemistry, University of Birmingham) for helpful discussions.

References

- Basnakova G, Macaskie LE (1999) Accumulation of zirconium and nickel by *Citrobacter* sp. J Chem Technol Biotechnol 74:509-514
- Baes CF, Mesmer RE (1986) The Hydrolysis of Cations. Krieger Publishing Company, Malabar, Florida, pp 152-159
- Bogdanov SG, Valiev EZ, Dorofeev YA et al (1997) Structure of zirconium phosphate gels produced by the sol-gel method. J Phys Cond Matter 9:4031-4039
- Clearfield A, Stynes JA (1964) The preparation of crystalline zirconium phosphate and some observations on its ion exchange behaviour. J Inorg Nucl Chem 26:117-129
- Clearfield A (1988) Role of ion exchange in solid-state chemistry. Chem Rev 88:125-148
- Finlay JA, Allan VJM, Conner A et al (1999) Phosphate release and heavy metal accumulation by biofilm-immobilised and chemically-coupled cells of a *Citrobacter* sp. pre-grown in continuous culture. Biotechnol Bioeng 63: 87-97.
- Graf von der Schulenburg DA, Holland DJ, Paterson-Beedle M et al (2008) Spatially resolved quantification of metal concentration in biofilm-mediated ion exchanger. Biotechnol Bioeng 99:821-829
- Jeong BC (1992). Studies on the atypical phosphatase of a heavy metal accumulating *Citrobacter* sp. D.Phil. Thesis, University of Oxford UK.
- Macaskie LE (1991) The application of biotechnology to the treatment of wastes produced from nuclear fuel cycle: biodegradation and bioaccumulation as a means of treating radionuclide-contaminated streams. Crit Rev Biotechnol 11: 41-112
- Macaskie LE, Empson RM, Cheetham AK et al (1992) Uranium bioaccumulation by a *Citrobacter* sp. as a result of enzymatically mediated growth of polycrystalline HUO_2PO_4 . Science 257: 782-784
- Macaskie LE, Yong P, Paterson-Beedle M, Thackray AC, Marquis PM, Sammons RL, Nott KP, Hall LD (2005) Novel non line of-sight method for coating hydroxyapatite onto surfaces of support materials by biomineralization. J Biotechnol 118: 187-200.
- Michaylova V, Kouleva N (1974) Spectrophotometric study of the reactions of arsenazo III with alkaline-earth metals. Talanta 21:523-532
- Nott P K, Heese F, Hall LD et al (2005) Measurement of flow field through biofilm reactors by three-dimensional magnetic resonance imaging. Am Inst Chem Eng J 51: 3072-3079
- Onishi H (1986) Photometric determination of traces of metals, Part IIA: Individual metals, aluminum to lithium, 4th edn. John Wiley & Sons, New York

- Paterson-Beedle M, Macaskie LE (2004) Use of PhoN phosphatase to remediate heavy metals. In: Barredo JL (ed) *Methods in Biotechnology: Microbial Products and Biotransformations*, Vol 18. Humana Press, Totowa, pp 413-436
- Paterson-Beedle M, Macaskie LE (2006) Utilisation of a hydrogen uranyl phosphate-based ion exchanger supported on a biofilm for the removal of cobalt, strontium and caesium from aqueous solutions. *Hydrometallurgy* 83:141-145
- Paterson-Beedle M, Macaskie LE, Readman JE, Hriljac JA (2009). Biorecovery of uranium from minewaters into pure mineral product at the expense of plant wastes *Adv. Mats Res.* 71-73, 621-624.
- Stylianou MA, Hadjiconstantinou MP, Inglezakis VJ et al (2007) Use of natural clinoptilolite for the removal of lead copper and zinc in fixed bed column. *J Hazard Mater* 143: 575–581.
- Trobajo C, Khainakov SA, Espina A et al (2000) On the synthesis of α -zirconium phosphate. *Chem Mater* 12:1787-1790
- Wong R (2006) Method of synthesizing zirconium phosphate particles. Available at <http://www.freepatentsonline.com/20060140840>. Accessed 29 Aug 2007
- Yong P, Macaskie LE (1995) Removal of the tetravalent actinide thorium from solution by a biocatalytic system. *J Chem Technol Biotechnol* 64:87-95
- Yong P, Macaskie LE (1998) Bioaccumulation of lanthanum, uranium and thorium, and use of a model system to develop a method for the biologically-mediated removal of plutonium from solution. *J Chem Technol Biotechnol* 71:15-26
- Yong P, Eccles H, Macaskie LE (1996) Determination of uranium, thorium and lanthanum in mixed solutions using simultaneous spectrophotometry. *Anal Chim Acta* 329:173-179

Figure 1. Break through curves for the sorption of Co^{2+} (●) and Sr^{2+} (○) on ZrP-biogel supported onto *Serratia* sp. biofilm immobilised onto polyurethane foam discs from system (ii) and packed in reactors. Reactors were exposed to $\text{Co}(\text{NO}_3)_2 \cdot 6\text{H}_2\text{O}$ (0.5 mM, pH 6.1) or $\text{Sr}(\text{NO}_3)_2$ (0.5 mM, pH 6.1). C = concentration of metal in the effluent (mg/l) and C_o = concentration of metal in the feed (mg/l) Flow-rate: 4.8 ml/h; column volume (without ZrP supported on biofilm, see Table 2): 7.83 ml and amount of Zr in column: ca. ~3 mg.

Table 1. Comparison between HUP biomaterial and some commercial inorganic materials.

Agent	CsTreat® ^a	SrTreat® ^a	CoTreat® ^a	Bio-HUP
Principle	Hexacyano-ferrate, granular	Ti oxide based, granular	Ti oxide based, granular	HUP on biomass, foam lattice
Bulk density (kg/l)	0.6	0.8	0.8	0.16 (dry weight, dw) ^b 0.71 (wet weight, ww) ^c
Grain size	0.25-0.85 mm	0.30-0.85 mm	0.30-0.85 mm	Nanoscale, surface array
Capacity (bed volumes, BV) ^d	6.0x10 ⁴ -2.4x10 ⁵	1.2x10 ⁵ -4.0x10 ⁵	2.0x10 ⁴ -4.0x10 ⁴	3x10 ⁷ -3x10 ¹⁰ (Cs) ^e 5x10 ⁷ -3x10 ¹⁰ (Sr) ^e ~8x10 ⁸ (Co) ^e
Capacity (l/kg)	1.0x10 ⁵ -4.0x10 ⁵	1.5x10 ⁵ -5.0x10 ⁵	2.5x10 ⁴ -5.0x10 ⁴	7.5x10 ⁸ -7.1x10 ¹¹ (dw) ^f 1.6x10 ⁸ -1.6x10 ¹¹ (ww) ^{f,c} 8.0x10 ⁹ -7.6x10 ¹² (dw) ^g 1.8x10 ⁹ -1.7x10 ¹² (ww) ^{g,c}
pH	1-13	>10	4-8	Full range not tested

^aSource: <http://www.fortum.com>. ^bCalculations based on maximum HUP loadings (16.6 g/g biomass) on biofilm immobilized onto polyurethane foam (cubes) packed in reactors as described in Paterson-Beedle et al. (2006). ^cEstimated using 78 % moisture content. ^dIn the bioreactor this is taken as 11 ml, but the interstitial volumes will vary according to how much HUP has been used in the ion exchange layer. ^eCalculations were based on ion exchange capacities of Bio-HUP (1.6 g/g biomass, 148.9 mg HUP/reactor) for ⁸⁵Sr (0.055 mmol), ¹³⁷Cs (0.11 mmol) and ⁶⁰Co (0.055 mmol), as described in Paterson-Beedle et al. (2006). For the estimation of the capacities (BV), typical concentrations (mg/l) of these elements in low active waste (Sr: 8.3 x 10⁻⁶; Cs: 4.1 x 10⁻⁵ and Co: 3.9 x 10⁻⁷) and in fuel rod storage pond stream (Sr: 1.4 x 10⁻⁸ and Cs: 4.3 x 10⁻⁸) (Macaskie 1991), were used. ^fCalculations based on the capacity (BV) in the range of 3x10⁷-3x10¹⁰ and Bio-HUP loading of 1.6 g/g biomass. ^gCalculations based Bio-HUP loading of 16.6 g/g biomass.

Table 2. Comparison of bioreactor systems, packed with *Serratia* sp. biofilm immobilized onto polyurethane foam with different formats, for the uptake of Zr from aqueous solutions, with and without citrate.

Description	With citrate ^a	Without citrate ^a	Without citrate ^b
Format of polyurethane foam	Cube	Cube	Disc
Volume of each foam (cm ³)	0.125	0.125	1.57
Number of foams with biofilm per reactor	88	88	8
Column volume (CV) (ml)	11	11	7.83
Flow-rate (ml/h)	7.8	7.8	8.2
Time (h)	72.6	72.6	66.6
Space velocity (1/h)	0.7	0.7	1.0
Biomass (dry weight) (mg per reactor)	88	88	120
Zr uptake (% of total Zr in inflow)	21	68	65
Total Zr uptake (mg)	9.94	31.97	21.42
Total Zr uptake (mmol)	0.11	0.35	0.24
Zr uptake (µg/h/ml CV)	12.45	40.03	41.05
Zr uptake (mg/g biomass)	0.11	0.36	0.18
Total P uptake (mg)	2.74	8.25	9.61
Total P uptake (mmol)	0.09	0.27	0.31
P uptake (µg/h/ml CV)	3.43	10.33	18.42
P uptake (mg/g biomass)	0.03	0.09	0.08
Zr : P (molar ratio)	1 : 0.82	1 : 0.76	1 : 1.32

^aReactors (1.5 cm x 9 cm) packed with cubes and exposed to Zr/G2P with and without citrate buffer (see text), pH 5. ^bReactors (2 cm x 5 cm) packed with discs and exposed to Zr/G2P, pH 5. The disc format was used since this avoided patchy ZrP deposition due to channeling (see text). The ‘ideal’ ratio of Zr:P for Zr(HPO₄)₂ is 1:2 (see text). Representative data are shown; each experiment was replicated as described in Materials and Methods with variations of within 7 % throughout.

Table 3. Comparison of two bioreactor systems, packed with ZrP supported on *Serratia* sp. biofilm immobilized onto polyurethane foam discs, for the uptake of Co^{2+} or Sr^{2+} from aqueous solutions.

Description	Co^{2+}		Sr^{2+}	
	System (i) ^a	System (ii) ^b	System (i) ^a	System (ii) ^b
Zr (mg/reactor) ^c	35.15	3.00	34.03	3.04
Zr (mmol/reactor) ^c	0.39	0.03	0.37	0.03
P (mg/reactor) ^c	4.19	3.65	4.04	3.52
P (mmol/reactor) ^c	0.14	0.12	0.13	0.11
Metal uptake(mg/reactor)^d	1.41	1.18	1.75	1.75
Metal uptake (mmol/reactor)^d	0.02	0.02	0.02	0.02
Zr:Metal (molar ratio)^d	0.06	0.61	0.05	0.60

^aSystem (i): packed-bed reactors containing Zr supported on *Serratia* sp. biofilm immobilized onto discs, exposed to Zr/G2P (14 ml/h for 22.5 h, then at 6.3 ml/h for a further 49.5 h), with a Zr:P molar ratio of 1:0.33 (see text). ^bSystem (ii): packed-bed reactors similar to system (i) but exposed to an intermittent flow Zr/G2P with ethanol, during 10 days, and with a Zr:P molar ratio of 1:3.4 (see text). ^cParameters before $\text{Co}^{2+}/\text{Sr}^{2+}$ addition. ^dUptake of test metals (in bold). Representative data are shown; each experiment was replicated as described in Materials and Methods with variations of within 8 % throughout.

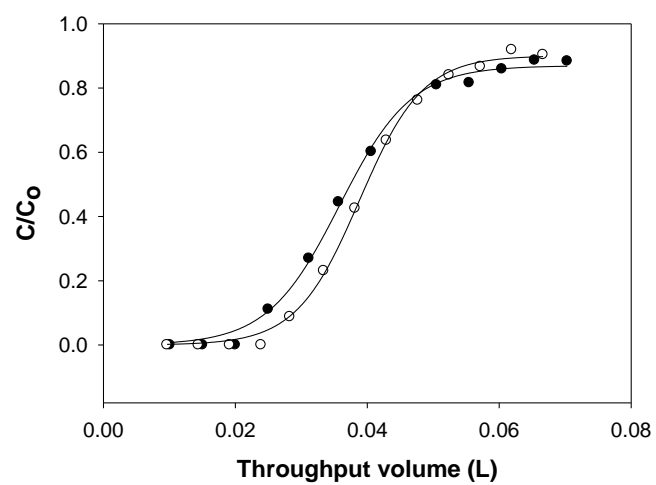


Figure 1

4 Chapter 4 Purification and partial characterisation of the phosphatases SP1 and SP2 from *Serratia* sp.

Context

Mennan *et al* (2010) have shown that biogenic ZrP removes Co^{2+} and Sr^{2+} to loads of 1.41 mg and 1.75 mg per reactor (respectively) before saturation (chapter 3). Greater loads can be obtained by co-crystalliation via doping with supplemental Zr(IV) and G2P. However, in a radioactive system radiotoxicity to the phosphatase could be problematic. Within the aim to produce a greater proportion of the radioresistant isoenzyme SP1 this chapter describes the purification and initial characterisation of SP1 and SP2.

4.1 Chapter summary

This chapter describes the methods used to purify SP1 and SP2 (previously called CPI and CPII) from *Serratia* sp. and discusses the differences between the enzymes based on their behaviour on chromatography media. Two methods of enzyme purification were used in this study. The first method was taken from a study carried out by Jeong (1992) who purified SP1 and SP2. The use of the previous method in this study proved unsuccessful since the column materials were not now commercially available and no direct substitutes were available. Hence an alternative purification protocol was sought. Methods detailing the culture conditions and the growth of cells prior to purification can be seen in chapter 2 (materials and methods). The results shown in this chapter are from the successful purification only; however, all purification methods used are discussed.

4.2 Introduction

The aim of this chapter was to purify SP1 and SP2 to homogeneity by designing a new purification protocol in order to produce mg quantities of phosphatase (SP1 and SP2) for analysis, biochemical tests, EPR studies, NMR studies, PIXE analysis and protein crystallisation, in order to elucidate a possible role for the enzyme and discover differences between the two isoforms and the reasons for these differences, relating these to the dissimilarity in the radiostability of SP1 and SP2 with a view to applications in radionuclide decontamination.

4.3 Results and Discussion

4.3.1 Purification of SP1 and SP2 using the method of Jeong (1992).

The *Serratia* phosphatase isoenzymes SP1 and SP2 were purified as described by Jeong (1992). The flowsheet (Fig. 12.a) summarises the purification of the isoenzymes SP1 and SP2 from *Serratia* according to Jeong's method. As previously noted (Jeong, 1992), this study also revealed that cell disruption using a French press gave no increase in phosphatase activity. The phosphatase specific activity before and after French pressing was 1510 and 1500 units (nmol product/min/mg protein) respectively. This was expected since an electron microscope study (Jeong *et al*, 1997) with immunogold labelling localised the phosphatase to the periplasmic space and extracellular polymeric matrix. It is also possible that the freeze thawing of *Serratia* biomass prior to French pressing had already caused cell lysis and the French press did not contribute further to the release of phosphatase from the cells. Jeong (1992) also found most of the phosphatase in 35 % - 60 % of the ammonium sulphate saturation, therefore this method was used in the current

study. In preliminary tests the phosphatase was then separated into two isoforms, SP1 and SP2 by cation exchange on SP-Sephadex C-50 (column dimensions: 1.6 cm × 20 cm). SP1 (unbound by cation exchange: overall negative charge) was collected from the column flow through and SP2 (bound by cation exchange: overall positive charge) was eluted from the column with a linear sodium chloride gradient (0.3 M). Jeong (1992) offered no explanation for this charge-dependent behaviour of two isoenzymes which were otherwise very similar in most respects; the relative molecular masses were 25 kDa (SP1) and 25 kDa (SP2), the isoelectric points were 8.9 (SP1) and 9.1 (SP2) and the K_m values for pNPP were 32 ± 11 (SP1) and 40 ± 10 (SP2) (Jeong, 1992). The only major difference observed by Jeong was in the sensitivity of SP2 to ionising radiation (^{60}Co γ source) which is discussed elsewhere in this thesis (chapter 5 and Appendix 9).

Large scale purification to produce mg quantities of pure enzyme was needed in order to carry out studies involving EPR and NMR (structural studies) which is discussed in the introduction (chapter 1). Although SP-Sephadex C-50 successfully separated SP1 and SP2, the use of this chromatography medium for large scale enzyme purification was not useful due to the large volume changes (shrinkage) associated with increasing concentrations of NaCl. This effect caused problems with pressure (when the sephadex medium returned to its original volume) in the column resulting in the loss of a number of batches of protein through leakages in the column fittings. Phosphatase activity was retained in both isoforms after resolution on this column, however after subsequent buffer exchange and concentrating, the (unbound) activity of SP1 dropped significantly and on some batches, lost all activity, although SP2 (bound and eluted) remained unaffected.

Active SP1 from the Sephadex C-50 (unbound) step was loaded onto a QAE-Sephadex A-50 column, equilibrated with buffer D and eluted with a sodium chloride gradient as shown in Fig.12.a. QAE-Sephadex is a strong anion exchange resin composed of cross

linked dextran with functional groups composed of diethyl-(2-hydroxy-propyl) aminoethyl. It has a protein binding capacity of 60 mg/ml resin (for phosphatase). QAE-Sephadex was tested with small injections (100 μ l at a concentration of 0.5 mg/ml) of phosphatase (SP1), protein was loaded at the top of the column and bound to the top layer of the resin in the column and could not be eluted, causing the resin to shrink and crack where the protein was bound. After several failed attempts at purification using this resin, HiTrap Q (small scale column: 1 cm \times 5 cm) or HiLoad Q (large scale column: 2.6 cm \times 10 cm) were substituted. HiTrap Q and HiLoad Q are strong anion exchange resins composed of a matrix of 6% spherical cross linked agarose with functional groups made up of quarternary ammonium (Q), which are recommended by GE Healthcare (UK) for the purification of phosphatases.

Unlike QAE-Sephadex, these have high protein binding capacity (180 mg/ml resin for phosphatase). However both gels were found to be subject to very large volume changes under variation in ionic strength in the NaCl gradient.

SP1 (C-50 unbound) retained 100 % activity after binding to and elution from HiTrap Q. However, enzyme activity was completely lost when the purification was scaled up and SP1 was applied to HiLoad Q following its recovery in the C-50 eluate. It is unclear why the scaled up purification was unsuccessful as both HiTrap Q and HiLoad Q are made from agarose and have the same functional groups. However, previous work by Jeong (1992) did not detail flow rates for column operation or note the difficulty of large volume changes observed with particular resins, such as sephadex. Hence it was difficult to fully replicate the conditions used in the previous study for a successful purification of both isoforms. It is possible that SP1 is sensitive to higher concentrations of NaCl, which would explain the loss of activity after HiLoad Q where higher NaCl concentrations

were needed for elution (0.4 M) in comparison with the retention of phosphatase activity after HiTrap Q where a lower NaCl concentration (0.2 M) was required for elution.

Incorporation of hydroxyapatite and phenyl sepharose columns (Jeong, 1992) did not adversely affect the activity of either SP1 or SP2. In the present study these additional columns did not have any effect on the purity of either isoform (in contrast to the work of Jeong (1992)) and both isoforms were not pure as shown by SDS-PAGE before and after purification on each column. It was concluded that the purification conferred by hydroxyapatite and phenyl sepharose in this study was of no benefit and their use was discontinued.

4.3.2 Phosphatase purification flowsheet taken from Jeong (1992)

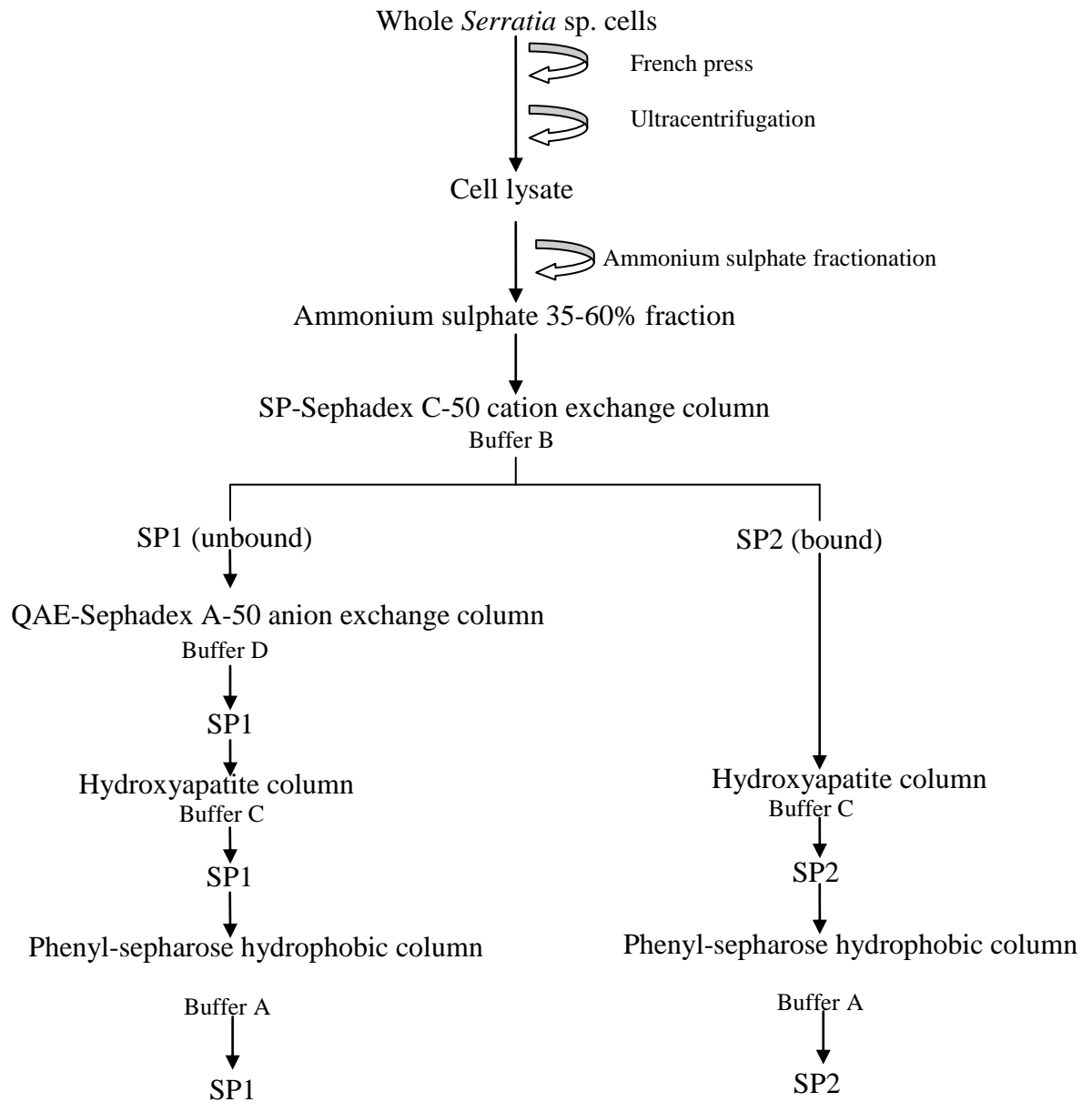


Figure 12.a. Overview of the purification of *Serratia* sp. phosphatases (SP1 and SP2) taken from Jeong (1992). This method of purification was used in this study along with modified versions involving the substitution of QAE-Sephadex with HiTrap and HiLoad Q columns (Fig 12.b.). This method including its modified versions involving HiTrap and HiLoad Q columns were found to be unsuccessful for the purification of SP1 and SP2. The composition of each buffer in the flowsheet can be seen in Table 3.a.

4.3.3 Phosphatase purification flowsheet for this study

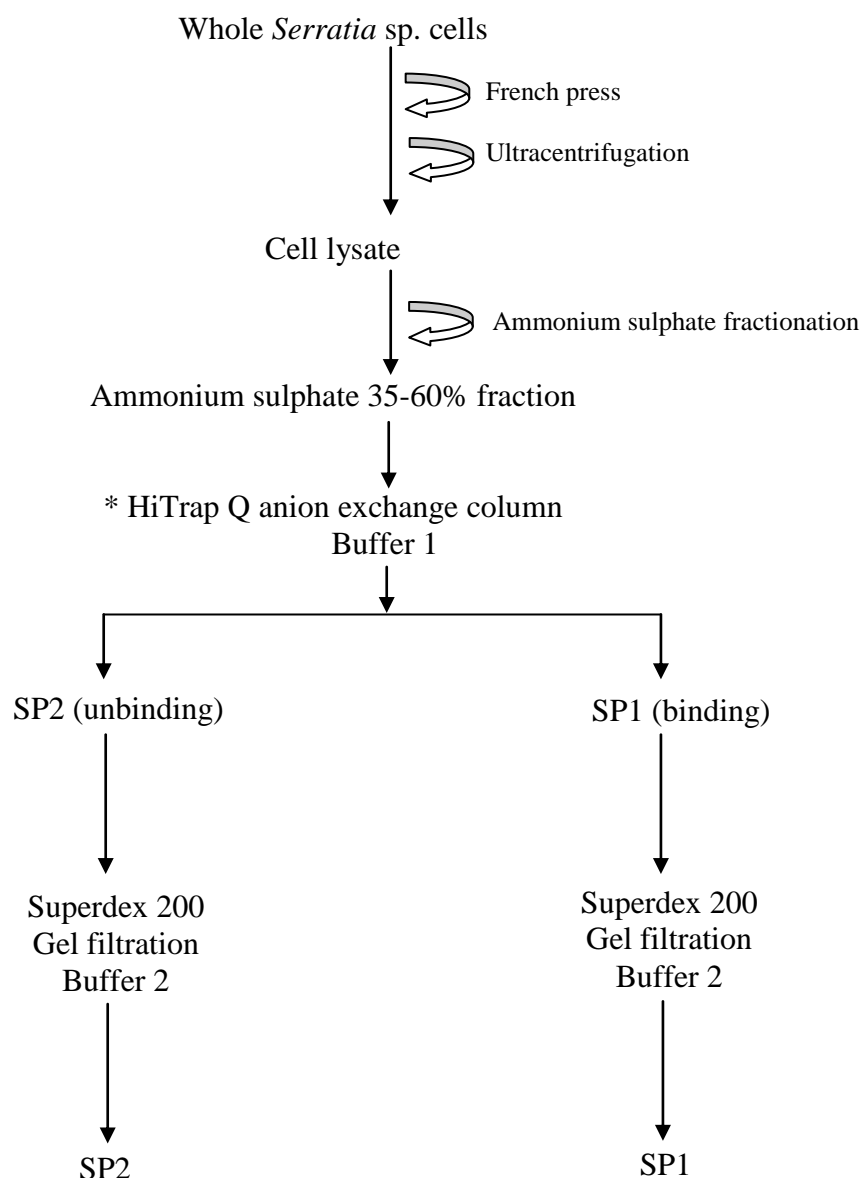


Fig. 12.b. Overview of the purification of *Serratia* sp. phosphatases (SP1 and SP2) used in this study. This method of purification was found to be successful. The composition of buffers used in this flowsheet can be seen in Table 3.b. below.

* Note: In the final purification scheme the Sephadex C-50 step was omitted and the HiTrap Q column was used in Tris buffer, pH 8.0 (see Table 3.b. and see text). Thus, the first separation step was an anion exchanger in this study, not the cation exchanger used by Jeong.

Table 3.a. Showing the composition of different buffers used during the purification of SP1 and SP2 in the flowsheet for purification (Fig 12).

Buffer	Buffer composition	Eluent
A	MOPS-NaOH (20 mM), β -mercaptoethanol (10 mM), Ammonium sulphate (25%) pH 7.0	Ammonium sulphate (25% - 0%) linear decreasing
B	MES-NaOH (20 mM), β -mercaptoethanol (10 mM) pH 6.0	NaCl (1 M)
C	KH ₂ PO ₄ (20 mM), β -mercaptoethanol (10 mM) pH 6.0	KH ₂ PO ₄ (800 mM)
D	Diethanolamine (20 mM), β -mercaptoethanol (10 mM) pH 9.4	NaCl (1 M)

Table 3.b. Showing the composition of different buffers used during the purification of SP1 and SP2 in the flowsheet for purification (Fig. 12.b).

Buffer	Buffer composition	Eluent
1	Tris (20 mM) pH 8.0	NaCl (1 M)
2	Tris (20 mM), NaCl (0.15 M) pH 8.0	N/A

4.3.4 Purification of SP1 and SP2 using two step ion exchange and gel filtration

Due to difficulties using Jeong's (1992) method of enzyme purification (Fig. 12.a.) attributable to problems with the ion exchange media and loss of (SP1) enzyme activity after the repeated buffer exchange necessary throughout the process, a different method of purification was sought. The use of gel filtration had previously been found to be unsuitable as the enzyme eluted as a very high molecular mass complex with unknown components (the same problem precluded electrophoresis of the native protein) (Jeong, 1992). However, gel filtration was re-tested on the assumption that the use of HiTrap Q as the first purification step would give an improved separation prior to the use of gel filtration making the latter step more effective than Jeong (1992) had previously found.

The isoelectric points of SPI and SP2 (8.9 and 9.1 respectively (Jeong, 1992)) and the use of an anion exchange column (HiTrap Q) at the start of the process meant that the buffers used in Jeong's protocol (which were designed for the ion exchange media in that protocol) were now unsuitable. Therefore the buffer was changed to Tris ($pK_a = 8.06$, 20 mM, pH 8.0) for use throughout the whole two step purification process. This also avoided loss of enzyme activity on exchanging buffers in Jeong's (1992) method, which was no longer necessary due to the use of Tris buffer throughout the new process. The previous use of mercaptoethanol was possibly inappropriate due to its effect as a reducing agent and therefore its unknown effect on a possible redox-active enzyme (SP1 and SP2, see chapter 5), for this reason its use in the buffer was discontinued.

The success of HiTrap Q in the purification process led to its continued use in the scaled up purification (instead of HiLoad Q) despite the fact that the column was designed for small scale use.

The alternative strategy involved using a buffer at pH 8.0 (on the lower side of the PIs of SP1 and SP2) to improve purification of the phosphatase and its separation from contaminating proteins. The assumption was that lowering the pH below the PIs of both isoforms would allow them both to be eluted in the flow through by leaving them positively charged and therefore unbound to the anion exchange column. This would then allow some contaminating proteins (retaining a negative charge) to be bound to the column. After loading the ammonium sulphate fraction onto HiTrap Q, SP2 (the more cationic protein) was eluted as a single peak in the flow through and SP1 bound to the column (Fig. 13). SP1 was then eluted at 0.1 M NaCl.

SDS-PAGE (Fig. 14. Lanes 6 and 7 corresponding to fractions 2 and 3 respectively) of fractions containing SP2 showed the presence of multiple bands and therefore a large number of contaminating proteins. However SP2 made up the greatest proportion of these proteins, which can be seen at the 25 kDa mark (the mass of a single phosphatase subunit: Jeong, 1992) as a thick band. SP1 was eluted from the column with 0.1M NaCl (Fig. 13) and also contained many contaminating proteins (Fig. 14, lanes 8 and 9 corresponding to fractions 17 and 18 respectively) and had a relatively thin band at the 25 kDa position when compared to SP2. The low concentration of NaCl required to unbind SP1 from the column shows how close the PIs of the two isoforms are as SP2 did not bind. The total protein after HiTrap Q for the fractions containing SP1 and SP2 was 17.85 mg and 78.75 mg respectively (Table 4 and 5). The total protein obtained by Jeong (1992) after the first ion exchange step (Fig. 12.a.) for SP1 and SP2 was 989.52 mg and 65.48 mg respectively, which is the converse to that obtained after HiTrap Q in this study (Table 2). However, other workers (H.Pflicke and M.Paterson-Beedle, unpublished) obtained evidence that after purification, if the two isoenzymes were pooled they re-fractionated in different proportions, suggesting that SP1 and SP2 are

interconvertible; a major premise underlying the current investigation (see chapter 4). The large amount of SP1 obtained at this stage in Jeong's study was possibly due to poor separation as SP1 was collected as one large peak in the flow through which would have contained all of the contaminants. During this study SP1 was separated much more efficiently from contaminating proteins on HiTrap Q and therefore less protein was collected.

The protein preparation was pigmented, which is normal in phosphatases (e.g. purple acid phosphatases) carrying transition metal ions (Kaija, 2002). Fig. 17.a, 1 and 2 show the pigment present in the ammonium sulphate fractionated proteins prior to de-salting, concentrating and loading onto HiTrap Q. The separation of pigments can be seen in the fraction collector after running the de-salted and concentrated ammonium sulphate fractionated protein on HiTrap Q (Fig. 17.c). No purple colour (Fig. 17.a) was visible in fractions containing SP1 or SP2, instead, a slightly yellow colour can be seen in the fractions containing SP2; however there was no visible pigment in the fractions known to contain SP1 (Fig. 17.c) (possible due to the relatively lower quantity of SP1 at this stage).

Fig. 17.b. shows the concentrated and purified SP2 showing a yellow/gold colour which was also observed in SP1 (See chapter 5). This coloration was also seen in crystals of SP2 (chapter 6). However the reasons for the gold/yellow colour in the purified enzyme (and any possible association with loss/gain in activity) is still unknown (see chapter 5).

Jeong (1992) found that gel filtration did not produce a good separation since the enzyme voided as a high molecular mass complex with other unidentified cellular components. However by pre-application of anion exchange (HiTrap Q) in this study (which produced a good separation), gel filtration was successfully applied using

Superdex 200. Fig. 16.a. shows the purification of SP2 from Superdex 200 gel filtration column.

SP2 was eluted as a single peak before contaminating proteins (but after the void volume). Comparison with known standards run on the column showed the whole protein had a M_r of ~100 kDa. SP1 behaved in the same way as SP2 on Superdex 200 (Fig. 16.b), the protein eluted before the contaminants and had a M_r of ~100 kDa; however the amount of protein was lower than that obtained for SP2. The total protein obtained for SP1 and SP2 after Superdex 200 was 2.96 mg and 12.12 mg (respectively) (Table 4 and 5). This compares well (for SP2) to the previous purification of this enzyme by Jeong (1992) who obtained total protein for SP1 and SP2 of 4.13 mg and 12.97 mg (respectively) at the end of the purification process. Following gel filtration on Superdex 200, both SP1 and SP2 were pure as shown by SDS-PAGE of pooled active fractions of each isoform (Fig. 18) both having a subunit molecular weight of 25 kDa (Fig. 18). Fig. 18 is not well represented photographically (the original gel was more intensely coloured) and in confirmation a subsample was also subject to mass spectroscopy analysis which showed only the single protein as shown in Fig. 18. This was also confirmed by MALDI (chapter 5).

Previous work by Jeong (1992) showed that the subunit bands of SP1 and SP2 on denaturing gels did not stain with the phosphatase substrate 5-bromo-4-chloro-3-indolyl phosphate (BCIP) (i.e. single subunits had no enzymatic activity). Subunits of both SP1 and SP2 were reacted to anti SP2 antibody and immunoblotting with conjugated antibodies gave bands corresponding to the coomassie blue stained phosphatase bands (Jeong, 1992). Non-denaturing PAGE showed that neither phosphatase migrated well, however it did show a broad smeared activity band against BCIP at that position and both reacted to anti SP2 antibody (Jeong, 1992). Non denaturing gels and staining with

BCIP were not repeated in this study as other workers (H.Pflicke, unpublished) had repeated this work and reported the same results as Jeong (1992). A summary of the phosphatase purification is shown in Table 4 and 5.

Purification Results

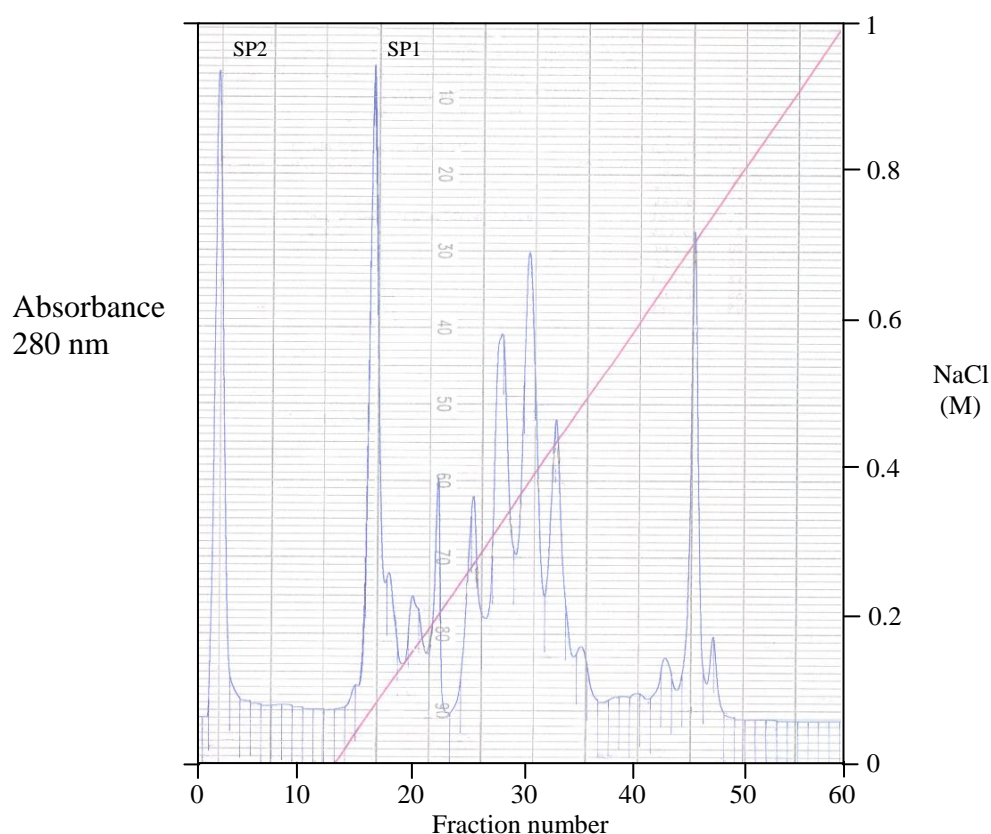


Fig. 13. HiTrap Q (anion exchange) chromatography of ammonium sulphate fractionated *Serratia* sp. phosphatases. The ammonium sulphate 35 % - 60 % fraction was de-salted and concentrated as described in materials and methods (chapter 2) was loaded (5 ml; 270 mg protein in a typical purification) was loaded onto the column (1.0 cm \times 5.0 cm) pre-equilibrated with buffer 1 (Table 3.b.). The column was washed (two column volumes) with buffer 1 at a flow rate of 2.5 ml/min followed by elution with a linear NaCl gradient (0M-1M NaCl in buffer 1). All fractions were collected and each checked for phosphatase activity. Of the voided phosphatase fractions collected, only fractions showing maximum activity were pooled and designated as SP2*. The eluted phosphatase fractions were collected and tested for activity in the same way as SP2 and those showing maximum activity were designated as SP1. The actual proportions of SP1 and SP2 varied between preparations, however this variation was minimal. The void volume is not

shown on the chromatogram as the fraction collector was started manually after the void volume had eluted from the column.

* The possibility of contamination of the voided SP2 with SP1 due to column overload was discounted by pooling the voided SP2 fractions and injecting them back onto the column to look for SP1. The SP2 fractions were pooled into two pools, those showing maximum phosphatase activity (for use in further purification) and those fractions showing little or no activity. Fractions were concentrated as above before injecting onto the HiTrap Q column. Column overload is also discounted due to the fact that the maximum total protein loading for this column is 600 mg. The maximum total protein injected at any one time was ~270 mg.

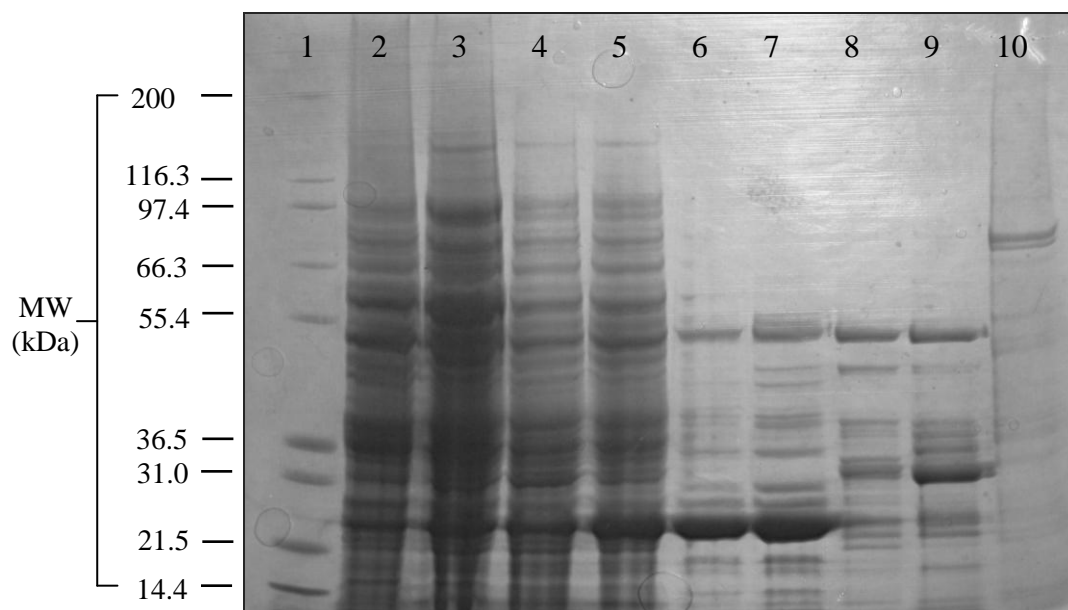


Fig.14. SDS-polyacrylamide gel electrophoresis of the proteins at various stages of phosphatase purification using two step ion exchange and gel filtration from *Serratia* sp. Lane 1, molecular weight standards. Lane 2, 35 % ammonium sulphate fractionated *Serratia* phosphatase. Lane 3, 60 % ammonium sulphate fractionated phosphatase. Lane 4, flow through from vivaspin 20 molecular weight concentrator (mw cut off 300 kDa). Lane 5, concentrated (5 ml) sample prior to loading onto HiTrap Q. Lane 6, fraction 2 (SP2) from HiTrap Q. Lane 7, fraction 3 (SP2) from HiTrap Q. Lane 8, fraction 17 (SP1). Lane 9, fraction 18 (SP1) from HiTrap Q. Lane 10, fraction 46 from HiTrap Q. Standards used were Invitrogen (Mark12) molecular weight standards: myosin (200 kDa), β -galactosidase (116.3 kDa), phosphorylase B (97.4 kDa), bovine serum albumin (66.3 kDa), glutamic dehydrogenase (55.4 kDa), lactate dehydrogenase (36.5 kDa), carbonic anhydrase (31.0 kDa), trypsin inhibitor (21.5 kDa), lysozyme (14.4 kDa).

Table 4. Relative amounts of SP1 and SP2 obtained from ion exchange fractionation by Jeong (1992: Sephadex C-50, QAE Sephadex A-50 cation and anion exchangers, hydroxyapatite and phenyl sepharose, flowsheet in Fig. 12.a.), and in this study (HiTrap Q anion exchange and Superdex 200 (as shown in Fig. 12.a. and 12.b.)). The amounts shown are the total amounts of protein from studies using comparable amounts of biomass and are shown for the purposes of comparison between the two studies.

Study	Total amount of protein recovered (mg)		Ratio of total protein material containing SP1 and SP2
	SP1 containing fractions	SP2 containing fractions	
Jeong (1992)	4.13	12.97	1:3
This study	2.96	12.12	1:4

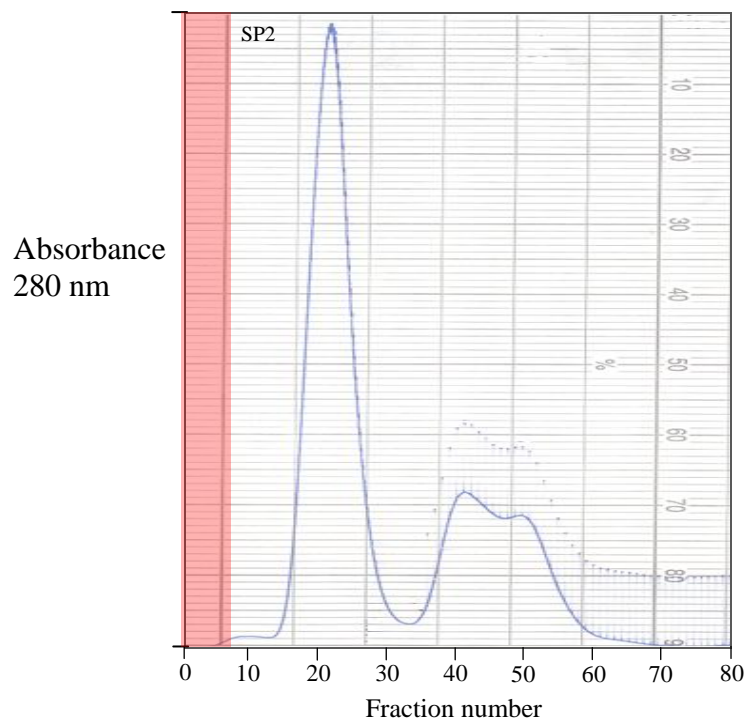


Fig. 15.a. Superdex 200 (gel filtration) chromatography of SP2. The voided phosphatase (SP2) from HiTrap Q was concentrated (0.5 ml) using vivaspin 20 centrifugal concentrators with a molecular weight cut off of 10 kDa. The sample (0.5 ml) (78 mg protein) was loaded onto the column (1.8 cm \times 60 cm) pre-equilibrated with buffer 2 at a flow rate of 1ml/min. Fractions showing phosphatase activity (10-25) were pooled and run on SDS-Page to check purity (Fig. 18). The pink shaded area denotes the column void volume.

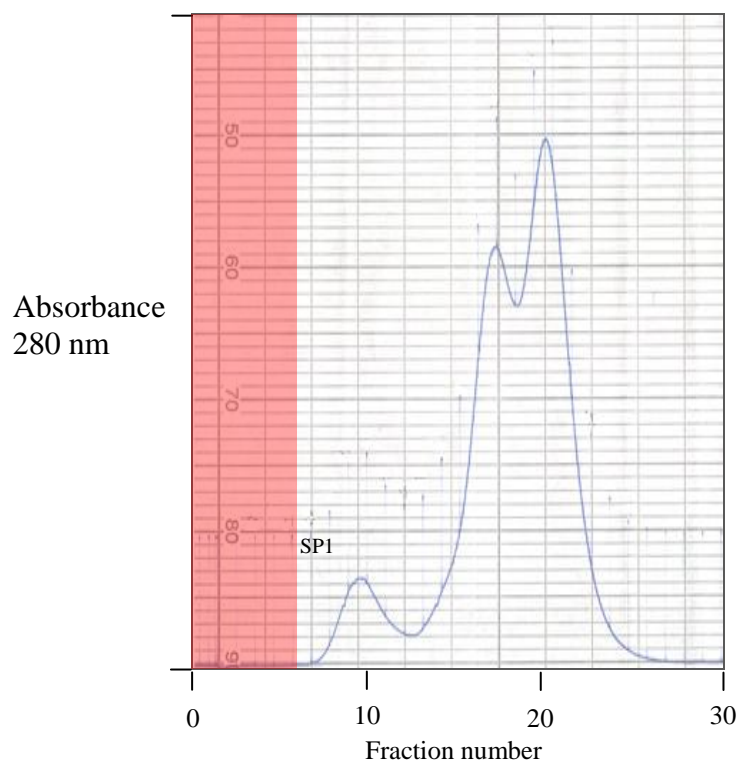


Fig. 16.a. Superdex 200 (gel filtration) chromatography of SP1. The eluted fractions designated as SP1 after HiTrap Q were de-salted and concentrated (0.5 ml) using vivaspin 20 centrifugal concentrators with a molecular weight cut off of 10 kDa. The sample (0.5 ml) (17 mg protein) was loaded onto the column (1.8 cm \times 60 cm) pre-equilibrated with buffer 2 at a flow rate of 1ml/min. Fractions showing phosphatase activity (6-10) were pooled and run on SDS-PAGE to check purity (Fig. 18). The pink shaded area denotes the column void volume.

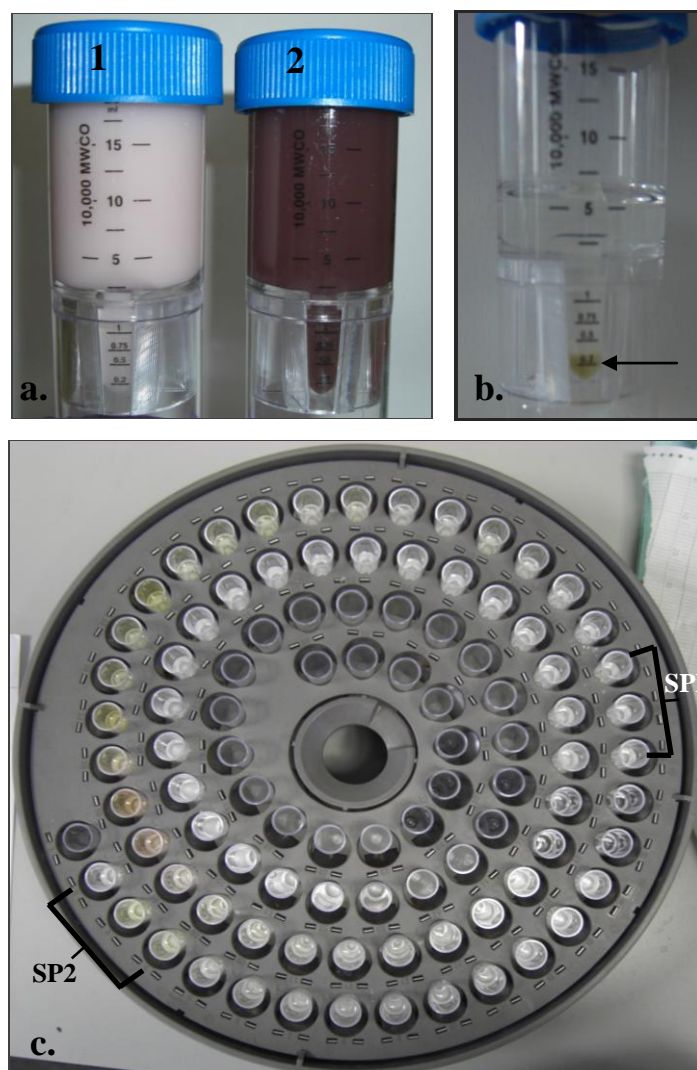


Fig. 17.(a)1. showing 35% 2. 60%, ammonium sulphate fractionated proteins prior to de-salting and concentrating. **(b)** Showing the pigment present in pooled fractions containing SP2 after elution from the HiTrap Q column and prior to loading onto Superdex 200 gel filtration (see later). The same pigment was observed in pooled fractions containing SP1 and in some pure protein crystals where the protein harvest was high (see chapter 6). **(c)** Fraction collector after HiTrap Q chromatography of 35% and 60% ammonium sulphate fractions, showing the different pigments present and their separation into different fractions. SP2 was found in fractions 2-4 and SP1 in fractions 17-19. However, gold colour was also observed in some fractions which did not contain either SP1 or SP2 so the significance of the colour may have little relevance.

* Note: The centre fractions in the above fraction collector are unused (empty tubes).

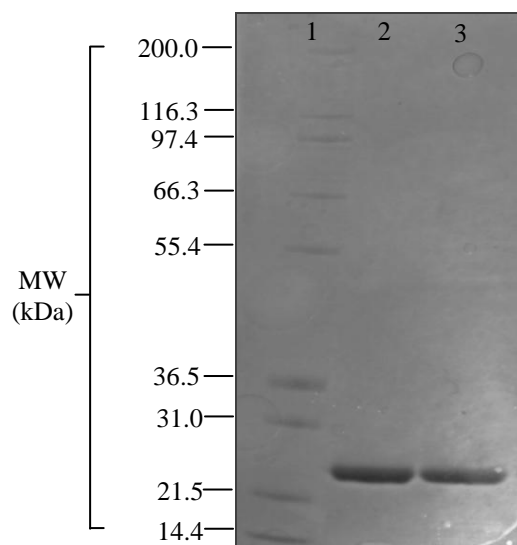


Fig. 18. SDS-polyacrylamide gel electrophoresis of *Serratia* sp. phosphatases (SP1 and SP2) after Superdex 200 gel filtration. Invitrogen (Mark12 unstained) molecular weight standards were: myosin (200 kDa), β -galactosidase (116.3 kDa), phosphorylase B (97.4 kDa), bovine serum albumin (66.3 kDa), glutamic dehydrogenase (55.4 kDa), lactate dehydrogenase (36.5 kDa), carbonic anhydrase (31.0 kDa), trypsin inhibitor (21.5 kDa), lysozyme (14.4 kDa). Lane 1, molecular weight standards, lane 2, SP2, Lane 3, SP1. The photographic representation does not show the depth of colour seen in the original gel. In confirmation the MALDI-ToF results (Fig 19) were obtained on a liquid sample of the protein (Chapter 2, section 2.5) and showed only one protein in accordance with the gel shown above.

Table 5. Purification of acid phosphatase (SP1 and SP2) from *Serratia* sp.

Purification step	Total activity (M units)	Total Protein (mg)	Specific activity (M units/mg)	Purification (fold)	Yield (%)
Cell lysate	3150	2100	1.5	1	100
Ammonium sulphate fractionation	567	270	2.1	1.4	18
HiTrap Q					
*SP1	29	17.85	1.6	1.1	0.93
*SP2	3098	78.75	3935	26.23	98
Superdex 200					
SP1	99	2.96	33.7	22.46	3.16
SP2	10	12.12	49.9	33.28	19

Purification of SP1 and SP2 from *Serratia* sp. The data given here are from a typical purification. 1 M unit = 1000 units.

*SP1 : *Serratia* phosphatase 1

*SP2 : *Serratia* phosphatase 2

4.4 Summary of the Results

- SP1 and SP2 were previously purified to homogeneity by Jeong (1992) but repetition of this method failed in this study.
- Successful purification of SP1 and SP2 (this study) was achieved by using HiTrap Q (anion exchange) and Superdex 200 (gel filtration).
- The behaviour on HiTrap Q (anion exchanger) shows SP1 retains a negative charge, whilst SP2 retains a positive charge under the conditions selected.
- Both SP1 and SP2 were eluted at the 100 kDa mark after Superdex 200.
- Both SP1 and SP2 have a subunit molecular weight of 25 kDa.
- Purified SP1 and SP2 show a yellow/gold pigmentation.

5 Chapter 5 Characterisation of *Serratia* sp. phosphatase SP1 and SP2: metal content and possible function of the enzyme

Context

Appendix 9 discusses the characterisation of SP2 and shows that SP2 potentiates free radical damage to deoxyribose. This chapter compares the isoenzymes SP1 and SP2 in this context and also with respect to other properties of the enzymes.

5.1 Chapter summary

This chapter details and discusses the differences between the two phosphatase isoenzymes SP1 and SP2 from *Serratia* sp. and discusses the possible function(s) of these two highly similar enzymes. SP1 and SP2 were compared using: micro-PIXE (for elemental analysis), MALDI, MS for phosphorylation detection and peptide mass fingerprinting with Swissprot and NCBI nr protein database searches. Amino acid sequences obtained in previous work (Macaskie *et al.* 2004; Jeong, 1992) were also used in this work to search databases using the Basic Local Alignment Search Tool (BLAST).

5.2 Introduction

Serratia sp. PhoN-type phosphatases SP1 and SP2 are highly similar isoenzymes with minor identifiable differences. Critically, SP1 was retained by an anion exchanger, whilst SP2 remained unbound. Their PIs were 8.9 and 9.1 for SP1 and SP2 respectively (Jeong, 1992) suggesting a charge difference which has not, as yet, been assigned to differences in amino acid composition, the presence of additional components or subtle conformational differences between the two enzymes. Previous work by Jeong (1992; Jeong *et al.* 1995) also showed that these enzymes differ slightly in their optimum pH, temperature, sensitivity to γ radiation and monovalent cations (chapter 1). It is not known why *Serratia* sp. phosphatase exists in two highly similar immunologically cross reactive isoforms (Jeong, 1992), however the existence of phosphatases as multiple forms of isoenzymes in the same cell is not an exceptional case (Uerkvitz & Beck, 1981; Pradel & Boquet, 1988; Pond *et al.* 1989). The true role of this acid type phosphatase still remains unclear. However one accepted role is that acid phosphatase acts as a scavenger of organic phosphate esters which are otherwise unable to pass through the cytoplasmic membrane (Uerkvitz

& Beck, 1981). It has been hypothesised more recently that acid phosphatase functions as a phosphate retrieval system in pathogenic bacteria, activated upon phagosomal containment (Felts *et al.* 2006), as well as playing an integral role in survival of the pathogen within the host's phagocytic cells (Aguirre-Garcia *et al.* 2000). Other studies have shown very high expression of the enzyme in carbon restricted continuous culture with parallel expression of multiple pili and curli although any possible association between these was not discussed (Allan *et al.* 2002).

This study aims to further the existing work on characterisation and identification of these enzymes as well as identifying other differences between them and in doing so to clarify the role(s) of SP1 and SP2 and subsequently their biological function and significance.

5.3 Results and discussion

5.3.1 Polyacrylamide Gel Electrophoresis and MALDI-ToF mass spectrometry of *Serratia* sp. phosphatase SP1 and SP2.

Initial testing of purified SP1 and SP2 involved analysis with MALDI-ToF to accurately measure the sub-unit molecular weight of both isoforms from a solution of the purified phosphatase (section 2.5) (Fig. 19.b and c).

Fig. 19.a. shows SDS-Page analysis of SP1 and SP2; both enzymes ran as a single band at the 25 kDa mark. This is corroborated by MALDI-ToF analysis of SP2 and SP1 (Fig. 19.b and c, respectively), showing the subunit molecular weight as 25,155 Da and 25,143 Da for SP2 and SP1, respectively. MALDI-ToF analysis was done from a solution of the purified phosphatase and not from an excised gel band (Chapter 2, section 2.5) proving that both proteins (SP1 and SP2) had been purified successfully. MALDI is capable of measuring masses to within 0.01 % of the molecular mass of the sample up to 40 kDa (Hillenkamp *et al.* 1991) and hence the subunit molecular mass was concluded to be identical within experimental error. As both SP1 and SP2 are known to be tetrameric (Jeong, 1992), and based on their behaviour on chromatography media

(chapter 4) it was concluded that the holoenzyme molecular weight of each isoform is ~ 100 kDa, (specifically; 100,620 Da SP2 and 100,572 Da SP1, assuming identical subunits make up each isoform). Earlier work by Jeong (1992) that determined the holoenzyme mass did not use MS analysis but the mass was found to be around 100 kDa using a Superose Q-6 sizing column.

Electrospray ionisation (ESI) was attempted in this study with SP1 and SP2, however results from ESI were not obtained, probably due to the presence of minute quantities of salt or other impurities in the original enzyme buffer, which are known to dramatically decrease the sensitivity and suppress ionisation of the sample (Canarelli *et al.* 2002). Therefore it is not known whether the apparent small mass differences between SP1 and SP2 suggested by MALDI analysis are significant.

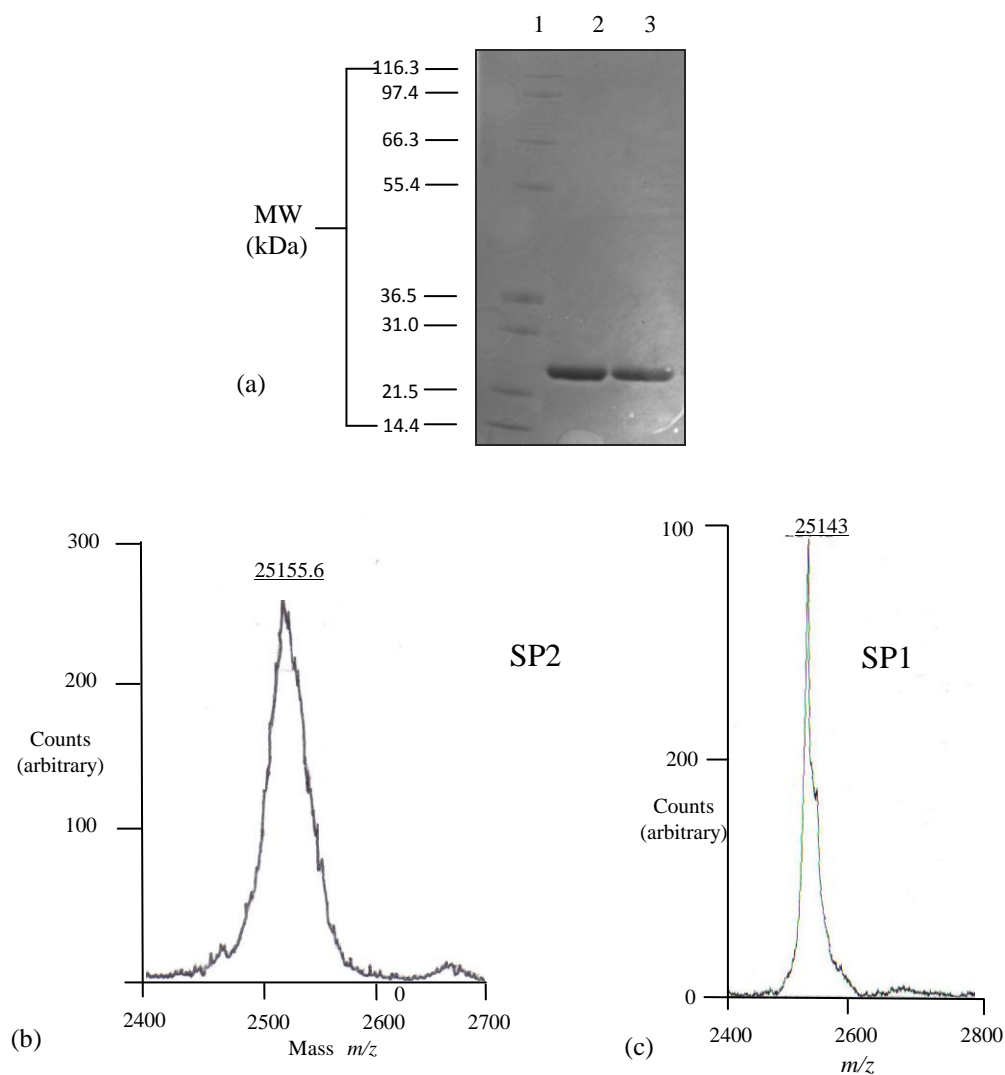


Fig. 19.(a) SDS-PAGE analysis of acid phosphatase from *Serratia* sp. after purification. Lane 1 Novex Mark12 molecular weight standards. Lane 2 phosphatase (SP2) (10 μ g) and lane 3 phosphatase (SP1) (10 μ g), stained with Coomassie blue (R-250). The subunit molecular weight of 25 kDa was obtained from a log plot of distance versus molecular mass and confirmed by MALDI-ToF as 25,155 kDa and 25,143 kDa for (b) SP2 and (c) SP1 respectively.

5.3.2 Analysis of *Serratia* phosphatase by mass spectrometry and identification of the protein by database interrogation

The phosphatase was subjected to tryptic digest and analysis by mass spectrometry as described in Materials and Methods (chapter 2). Trypsin was used for protein digestion as it is the most suitable enzyme for mass spectrometric studies, firstly, trypsin cleaves on the C-terminal side of arginine and lysine, which makes it eminently suitable for positive ionisation mass spectrometric analysis, secondly, putting the basic residues at the C-terminus also makes the peptides fragment in a more predictable manner throughout the length of the peptide. The other advantage of trypsin digestion is that useable collision induced dissociation (CID) data can only be obtained from peptides less than 2-3 kDa and trypsin generally produces peptides of this size.

Following trypsin digestion, a peak list file (pkl) was generated from the mass spectrometry results for SP1 and SP2, which was used to interrogate the protein data bank for possible sequence matches to this protein. Databases were interrogated through the MASCOT (MS/MS Ions) search engine. NCBIInr and Swissprot were searched and results showed no significant homology (only showing partial peptide matches to one or two peptides) to any protein in the databases. The results of the database searches can be seen in appendix 8. The only two partial matches were for the following (see appendix 8): 1. (NCBIInr) two partial peptide matches with acid phosphatase of *Bacteroides vulgates*. 2. (NCBIInr) PhoN1 (candidate division TM7 single-cell clinical isolate TM7), two partial peptides.

Fig. 20. shows the partial peptide mass fingerprints of SP1 and SP2 (further ‘screenshots’ can be seen in Appendix 6). These screenshots show that SP1 and SP2 are almost identical apart from small differences in relative peak intensities (as indicated by the grey highlighted areas). Small sections of the screen shots were enlarged in order to zoom in and compare small details of the traces (Fig. 20). Comparison by superimposition showed that the traces are virtually superimposable and SP1 and SP2 contained no differing peptides which would set the two enzymes

apart. This does not mean that the full protein sequences (which are unknown) of SP1 and SP2 are identical. However, the N-terminal sequences (Appendix 3.1) were found to be exactly the same (Jeong, 1992).

The amino acid sequences of two peptide fragments of purified *Serratia* phosphatase obtained in earlier work (Jeong, 1992; Macaskie *et al.* 1994) were compared with known polypeptide sequences using the Basic Local Alignment Search Tool (BLAST) to interrogate six databases (non redundant protein sequences, swissprot, patented protein sequences, reference proteins, protein data bank and environmental samples) and returned several partial matches to PhoN and PhoC of several microorganisms. Partial sequences searched were: Fragment 1 (F1) N-terminal sequence of *Serratia* acid phosphatase (Jeong, 1992) and Fragment 2 (F2) *Serratia* acid phosphatase (Macaskie *et al.* 1994).

Results using fragment 1 for database interrogation showed matches for several members of the enterobacteriaceae, many of which are pathogenic (Table 6). Homology can be seen (amongst others) between the *Serratia* peptide fragments and *P.stuartii* and *M. morganii* (PhoN and PhoC respectively) (K. Choi, pers. Comm.) showed that the removal of one amino acid can convert PhoC to PhoN), PhoN was noted previously for its low G+C content and possible involvement in the horizontal transfer of *phoN* between organisms in the environment was postulated (Groisman *et al.* 1992; 1993; 2001). Results using fragment 2 (Table 6) showed a match for the active site conserved domain for PAP2 acid phosphatases and PAP2-like superfamily. The latter are a super family of histidine phosphatases and vanadium haloperoxidases. The group includes glucose-6-phosphatase and bacterial acid phosphatase, vanadium bromoperoxidases and vanadium chloroperoxidases. However the *Serratia* enzyme contained no vanadium (see later).

The phosphatases of *M. morganii* (*phoC*), *P. stuartii* (*phoN*), *S. flexneri* and *S. typhimurium* (*phoN*), which all share gene sequence homology with *Serratia phoN* (and all fit into the Class A phosphatases (Rossolini *et al.* 1998)) also share sequence homology and active site conserved

domain matches with vanadium peroxidases (Hemrika *et al.* 1997). It is not possible to compare *Serratia phoN* for sequence homology with vanadium peroxidase as the full amino acid sequence of the *Serratia phoN* is not yet known, because there are no genomic data available for the organism; however it has been shown that Class A phosphatases and vanadium haloperoxidases have a conserved active site (Tanaka *et al.* 2002). The vanadium-containing chloroperoxidase from *Curvularia inaequalis* was found to have phosphatase activity in addition to peroxidase activity, indicating that the active site of this enzyme is indeed similar to that of other acid phosphatases (Hemrika *et al.* 1997). The active site structure of acid phosphatase from *Escherichia blattae* shows remarkable similarity to the vanadium-chloroperoxidase from *C. inaequalis* (Tanaka *et al.* 2002) and sulfate cocrystallises with the active site of the phosphatase in the same way as vanadium in the active site of the vanadium chloroperoxidase (Tanaka *et al.* 2002). The similarity between the enzymes from the organisms noted above indicates that the vanadium-containing haloperoxidases and this group of phosphatases may have divergently evolved from a common ancestor (Hemrika *et al.* 1997). This is further corroborated by the fact that vanadate is a potent inhibitor of the phosphohydrolase activity of the above phosphatases (Tanaka *et al.* 2002) and that all these organisms show significant homology of their phosphatases with each other (see sequence homology, Table 6). However an extensive search failed to show any vanadium component of the *Serratia* enzyme (see below); indeed, the activity of the enzyme was inhibited by vanadyl sulphate (Jeong, 1992) (Table 8).

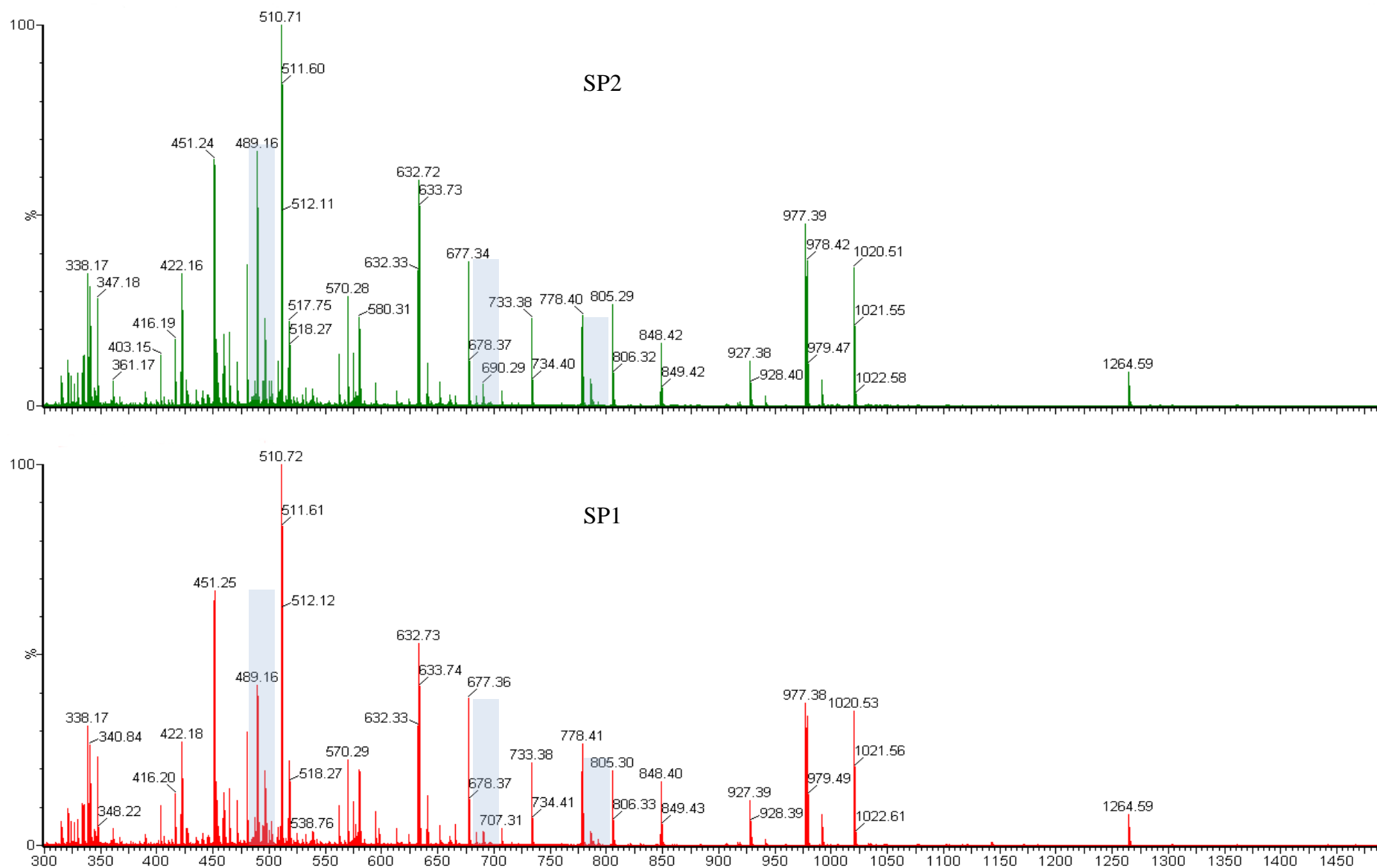


Fig.20 Showing screenshots from the MS analysis (peptide mass fingerprints) of SP1 and SP2 (5 min sections of the LC trace were combined and the MS spectra plotted). This screenshot was taken from 10-15 min retention time on the LC column run. Apart from small differences in intensity, the traces for SP1 and SP2 are super imposable and show no additional peptides. Further screenshots from 15-20, 20-25 and 25-30 min retention times can be seen in Appendix 6.

* Highlighted areas indicate small differences in peak intensities which are of no significance in terms of differing peptides between SP1 and SP2 (S. Slade, Warwick University. Pers comm).

Table 6. A new database search (using BLAST) of the amino acid sequences of two peptide fragments of *Serratia* phosphatase which were obtained in an earlier study (Jeong, 1992; Macaskie *et al.* 1994).

N-terminal sequence:

<i>Serratia</i> phosphatase (F1)	ARDVTTTPDFYYLKEAQSIDSLSLLPPPPPAVDSIDFLND
<i>Klebsiella pneumoniae</i>	GNDVTTKPDLYYLTNAOAIDSLALLPPPPAVGSI AFLND
<i>Providencia stuartii</i>	GNDVTTKPDLYYLNKNSQAIDSLALLPPPPPEVGSILFLND
<i>Morganella morganii</i> (PhoC)	DATTKPDLYYLNKNEQAIDSLKLLPPPPPEVGSIQFLND
<i>Shigella dysenteriae</i> (Periplasmic NSAP)	DVTTKPDLYYLTNDNAIDSLALLPPPPQIGSIAFLND
<i>Shigella flexneri</i> (Periplasmic NSAP PhoN1)	DVTTKPDLYYLTNDNAIDSLALLPPPPQIGSIAFLND
<i>Escherichia blattae</i>	DTTKPDLYYLNKNSAIDSLALLPPPPAVGSI AFLND
†Consensus	D-TT-PD-YYL-----IDSL-LLPPPP---SI-FLND
* <i>Francisella novicida</i> / <i>F.tularensis</i>	NSLALLPPPPATDSIAFMND
†Consensus	-----SL-LLPPPP---SI-F-ND

* Hypothetical protein *Francisella novicida* of similar to membrane associated phospholipid phosphatase of *Francisella tularensis* sub species *novicida*.

<i>Serratia</i> phosphatase (F2)	VICGYHNQSDVTAG
<i>Klebsiella pneumoniae</i>	VICGYHWQSDVDA
*(PAP2 family protein PhoN1)	
<i>Klebsiella pneumoniae</i> (PhoC)	VICGYHWQSDVDA
<i>Rahnella sp</i> (NSAP)	VICGYHWQSDVDA
<i>Shigella dysenteriae</i> (PhoN1)	VICGYHWQSDVDA
<i>Shigella flexneri</i> (PhoN1 NSAP)	VICGYHWQSDVDA
*PhoN (NSAP)	VICGYHWQSDVDA
<i>Salmonella typhimurium</i> (PhoN)	VICGAHWQSDVDAG
<i>Escherichia blattae</i>	VICGYHWQSDVDA
†Consensus	VICG-H-QSDV-A-

* PAP2 (Purple Acid Phosphatase). NSAP: Nonspecific acid phosphatase.

†Consensus: sequences found in six other enterobacterial phosphatases.

Table 6 compares previously published data (Jeong, 1992; Macaskie *et al.* 1994) with current protein databases.

F1: fragment 1; F2: fragment 2 (from Jeong, 1992).

At the time of the original investigation (Jeong, 1992) the reference databases and available comparator sequences were limited.

5.3.3 Examination of transition metal associations with *Serrratia* phosphatase by micro PIXE analysis

A previous study Jeong *et al* (1998) suggested that this phosphatase was probably not a metalloenzyme since its activity was unaffected by EDTA. However other studies (e.g. Reynolds & Schlesinger, 1969) noted that extended incubation with EDTA may be necessary to chelate metal atoms that are sequestered within a protein. Accordingly, SP1 and SP2 were treated with 10 mM EDTA for 24 h which, similarly, had no effect on their activity (Table 8). However even some EDTA resistant enzymes have been later shown to be metalloenzymes (Sugiura *et al.* 1981; Reilly *et al.* 1996 & Felts *et al.* 2006). Therefore, in an attempt to identify any bound metals, the *Serratia* phosphatases (SP1 and SP2) were examined using PIXE which, being able to detect X-ray emissions from both outer and inner shell electrons under bombardment with a high energy proton beam enables highly sensitive, element-specific detection at very low levels against the background at a spatial resolution of a few microns (Grime & Watt, 1990) (Fig. 21). Different areas of a specimen will have different metal contents according to thickness, therefore each metal is normalized against an internal standard, in this case chloride which was present in the suspension buffer. Only Zn (a common metal within phosphatases), Fe and Cu were found at levels above the background chloride and calcium (which is not a component of enzymes) was used as the reference to normalise the metal concentrations to overcome any heterogeneities in the sample points. Due to difficulties with the purification of SP1 (chapter 4), this isoform was not analysed by PIXE until much later in this study, therefore there is only one analysis of SP1 versus two PIXE analyses of SP2 (Table 7). Fig. 21.a. shows the protein drying ring used to create elemental maps during the analysis and Fig. 21.b and c shows the elemental maps of SP1 and SP2. Table 7 shows the two results for PIXE analysis of SP2 together with the single analysis of SP1.

It is strongly indicated that, like SP2, SP1 contains no bound metals since none were detected at a significant level above Ca^{2+} .

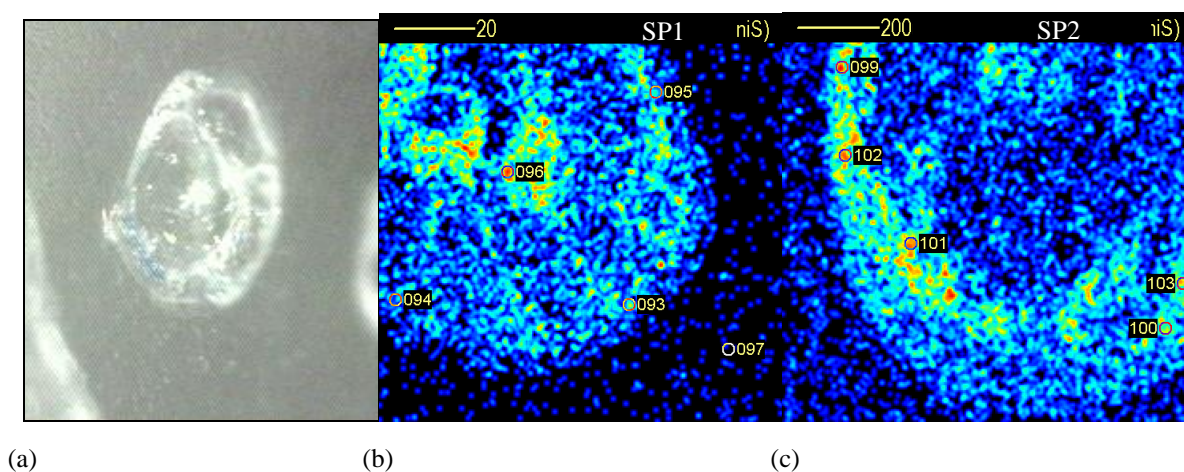


Fig. 21 (a) The protein drying ring on the target prior to PIXE analysis. (b) The PIXE map of the protein SP1 (c) SP2 with numbered circles indicating points selected for analysis of elemental composition. Pale areas show localisations of high sulphur content; numbers indicate sampling points. Analyses were compared to points outside the protein ring (buffer background).

Table 7 (a) Trace metal content of *Serratia* phosphatase SP1 and SP2 (atomic ratios of metal to Ca and metal to S)

Prep.		Metal concentration (atomic ratio to Ca)						
	No	Ca	Zn:Ca	Fe:Ca	Cu:Ca	[Cu + Fe]:Ca	Ti:Ca	Si:Ca
SP2	I	1.0	0.092	0.111 ± 0.015	0.060 ± 0.01	0.172 ± 0.052	0.020 ± 0.003	1.98
	II	1.0	0	0.179	0.018	0.196	0.029	0.456
SP1	II	1.0	0	0.243	0.043	0.286	0.029	0.457

		Metal concentration (atomic ratio to S)						
		S	Zn:S	Fe:S	Cu:S	[Cu + Fe]:S	Ti:S	Si:S
SP2	I	1.0	0.0054	0.0065	0.0032	0.0098	0.0015	0.111
	II	1.0	0.001	0.011	0.003	0.0113	0.001	0.041
SP1	II	1.0	0	0.010	0.001	0.011	0.001	0.037

(b) Metal concentration (ppm) over its detection limit (ppm) at that point for the lowest concentration found in each test

Prep.	Ca	Zn	Fe	Cu	Ti	Si	
SP2-[I	394/ 7	62/ 1	48/ 1	37/ 1	23/ 15	627/ 21
	II	NR					
SP1	II	NR					

(a) Trace metals were referenced to calcium since this is a background ubiquitous contaminant and to sulphur which is associated with the protein. The concentrations of Ti and Si are also shown since these are not known to be enzyme components or cofactors.

(b) Detection limits (ppm) are shown for each element in each particular spot; this has to be determined for each point individually since it depends on the sample thickness, which is not homogeneous (see the 'drying ring' in Fig.21 (b) using sulphur as the enzyme locator). Data in (b) are the lowest concentration in each point (ppm) from several replicates compared to its detection limit (ppm) at that point (bold). PIXE analysis gives the total metal composition; metals not shown were not present. The detection limits and PIXE technique is described by (Grime & Watt, 1990). The emission intensity for vanadium (see text) is such that an analysis detecting Ti will also detect V, since the limits of these are similar and PIXE detects all elements present. Data are means ± SEM for three of four determinations from random points within the protein spot. Data without ± SEM are all within 10 % error. NR: data not recorded.

Data from two independent preparations are shown (I and II): Preparation I was an earlier PIXE analysis of SP2 prior to the purification of SP1. Preparation II is the second analysis of SP2 and the first analysis of SP1. NR: Data not recorded.

Metal analysis of the *Serratia* phosphatase SP1 and SP2 is shown in Table 7, with individual results shown for two independent protein preparations for SP2 only (SP1 was analysed on one occasion) (each datum is the mean from at least three replicate determinations) since inter-batch variations were seen. The literature reports that transition metals can be interchangeable in metalloenzymes (e.g. Beck *et al.* 1988; Schenk *et al.* 1999) and hence pooled data for Fe and Cu in each analytical spot were also calculated. Titanium was examined as a ‘pathfinder’ element for vanadium since it is detectable by PIXE at lower levels than V. Ti was present only at the detection limit (within experimental error), therefore it was concluded that vanadium was absent. Cu and Fe were consistently present at more than 2-fold over the detection limits but at varying proportions. However the amounts (even pooled) were very small as compared to Ca and sulphur and their presence was concluded to be not biologically significant and probably attributable to non specific binding of trace metal impurities to the protein.

Using sulphur as a reference (16 atoms per tetrameric holoenzyme: Jeong *et al.* 1998) the number of atoms of Cu and Fe per molecule was too low to attribute any biological significance since the concentration was generally a few atoms per thousand sulphur atoms and, indeed, the transition metals were present at well below the levels of Si, a ubiquitous contaminant, and calcium, which is not known to have a biochemical role in the context of this study (Table 7). Hence from the elemental analysis it can be concluded that the *Serratia* phosphatases SP1 and SP2 are not metalloenzymes and that the very low levels of transition metals detected rule out any function in enzyme structure or function, although it cannot be precluded that metals associated with the surface of the protein and loosely bound were not lost during the preparation. Importantly, SP1 does not contain any trace metal which is absent from SP2.

Since PIXE provides a full elemental analysis the opportunity was taken to determine the P:S ratio. This was ~1:10 in preparation II (SP2 and SP1), and zero in preparation I for SP2, hence

no firm conclusions are possible about possible phosphorylation of the purified protein from micro PIXE analysis but phosphorylation seems unlikely. In accord with this, analysis with mass spectrometry at Warwick University concluded that the enzyme was not phosphorylated. The collision energy on MS scans is elevated in this type of analysis to determine if the neutral loss of H_3PO_4 occurs from a phosphorylated peptide. None of the peptides in the protein sample showed neutral loss of H_3PO_4 (data not shown).

5.3.4 Effect of various compounds on *Serratia* sp. phosphatase

SP1 and SP2 differ in their response to the effect of different chemicals and metals. Table 8 shows that both SP1 and SP2 are sensitive to inhibition by L-(+)-sodium tartrate, vanadium and fluoride, although they both show sensitivity to these substances, the degree of sensitivity varies between them (Table 8). Inhibition by L-(+)-sodium tartrate has been ‘classically’ used to identify acid phosphatases from lysosomal or prostatic origin in higher eukaryotes, which are glycoproteins (Oddie *et al.* 2000). However, it has been shown that the structure of the active site of tartrate-resistant and tartrate sensitive acid phosphatases are different in the two enzyme species (Lindqvist *et al.* 1993). Tartrate resistance for example, confers a completely different active site topology compared to tartrate sensitive enzymes (LaCount *et al.* 1998). Subsequently tartrate was used and tested as an effector substance in enzyme studies to allow comparison and classification of acid phosphatases e.g. by Rossolini *et al.* (1998), where phosphatases are divided into categories and sub categories depending on their similarities and behaviour towards effector substances. Sequencing studies on *Salmonella* PhoN and its PhoC homologue, revealed the PhoN phosphatase was missing one particular amino acid, when this was present, the new sequence was indistinguishable from PhoC (K.Choi, University of Pohang, pers comm. to L.E. Macaskie). This same classification approach is applied to the use of fluoride as an effector substance. However such methodologies have become less critical since the widespread

adoption of highly sophisticated methodologies where highly accurate mass analysis can reveal very subtle differences. Fluoride is a potent inhibitor of many acid phosphatases (Panara *et al.* 1990), however, SP2 was more sensitive to fluoride than SP1 retaining 15 % of initial activity after incubation with 4 mM, whilst SP1 retained 32 % of the initial activity. The effect of vanadium as a potent inhibitor of SP1 and SP2 is also relevant to the structure of the active site of the enzyme (Hemrika *et al.* 1997), and the classification of the phosphatases and indeed is critical in the function of vanadium haloperoxidases which are evolutionarily related to this phosphatase (Appendix 9). Both SP1 and SP2 were strongly inhibited by vanadyl sulphate (0.5 mM), retaining only 12 and 5 % of the initial activity, respectively. Because vanadyl sulphate is the lower valence form of vanadate and will readily donate electrons, it is possible that vanadyl became oxidised in the reaction, donating electrons to the phosphatase (effectively behaving as a reducing agent), however this effect is unlikely to be the cause of the inhibition as β -mercaptoethanol activated SP2 but it had no effect on SP1 (see below). Although redox effects of vanadyl cannot be ruled out from this experiment alone, it is more likely that vanadyl inhibition was via vanadyl occupation of the active site of both isoforms or by binding to key peptides.

EDTA is a chelator of divalent cations and is a potent inhibitor of metalloenzymes (Ackermann & Ahlers, 1976). Initial tests using EDTA found that it had no effect on either isoform after incubation for 1 h (Jeong, 1992). Tests using EDTA (this study) showed that it had no effect on SP1 or SP2 despite incubation with phosphatases for over 24 h, both SP1 and SP2 retained 100 % of initial activity after incubation (Table 8). This result is in accordance with the negative results obtained by PIXE analysis.

The effects of β -mercaptoethanol and H_2O_2 on SP1 and SP2 are shown in Table 8. Incorporation of β -mercaptoethanol (30 mM) increased the initial activity of SP2 by 30 % whilst SP1 remained unaffected. Conversely, H_2O_2 (50 mM) had no effect on SP2, but decreased the

initial activity of SP1 by ~ 70 %. These results suggest that the two enzymes are differentially sensitive to redox-active agents as SP2 is activated by the reducing agent β -mercaptoethanol and SP1 is inactivated by the oxidising agent H_2O_2 .

These effects of reducing/oxidising agents (i.e. β -mercaptoethanol and H_2O_2) on the phosphatase might be expected if the active site contained redox active metals like Fe, Cu or Mn, however this is unlikely due to the lack of effect of EDTA and from the micro-PIXE analysis. Purple acid phosphatases contain a binuclear iron centre, consequently the enzyme exists in two interconvertible states: enzymatically active reduced form (pink) Fe(II)-Fe(III) and an enzymatically inactive oxidised form (purple) Fe(III)-Fe(III) (Kaija, 2002). However SP1 and SP2 do not contain iron (Table 7). Before treatment with β -mercaptoethanol and H_2O_2 , SP2 (the more active form) could have been in an oxidised state and SP1 (the reduced activity form) in a reduced state, it is also possible that both isoforms were in a 'neutral' state prior to treatment with β -mercaptoethanol and H_2O_2 and reacted differently to the agents.

According to this study (from EDTA testing and PIXE analysis) it is unlikely that either SP1 or SP2 contain metals hence it follows that SP2 would have had to be in an oxidised state and SP1 in a reduced state, by virtue of their cystine/cysteine groups (4 per unit; Jeong, 1992) for β -mercaptoethanol to have reduced SP2 and H_2O_2 to have oxidised SP1.

In summary, a comprehensive study has revealed that although SP1 and SP2 are almost identical the critical difference between them is in their sensitivity to redox active agents. This, together with their differential sensitivity to ^{60}Co gamma irradiation (or more specifically the radicals which form from radiation effects on water; Paterson-Beedle *et al.* unpublished) allow speculation that the true role of the enzyme may be rooted in moderating the effects of free radicals on either the bacterial cell (a defensive function) or the host cell in pathogenic species (an attack function). Therefore attention was focussed on the comparative ability of SP1 and SP2 to affect the free radical damage on a target molecule.

Table 8. The effect of different chemicals on the enzyme activity of SP1 and SP2.

Effector substance	Effector concentration (mM)	Enzyme specific activity (%)	
		SP2	SP1
Control	0	100 \pm 2	100 \pm 2
L-(+)-Sodium tartrate	1	48 \pm 5	51 \pm 2
*EDTA	10	100 \pm 3	100 \pm 3
β-Mercaptoethanol	30	130 \pm 7	100 \pm 2
H₂O₂	50	100 \pm 2	31 \pm 3
^a Vanadyl sulphate	0.5	5 \pm 3	12 \pm 2
[†] Fluoride	4	15 \pm 5	32 \pm 1

* In the case of EDTA mixtures were left for 24 h before testing with the same result as shown.

^a Vanadium results taken from Jeong (1992).

[†] Fluoride results taken from Jeong (1992).

The activity was determined in 40mM MOPS-NaOH, pH 7.0. The activity was expressed as a percentage of that observed without effector substance. Data are mean \pm SEM of 3 experiments.

Key differences between SP1 and SP2 are shown in bold.

5.3.5 Phosphatase as a potentiator of free radical damage

Since the *Serratia* sp. phosphatase showed a resistance to radical generating molecules such as H_2O_2 and also to free radicals generated by γ irradiation (Chapter 1; Jeong, 1992), a possible involvement of the enzyme itself in free radical mediated reactions was tested using Fe(III) as an exogenous radical generator.

Fig. 22 shows the effect of purified SP1 and SP2 on the free radical damage to deoxyribose. Both enzymes are shown to potentiate free radical damage. SP2 shows an identical potentiating rate to SP1; rate constants for SP1 and SP2 were $-0.9 \times 10^{15} \text{ M}^{-1} \text{ S}^{-1}$ and $-1.0 \times 10^{15} \text{ M}^{-1} \text{ S}^{-1}$, respectively.

Free radical tests carried out by Halliwell & Gutteridge (1987) with superoxide dismutase gave a rate constant for radical scavenging ability using a simple test tube method, comparable to that observed with the more precise method of pulse radiolysis (Halliwell & Gutteridge, 1987). This method was used in this study with purified *Serratia* sp. acid phosphatase (SP1 and SP2) in comparison with ethanol (Fig. 22). Ethanol is a known scavenger of free radicals and a rate constant of $1.0 \times 10^9 \text{ M}^{-1} \text{ S}^{-1}$ was obtained which agrees with the published rate constant (for ethanol) of $1.4 \times 10^9 \text{ M}^{-1} \text{ S}^{-1}$ (Halliwell *et al.* 1987) and was similar to that seen using superoxide dismutase ($1.8 \times 10^9 \text{ m}^{-1} \text{ s}^{-1}$; Rotilio *et al.* 1972).

Denatured phosphatase was used as a control in these experiments and showed no effect on the free radical damage to deoxyribose (Fig. 22), whereas the active phosphatase; SP1 and SP2, were clear potentiators of free radical damage (Fig. 22). Halliwell & Gutteridge (1981) showed that superoxide dismutase moderated free radical damage to deoxyribose by 96 %, but when the enzyme was denatured, the same level of activity was observed, suggesting a largely chemical effect due to bound transition metal.

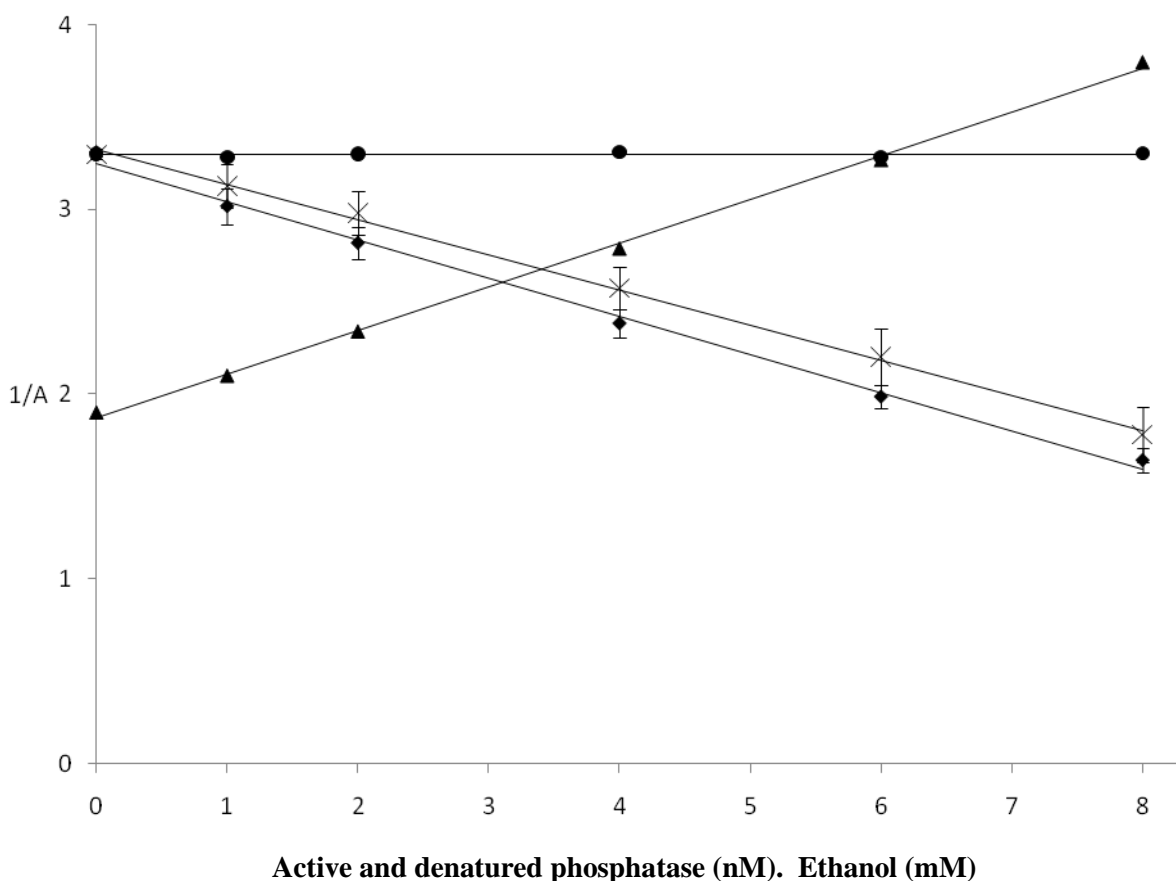


Fig. 22. The effect of phosphatase (SP2 and SP1), denatured phosphatase and ethanol on the free radical damage to deoxyribose: For phosphatase data are means \pm SEM from three experiments, where no error bars are shown, these were within the symbol dimensions. Denatured phosphatase and ethanol were each calculated from two separate experiments where errors were less than 5%, the means are displayed. The rate constant was determined from the slope of the line ($k = \text{slope} \times K_{\text{DR}} \times [\text{DR}] \times A^0$) as described in the text, giving a value of $-1 \times 10^{15} \text{ M}^{-1} \text{ S}^{-1}$. A is absorbance at 532 nm.

Phosphatase SP2 (♦), phosphatase SP1 (×), denatured phosphatase (●) and ethanol (▲).

The superoxide dismutase used in the published study was a copper protein and it is likely that Cu^{2+} (released upon denaturation; Halliwell & Gutteridge, 1981) was responsible for this effect, since free Cu^{2+} and copper amino acid complexes can scavenge O^{2-} (Klug-Roth *et al.* 1976) and hence generate free radicals by Fenton chemistry. In contrast (and in accordance with the absence of Fe and Cu in the protein) denatured phosphatase shows no effect on the free radical damage to deoxyribose. The rate constant using active enzyme (SP2, $-1 \times 10^{15} \text{ M}^{-1} \text{ S}^{-1}$; SP1, $-0.9 \times 10^{15} \text{ M}^{-1} \text{ S}^{-1}$; Fig. 22) showed that both of the *Serratia* phosphatases are effective potentiators of free radical damage; this effect is enzymatic since the heat inactivated enzyme was ineffective.

Peroxidases are usually associated with detoxification *in vivo* e.g. breaking down the H_2O_2 produced via oxic metabolism (Renirie *et al.* 2000). In the presence of Fe or Cu as a Fenton reagent, peroxidase activity is a powerful source of free radicals (single unpaired electrons) and from the effect on deoxyribose it can be concluded that the non-denatured phosphatase is behaving as a metal-unsubstituted peroxidase. Examination of the enzyme using electron paramagnetic resonance in the laboratories of Bruker Biospin failed to detect any evidence of unpaired electrons *per se* or indeed Fe or Cu (Paterson-Beedle *et al.* unpublished). However an association of the added Fe (III) with the enzyme during the free radical test (and *in vivo*) cannot be precluded.

Table 8 shows that SP2 remains unaffected by H_2O_2 , whilst SP1 is 70 % inhibited, however in Fig. 22 the pattern of behaviour of the enzymes is identical. This could suggest that having a target molecule on which to unload free radicals prevents inhibition of SP1. Fig. 22 shows the ability of the phosphatase enzyme to potentiate the effect of free radicals on the target molecule, however it does not show if this is because the enzyme has been itself stimulated or inhibited and is then only showing an enhanced activity. Further testing will need to be done to determine what happens to the enzyme activity of both SP1 and SP2 during and following the deoxyribose

reaction, however, it is clear that the reaction is enzymic and therefore it is clear that both SP1 and SP2 do retain some or all of their enzyme activity during the reaction.

5.4 Summary of the results

Similarities between SP1 and SP2

- They have similar (holoenzyme) molecular weight; 100,620 Da SP2 and 100,572 Da SP1, consisting of 4 subunits (~25 kDa).
- They have the same N-terminal sequences (up to 15 residues) (Jeong, 1992).
- Both were sensitive to inhibition by; L-(+)-sodium tartrate, vanadium and fluoride.
- Both resistant to EDTA.
- Peptide mass fingerprints of both enzymes showed they were identical.
- Neither enzyme is phosphorylated.
- They are not metalloenzymes.
- They both potentiate free radical damage.
- They have phosphomonoesterase activity and transphosphorylase activity (Jeong, 1992).
- They are immunologically cross reactive (Jeong, 1992).

Differences

- SP1 is less active than SP2.
- The activity of SP1 was reduced by H₂O₂, SP2 was unaffected (this study, Table 8).
- The activity of SP2 was increased by β -mercaptoethanol, SP1 was unaffected (this study, Table 8).
- SP1 has a PI of 8.9, SP2 has a PI of 9.1 (Jeong, 1992).
- SP1 has a negative charge, SP2 has a positive charge.
- They have slightly different amino acid compositions (Jeong, 1992; Chapter 1).
- SP1 was more thermostable than SP2 (Jeong, 1992)*.
- SP1 was more radiostable than SP2 (Jeong, 1992)*.

* Radiostability:

Jeong (1992) found that SP1 and SP2 differed from each other in their response to irradiation with a ⁶⁰Co gamma source. SP1 was more resistant, retaining 50 % of the initial activity after 7 h, whilst SP2 was radiation-sensitive, losing 50 % of the initial activity after 2-3 h.

6 Chapter 6 Crystallisation of *Serratia* sp. phosphatase SP2

Context

The previous chapter shows that there are very small differences between SP1 and SP2 but the most striking is their response to redox active agents. The purpose of this study is to crystallise the proteins in order to perform X-ray diffraction analysis to reveal any structural differences between them.

6.1 Chapter summary

This chapter discusses the results obtained in the attempt to successfully crystallise SP2. SP1 was not crystallised due to the limited quantity of purified protein produced. Crystallisation experiments using SP2 produced many different crystals, however a diffractable 3D crystal suitable for analysis was not obtained in this work. All crystal “screens” (i.e. buffers used) are discussed as well as the number and type of crystals produced in each case. One of the most intriguing findings of this work was that many of the crystals showed a gold or brown pigmentation, which is also discussed in this chapter.

6.2 Introduction

So far, all attempts to identify SP1 and SP2 using partial sequences and peptide mass fingerprints (chapter 5) to search protein data bases, have failed to find any protein matches. Obtaining crystal structures of SP1 and SP2 would allow comparison with the structures of other proteins already held in the protein data bank whose functions are already known. It is also possible that a protein match may be found for one or both of the *Serratia* phosphatases. If a match is not found, comparison to structurally similar enzymes may elucidate a role and function of these two enzymes. It was shown in chapter 5 that SP1 and SP2 are very similar in many ways but have important differences (e.g. in charge and susceptibility to radiation damage). It is possible that the two proteins are interchangeable conformationally and a successful x-ray diffraction analysis would confirm this and gain insight into the mechanistic function of the enzyme.

Further crystallisation work beyond initial crystal structures would involve the addition of metal ions such as Fe, Cu and V, in order to observe their possible effect on the protein

structure and enzyme activity. Adding metal ions such as vanadium would allow greater understanding of the enzymes relationship to vanadium peroxidase (chapter 5). The aim of using vanadium would be to determine if phosphohydrolase activity was inhibited (chapter 5) whilst looking at the possibility of the potentiation of peroxidase activity, i.e. a ‘switchable’ enzyme according to its function.

Serratia phosphatase SP2 was purified according to Materials and Methods chapter 2 and is also detailed and discussed in chapter 4. SP1 was not used in crystallisation experiments (i.e. initial screening) as the low recovery of the enzyme gave insufficient protein to set up initial screens. As SP1 and SP2 apparently have few differences (Jeong, 1992 and see earlier) the crystallisation experiments were set up using SP2 on the assumption that if the correct (crystallisation) buffer conditions were found, then an attempt to grow SP1 crystals under the same conditions would be attempted, therefore reducing unnecessary loss of SP1 in initial screening.

6.3 Methods

6.3.1 Set up of initial crystal screens to establish crystal growing conditions

Purified SP2 (of varying concentrations) was de-salted (as described in Materials and Methods) and washed with fresh Tris-HCl buffer (20 mM, pH 8.0) prior to crystallisation experiments (“crystal screens”). Purified protein was stored at 4 °C for no longer than 48 h prior to use in crystallisation experiments. Buffer compositions used in crystal screens can be seen in the results section of this chapter. Initial screens used SP2 at a concentration of 18 mg/ml in initial tests and a concentration of between 20-30 mg/ml in later tests. Buffer screens each hold 96 different buffer conditions contained within a plate which contains 96 small wells, each well holding one of these 96 different buffers. Plates were purchased from Qiagen, UK. Three separate buffer screens were used initially; Index (Hampton Research, USA), screens SW2 and

SW3 (designed and made by Dr Scott White, University of Birmingham, results not shown). In each crystallisation plate a control well was set up which contained buffer without protein so that any crystal growth in remaining buffers containing protein could be attributed to the presence of protein and not salts or other additives.

A robotic liquid handler (mosquito®, TTP Labtech) was used to pipette the buffers (1 µl) and protein (SP2, 1 nl, 18 mg/ml) into each well. Wells were then covered (“crystal clear” sealing tape), left overnight at 18 °C and then examined under a microscope daily with minimal disturbance until crystal growth was observed.

6.3.2 Set up of secondary crystal screens

Based on the results from the three initial crystal screens (Index, SW2 and SW3), further screens (screens 4 and 5) were made in an attempt to optimise the buffer conditions, with the aim of growing larger crystals and obtaining more crystal ‘hits’ (i.e. crystal growth in more of the buffer conditions).

From the initial screens it was evident that buffers containing phosphate and ammonium sulphate at pH 6.5, 7.0 and 7.5 contained protein crystals. New buffers were made (as shown below) using varying concentrations of di-sodium hydrogen orthophosphate (Pi) ($\text{HNa}_2\text{O}_4\text{P} \cdot 12\text{H}_2\text{O}$) (25 or 50 mM), sodium pyrophosphate (PPi) ($\text{Na}_4\text{P}_2\text{O}_7$) (5 or 10 mM), sodium tripolyphosphate (PPPi) ($\text{Na}_5\text{P}_3\text{O}_{10}$) (25 or 50 mM) and ammonium sulphate (1.3, 1.5 or 1.7 mM).

6.3.3 Preparation of buffer stock solutions

Stock solutions of the following chemicals were made:

Ammonium sulphate (AS) (4 M); di-sodium hydrogen orthophosphate (Pi) (500 mM); sodium pyrophosphate (PPi) (100 mM); sodium tripolyphosphate (PPPi) (300 mM). All solutions used ultrapure water. Three stock solutions of imidazole (1 M) were also made and the pH was adjusted to 6.5, 7.0 and 7.5 for the three imidazole solutions using HCl (1 M) and NaOH (1 M) (dependent on required pH). Imidazole stock solutions (1 M) were used to adjust the pH of the crystallisation buffers. All solutions were then filtered using syringe filters (Millipore, UK) (pore size; 0.45 µm) and stored at 4 °C prior to use. Large quantities (1 L stocks) of all the above phosphate stock solutions were frozen at -70 °C for use in future screens to avoid the variability associated with making up fresh solutions since conditions yielding good crystals are difficult to re create due to the small and inevitable changes in buffer concentration when making new stock solutions.

6.3.4 Preparation and set up of optimisation screens (Index, screen 2 (SW2) and screen 3 (SW3))

After initial screening using the three screens (Index, screens SW2 and SW3), a total of seven further screens were set up sequentially (based on the previous results of each screen). The volumes of protein used in these screens was increased from the small quantities used in the initial screens (nl) to larger volumes (µl) as larger crystals were required. These optimisation screens utilised a number of different variables in addition to variation of buffer composition, such as protein concentration (typically 20-30 mg/ml, as SP2 is very soluble, therefore a higher concentration is needed), protein drop to buffer drop ratio (in order to add further variability to the buffer and protein concentration) and the use of additives such as glycerol-2-phosphate and

glycerol to potentially stabilise the protein. Buffer drop volumes of 1 μ l were used in optimisation screens. Protein drop volumes (variable concentrations) of 1, 2 and 3 μ l were also used (dependent on the quantity of protein available at the time of screening). Crystallisation plates were set up by pipetting the required volume of buffer (1-3 μ l) into the well followed by the protein. The protein droplet was pipetted onto the buffer droplet and then the buffer drop (containing protein) was pipetted up and down three times to ensure good mixing and dispersion of protein. Care was taken to ensure air bubbles did not enter the protein/buffer droplet on mixing as this would have disrupted crystallisation.

6.4 Results and discussion

6.4.1 Initial screens using Index, screens SW2 and SW3.

6.4.1.1 Screen: “Index” (✓ denotes crystals apparent)

Well no	Salt	Buffer	Precipitant	Crystals	
A	1	None	0.1 M Citric acid pH 3.5	2.0 M Ammonium sulphate	✗
	2	None	0.1 M Sodium acetate trihydrate pH 4.5	2.0 M Ammonium sulphate	✗
	3	None	0.1 M BIS-TRIS pH 5.5	2.0 M Ammonium sulphate	✓
	4	None	0.1 M BIS-TRIS pH 6.5	2.0 M Ammonium sulphate	✓
	5	None	0.1 M HEPES pH 7.5	2.0 M Ammonium sulphate	✗
	6	None	0.1 M Tris pH 8.5	2.0 M Ammonium sulphate	✗
	7	None	0.1 M Citric acid pH 3.5	3.0 M Sodium chloride	✓
	8	None	0.1 M Sodium acetate trihydrate pH 4.5	3.0 M Sodium chloride	✓
	9	None	0.1 M BIS-TRIS pH 5.5	3.0 M Sodium chloride	✗
	10	None	0.1 M BIS-TRIS pH 6.5	3.0 M Sodium chloride	✗
	11	None	0.1 M HEPES pH 7.5	3.0 M Sodium chloride	✗
	12	None	0.1 M Tris pH 8.5	3.0 M Sodium chloride	✗
B	1	None	0.1 M BIS-TRIS pH 5.5	0.3 M Magnesium formate dihydrate	✗
	2	None	0.1 M BIS-TRIS pH 6.5	0.5 M Magnesium formate dihydrate	✗
	3	None	0.1 M HEPES pH 7.5	0.5 M Magnesium formate dihydrate	✗
	4	None	0.1 M Tris pH 8.5	0.3 M Magnesium formate dihydrate	✗
	5	None	None - pH 5.6	1.26 M Sodium phosphate monobasic monohydrate 0.14 M Potassium phosphate dibasic	✗
	6	None	None - pH 6.9	0.49 M Sodium phosphate monobasic monohydrate 0.91 M Potassium phosphate dibasic	✓
	7	None	None - pH 8.2	0.056 M Sodium phosphate monobasic monohydrate 1.344 M Potassium phosphate dibasic	✗
	8	None	0.1 M HEPES pH 7.5	1.4 M Sodium citrate tribasic dihydrate	✗
	9	None		1.8 M Ammonium citrate tribasic pH 7.0	✗
	10	None		0.8 M Succinic acid pH 7.0	✗
	11	None		2.1 M DL-Malic acid pH 7.0	✗
	12	None		2.8 M Sodium acetate trihydrate pH 7.0	✗
C	1	None		3.5 M Sodium formate pH 7.0	✗
	2	None		1.1 M Ammonium tartrate dibasic pH 7.0	✗
	3	None		2.4 M Sodium malonate pH 7.0	✓
	4	None		35% v/v Tacsimate pH 7.0	✗
	5	None	None	60% v/v Tacsimate pH 7.0	✓
	6	0.1 M Sodium chloride	0.1 M BIS-TRIS pH 6.5	1.5 M Ammonium sulfate	✓
	7	0.8 M Potassium sodium tartrate tetrahydrate	0.1 M Tris pH 8.5	0.5% w/v Polyethylene glycol monomethyl ether 5,000	✗
	8	1.0 M Ammonium sulphate	0.1 M BIS-TRIS pH 5.5	1% w/v Polyethylene glycol 3,350	✗
	9	1.1 M Sodium malonate pH 7.0	0.1 M HEPES pH 7.0	0.5% v/v Jeffamine ED-2001 ® pH 7.0	✗
	10	1.0 M Succinic acid pH 7.0	0.1 M HEPES pH 7.0	1% w/v Polyethylene glycol monomethyl ether 2,000	✗
	11	1.0 M Ammonium sulphate	0.1 M HEPES pH 7.0	0.5% w/v Polyethylene glycol 8,000	✗
	12	15% v/v Tacsimate pH	0.1 M HEPES pH 7.0	2% w/v Polyethylene glycol 3,350	✗

		7.0			
D	1	None	None	25% w/v Polyethylene glycol 1,500	✗
	2	None	0.1 M HEPES pH 7.0	30% v/v Jeffamine M-600 @ pH 7.0	✗
	3	None	0.1 M HEPES pH 7.0	30% v/v Jeffamine ED-2001 @ pH 7.0	✗
	4	None	0.1 M Citric acid pH 3.5	25% w/v Polyethylene glycol 3,350	✗
	5	None	0.1 M Sodium acetate trihydrate pH 4.5	25% w/v Polyethylene glycol 3,350	✗
	6	None	0.1 M BIS-TRIS pH 5.5	25% w/v Polyethylene glycol 3,350	✗
	7	None	0.1 M BIS-TRIS pH 6.5	25% w/v Polyethylene glycol 3,350	✗
	8	None	0.1 M HEPES pH 7.5	25% w/v Polyethylene glycol 3,350	✗
	9	None	0.1 M Tris pH 8.5	25% w/v Polyethylene glycol 3,350	✓
	10	None	0.1 M BIS-TRIS pH 6.5	20% w/v Polyethylene glycol monomethyl ether 5,000	✗
	11	None	0.1 M BIS-TRIS pH 6.5	28% w/v Polyethylene glycol monomethyl ether 2,000	✗
	12	0.2 M Calcium chloride dehydrate	0.1 M BIS-TRIS pH 5.5	45% v/v (+/-)-2-Methyl-2,4-pentanediol	✗
E	1	0.2 M Calcium chloride dehydrate	0.1 M BIS-TRIS pH 6.5	45% v/v (+/-)-2-Methyl-2,4-pentanediol	✗
	2	0.2 M Ammonium acetate	0.1 M BIS-TRIS pH 5.5	45% v/v (+/-)-2-Methyl-2,4-pentanediol	✗
	3	0.2 M Ammonium acetate	0.1 M BIS-TRIS pH 6.5	45% v/v (+/-)-2-Methyl-2,4-pentanediol	✗
	4	0.2 M Ammonium acetate	0.1 M HEPES pH 7.5	45% v/v (+/-)-2-Methyl-2,4-pentanediol	✗
	5	0.2 M Ammonium acetate	0.1 M Tris pH 8.5	45% v/v (+/-)-2-Methyl-2,4-pentanediol	✗
	6	0.05 M Calcium chloride dehydrate	0.1 M BIS-TRIS pH 6.5	30% v/v Polyethylene glycol monomethyl ether 550	✗
	7	0.05 M Magnesium chloride hexahydrate	0.1 M HEPES pH 7.5	30% v/v Polyethylene glycol monomethyl ether 550	✗
	8	0.2 M Potassium chloride	0.05 M HEPES pH 7.5	35% v/v Pentaerythritol propoxylate (5/4 PO/OH)	✗
	9	0.05 M Ammonium sulphate	0.05 M BIS-TRIS pH 6.5	30% v/v Pentaerythritol ethoxylate (15/4 EO/OH)	✗
	10	None	0.1 M BIS-TRIS pH 6.5	45% v/v Polypropylene glycol P 400	✗
	11	0.02 M Magnesium chloride hexahydrate	0.1 M HEPES pH 7.5	22% w/v Poly(acrylic acid sodium salt) 5,100	✗
	12	0.01 M Cobalt (II) chloride hexahydrate	0.1 M Tris pH 8.5	20% w/v Polyvinylpyrrolidone K 15	✗
F	1	0.2 M L-Proline	0.1 M HEPES pH 7.5	10% w/v Polyethylene glycol 3	✗
	2	0.2 M Trimethylamine N-oxide dihydrate	0.1 M Tris pH 8.5	20% w/v Polyethylene glycol monomethyl ether 2	✗
	3	5% v/v Tacsimate pH 7.0	0.1 M HEPES pH 7.0	10% w/v Polyethylene glycol monomethyl ether 5	✗
	4	0.005 M Cobalt (II) chloride hexahydrate 0.005 M Nickel (II) chloride hexahydrate 0.005 M Cadmium chloride hydrate 0.005 M Magnesium chloride hexahydrate	0.1 M HEPES pH 7.5	12% w/v Polyethylene glycol 3	✗
	5	0.1 M Ammonium acetate	0.1 M BIS-TRIS pH 5.5	17% w/v Polyethylene glycol 10	✓
	6	0.2 M Ammonium sulphate	0.1 M BIS-TRIS pH 5.5	25% w/v Polyethylene glycol 3	✗
	7	0.2 M Ammonium sulphate	0.1 M BIS-TRIS pH 6.5	25% w/v Polyethylene glycol 3	✓
	8	0.2 M Ammonium sulphate	0.1 M HEPES pH 7.5	25% w/v Polyethylene glycol 3	✓
	9	0.2 M Ammonium sulphate	0.1 M Tris pH 8.5	25% w/v Polyethylene glycol 3	✗
	10	0.2 M Sodium chloride	0.1 M BIS-TRIS pH 5.5	25% w/v Polyethylene glycol 3	✗

	11	0.2 M Sodium chloride	0.1 M BIS-TRIS pH 6.5	25% w/v Polyethylene glycol 3	✗
	12	0.2 M Sodium chloride	0.1 M HEPES pH 7.5	25% w/v Polyethylene glycol 3	✓
G	1	0.2 M Sodium chloride	0.1 M Tris pH 8.5	25% w/v Polyethylene glycol 3	✓
	2	0.2 M Lithium sulphate monohydrate	0.1 M BIS-TRIS pH 5.5	25% w/v Polyethylene glycol 3	✗
	3	0.2 M Lithium sulphate monohydrate	0.1 M BIS-TRIS pH 6.5	25% w/v Polyethylene glycol 3	✗
	4	0.2 M Lithium sulphate monohydrate	0.1 M HEPES pH 7.5	25% w/v Polyethylene glycol 3	✓
	5	0.2 M Lithium sulphate monohydrate	0.1 M Tris pH 8.5	25% w/v Polyethylene glycol 3	✓
	6	0.2 M Ammonium acetate	0.1 M BIS-TRIS pH 5.5	25% w/v Polyethylene glycol 3	✓
	7	0.2 M Ammonium acetate	0.1 M BIS-TRIS pH 6.5	25% w/v Polyethylene glycol 3	✗
	8	0.2 M Ammonium acetate	0.1 M HEPES pH 7.5	25% w/v Polyethylene glycol 3	✓
	9	0.2 M Ammonium acetate	0.1 M Tris pH 8.5	25% w/v Polyethylene glycol 3	✗
	10	0.2 M Magnesium chloride hexahydrate	0.1 M BIS-TRIS pH 5.5	25% w/v Polyethylene glycol 3	✓
	11	0.2 M Magnesium chloride hexahydrate	0.1 M BIS-TRIS pH 6.5	25% w/v Polyethylene glycol 3	✗
	12	0.2 M Magnesium chloride hexahydrate	0.1 M HEPES pH 7.5	25% w/v Polyethylene glycol 3	✗
H	1	0.2 M Magnesium chloride hexahydrate	0.1 M Tris pH 8.5	25% w/v Polyethylene glycol 3	✓
	2	0.2 M Potassium sodium tartrate tetrahydrate	None	20% w/v Polyethylene glycol 3	✗
	3	0.2 M Sodium malonate pH 7.0	None	20% w/v Polyethylene glycol 3	✗
	4	0.2 M Ammonium citrate tribasic pH 7.0	None	20% w/v Polyethylene glycol 3	✓
	5	0.1 M Succinic acid pH 7.0	None	15% w/v Polyethylene glycol 3	✓
	6	0.2 M Sodium formate	None	20% w/v Polyethylene glycol 3	✗
	7	0.15 M DL-Malic acid pH 7.0	None	20% w/v Polyethylene glycol 3	✗
	8	0.1 M Magnesium formate dihydrate	None	15% w/v Polyethylene glycol 3	✓
	9	0.05 M Zinc acetate dehydrate	None	20% w/v Polyethylene glycol 3	✗
	10	0.2 M Sodium citrate tribasic dihydrate	None	20% w/v Polyethylene glycol 3	✗
	11	0.1 M Potassium thiocyanate	None	30% w/v Polyethylene glycol monomethyl ether 2	✗
	12	0.15 M Potassium bromide	None	30% w/v Polyethylene glycol monomethyl ether 2	✗

* Index was purchased as a readymade screen from Hampton Research (USA). Chemical information in the above table is the information used and distributed by the company.

From the Index screen, it can be seen that no clear patterns emerge. Specific precipitants could not be seen to be promoting crystallisation under any conditions, therefore it was decided that the most commonly used precipitant (ammonium sulphate) would be used in further screens.

6.4.1.2 Screen: 2 (SW1)

Buffer composition not recorded (NR)

Well no	Buffer pH 7.0	Crystals
A 1-9		✓
10-12		✗
B 1-2		✓
3-8		✗
9		✓
10		✗
11-12		✓
C 1-12		✗
D 1-12		✗
E 1-12		✗
F 1-12		✗
G 1-12		✓
H 1-5		✗
6		✓
7-9		✗
10-11		✓
12		✗

Screen 2 (developed by S. White) shows little difference in the use for pH 7 or pH 8 with respect to crystallisation outcomes.

6.4.1.3 Screen: 3 (SW2)

Buffer composition not recorded (NR)

Well no	Buffer pH 8.0	Crystals
A 1		✓
2		✗
3-10		✓
11-12		✗
B 1		✗
2		✓
3		✗
4		✓
5		✗
6		✓
7		✗
8		✓
9		✗
10		✓
11-12		✗
C 1-12		✗
D 1-12		✗
E 1-12		✗
F 1-12		✗
G 1-5		✓
6		✗
7-12		✓
H 1-7		✓
8		✗
9-12		✓

6.4.2 Optimisation Screen 4

Well number	Buffer conditions			Crystals	Crystal type	Crystal images	Pigment
	pH	Phosphate (mM)	Ammonium sulphate (AS) (M)				
A	1	7	Pi 25	1.5	× control	Control (no protein)	×
	2	7.5	Pi 50	1.7	✓	Small crystals	×
	3	7.5	Pi 25	1.5	✓	Small crystals	×
	4	6.5	Pi 25	1.5	×		×
	5	7	Pi 50	1.5	✓	Thin needles	×
	6	7	0	1.5	✓	Very few needles	×
	7	7	0	1.3	×		×
	8	7.5	0	1.3	×		×
	9	7.5	PPi 10	1.7	✓	Large needles	×
	10	7.5	PPi 5	1.5	×		×
	11	7	PPi 5	1.3	×		×
	12	7	PPi 10	1.5	×		×
B	1	6.5	0	1.7	×		×
	2	6.5	0	1.3	×		×
	3	7	Pi 25	1.3	×		×
	4	7	Pi 25	1.7	✓	Small 3D crystals	×
	5	7	Pi 50	1.3	×		×
	6	7	Pi 50	1.7	✓	Oil drops	×
	7	7	PPi 5	1.5	×		×
	8	7.5	0	1.7	✓	Needles	×
	9	7	PPi 5	1.7	✓	Thin needles	×
	10	6.5	PPi 5	1.5	×		×
	11	7	PPi 10	1.3	×		×
	12	7	PPi 10	1.7	✓	Large thin needle cluster	×
C	1	7	PPPi 25	1.5	×		×
	2	7.5	PPPi 50	1.7	✓	Small needle clusters	×
	3	7	PPPi 25	1.7	✓	Very large fine needle cluster	×
	4	7	PPPi 25	1.3	×		×
	5	7	PPPi 50	1.3	×		×

D	1	6.5	PPPi 25	1.5	×		×
	2	7.5	PPPi 25	1.5	✓	Large fine needle cluster	×
	3	7	PPPi 50	1.7	✓	Fine needle clusters	×
	4	7	PPPi 50	1.5	×		×

Key: Pi (di-sodium hydrogen orthophosphate): PPi (sodium pyrophosphate): PPPi (sodium tripolyphosphate).

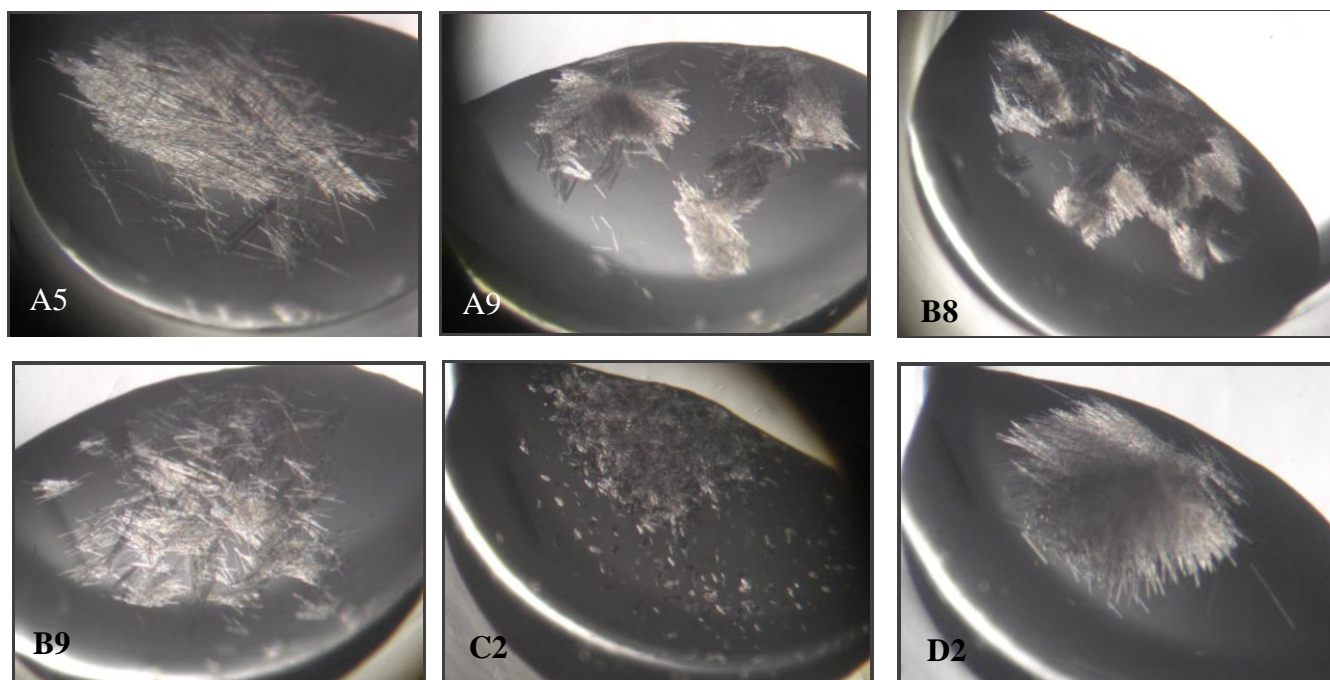


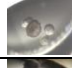
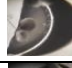



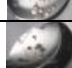
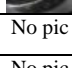



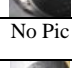







Fig. 23. Pictures of *Serratia* phosphatase SP2 crystals from a selection of buffer conditions taken from optimisation screen 4. The picture number relates to the well number in the optimisation screen showing the buffer conditions for each crystal.

The majority of crystals from optimisation screen 4 were needles (Fig. 23). A5 shows single needles, which were very thin, indicating that the nucleation rate was too high. A9, B8, B9 and C2 all show various forms of needles and D2 shows a thin needle cluster originating from a single nucleation point. These results suggested that the next screen needed to have a reduced protein concentration and/or precipitant concentration in order to reduce the nucleation rate. Pigment was not observed in crystals from this screen.

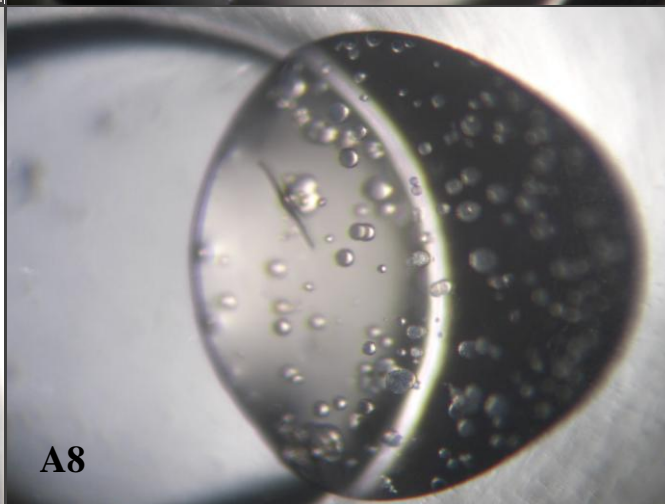
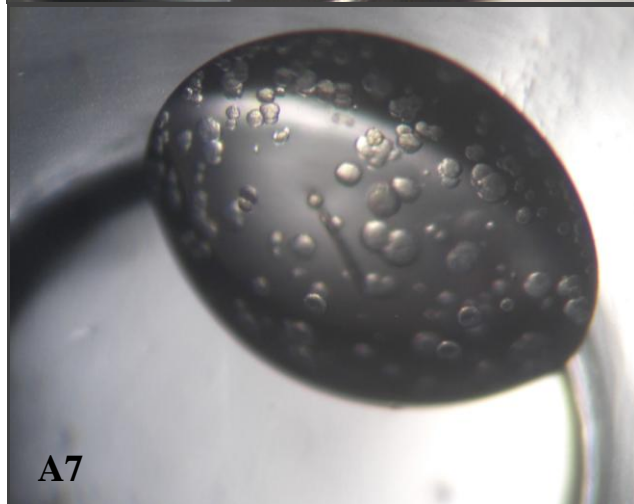
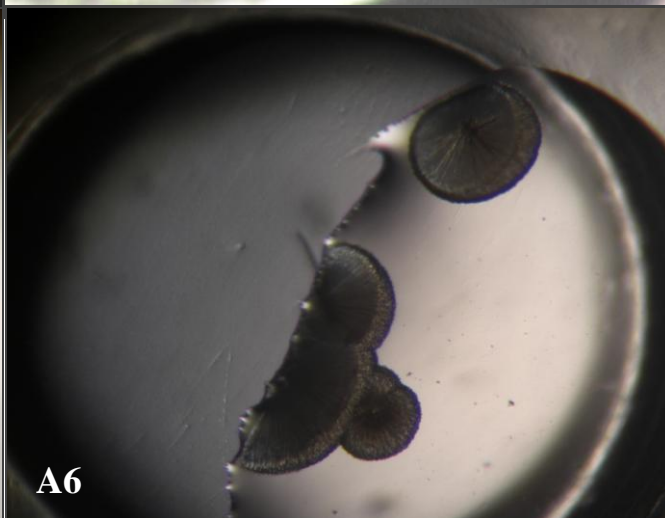
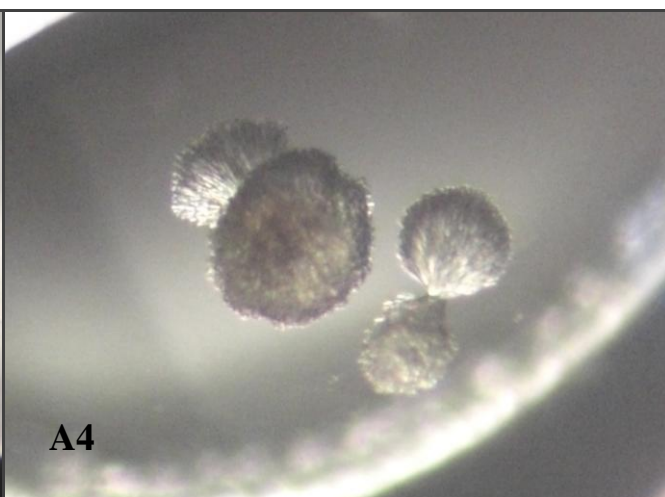
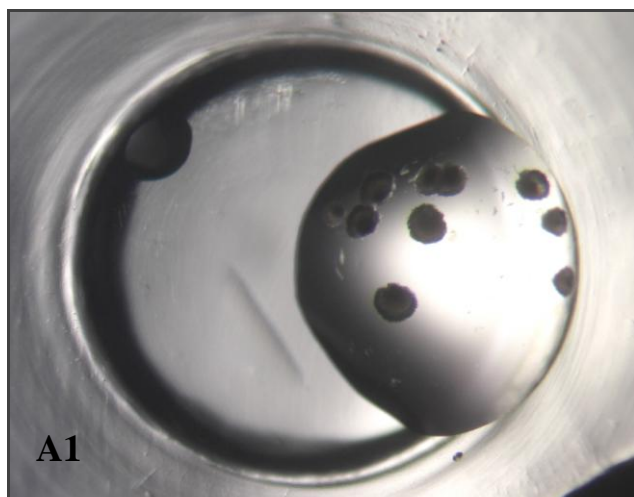
Unusable protein crystals were sacrificed in order to confirm the crystals were in fact protein and not crystals of salt, this was achieved by removing the crystal from the buffer solution and running a sample on SDS-PAGE to visualise the protein bands as shown in chapter 4 (Fig. 18), a sample of the buffer was also run on the gel alongside the crystal sample. A single band was seen as in chapter 4 Fig. 18.

6.4.3 Optimisation screen 5

Well number	Buffer conditions			Other variables Ammonium sulphate (1.5 M)		Crystals	Crystal pictures	Pigment
	P (mM)		PH	Protein drop: Buffer Drop volume (μL) (1:1 2:1 3:1)	Protein concentration (mg/mL)			
A 1	Pi	25	6.5	1	30	✓		✓
2		25	6.5	2	20	×		✓
3		25	6.5	2	30	✓		✓
4		25	6.5	3	20	✓		✓
5		25	6.5	3	30	✓		✓
6		25	7	1	30	✓		✓
7		25	7	2	20	✓		✓
8		25	7	2	30	✓		✓
9		25	7	3	20	✓		✓
10		25	7	3	30	✓		✓
11		25	7.5	1	30	✓	No pic	×
12		25	7.5	2	20	✓	No pic	×
B 1		25	7.5	2	30	✓		✓
2		25	7.5	3	20	✓		✓
3		25	7.5	3	30	✓		×
4		50	6.5	1	30	✓		×
5		50	6.5	2	20	×	No Pic	×
6		50	6.5	2	30	✓		×
7		50	6.5	3	20	×	No Pic	×
8		50	6.5	3	30	✓		✓
9		50	7	1	30	✓		✓
10		50	7	2	20	✓	No Pic	×
11		50	7	2	30	✓		✓
12		50	7	3	20	✓		✓
C 1		50	7	3	30	✓	No Pic	✓
2		50	7.5	1	30	✓	No Pic	×
3		50	7.5	2	20	✓	No Pic	×
4		50	7.5	2	30	✓	No Pic	×
5		50	7.5	3	20	✓	No Pic	✓
6		50	7.5	3	30	✓	No Pic	✓
7	PPi	5	6.5	1	30	✓	No Pic	✓

	8	5	6.5	2	20	✓	No Pic	×
	9	5	6.5	2	30	✓	No Pic	×
	10	5	6.5	3	20	✓	No Pic	×
	11	5	6.5	3	30	✓	No Pic	✓
	12	5	7	1	30	✓	No Pic	✓
D	1	5	7	2	20	✓	No Pic	✓
	2	5	7	2	30	✓	No Pic	×
	3	5	7	3	20	✓	No Pic	✓
	4	5	7	3	30	✓	No Pic	×
	5	5	7.5	1	30	✓	No Pic	×
	6	5	7.5	2	20	✓	No Pic	×
	7	5	7.5	2	30	✓	No Pic	×
	8	5	7.5	3	20	✓	No Pic	✓
	9	5	7.5	3	30	✓	No Pic	✓
	10	10	6.5	1	30	✓	No Pic	×
	11	10	6.5	2	20	×	No Pic	×
	12	10	6.5	2	30	✓	No Pic	✓
E	1	10	6.5	3	20	×	No Pic	×
	2	10	6.5	3	30	×	No Pic	×
	3	10	7	1	30	*NO PROTEIN		×
	4	10	7	2	20	✓	No Pic	×
	5	10	7	2	30	*NO PROTEIN		×
	6	10	7	3	20	*NO PROTEIN		×
	7	10	7	3	30	*NO PROTEIN		×
	8	10	7.5	1	30	*NO PROTEIN		×
	9	10	7.5	2	20	✓	No Pic	×
	10	10	7.5	2	30	*NO PROTEIN		×
	11	10	7.5	3	20	✓	No Pic	×
	12	10	7.5	3	30	*NO PROTEIN		×

* NO PROTEIN. This was due to the fact that the screen was designed before the protein was purified and there was not enough protein available to add to all buffer conditions.



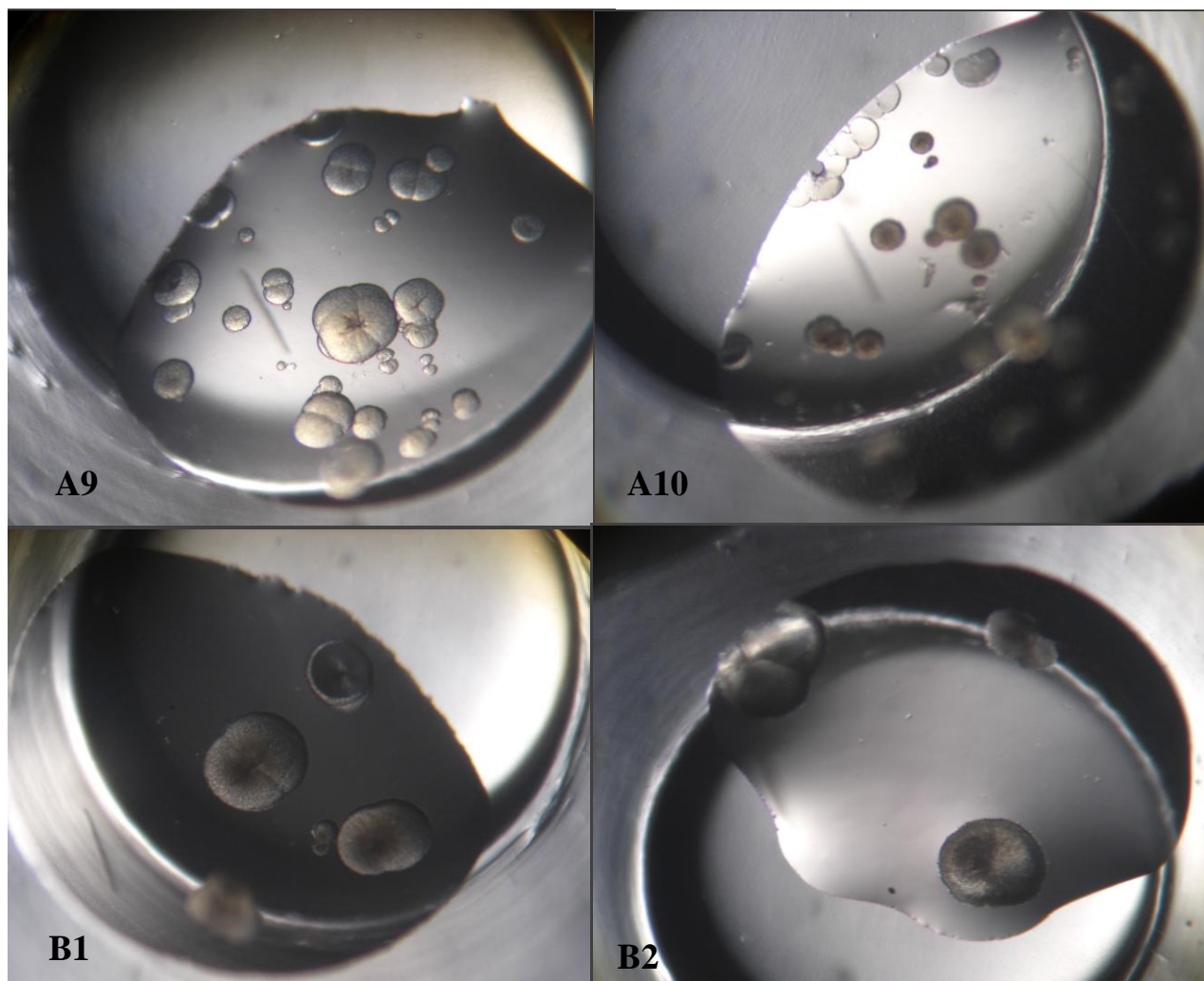


Fig. 24. Crystal pictures (SP2) from optimisation screen 5. A4 and A5 show needle haystacks and needles (respectively). The remaining pictures all show spherulites.

Optimisation screen 5 showed a large number of buffer conditions yielding protein crystals. Unfortunately none of the conditions grew a 3D crystal large enough for analysis, however, spherulites or needles grew in 47 out of 53 buffer conditions containing protein (SP2). Spherulites (Fig. 24. A9, A10, B1, B2) represent a crystal phase which shows that the conditions are improving towards crystallisation and that further optimisation of the conditions around the condition which yielded spherulites should lead to crystal growth worthy of analysis.

Pictures A1-B2 (Fig. 24) show some of the crystals representative of optimisation screen 5. A1, A6, A9, A10, B1 and B2 all show spherulites. A7 and A8 were also spherulites as they were probed with a needle and found to be “crunchy” which would not be the case if they were oil drops. A4 and A5 show needle haystacks and needles (respectively). Some of the spherulites showed a deep yellow/gold or brown pigmentation, which has not been captured sufficiently well in the above photographs, however yellow pigment was seen in the centre of crystals (spherulites) in A9 (an enlarged picture can be seen in Fig. 25 below). Other pictures show the brown pigment which sometimes appeared as a deep red/brown pigment although it is currently unknown what causes this pigmentation in the crystallised enzyme.

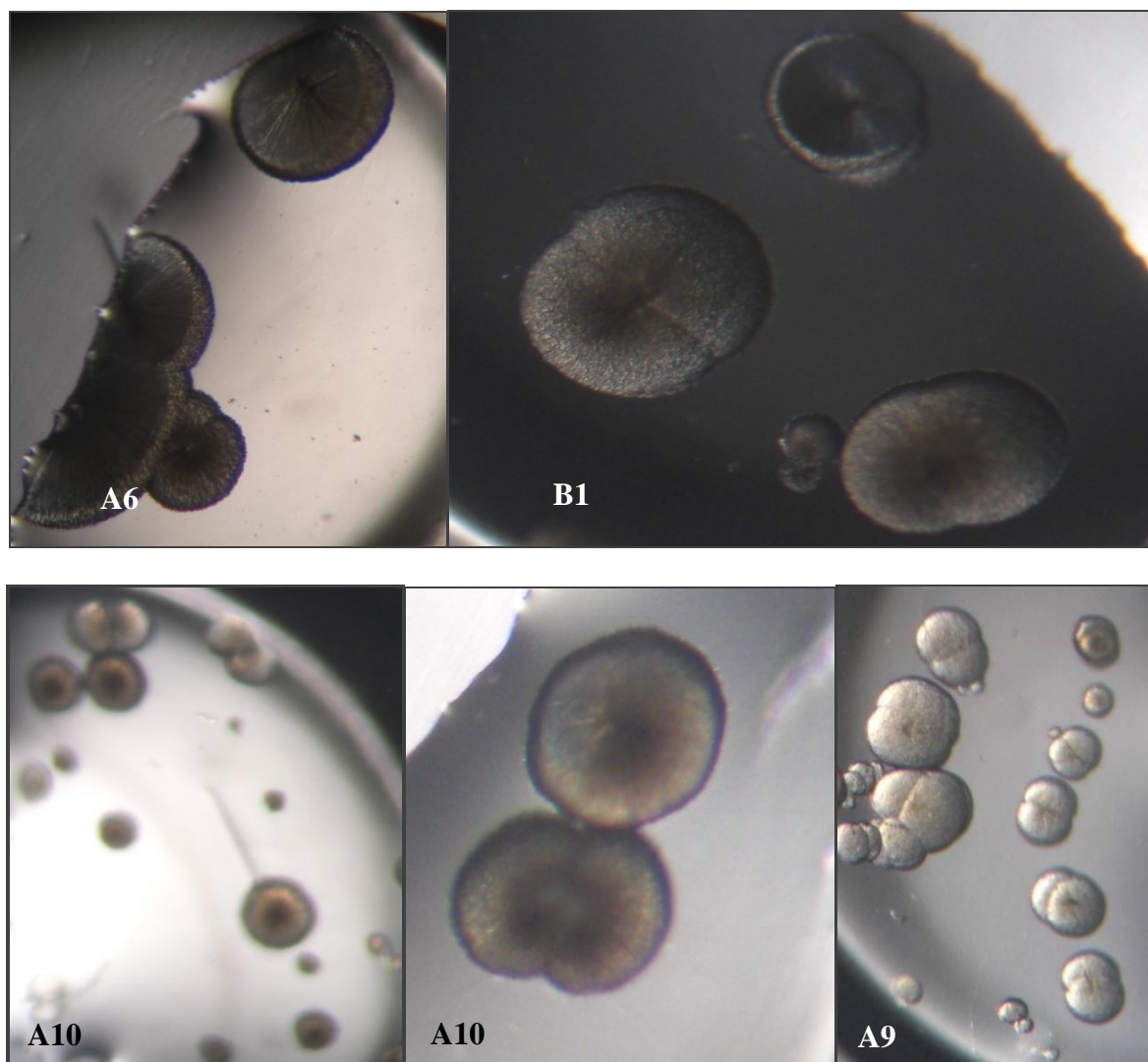


Fig. 25. Enlarged images of crystals found in optimisation screen 5, showing visible pigmentation of spherulites. A6 and B1 show spherulites with a dark brown pigmentation, this colour looked slightly red to the naked eye but was not captured well on camera. A10 shows a slightly red/brown pigmentation and A9 shows a yellow/gold pigmentation present at the centre of the spherulites (this colour was also vivid to the naked eye).

6.4.4 Optimisation screen 6 - addition of glycerol to promote stability

Ammonium sulphate (1.5 M), glycerol (5%), pH 7.0.					
Well no	Pi, PPI, PPPi (mM)		Protein drop volume (μl)	Crystals	Pigment
A	1	Pi 25	1	✓	x
	2	25	2	x	x
	3	50	1	✓	x
	4	50	2	✓	x
	5	PPI 5	1	x	x
	6	5	2	✓	x
	7	10	1	✓	x
	8	10	2	✓	x
	9	PPPi 25	1	✓	x
	10	25	2	✓	x
	11	50	1	✓	x
	12	50	2	✓	x

6.4.5 Optimisation screen 7 addition of glycerol-2-phosphate to promote crystallisation

Glycerol-2-phosphate (5 mM), ammonium sulphate (1.5 M), pH 7.0.					
Well no	Pi, PPI, PPPi (mM)		Protein drop volume (μl)	Crystals	Pigment
B	1	Pi 25	1	x	x
	2	25	2	x	x
	3	50	1	✓	x
	4	50	2	✓	x
	5	PPI 5	1	x	x
	6	5	2	x	x
	7	10	1	x	x
	8	10	2	x	x
	9	PPPi 25	1	x	x
	10	25	2	✓	x
	11	50	1	✓	x
	12	50	2	✓	x

Optimisation screens 6 and 7 were set up with a limited amount of protein available, hence the limited number of buffer conditions (above). Glycerol was used in screen 6 and glycerol-2-phosphate in screen 7 to see if 3D crystals (instead of needles) would grow. Glycerol is known to add stability to the protein in aqueous solutions and it is also a known cryoprotectant, which would help prevent crystals cracking during the flash freezing process used before structural analysis. All crystals grown in screen 6 were needles, however it was apparent that the needles were not as thin as those seen in previous screens, which could mean that glycerol added some stability to the solution. Screen 7 (with glycerol-2-phosphate in lieu of glycerol) also grew needles and spherulites. G2P is the preferred substrate of SP2 (the relative k_m values for G2P for SP1 and SP2 are; 1963 μm and 938 μm , respectively; Jeong, 1992), therefore it was hypothesised that binding of this to the active site might add some stability to the protein and promote the growth of better crystals. No obvious differences were apparent between screens 6 and 7.

6.5 Discussion

For crystal growth the best conditions were those which used a high concentration of protein ~ 30 mg/ml; due to the high solubility of the protein, ammonium sulphate is also a requirement as it helps precipitation of the protein. Varying concentrations of phosphate were also found to promote crystal formation. At this stage it is unknown whether or not the phosphate promoted crystallisation by acting as an additive or a precipitant. As phosphate is a product of phosphatase, the crystals could be forming as a result of the binding of the phosphate within the active site of the protein, rather than its effect as a precipitant. The most useful and well understood additives are those which (for physiological reasons) bind to the protein causing favourable changes in its conformation or physical chemical properties, the optimal end result being the formation of a crystal. Additives which form a substrate enzyme complex (e.g. G2P), do not add rigidity to the protein (the more rigid the protein, the more likely it is to crystallise) but they are inherently more scientifically interesting and revealing once analysed. Precipitants, however, are used solely to induce supersaturation and promote crystal formation.

It is desirable to separate out these effects i.e. binding or precipitation (additive or precipitant) so that they may be carefully controlled in order to better control the parameters that affect crystallisation in future experiments. This in turn increases the probability of the growth of good quality crystals for structural analysis.

After the first three initial screens and the first optimisation screen (screen 4), optimisation screen 5 showed the greatest number of buffers yielding crystals. Optimisation screen 5 shows that ~ 90 % of the buffers containing protein grew crystals. Screen 5 used a high concentration of protein as mentioned above, as well as 1.5 M ammonium sulphate, variable pH of: 6.5, 7.0 and 7.5 and three different phosphates (of variable concentration) (see screen 5). Until further screens are made which generate diffractable 3D crystals it is impossible to pin point the exact conditions which will promote such crystal growth, however screening around the conditions

set up in screen 5 with slight modification to any of the variables within the screen could grow a diffractable crystal. This would then allow structural analysis of the protein, giving insight into a possible role, function and hopefully reveal the biological significance of the enzyme. Due to the overall similarity of SP1 and SP2, successful crystal growth and analysis of SP2 crystals could theoretically allow crystallisation of SP1 using similar conditions (although there are some significant differences including charge). This would provide the advantage of growing crystals of SP1 in a shorter space of time and with less waste of purified protein which would otherwise be used for initial crystal screens. Once diffractable crystals of SP1 and SP2 have been grown, analysed and their structure identified, it may be possible to elucidate the reasons for the subtle differences between these two isoenzymes.

The most interesting observation from this work was the appearance of brown/red or gold pigmentation in some preparations, which lacked added glycerol or G2P. Initially it was assumed that pigmentation was due to the presence of one or more metals and that the enzyme was a metalloenzyme, however this was found to be incorrect as PIXE analysis (chapter 5) showed that there are no metals present in this enzyme.

Pigmentation is commonly attributed to the presence of metallic ions (e.g. the binuclear iron in purple acid phosphatase, arising from the tyrosine to iron charge transfer transition (Kaija, 2002)). However, the presence of pigment can also be due to tyrosine alone and/or tyrosine and cysteine (Casadevall & Nosanchuk, 2000). Tyrosine is a precursor to the pigment melanin (Nosanchuk & Casadevall, 2003), which can give brown, red (Land *et al.* 2003) and yellow/gold pigments. Melanin has been shown to have a role in virulence by protecting melanised bacterial cells from the oxidative burst of activated immune system cells (Nosanchuk & Casadevall, 2003), this is thought to be achieved by iron binding to melanin and offering protection from damage against H₂O₂ (Page & Shivprasad. 1995). On storage, cell pellets of the *Serratia* sp. have sometimes been seen to develop black pigmentation (L.E. Macaskie,

unpublished). However it is unknown whether melanin production in the bacterial cell (of which there are many examples: Nosanchuk & Casadevall, 2003; Langunas-Munoz *et al.* 2006; Tsai & Lee. 1998) relates to any pigmentation of the purified acid phosphatase enzyme in this case. Future crystallisations would aim to obtain sufficient protein in crystal form for PIXE analysis as well as a diffractable crystal for structural analysis.

6.6 Summary of the results

- Crystals were grown for SP2 only as purification of SP1 did not yield enough protein for crystallisation studies.
- None of the crystals grown were suitable for structural analysis.
- Optimisation screen 5 showed gave the highest number of buffer conditions yielding crystals.
- The phosphatase enzyme was shown to be very soluble and therefore higher concentrations of protein (~30 mg/ml) were needed to produce crystals consistently.
- Red, brown and gold pigmentation was observed in some of the crystals grown, however the reason for pigmentation is currently unknown.
- Addition of glycerol and glycerol-2-phosphate to crystal buffers did not improve crystallisation further.

7 Chapter 7 Discussion

7.1 Hypothesis and future work

7.1.1 Zr work, biomineralisation and possible roles of *Serratia* phosphatase

Until now the majority of work concerning the biomineralisation of metal phosphates with *Serratia* sp. has focussed on hydrogen uranyl phosphate (HUP), due to its ease of bioaccumulation (whole-cell loads of up to 9 g accumulated uranium per gram of biomass; 900 % of the cellular dry weight; Yong & Macaskie, 1995) and its excellent ion exchange properties (Paterson-Beedle *et al.* 2006). However zirconium phosphate (ZrP) has now offered a potentially viable alternative where a non toxic and non radioactive metal is needed e.g. for decontamination of potable and irrigation waters (Mennan *et al.* 2010). Like HUP ZrP bioaccumulates very well (~95 % of the initial metal concentration; Mennan *et al.* 2010) under certain conditions and acts as a suitable ion exchanger for cold “surrogates” of ^{60}Co and ^{90}Sr (Co^{2+} and Sr^{2+}). Like HUP, the estimated Sr^{2+} and Co^{2+} uptake capacities obtained from ZrP reactors are ~2 fold greater than for commercially available materials (chapter 3; Mennan *et al.* 2010). The biogenic ZrP created in this study has amorphous, gel like properties and contained few crystalline phases (shown by XRD). It is hypothesised (chapter 3) that biogenic ZrP is a crude, amorphous phase precursor to crystalline α -ZrP, also suggested in other work using x-ray powder diffraction and pair distribution function analysis (Readman *et al.* Unpublished).

α -ZrP is an excellent ion exchanger (Clearfield, 1988), but is time consuming to make (Clearfield, 1988). Therefore the *Serratia* sp.-produced ZrP confers advantages: it is potentially cheaper to make than chemically produced α -ZrP, it is easily made *in situ*, scalably, and it retains good ion exchange properties despite (perhaps because of) its amorphous, crude nature. On the basis of the comparisons with commercially available materials (chapter 3) and its advantages over chemically-produced α -ZrP, the potential for ZrP-biogel to be used in wastewater decontamination warrants more detailed study and elucidation of the structure of the ZrP

biomaterial. The ultimate aim is the development of an inert, non-toxic, portable ion exchanger which could be made quickly and cheaply in the event of an emergency such as a radioterrorist attack or an accident involving radioactive material. Work done so far shows that biogenic ZrP shows a great deal of promise for such use.

The current study focussed on its application as an ion exchanger. However other work (Paterson-Beedle *et al.* 2009) has shown removal of Co^{2+} and Sr^{2+} by a co-crystallisation method where the chemical ‘cage’ of metal phosphate (HUP or ZrP) is built around the target ion. Under such circumstances where continued enzymatic activity is a pre-requisite for the continued synthesis of ZrP a radiotolerant system is required since over time ^{60}Co , ^{137}Cs and ^{90}Sr will accumulate to quite high concentrations very close to the enzyme. The radiotolerance of the mediating phosphatase was documented previously (Jeong, 1992) and the potential need for this tolerance inspired the fundamental study of the metal-accumulating phosphatase in this work. Since radiation damage to proteins is mediated by the effects of free radicals (generated via radiolysis of water) this study sought parallels in natural circumstances where bacteria come under targeted free radical attack, i.e. the host response.

The use of micro-organisms for the removal and subsequent bio accumulation of heavy metals from solution, for the bioremediation of wastes and sites contaminated with metals, is a relatively well known process (Macaskie *et al.* 1996; Lovley, 2003; Lloyd & Renshaw, 2005). However, little is known of the exact cellular localisations of the two *Serratia* phosphatase isoenzymes *in vivo*. Previous studies using electron microscopy with immunogold labelling of *Serratia* sp. found the phosphatase to be located in the periplasm and exocellularly (Jeong, 1992), but the immunological method could not differentiate between the two phosphatase isoenzymes. Macaskie *et al* (2000) found involvement of the phosphate of the lipid A component of LPS (which are produced exocellularly in association with the phosphatase) in formation of metal phosphate nucleation sites. Mineral deposits were not seen in the periplasmic

space, but were found at high metal loadings outside of the cell (Jeong, 1992; Macaskie *et al.* 1994). The accumulation of metal phosphate ‘tethered’ to the LPS as well as the exocellular location of the phosphatase is thought to prevent fouling of the cell surface and is consistent with a possible role of phosphatase in metal resistance (Macaskie *et al.* 2000). Although phosphatase has a proven role in the biomineralisation of metal phosphates, other factors besides phosphate release from the activity of phosphatase are implicated in effective metal removal (Macaskie *et al.* 1995); In proof of the role of the enzyme, a strain of *E.coli* expressing *Salmonella phoN* biomineralised HUP as effectively as the *Serratia* sp. while the parent strain of *E.coli* was ineffective (Basnakova *et al.* 1998). The role of phosphatase activity in the removal of metals has also been shown previously by the use of a *Serratia* phosphatase deficient mutant, which was unable to remove metals (Jeong *et al.* 1997). Other enterobacteria containing *phoN* and producing acid phosphatase removed little heavy metal from solution (Macaskie *et al.* 1994). Hence, it is postulated that the production of acid phosphatase alone is not sufficient to allow metal bioaccumulation to occur, and that it is the combination of phosphate release and suitable nucleation sites on the cell surface that permit initiation of nucleation prior to continued metal phosphate accumulation and crystal growth. *Serratia* sp. NCIMB 40259 atypically seems to have an appropriate combination of phosphatase overproduction and cell surface structure/nucleation sites to confer such good metal accumulating properties. It has been suggested that this may have been selected during prolonged stress in a metal-polluted environment (Macaskie *et al.* 1994).

It was anticipated that successful purification and characterisation of the *Serratia* phosphatase (PhoN) isoenzymes (SP1 and SP2) would give further insight into their specific role in the biomineralisation of metals, their radiotolerance (Jeong, 1992) and also their specific role(s) and function(s) within the bacterial cell. By knowing the precise function it becomes easier to produce a molecular toolkit for strain improvement. Furthermore, despite more than 30 years of

research the precise role of acid phosphatase in bacteria is still not known, although the natural occurrence of *phoN* in some pathogenic strains points to a possible role in pathogenicity determination.

Previous work by Jeong (1992) showed that SP1 and SP2 are each composed of four identical subunits, immunologically cross reactive and with the same molecular weight, N-terminal sequence and similar amino acid composition. The enzymes were not affected by EDTA (Jeong, 1992) and accordingly, this study found that neither SP1 nor SP2 are metalloenzymes despite having redox capability, it would be expected that redox capability would involve metal(s). Neither enzyme was found to contain phosphorylated peptides, which could have provided a possible explanation for the difference in charge between SP1 and SP2. The reasons for their slight differences, such as; thermostability, radiostability, pH optimum, substrate specificity, charge, sensitivity to certain metals and their different activities are still unknown. The striking similarity between these two enzymes raises the question of the reason for the presence of two such similar phosphatases in *Serratia* sp. However, many organisms harbour multiple phosphatases, such as *E.coli*, *Salmonella typhimurium* and *Shigella flexneri* (Rossolini *et al.* 1998). The location of these phosphatases (either periplasmic or extracellular) allows them to hydrolyse phosphate esters and the corresponding alcohol (Jeong, 1992) outside the cells main permeability barrier, the cytoplasmic membrane (which is considered to be relatively impermeable to phosphate esters which are not actively transported) (Kier *et al.* 1976). It is also possible that the phosphatase functions to provide a phosphate buffering system to the cell. The acid phosphatase (pH 2.5) from *Salmonella typhimurium* is thought to hydrolyse polyphosphate, generating phosphate buffer within the periplasm (Dassa *et al.* 1982). A similar role could be envisaged for the *Serratia* phosphatase exocellularly, due to its pH optimum of 5.0-7.0 (Jeong *et al.* 1998), and phosphatase is known to scavenge orthophosphate from membrane phospholipids as it is released (Kadurugamuwa & Beveridge, 1995).

Serratia phosphatase shows homology to the PhoN phosphatase of several pathogenic enterobacteria and, based on work by Rossolini *et al* (1998) on the classification of phosphatases, the *Serratia* phosphatase fits into Class A (subclass A2). This is based on its resistance to EDTA, Mg^{2+} , Mn^{2+} , Zn^{2+} , sensitivity to fluoride and mercuric ions (Jeong, 1992) and its homotetrameric form. The very high activity of the phosphatase (SP2) (up to 71000 units/mg; Jeong, 1992) is over twice the activity of that of *Francisella tularensis* acid phosphatase (13000-30000 units/mg) which is claimed to have the highest phosphatase activity recorded. It is noteworthy and key to this discussion that the highest acid phosphatase activities come from those strains showing pathogenicity and survival in the phagolysosome (Reilly *et al.* 1996; Baca *et al.* 1993; Olivier *et al.* 2005).

Although *Serratia* is not considered to be a pathogenic member of the *Enterobacteriaceae*, the presence of PhoN (which is associated with pathogenicity: see above and introduction) and its homology to the phosphatases of several pathogenic species of *Enterobacteriaceae* suggest that PhoN has been acquired from another possibly pathogenic species in the environment (Groisman *et al.* 1992) and that it is a relic of divergent evolution. The homology with other *Enterobacterial* phosphatases in addition to the conserved active site of vanadium peroxidases (see later) suggests that PhoN has a common ancestor and has simply diversified depending on the species in which it resides.

Serratia PhoN phosphatase is upregulated by carbon and phosphate starvation (Kasahara *et al.* 1991), by osmotic stress and by shift into anaerobiosis (Hallett *et al.* 1991), and is regulated via the *phoP/phoQ* (sensor/regulator) regulon (Groisman *et al.* 1989; Miller *et al.* 1989). PhoN is activated by the PhoP/PhoQ system as a stress response (Miller *et al.* 1989). It has been postulated that the products of PhoP/PhoQ are able to “sense” starvation and low pH (the latter would be encountered in the phagolysosome) (Miller *et al.* 1989). In the case of *Serratia* phosphatase it is possible that the enzyme would provide a localised phosphate buffer (activated

upon phagosomal containment) (Felts *et al.* 2006) and that a second function that is suggested by this study may be to redirect and amplify a free radical attack back at the phagocytic cell using its redox capability. Although this may be controversial, it is possible that the *Serratia* phosphatase is able to function with a defensive role, particularly as some phosphatases are thought to aid in the escape of the pathogen from the phagolysosome or immune system cells (Felts *et al.* 2006). However, it is not known whether *Serratia* phosphatase possesses this capability. It is implied that due to a structural similarity between *F. tularensis* acid phosphatase and phospholipase C, that the phosphatase could facilitate phagosomal escape by hydrolysing phospholipids of the phagosomal inner membrane (Felts *et al.* 2006) but this does not rule out a role in free radical trafficking.

The location of the *Serratia* phosphatase enzymes both in the periplasm and exocellularly is also consistent with a defensive role. However, due to the lack of any metal elements in either phosphatase, it is (currently) not known how the enzyme exhibits redox activity and why SP1 is strongly inhibited by the oxidising agent H₂O₂ while SP2 is unaffected, whilst the reducing agent β-mercaptoethanol inactivates SP1 and stimulates SP2. It would be expected that SP1 would remain unaffected by H₂O₂ in line with its radioresistance (see later), however the reasons for the differentially sensitive nature of SP1 and SP2 to redox active agents whilst being comparatively radioresistant (SP1) and radiosensitive (SP2) are unknown.

Some redox active enzymes (such as peroxidases) which do not contain metal elements, contain redox active cysteine or selenocysteine residues instead (Stadtman, 1996; Battacharyya *et al.* 2009). However *Serratia* sp phosphatase has a low cysteine content (1 cysteine per subunit; Jeong, 1992), but this does not mean that the existing cysteines are not redox active. Redox active peroxidases can be divided into two categories based on the number of catalytically active cysteines; the 1-Cys and 2-Cys peroxidases (Chae *et al.* 1994). However it is unknown whether the existing cysteines present in SP1 and SP2 are located in or near the active site of the

enzyme (see later). Certainly the presence of cysteine in the protein *per se* does not mean that this residue has a critical function, nor does it establish what that function may be (Fomenko *et al.* 2005). Although the presence of redox active cysteine could be an explanation for the redox ability of *Serratia* phosphatase, it has not been proven (so far) that redox capability is related to the presence of cysteines in this case. Nevertheless, the combination of redox capability and parallels with pathogenic enterobacterial species would seem to point to a defensive role for the phosphatase in relation to the bacterial cell or even an ‘attack’ function with respect to its ability to potentiate free radical damage on biological molecules (chapter 5).

Phosphatases with a proven defensive role come from organisms such as *Leishmania donovani* and *Francisella tularensis*. The method of their defensive role comes via amelioration of the respiratory burst from activated neutrophils, which would otherwise kill the invading bacteria in the phagolysosome (Reilly *et al.* 2005). However the link of *Serratia* sp. phosphatase with classical defensive mechanisms brought about by the immune response remains tenuous and more work would need to be done in order to determine if this phosphatase confers such defensive mechanisms. In this respect, *Salmonella phoN* has been expressed in *E.coli* and it would be useful in future work to determine which, if any, new pathogenic properties would be conferred by this change. Possibly the enzyme simply played an ancestral part in the survival of the pathogen within the host cell and now resides in non pathogenic species of bacteria and has subsequently diversified towards a role in resistance to toxic metals via their precipitation as phosphates.

The three most plausible explanations for the existence of SP1 and SP2 and their high degree of similarity is that (i) they are isoenzymes diverging over time (ii) one is a precursor of the other e.g. in the periplasm waiting to be exported to its final exocellular location (iii) they are interconvertible and any one ‘snapshot’ contains SP1 and SP2 according to what form they are in at the time of the snapshot. However, SP1 and SP2 were suggested to be interconvertible since a

combination of SP1 and SP2 inadvertently mixed, gave different proportions of SP1 and SP2 than in the known proportions added together (H. Pflicke & M. Paterson-Beedle, unpublished). It is also possible that they may differ slightly in amino acid sequence (although sequencing work has not been done so far). It is unlikely that this could account for the difference in charge (SP1 has a negative charge and SP2 a positive charge at pH 8.0) between the two enzymes. Examination of the amino acid compositions (Jeong, 1992; Appendix 3) showed aspartic acid, proline, tyrosine, leucine, phenylalanine and lysine differed between the two enzymes by one residue per subunit higher in SP1 with the exception of proline which is one residue per subunit higher in SP2, Appendix 3) as the difference in positively (histidine, arginine and lysine) and negatively charged amino acids (aspartic acid and glutamic acid) between SP1 and SP2 does not reflect the actual charges on the enzymes. SP2 contains two more aspartic acid residues (- charged) per subunit than SP1 and one less lysine (+ charged) per subunit than SP1. The existence of enzyme isoforms is thought to permit the fine tuning of cell metabolism. This could account for the different K_m (Michaelis-Menten constant. The substrate concentration required for an enzyme to reach one-half its maximum velocity) values for SP1 and SP2 for glycerol-1-phosphate and glycerol-2-phosphate (SP1 K_m glycerol-1-phosphatase = 190, SP2 = 354; SP1 K_m glycerol-2-phosphate = 1963, SP2 = 938). The difference in radiosensitivity between SP1 and SP2 (SP2 being comparatively radiosensitive and SP1 being comparatively radiostable) is one of the most profound differences between the two isoforms. However, the reasons for this difference remain unknown. Incorporation of Bovine Serum Albumin (BSA) into the reaction mixture during radiostability experiments conferred some radiostability onto the sensitive SP2 but the more resistant SP1 was not further stabilised by BSA (Jeong, 1992). This could indicate that SP1 contains less associated water, which would mean fewer 'local' free radicals during irradiation.

The radicals formed when ionizing radiation passes through water are among the strongest oxidizing agents that can exist in aqueous solution. Molecular oxygen (because of its bi-radical nature) readily accepts unpaired electrons, subsequently creating a series of partially reduced species known as reactive oxygen species (ROS). These include superoxide ($O_2^{\cdot-}$), hydrogen peroxide (H_2O_2), hydroxyl radical (HO^{\cdot}) and peroxy (ROO^{\cdot}) and alkoxy (RO^{\cdot}) radicals which may be involved in the initiation and proliferation of free radical chain reactions and which can be highly damaging to cells. Proteins such as BSA generally offer a stabilising effect during irradiation, possibly by lowering the water concentration around affected protein (Coggle, 1983) which is most probably why BSA conferred some radiostability onto SP2.

It is also possible that SP1 has a more “closed” structure than SP2, with fewer or smaller aqueous channels to the metal sensitive site. Jeong (1992) suggested that this may suggest subtle differences in the geometry of the active sites of SP1 and SP2, in agreement with the different K_m values for glycerol-1-phosphate and glycerol-2-phosphate.

The most likely reasons for the existence of SP1 and SP2 (other than existing as different isoforms which have diverged) probably lie in the survival of the organism in a metal-polluted environment and the divergence of PhoN from a pathogenic species now diversified for the aim of survival in hostile conditions. It is postulated that due to the radioresistance (i.e. postulated free radical resistance) of SP1, this form of the phosphatase is favoured by the cell and exported extracellularly during unfavourable conditions (such as metal toxicity or entrapment in the phagolysosome), possibly acting as a phosphate scavenger and providing a localised phosphate buffer that provides more favourable conditions for bacterial survival in adverse conditions. SP2 is possibly used routinely by the cell in normal (favourable) conditions, which would account for its lower radioresistance (as a radioresistant form would not be required in favourable conditions). It is still unproven that the two isoforms are interconvertible or indeed if they exist in two different cellular locations. However, until crystallographic structural analysis of SP1 and

SP2 is complete along with the full amino acid sequence for both isoforms it is impossible to say with certainty why these enzymes exist.

7.2 Further work

Although promising results were obtained in the biomineralisation of a ZrP gel with good ion exchange properties, more work will need to be carried out, firstly to fully characterise the ZrP gel and secondly to analyse the structure (post ion exchange) to assess if and for how long radionuclides will be held stably inside the ZrP matrix without release. Further ion exchange studies will need to be done with Cs^{2+} (as this was not carried out in this study) and then with real nuclear wastes to fully test the material. Also, the selectivity of ZrP needs to be tested, for example, Cs versus Na^+ and K^+ , Sr versus Ca^{2+} .

Economic assessment of HUP as a waste water treatment process showed a major potential limitation was the cost of the phosphate feed supplement (G2P) which contains 1 mol/mol phosphate (Paterson-Beedle *et al.* 2009). Phytic acid (inositol phosphate) is a ubiquitous plant waste which is relatively cheap and contains 6 mol phosphate/mol (Paterson-Beedle *et al.* 2009).

Initial work (Mennan *et al.* unpublished; Paterson-Beedle *et al.* 2009) used *E.coli* containing phytase to break down sodium phytate and then used the phosphate as a feed for *Serratia* sp. biomineralisation of metals, thereby utilising a cheap source of phosphate. However a strain of *E.coli* with cloned *phoN* could provide both enzymes (phytase and phosphatase) and be of more benefit than the *Serratia* sp. This recombinant *E.coli* was shown to biomineralise HUP comparably to *Serratia* sp. (Basnakova *et al.* 1998).

Finally, the process will need to be scaled up, the final aim being a highly portable reactor which could be deployed in the event of an emergency, such as a radioterrorist attack or radioactive leak or accident.

Further work on the characterisation of SP1 and SP2 would involve further analysis with MALDI-ToF and successful use of electrospray for confirmation of subunit and holoenzyme molecular weights to measure accurately any observable differences in molecular weight between the two isoforms beyond those observed in this study using MALDI-ToF. This technique was not available at the time of the original study (Jeong, 1992).

Continued protein database searches will need to be carried out using both the N-terminal sequences of SP1 and SP2 and the pkl files of peptide mass fingerprints obtained by mass spectrometry. This is important in continuing to identify the protein by finding a protein match, as new proteins are continually added to the databases.

Due to the sequence homology with vanadium peroxidase, work should be done to test the phosphatase for peroxidase activity, as it has been shown that some phosphatases possess peroxidase activity and vice versa (Hemrika *et al.* 1997; Renirie *et al.* 2000; Tanaka *et al.* 2002). Particularly noteworthy is that the vanadium haloperoxidases and the bacterial class A acid phosphatases have a conserved active site (Tanaka *et al.* 2002) and that vanadate-substituted recombinant acid phosphatases from *Shigella flexneri* and *Salmonella typhimurium* are able to function as vanadium haloperoxidases (Tanaka *et al.* 2002; Hemrika *et al.* 1997). Testing the *Serratia* phosphatase for peroxidase activity would show if any of the function(s) of the related peroxidase has been retained in the phosphatase and would subsequently help assign a specific role and function to the enzyme. The vanadium substitution work would need to be related to the structure and function analysis via the crystallographic study.

Initial tests using the deoxy ribose method will also need to be revisited with the aim of recovering the enzyme to determine its activity during and after the reaction. This would show how the phosphatase survives the free radical reaction in more detail, that is if potentiating the effect of free radicals inactivates the phosphatase or one enzyme preferentially. During initial tests, the quantity of phosphatase was very limited and the final stage of the experiment involved

heating the reaction mixture (with the phosphatase) to 100°C, which would have denatured the protein (post-reaction) before activity tests could be done.

Due to the evolutionary relatedness of the *Serratia* PhoN to the PhoN of other pathogenic enterobacteria, its redox ability and the fact that some phosphatases actively aid in a pathogen's survival and or escape from the immune system cells (for example, *F.tularensis* phosphatase preventing the respiratory burst from activated neutrophils) the phosphatase needs to be tested for its ability to prevent the respiratory burst from neutrophils in a similar way. Although this ability is unlikely from *Serratia* phosphatase, it should be tested, as it is possible that the phosphatase aids bacterial survival in the host, especially as PhoN does not normally occur in *Serratia* sp. and it is unknown from which organism *phoN* was acquired. Indeed, this gene could have been picked up from an organism which did possess the capacity to prevent respiratory burst and aid in escape and survival from the immune system. Its function in metal phosphate deposition may be serendipitous but the gene may be retained as conferring a selective advantage in a metal polluted environment, e.g. containing redox-active metals.

Finally, crystallisation studies on SP1 and SP2 need to be finished and a suitable 3D diffractable crystal grown for each isoform. Whilst this work is ongoing the full sequence of each isoform needs to be determined, which is currently underway (D. Chismon & D. Lee, unpublished) to add to the structural data obtained from crystallographic studies. Once the first structures of each isoform have been determined, it will be possible to look at structural differences and similarities between SP1 and SP2 as well as looking for any other structural matches in the protein database. After this, it should be possible to crystallise SP1 and SP2 with different substrates and metals (such as vanadium) to look at the active site of the enzyme comparing SP1 and SP2 with related enzymes for which structural information is available. One particularly interesting comparison will be that of the related vanadium peroxidases.

By comparing the crystal structures of the acid phosphatase from *Escherichia blattae* co-crystallised with sulfate and vanadate in chloroperoxidase it was found that these families were evolutionarily related and shared a common ancestor (Tanaka *et al.* 2002; Hemrika *et al.* 1997). Observing pNPP and then vanadium in the active site of the phosphatase through its crystal structure should allow similar comparisons to be made and such evolutionary links to be confirmed, shedding more light on the evolutionary past of the phosphatase and its current role and function after diversification in an organism which most probably acquired *phoN* from another organism in the environment.

8 References

- Ackermann, B.P & Ahlers, J. (1976).** Influence of complexing agents on stability and activity. *Biochemical Journal*. **153**: 151–157.
- Aguirre-García, M. M., Cerbón, J & Talamás-Rohana, P. (2000).** Purification and properties of an acid phosphatase from *Entamoeba histolytica* HM-1:IMSS. *International Journal of Parasitology*. **30**: 585–591.
- Allan, V.J.M., Callow, M.E., Macaskie, L.E & Paterson-Beedle, M. (2002).** The effect of nutrient limitation on biofilm formation and phosphatase activity of a *Citrobacter* sp. *Microbiology* **148**: 277–288.
- Baca, O. G., Roman, M. J., Glew, R. H., Christner, R. F., Buhler, J. E & Aragon, A. S. (1993).** Acid phosphatase activity in *Coxiella burnettii*: a possible virulence factor. *Infection & Immunity*. **61**: 4232–4239.
- Barford, D. (2004).** The role of cysteine residues as redox-sensitive regulatory switches. *Current Opinion in Structural Biology*. **14**: 679–686.
- Barkay, T & Schaefer, J. (2001).** Metal and radionuclide bioremediation: issues, considerations and potentials. *Current Opinion in Microbiology*. **4**: 318–323.
- Basnakova, G & Macaskie, L.E. (1997).** Microbially enhanced chemisorption of nickel into biologically synthesized hydrogen uranyl phosphate: a novel system for the removal and recovery of metals from aqueous solutions. *Biotechnology & Bioengineering*. **54**: 319–328.
- Basnakova, G & Macaskie, L.E. (1999).** Accumulation of zirconium and nickel by *Citrobacter* sp. *Journal of Chemical Technology & Biotechnology*. **74**: 509–514.
- Basnakova, G & Macaskie, L.E. (2001).** Microbially-enhanced chemisorption of Ni^{2+} ions into biologically-synthesised hydrogen uranyl phosphate (HUP) and selective recovery of concentrated Ni^{2+} using citrate or chloride ion. *Biotechnology Letters*. **23**: 67–70.

Basnakova, G., Spencer, A.J., Palsgard, E., Grime, G & Macaskie, L.E. (1998). Identification of the Nickel Uranyl Phosphate Deposits on *Citrobacter* sp. Cells by Electron Microscopy with Electron Probe X-ray Microanalysis and by Proton-Induced X-ray Emission Analysis. *Environmental Science & Technology*. **32**: 760-765.

Basnakova, G., Stephens, E.R., Thaller, M.C., Rossolini, G.M & Macaskie, L.E. (1998).

The use of *Escherichia coli* bearing a *phoN* gene for the removal of uranium and nickel from aqueous flows. *Applied Microbiology and Biotechnology*. **50**: 266-272

Beck, J. L., McArthur, M. J., De Jersey, J. & Zerner, B. (1988). Derivatives of the purple phosphatase from red kidney bean: Replacement of zinc with other divalent metal ions. *Inorganica Chimica Acta*. **153**: 39-44.

Belle, C & Pierre, J.L. (2003). Asymmetry in Bridged Binuclear Metalloenzymes: Lessons for the Chemist. *European Journal of Inorganic Chemistry*. 4137-4146.

Benhamza, H., Barboux, P., Bouhaouss, A., Josien, F & Livage, J. (1991). Sol-gel synthesis of $\text{Zr}(\text{HPO}_4)_2 \cdot \text{H}_2\text{O}$. *Journal of Materials Chemistry*. **1**: 681-684.

Britton, G & Friehofer, V. (1978). Influence of extracellular polysaccharides on the toxicity of copper and cadmium towards *Klebsiella aerogenes*. *Microbial Ecology*. **4**: 119-125.

Bogdanov, S.G., Valiev, E.Z., Dorofeev, Y.A & Pirogov, A.N. (1997). Structure of zirconium phosphate gels produced by the sol-gel method. *Journal of Physics Condensed Matter*. **9**: 4031-4039.

Bolton, P.G & Dean, A.C.R. (1972). Phosphatase synthesis in *Klebsiella (Aerobacter) aerogenes* growing in continuous culture. *Biochemical Journal*. **127**: 87-96.

Bonthrone, K. M., Basnakova, G., Lin, F & Macaskie, L. E. (1996). Bioaccumulation of nickel by intercalation into polycrystalline hydrogen uranyl phosphate deposited via an enzymatic mechanism. *Nature Biotechnology*. **14**: 635-638.

Bonthrone, K.M., Quarmby, J., Hewitt, C., Allan, V.J.M., Paterson-Beedle, M., Kennedy, J.F & Macaskie, L.E. (2000). The effect of the growth medium on the composition and metal binding behaviour of the extracellular polymeric material of a metal-accumulating *Citrobacter* sp. *Environmental Technology*. **21**: 123-134.

Bradford, M. M. (1976). A rapid and sensitive method for quantitation of microgram quantities of protein utilizing the principle of protein-dye-binding. *Analytical Biochemistry*. **72**: 248-254.

Campbell, H.D & Zerner, B. (1973). A low molecular weight acid phosphatase which contains iron. *Biochemical Biophysics Research Communications*. **54**: 1498-1503.

Canarelli, S., Fisch, I & Freitag, R. (2002). On-line microdialysis of proteins with high-salt buffers for direct coupling of electrospray ionization mass spectrometry and liquid chromatography. *Journal of Chromatography A*. **948**: 139-149.

Casadevall, A., Rosas, A.L & Nosanchuk, J.D. (2000). Melanin and virulence in *Cryptococcus neoformans*. *Current Opinion in Microbiology* **3**: 354–358.

Castro, I.M ., Fiettoa, J.L.R., Vieira, R.X., Trópiiaa, M.J.M., Campos, L.M.M., Paniagoc, E.B & Brandãoa, R.L. (2000). Bioleaching of zinc and nickel from silicates using *Aspergillus niger* cultures. *Hydrometallurgy*. **57**: 39-49.

Chae, H. Z., Robison, K., Poole, L. B., Church, G., Storz, G. & Rhee, S. G. (1994). Cloning and sequencing of thiol-specific antioxidant from mammalian brain: Alkyl hydroperoxide reductase and thiol-specific antioxidant define a large family of antioxidant enzymes. *Proceedings of the National Academy of Sciences*. **91**: 7017–7021.

Chakrabarty, A.M. (1996). Why and how *Pseudomonas aeruginosa* makes alginate under starvation conditions. In *Microbial Biofilms* (Proceedings, ASM Conference, Snowbird, Utah, USA). Washington, DC: American Society for Microbiology.

Choppin, G.R & Wong, P.J. (1998). The Chemistry of Actinide Behavior in Marine Systems. *Aquatic Geochemistry*. **4**: 77-101.

Clearfield, A. (1988). Role of ion exchange in solid-state chemistry. *Chemical Reviews*. **88**: 125-148.

Clearfield, A., Bortun, A.I., Bortun, L.N & Garcia, J.R. (1998). Direct hydrothermal synthesis of zirconium phosphate and zirconium arsenate with a novel basic layered structure in alkaline media. *Inorganic Chemistry Communications*. **1**: 206-208

Clearfield, A & Smith, G.D. (1969). Crystallography and structure of alpha-zirconium bis(monohydrogen orthophosphate) monohydrate. *Inorganic Chemistry*. **8**: 431-436.

Coggle, J. E. (1983). Biological Effects of Radiation. Taylor and Francis Ltd. London.

Costerton, J.W. (2000). Biofilms in the new Millennium: musings from a peak in Xanadu. In: Allison, D., Gilber, P., Lappin-Scott, H., Wilson, M. eds. *SGM symposium 59: Community structure and cooperation in biofilms*. Cambridge: Cambridge University Press. 329-345.

Costerton, J.W., Lewandowski, Z., Caldwell, D.E., Korber, D.R & Lappin-Scott, H.M. (1995). Microbial biofilms. *Annual Reviews in Microbiology*. **49**: 71-45.

da Cruza, A., de Melo Silvaa, D., da Silvaa, C.C., Nelson, R.J., Ribeiroa, L.M., Pedrosa, E.R., Jayme, J.C & Curadoa, M.P. (2008). Microsatellite mutations in the offspring of irradiated parents 19 years after the Cesium-137 accident. *Mutation Research/Genetic Toxicology and Environmental Mutagenesis*. **652**: 175-179.

Dassa, M., Cahu, B., Desjoyaux, C & Boquet, P.L. (1982). The acid phosphatase with optimum pH of *Escherichia coli*. *Journal of Biological Chemistry*. **257**: 6669–6676.

De Boer, E., Vankooyk,Y., Tromp, M.G.M., Plat, H & Wever, R. (1986). Bromoperoxidase from *Ascophyllum nodosum*: a novel class of enzymes containing vanadium as a prosthetic group? *Biochimica et Biophysica Acta*. **869**: 48–53.

Duff, S.M., Sarath, G & Plaxton, W.C. (1994). The role of acid phosphatases in plant phosphorous metabolism. *Physiology Plant*. **90**: 791-800.

Dyer, A., Shabeen, T & Zamin, M. (1997). Ion exchange of strontium and caesium into amorphous zirconium phosphates. *Journal of Material Chemistry*. **7**: 1895-1899.

Ek-Rylander, B., Barkhem, T., Ljusberg, J., Ohman, L., Andersson, K & Andersson, G. (1997). Comparative studies of rat recombinant purple acid phosphatase and bone tartrate-resistant acid phosphatase. *Journal of Biochemistry*. **321**: 305-311.

Ellwood, D. C., Keevil, C. W., Marsh, P. D., Brown, C. M. & Wardell, J. D. (1982). Surface-associated growth. *Philosophical Transactions of the Royal Society B: Biological Sciences*. **297**: 517-523.

Felts, R. L., Reilly, T. J. & Tanner, J. J. (2006). Structure of *Francisella tularensis* AcpA. Prototype of a unique superfamily of acid phosphatases and phospholipases C. *Journal of Biological Chemistry*. **281**: 30289-30298.

Fields, P. I., Groisman, E. A. & Hefron, F. (1989). A Salmonella locus that controls resistance to microbicidal proteins from phagocytic cells. *Science*. **243**: 1059-1062.

Finlay, J.A., Allan, V.J.M., Conner, A., Callow, M.E., Basnakove, G & Macaskie, L.E. (1999). Phosphate release and heavy metal accumulation by biofilm-immobilised and chemically-coupled cells of a *Citrobacter* sp. pre-grown in continuous culture. *Biotechnology & Bioengineering*. **63**: 87-97.

Fomenko, D.E., Xing, W., Adair, B.M., Thomas, D.J & Gladyshev, V.N. (2007). High-throughput identification of catalytic redox-active cysteine residues. *Science*. **315**: 387-389.

Forster, C & Wase, J. (2003). Biosorbents for Metal Ions. Taylor & Francis Ltd. 1-229.

Frolund, B., Griebe, T. & Nelson, P. H. (1995). Enzymatic activity in the activated sludge floc matrix. *Applied Microbiol Biotechnology*. **43**:755-761.

Gadd, G. M. (2009). Biosorption: critical review of scientific rationale, environmental importance and significance for pollution treatment. *Journal of Chemical Technology & Biotechnology*. **84**: 13-28.

- Garlanda, J.A & Wakeford, R. (2007).** Atmospheric emissions from the Windscale accident of October 1957. *Atmospheric Environment*. **41**: 3904–3920.
- Garret, I.R., Boyce, B.F., Oreffo, R.O., Bonewald, L., Poser, J & Mundy, G.R. (1990).** Oxygen-derived free radicals stimulate osteoclastic bone resorption in rodent bone in vitro and in vivo. *Journal of Clinical Investigation*. **85**: 632-639.
- Giles, N., Watts, A., Giles, G., Fry, F., Littlechild, J & Jacob, C. (2003).** Metal and Redox Modulation of Cysteine Protein Function. *Chemistry & Biology*. **10**: 677-693.
- Graf von der Schulenburg, D.A., Holland, D.J., Paterson-Beedle, M & Macaskie, L.E. (2008).** Spatially resolved quantification of metal concentration in biofilm-mediated ion exchanger. *Biotechnology & Bioengineering*. **99**: 821-829.
- Grime, G. W. & Watt, F. (1990).** Nuclear microscopy & elemental mapping using high-energy ion beam techniques. *Nuclear Instruments and Methods in Physics*. **50**: 197-207.
- Groisman, E. A. (2001).** The pleiotropic two-component regulatory system PhoP-PhoQ. *Journal of Bacteriology*. **183**: 1835-1842.
- Groisman, E. A., Saier, J., M. H. & Ochman, H. (1992).** Horizontal transfer of a phosphatase gene as evidence for mosaic structure of the *Salmonella* genome. *EMBO J*. **11**: 1309-1316.
- Groisman, E. A., Sturmoski, M. A., Solomon, F. R., Lin, R. & Ochman, H. (1993).** Molecular, functional and evolutionary analysis of sequences specific to *Salmonella*. *Proceedings of the National Academy of Sciences*. **9**: 1033-1037.
- Hadler, K.S., Huber, T., Cassady, I., Weber, J., Robinson, J., Burrows, A., Kelly, G., Guddat, L.W., Hume, D.A., Schenk, G & Flanagan, J.U. (2008).** Identification of a non-purple tartrate-resistant acid phosphatase: an evolutionary link to Ser/Thr protein phosphatases? *BMC Research Notes*. **1**: 78.

- Hallett, D. S., Clark, P & Macaskie, L. E. (1991).** Phosphatase production by a *Citrobacter* sp. growing in batch culture retarded by anaerobic or osmotic stress and the effect of the osmoprotectant glycinebetaine. *FEMS Microbiology Lett.* **78**: 7-10.
- Halliwell, B & Gutteridge, J. M. C. (1981).** Formation of a thiobarbituric acid reactive substance from deoxyribose in the presence of iron salts. The role of superoxide and hydroxyl radicals. *FEBS Letters.* **128**: 347-351.
- Halliwell, B., Gutteridge, J. M. C & Aruoma, O. I. (1987).** The Deoxyribose Method: A simple “test-tube” assay for determination of rate constants for reactions of hydroxyl radicals. *Analytical Biochemistry.* **165**: 215-219.
- Harder, W & Dijkhuizen, L. (1983).** Physiological responses to nutrient limitation. *Annual Review of Microbiology.* **37**: 1-23.
- Hemrika, W., Ranirie, R., Dekker, H., Barnett, P. & Wever, R. (1997).** From phosphatases to vanadium peroxidases: A similar architecture of the active site. *Biochemistry.* **94**: 2145-2149.
- Hillenkamp, F., Karas, M., Beavis, R.C & Chait, B.T. (1991).** Matrix-assisted laser desorption/ionization mass spectrometry of biopolymers. *Analytical Chemistry.* **63**: 1193-1202.
- Hollander, V.P. (1971).** Acid Phosphatases: P.D. Voyer (Ed). The Enzymes. 3rd Edition. Academic Press, New York. **4**: 449-498.
- Hunter, R. L & Merkert, C.L. (1957).** Histochemical demonstration of enzymes separated by zone electrophoresis in starch gels. *Science.* **125**: 1294-1295
- Janning, K.J., Harremoes, P & Nielson, M. (1995).** Evaluating and modelling the kinetics in a full scale submerged denitrification filter. *Water Science Technology.* **32**: 115-13.
- Jeong, B. C. (1992).** D.Phil. Thesis. Oxford.

Jeong, B. C., Hawes, C., Bonthron, K. M & Macaskie, L. E. (1997). Localisation of enzymically enhanced heavy metal accumulation by *Citrobacter* sp. and metal accumulation in vitro by liposomes containing entrapped enzyme. *Microbiology*. **143**: 2497-2507.

Jeong, B.C & Macaskie, L.E. (1995). PhoN-type acid phosphatases of a heavy metal-accumulating *Citrobacter* sp.: resistance to heavy metals and affinity towards phosphomonoester substrates. *FEMS Microbiology Letters*. **130**: 211-214.

Jeong, B.C., Poole, P.S., Willis, A.C & Macaskie, L.E. (1998). Purification and characterization of acid-type phosphatases from a heavy-metal-accumulating *Citrobacter* sp. *Archives of Microbiology*. **169**: 166–173.

Kadurugamuwa, J.L & Beveridge, T.J. (1995). Virulence factors are released from *Pseudomonas aeruginosa* in association with membrane vesicles during normal growth and exposure to gentamicin: a novel mechanism of enzyme secretion. *Journal of Bacteriology* **177**: 3998–4008.

Kaija, H. (2002). Tartrate resistant acid phosphatase: Three dimensional structure and structure based functional studies. Academic dissertation. Oulu.

Kaiser, D & Losick, R. (1993). How and why bacteria talk to each other. *Cell*. **73**: 873-85.

Kaplon, J.B., Ragunath, C., Ramasubbu, N & Fine, D.H. (2003). Detachment of *Actinobacillus actinomycetemcomitans* biofilm cells by an endogenous β -hexosaminidase activity. *Journal of Bacteriology*. **185**: 4693-4698.

Karavaeva, E.N., Molchanova, I.V & Mikhailovskaya, L.N. (2008). Mobility of technogenic radionuclides in the soil-plant system. *Russian Journal of Ecology*. **39**: 541-543.

Karthikeyan, M., Jayakumar, V., Radhika, K., Bhaskaran, R., Velazhahan, R & Alice, D. (2005). Induction of resistance in host against the infection of leaf blight pathogen (*Alternaria palandui*) in onion (*Allium cepa* var *aggregatum*). *Indian Journal of Biochemistry & Biophysics*. **42**: 371-7.

Kasahara, M., Nakata, A. & Shinagawa, H. (1991). Molecular analysis of the *Salmonella typhimurium* *phoN* gene which encodes a nonspecific acid phosphatase. *Journal of Bacteriology*. **173**, 6760-6765.

- Kier, L.D., Weppelman, R.M & Ames, B.N. (1979).** Regulation of nonspecific acid phosphatase in *Salmonella*: *phoN* and *phoP* genes. *Journal of Bacteriology*. **138**: 155-161.
- Kinchen, J.M & Ravichandran, K.S. (2008).** Phagosome maturation: going through the acid test. *Nature Reviews Molecular Cell Biology*. **9**: 781-795.
- Klug-Roth, D. & Rabani, J. (1976).** Pulse radiolytic studies on reaction of aqueous superoxide radicals with copper (II) complexes. *Journal of Physical Chemistry*. **80**: 558-591.
- Korber, D.R., Lawrence, J.R., Lappin-Scott, H.M & Costerton, J.W. (1995).** Growth of microorganisms on surfaces. *Microbial Biofilm*. Cambridge: Cambridge University Press. 15-45.
- LaCount, M.W., Handy, G & Lebioda, L. (1998).** Structural origins of L(+)-Tartrate inhibition of human prostatic acid phosphatase. *The Journal of Biological Chemistry*. **273**: 30406-30409.
- Laemmli, U.K. (1970).** Cleavage of structural proteins during the assembly of the head of bacteriophage T4. *Nature*. **227**: 680-685.
- Lagunas-Munoz, V.H., Cabrera-Valladares, N., Bolivar, F., Gosset, G & Martinez, A. (2006).** Optimum melanin production using recombinant *Escherichia coli*. *Journal of Applied Microbiology*. **101**: 1002–1008.
- Land, E.J., Ramsden, C.A & Riley, P.A. (2003).** Tyrosinase autoactivation and the chemistry of ortho-quinone amines. *Accounts of Chemical Research*. **36**: 300-308.
- Lindqvist, Y., Schneider, G & Vihkon, P. (1993).** Three dimensional structure of rat acid phosphatase in complex with L(+)-Tartrate. *The journal of biological chemistry*. **268**: 20744-20746.
- Lloyd, J.R. (2002).** Bioremediation of metals; the application of micro-organisms that make and break minerals. *Microbiology Today*. **29**: 67-69.
- Lloyd, J.R & Renshaw, J.C. (2005).** Bioremediation of radioactive waste: radionuclide–microbe interactions in laboratory and field-scale studies. *Current Opinion in Biotechnology*. **16**: 254–260.

Lovley, D. (2000). Environmental microbe-metal interactions. ASM Press. American Society for Microbiology. Washington DC.

Lovley, D.R. (2003). Cleaning up with genomics: applying molecular biology to bioremediation. *Nature Reviews in Microbiology*. **1**: 35-44.

Lovley, D.R & Coates, J.D. (1997). Bioremediation of metal contamination. *Current Opinion in Biotechnology*. **8**: 285-289.

Macaskie, L. E., Bonthron, K. M., Yong, P. & Goddard, D.T. (2000). Enzymically mediated bioprecipitation of uranium by a *Citrobacter* sp.: a concerted role for exocellular lipopolysaccharide and associated phosphatase in biomineral formation. *Microbiology*. **146**: 1855-1867.

Macaskie, L. E. & Dean, A. C. R. (1982). Cadmium accumulation by micro-organisms. *Environmental Technology Letters*. **3**: 49-56.

Macaskie, L.E. & Dean, A.C. R. (1984). Cadmium accumulation by immobilised cells of *Citrobacter* sp., *Environmental Technology Letters*. **5**: 177–186.

Macaskie, L.E. & Dean, A.C. R. (1985). Strontium accumulation by immobilised cells of a *Citrobacter* sp., *Biotechnology Letters*. **7**: 457–462.

Macaskie, L. E., Empson, R. M., Cheetham, A. K., Grey, C. P. & Skarnulis, A. J. (1992). Uranium bioaccumulation by a *Citrobacter* sp. as a result of enzymically-mediated growth of polycrystalline HUO_2PO_4 . *Science*. **257**: 782-784.

Macaskie, L. E., Jeong, B. C. & Tolley, M. R. (1994). Enzymically accelerated biomineralization of heavy metals: application to the removal of americium and plutonium from aqueous flows. *FEMS Microbiology Reviews*. **14**: 351-368.

Macaskie, L.E., Hewitt, C.J., Shearer, J.A & Kent, C.A. (1995). Biomass production for the removal of heavy metals from aqueous solutions at low pH using growth-decoupled cells of a *Citrobacter* sp. *International Biodeterioration and Biodegradation*. **7**: 3-92.

Macaskie, L. E., Lloyd J. R., Thomas, R. A. P & Tolley, M. R. (1996). The use of micro-organisms for the remediation of solutions contaminated with actinide elements, other radionuclides, and organic contaminants generated by nuclear fuel cycle activities. *Chemistry of the nuclear fuel cycle. Nuclear energy*. **35**: 257-271.

Mennan, C., Paterson-Beedle, M & Macaskie, L.E. (2010). Accumulation of zirconium phosphate by *Serratia* sp.: A benign system for the removal of radionuclides from aqueous flows. *Biotechnology Letters*. **32**: 1419-1427.

Michaylova, V & Kouleva, N. (1974). Spectrophotometric study of the reactions of arsenazo III with alkaline-earth metals. *Talanta*. **21**: 523-532.

Miller, S. I., Kukral, A. M. & Mekalanos, J. J. (1989). A two component regulatory system (*phoP phoQ*) controls *Salmonella typhimurium* virulence. *Genetics*. **86**: 5054-5058.

Mittleman, M.W., Nivens, D.E., Low, C & White, D.C. (1990). Differential adhesion, activity, and carbohydrate: protein ratios of *Pseudomonas atlantica* monocultures attaching to stainless steel in a linear shear gradient. *Microbial Ecology*. **19**: 269 278.

Mishra, S.P & Tiwari, D. (2002). Inorganic ion exchangers in radioactive waste management. Part XII: Removal behaviour of stannic and zirconium phosphates for strontium. *Journal of Radioanalytical and Nuclear Chemistry*. **253**: 421-426.

Nesmeyanova, M. A., Tsfasman, I. M., Karamyshev, A. L & Suzina, N. E. (1991). Secretion of the overproduced periplasmic PhoA protein into the medium and accumulation of its precursor in *phoA*-transformed *Escherichia coli* strains: involvement of outer membrane vesicles. *World Journal of Microbiology & Biotechnology*. **7**: 394-406.

Nosanchuk, J.D & Casadevall, A. (2003). The contribution of melanin to microbial pathogenesis. *Cellular Microbiology*. **5**: 203–223.

Nott, P.K., Heese, F., Hall, L.D., Macaskie, L.E & Paterson-Beedle, M. (2005). Measurement of flow field through biofilm reactors by three-dimensional magnetic resonance imaging. *American Institute of Chemical Engineers*. **51**: 3072-3079.

Nuttleman, P.R & Roberts, R.M. (1990). Transfer of iron from utoferrin (purple acid phosphatase) to transferring related to acid phosphatase activity. *Journal of Biological Chemistry*. **265**: 12192-12199.

Oddie, G.W., Schenk, G., Angel, N.Z., Walsh, N., Guddat, L.W., De Jersey, J., Cassady, A.I., Hamilton, S.E & Hume, D.A. (2000). Structure, function, and regulation of tartrate-resistant acid phosphatase. *Bone*. **27**:575–584.

Olivier, M., Gregory, D. J. & Forget, G. (2005). Subversion mechanisms by which *Leishmania* parasites can escape the host immune response: a signalling point of view. *Clinical Microbiology Reviews*. **18**: 293-305.

Onishi, H. (1986). Photometric determination of traces of metals, Part IIA: Individual metals, aluminum to lithium, 4th edn. John Wiley & Sons, New York.

Page, W & Shivprasad, S. (1995). Iron binding to *Azotobacter salinestris* melanin, iron mobilization and uptake mediated by siderophores. *Biometals*. **8**: 59–64.

Panara, F., Pasqualini, S & Antonielli, M. (1990). Multiple forms of barley root acid phosphatase: purification and some characteristics of the major cytoplasmic isoenzyme. *Biochimica et Biophysica Acta*. **1037**: 73-80.

Pattanapipitpaisal, P., Mabbett, A.N., Finlay, J.A., Beswick, A.J., Paterson-Beedle, M., Essa, A., Wright, J., Tolley, M.R., Badar, U., Ahmed, N., Hobman, J.L., Brown, N.L., Macaskie, L.E. (2002). Reduction of Cr(VI) and bioaccumulation of chromium by Gram positive and Gram negative microorganisms not previously exposed to Cr-stress. *Environmental Technology*. **73**: 731-45.

Paterson-Beedle, M & Macaskie, L.E. (2004). ‘Removal of Co, Sr and Ce from aqueous solutions sing native biofilm of *Serratia* sp. and biofilm pre-coated with hydrogen uranyl phosphate’ in

Biohydrometallurgy: A Sustainable Technology in Evolution, eds., M. Tsezos, A. Hatzikioseyan and E. Remoundaki, National Technical University of Athens, Athens, pp. 1155-1162.

Paterson-Beedle, M & Macaskie, L.E. (2006). Utilisation of a hydrogen uranyl phosphate-based ion exchanger supported on a biofilm for the removal of cobalt, strontium and caesium from aqueous solutions. *Hydrometallurgy*. **83**: 141-145.

Paterson-Beedle, M., Macaskie, L.E., Readman, J.E & Hriljac, J.A. (2009). Biorecovery of uranium from minewaters into pure mineral product at the expense of plant wastes. *Advanced Materials Research*. **71-73**: 621-624.

Pond, J.L., Eddy, C.K., Mackenzie, K.F., Conway, T., Borecky, D.J & Ingram, L. (1989). Cloning, sequencing, and characterization of the principal acid phosphatase, the *phoC*⁺ product, from *Zymomonas mobilis*. *Journal of Bacteriology*. **171**: 767-764.

Pradel, E & Boquet, P. (1988). Acid phosphatases of *Escherichia coli*: molecular cloning and analysis of *agp*, the structural gene for a periplasmic acid glucose phosphatase. *Journal of Bacteriology*. **170**: 4916–4923.

Räisänen, S.R., Alatalo, S.L., Ylipahkala, H., Halleen, J.M., Cassady, I., Hume, D.A & Väänänen, H.K. (2005). Macrophages overexpressing tartrate-resistant acid phosphatase show altered profile of free radical production and enhanced capacity of bacterial killing. *Biochemical and Biophysical Research Communications*. **331**: 120-126.

Reilly, T. J., Baron, G. S., Nano, F. E. & Kuhlenschmidt, M. S. (1996). Characterisation and sequencing of a respiratory burst-inhibiting acid phosphatase from *Francisella tularensis*. *Journal of Biological Chemistry*. **271**: 10973-10983.

Renirie, R., Hemrika, W. & Wever, R. (2000). Peroxidase and phosphatase activity of active site mutants of vanadium chloroperoxidase from the fungus *Curvularia inaequalis*. *Journal of Biological Chemistry*. **275**: 11650-11657.

Reynolds, A. & Schlesinger, M. J. (1969). Alterations in the structure and function of *Escherichia coli* alkaline phosphatase due to Zn^{2+} binding. *Biochemistry*. **8**: 588-593.

Rossolini, G. M., Schippa, S., Riccio, M. L., Berlutti, F., Macaskie, L. E. & Thaller, M. C. (1998). Bacterial nonspecific acid phosphohydrolases: physiology, evolution and use as tools in microbial biotechnology. *Cellular & Molecular Life Sciences*. **54**: 833-850.

Rotilio, G., Bray, R. C. & Fielden, E. M. (1972). A pulse radiolysis study of superoxide dismutase. *Biochimica et Biophysica Acta*. **268**: 605–609.

Saha, A. K., Dowling, J.N., Pasculle, A.W & Glew, R.H. (1988). *Legionella micdadei* phosphatase catalyzes the hydrolysis of phosphatidylinositol 4,5- biphosphate in human neutrophils. *Archives of Biochemistry Biophysics*. **265**: 94–104.

Salmeen, A & Barford, D. (2005). Functions and mechanisms of redox regulation of cysteine-based phosphatases antioxidants & redox signaling. *Institute of Cancer Research Repository*. **7**: 560-577.

Schenk, G., Boutchard, C. L., Carrington, L. E., Noble, C. J., Moubaraki, B., Murray, K. S., de Jersey, J., Hanson, G. R. & Hamilton, S. (2001). A purple acid phosphatase from sweet potato contains an antiferromagnetically coupled binuclear Fe-Mn Center. *Journal of Biological Chemistry*. **276**: 19084-19088.

Schenk, G., Elliott, T.W., Leung, E., Carrington, L.E., Mitić, N., Gahan, L.R & Guddat, L.W. (2008). Crystal structures of a purple acid phosphatase, representing different steps of this enzyme's catalytic cycle. *BMC Structural Biology*. **8**: 1-13

Schenk, G., Ge, Y., Carrington, L. E., Wynne, C. J., Searle, I. R., Carroll, B. J., Hamilton, S. & de Jersey, J. (1999). Binuclear metal centers in plant purple acid phosphatases: $\text{Fe}\pm\text{Mn}$ in Sweet Potato and $\text{Fe}\pm\text{Zn}$ in Soybean. *Archives of Biochemistry & Biophysics*. **370**: 183–189.

Schenk, G., Korsinczky, M.L.J., Hume, D.A., Hamilton, S & DeJersey, J. (2000). Purple acid phosphatases from bacteria: similarities to mammalian and plant enzymes. *Gene*. **255**: 419-424.

Spitznagel, J.K. (1983). Microbial Interactions with Neutrophils. *Reviews of Infectious Diseases*. The University of Chicago Press. 806-822.

Stadtman, T. C. (1996). Selenocysteine. *Annual Review of Biochemistry*. **65**: 83-100.

Stylianou, M.A., Hadjiconstantinou, M.P., Inglezakis, V.J., Moustakas, K.G & Loizidou, M.D. (2007). Use of natural clinoptilolite for the removal of lead copper and zinc in fixed bed column. *Journal of Hazardous Materials*. **143**: 575–581.

Sugiura, Y., Kawabe, H., Tanaka, H., Fujimoto, S. & Ohara, A. (1981). Purification, enzymatic properties and active site environment of a novel manganese (III)-containing acid phosphatase. *Journal of Biological Chemistry*. **256**: 10664-10670.

Szalewicz, A., Radomska, B., Strzelczyk, B & Kubicz, A. (1999). A novel 35 kDa frog liver acid metallophosphatase. *Biochimica et Biophysica Acta*. **1431**: 199-211.

Tanaka, N., Dumay, V., Liao, Q., Lange, A. J. & Wever, R. (2002). Bromoperoxidase activity of vanadate-substituted acid phosphatases from *Shigella flexneri* and *Salmonella enterica* ser. Typhimurium. *European Journal of Biochemistry*. **269**: 2162–2167.

Tempest, D. W & Wouters, J. T. M. (1981). Properties and performance of microorganisms in chemostat culture. *Enzyme and Microbial Technology*. **3**: 283-90.

Tolley, M.R., Macaskie, L.E., Moody, J.C. & Strandling, G.N. (1991). Actinide and lanthanum accumulation by immobilised cells of *Citrobacter* sp., Proceedings of the 201st Meeting American Chemical Society. **31**: 213–216.

Trobajo, C., Khainakov, S.A., Espina, A. Garcia, J.R. (2000). On the synthesis of α -zirconium phosphate. *Chemistry of Materials*. **12**:1787-1790.

Tsai, T.Y & Lee, Y.H. (1998). Roles of copper ligands in the activation and secretion of *Streptomyces tyrosinase*. *Journal of Biological Chemistry*. **273**: 19243–19250.

- Uerkvitz, W & Beck, C. F. (1981).** Periplasmic phosphatases in *Salmonella typhimurium* LT2. A biochemical, physiological and partial genetic analysis of three nucleoside monophosphate dephosphorylating enzymes. *Journal of Biological Chemistry*. **256**: 382–389.
- Uchiya, K. I., Tohsuji, M., Nikai, T., Sugihara, H. & Sasakawa, C. (1996).** Identification and characterization of *phoN-Sf*, a gene on the large plasmid of *Shigella flexneri* 2a encoding a nonspecific phosphatase. *Journal of Bacteriology*. **178**: 4548–4554.
- Vanhaecke, E. Remon, J.P., Moors, M., Raes, F., De Rudder, D & Van Peteghem, A. (1990).** Kinetics of *Pseudomonas aeruginosa* adhesion to 304 and 316 L stainless steel: role of cell surface hydrophobicity. *Applied Environmental Microbiology*. **56**: 788-795.
- Van Schijndel, J.W.P.M., Vollenbroek, E.G.M & Wever, R. (1993).** The chloroperoxidase from the fungus *Curvularia inaequalis*: a novel vanadium enzyme. *Biochimica et Biophysica Acta*. **1161**: 249–256.
- Volesky, B & Holan, Z.R. (1995).** Biosorption of heavy metals. *Biotechnology Progress*. **11**: 235-50.
- Wain, J., House, D., Pickard, D., Dougan, G & Frankel, G. (2001).** Acquisition of virulence-associated factors by the enteric pathogens *Escherichia coli* and *Salmonella enterica*. *Philosophical transactions of Royal Society Series B: Biological Sciences*. **356**: 1027-1034.
- Yong, P., Eccles, H & Macaskie, L.E. (1996).** Determination of uranium, thorium and lanthanum in mixed solutions using simultaneous spectrophotometry. *Analytica Chimica Acta*. **329**:173-179.
- Yong, P & Macaskie, L. E. (1995).** Enhancement of uranium bioaccumulation by a *Citrobacter* sp. via enzymically-mediated growth of polycrystalline $\text{NH}_4\text{UO}_2\text{PO}_4$. *Journal of Chemical Technology & Biotechnology*. **63**: 101-108.
- Yong, P. & Macaskie, L. E. (1998).** Bioaccumulation of lanthanum, uranium and thorium and use of a model system to develop a method for the biologically-mediated removal of plutonium from solution. *Journal of Chemical Technology & Biotechnology*. **71**: 15-26.

9 Appendices

Appendix 1 Protein measurement

Protein concentration was determined by the method of Bradford for soluble proteins, using dried bovine serum albumin (Sigma-Aldrich) as a standard in each case.

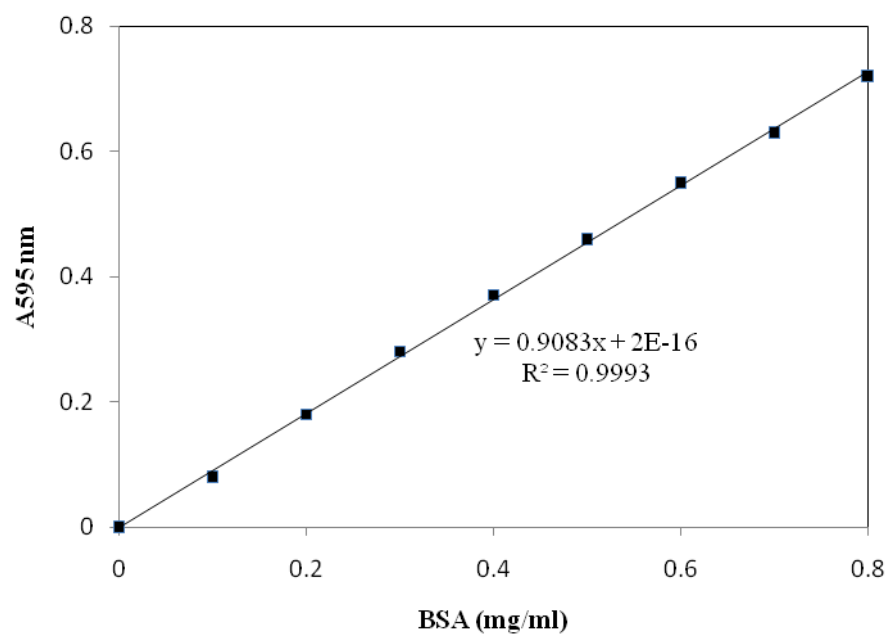
Bradford method (Bradford, 1976)

Coomassie brilliant blue (100 mg) G-250 was dissolved in 95% ethanol (50 mL). Phosphoric acid 85% (w/v) (100 mL) was then added. The reagent was made up to a total volume of 1 L with deionised water and then filtered with Whatmann No.1 filter paper to remove any undissolved dye. A solution of NaOH (1 M) was also prepared for use in the assay.

Standard method (for 0.1 mg/ml – 1.0 mg/ml protein)

Protein sample (30 μ L), NaOH (1 M) (50 μ l) were added together and mixed, before the addition of coomassie blue reagent (1 ml). Samples were incubated for 20 min and the absorbance measured at 595 nm against a reagent blank.

Calibration curve of protein using the Bradford method



Appendix 2 Phosphatase specific activity

Phosphatase activity was determined by measuring the liberation of p-nitrophenol (pNP) from p-nitrophenyl phosphate (pNPP). One unit of enzyme activity is defined as 1 nmol of pNP liberated per minute, per mg of bacterial protein.

Cell suspension (1 mL) was added to test tubes A and B, MOPS NaOH buffer (1 mL) was also added to A and B, which were then left to equilibrate in a water bath at 30°C for 15 mins. Phosphatase activity was stopped in test tube B by the addition of NaOH (5 mL, 0.2 M). The reaction was initiated in test tube A by the addition of pNPP solution (0.4 mL, 12 mg/mL), a timer was set and the solution mixed. This solution was also added to test tube B. As soon as the solution in tube A showed yellow colouration the reaction was stopped by the addition of NaOH (5 mL, 0.2 M) and the timer was stopped. The absorbance of the original cell suspension was measured at 600 nm against deionised water. The absorbance of test tube A was measured at 410 nm against reagent blank B.

Phosphatase activity was calculated by the following equation:

$$\text{Phosphatase specific activity} = \frac{A_{410} \times 10^9}{t \times 18472} \times \frac{7.4}{10^3} \times \frac{1}{0.552 \times A_{600}}$$

Where t is the time of the reaction from the addition of pNPP solution to the time when the reaction is stopped by NaOH; 18,472 is the molar extinction coefficient ($\text{M}^{-1}, \text{cm}^{-1}$) for the above conditions and 0.552 is the protein conversion factor (Jeong, 1992).

Appendix 3 Differences between SP1 and SP2 from previous work (Jeong, 1992)

Amino acid composition of *Serratia* sp. phosphatases SP1 and SP2 (Jeong, 1992).

Amino Acid	Number of residues per subunit	
	SP1	SP2
Cysteine	1	1
Aspartic acid	19	21
Glutamic acid	21	21
Serine	14	14
Glycine	31	31
Histidine	4	4
Arginine	13	13
Threonine	14	14
Alanine	37	37
Proline	11	12
Tyrosine	7	6
Valine	10	10
Methionine	3	3
Isoleucine	8	8
Leucine	18	17
Phenylalanine	5	4
Lysine	9	8
Total residues per subunit:	224	224

* Differences in the number of amino acids between SP1 and SP2 are highlighted in bold text.

3.1 N-terminal amino acid sequences of *Serratia* sp. phosphatases SP1 and SP2 (Jeong, 1992).

SP1: Ala-Arg-Asp-Val-Thr-Thr-Thr-Pro-Asp-Phe-Tyr-Tyr-Leu-Lys-Glu

SP2: Ala-Arg-Asp-Val-Thr-Thr-Thr-Pro-Asp-Phe-Tyr-Tyr-Leu-Lys-Glu

3.2 Temperature optima of SP1 and SP2:

SP1 = 50 °C, SP2 = 45°C (Jeong, 1992).

3.2.1 pH optima of SP1 and SP2:

SP1 = 5.75, SP2 = 6.25 Range: SP1 activity decreased significantly outside range of 4.5-6.25 and had only 15 % of the maximum activity below pH 4.5 or above pH 9.0. SP2 the retention of activity was 46 % and 37 % of the maximum at pH 4.5 and pH 10.00, respectively. SP1 can be classified as an acid-type phosphatase and SP2 as more of a 'neutral' phosphatase with some alkaline phosphatase activity.

Appendix 4 Calculation of a rate constant for the deoxyribose method

The calculation of the rate constant for a scavenger of free radicals is calculated from the following equation:

$$\frac{1}{A} = \frac{1}{A^0} \left(1 + \frac{K_p [P]}{K_{DR} [DR]} \right)$$

Where A = absorbance, A^0 = absorbance in the absence of a scavenger, P = scavenger, [P] = concentration of scavenger, [DR] = deoxyribose, K = rate. Concentration is in moles.

A plot of $1/A$ against [S] should give a straight line of slope $K_s / K_{DR} [DR] A^0$ with an interception on the y-axis of $1/A^0$. The rate constant for reaction of S with free radicals can be obtained from the slope of the line.

The results for purified phosphatase are presented in this way to enable direct comparison for other enzymes with scavenging ability cited in the literature with rate constants.

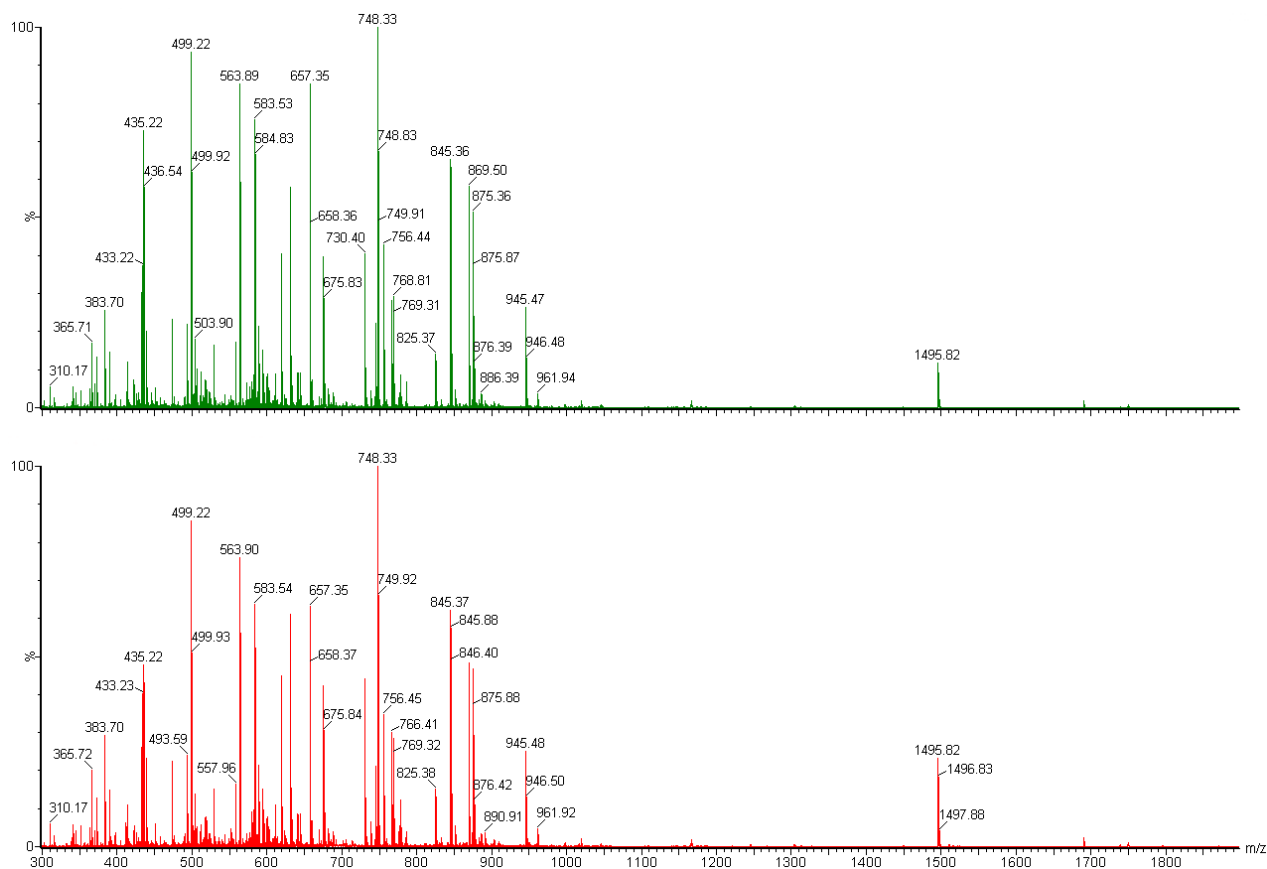
Appendix 5 Peptide separation by in-line liquid chromatography, electrospray ionisation mass spectrometry and data dependent analysis of gel based samples for protein identification (separation and analysis was done by Susan Slade, Biological mass spectrometry and proteomics department, University of Warwick).

The extracted tryptic peptides (as described in materials and methods) were resolved using an in-line NanoAcquity LC and autosampler system. A 4.9 μL aliquot of each sample was loaded onto a nanoACQUITY UPLC™ trapping column 10 kpsi Symmetry C18 180 μm x 20 mm 5 μm (Waters) equilibrated in 1 % aqueous acetonitrile containing 0.1 % formic acid, the column was then flushed at 15 μLmin^{-1} for 1 min to waste. The peptides were then eluted onto a nanoACQUITY UPLC BEH C18 Column, 1.7 μm , 100 μm x 100 mm, 10 kpsi column (Waters) at 0.4 μLmin^{-1} using a linear gradient of formic acid (1 %) in acetonitrile (1 %).

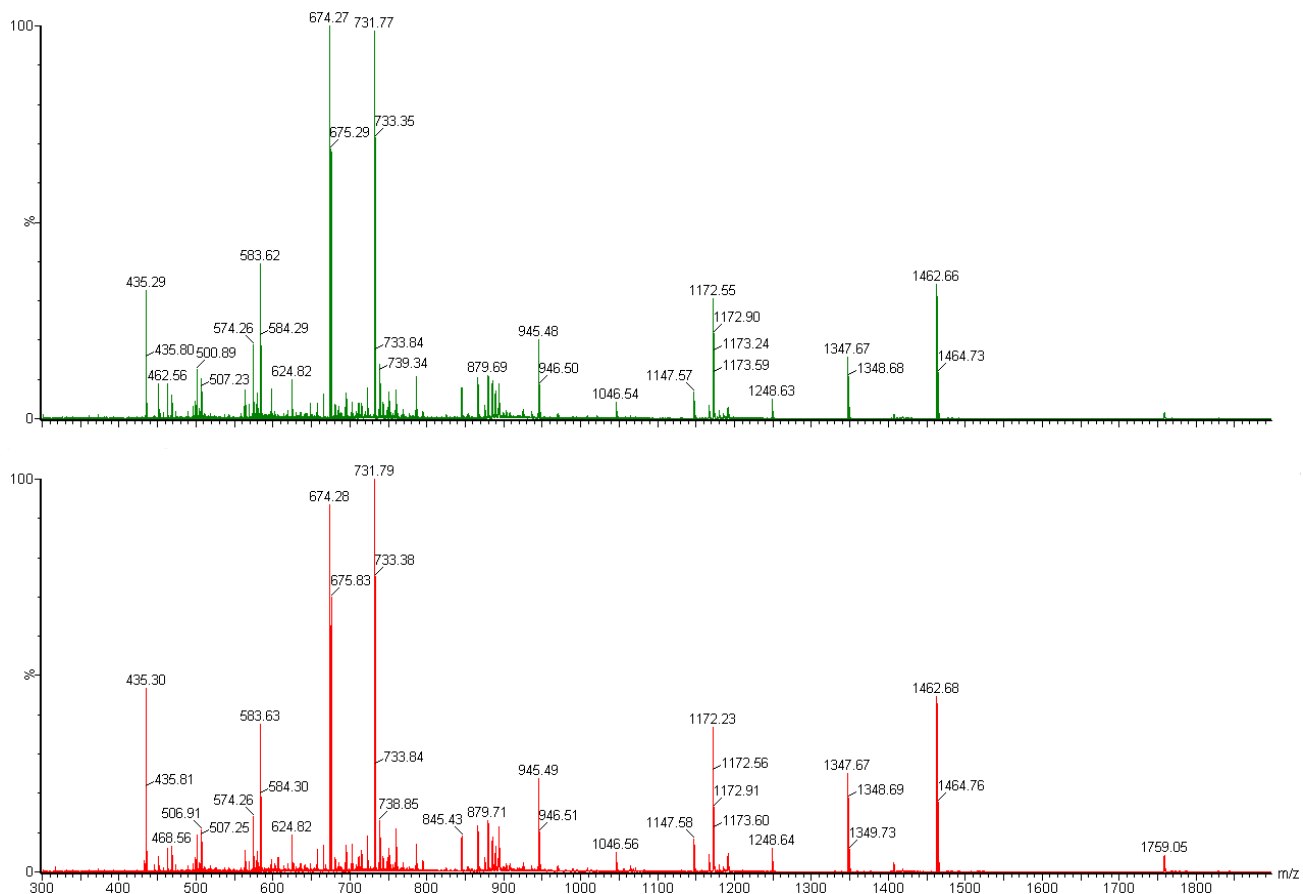
The eluted peptides were analysed on a Waters Micromass Q-ToF Global Ultima mass spectrometer fitted with a nano-LC emitter (New Objective) with an applied capillary voltage of 3-4 kV. The instrument was operated in ESI-MS positive ion mode over the mass/charge (m/z) range 300-2000 using a 0.6 sec scan time. A calibration was done using a collisionally induced decomposition (CID) spectrum of the doubly charged precursor ion of [glu¹]-fibrinopeptide B (GFP – Sigma-Aldrich F3261). A calibration was accepted when the average error obtained on a subsequent acquisition was <10 ppm. Sensitivity was assessed by an injection of 50 fmol of a phosphorylase B (for tryptic digest) on the column giving a base peak intensity >1000 counts sec^{-1} in MS mode on the most intense peptide.

The instrument was operated in data dependent acquisition (DDA) mode over the mass/charge (m/z) range of 50-2000. During the DDA analysis, both MS and tandem mass spectrometry (CID) were done on the three most intense peptides as they eluted from the column. The uninterpreted MS/MS data were processed using the Waters ProteinLynx Global Server v2.3 software package (smoothed, background subtracted, centred and deisotoped) then mass corrected against the doubly charged GFP peptide infused at 0.5 μLmin^{-1} in 50 % aqueous acetonitrile/0.1% formic acid through the nanoflow lock mass line. A peak list file (pkl) was created for each sample and used for database interrogation.

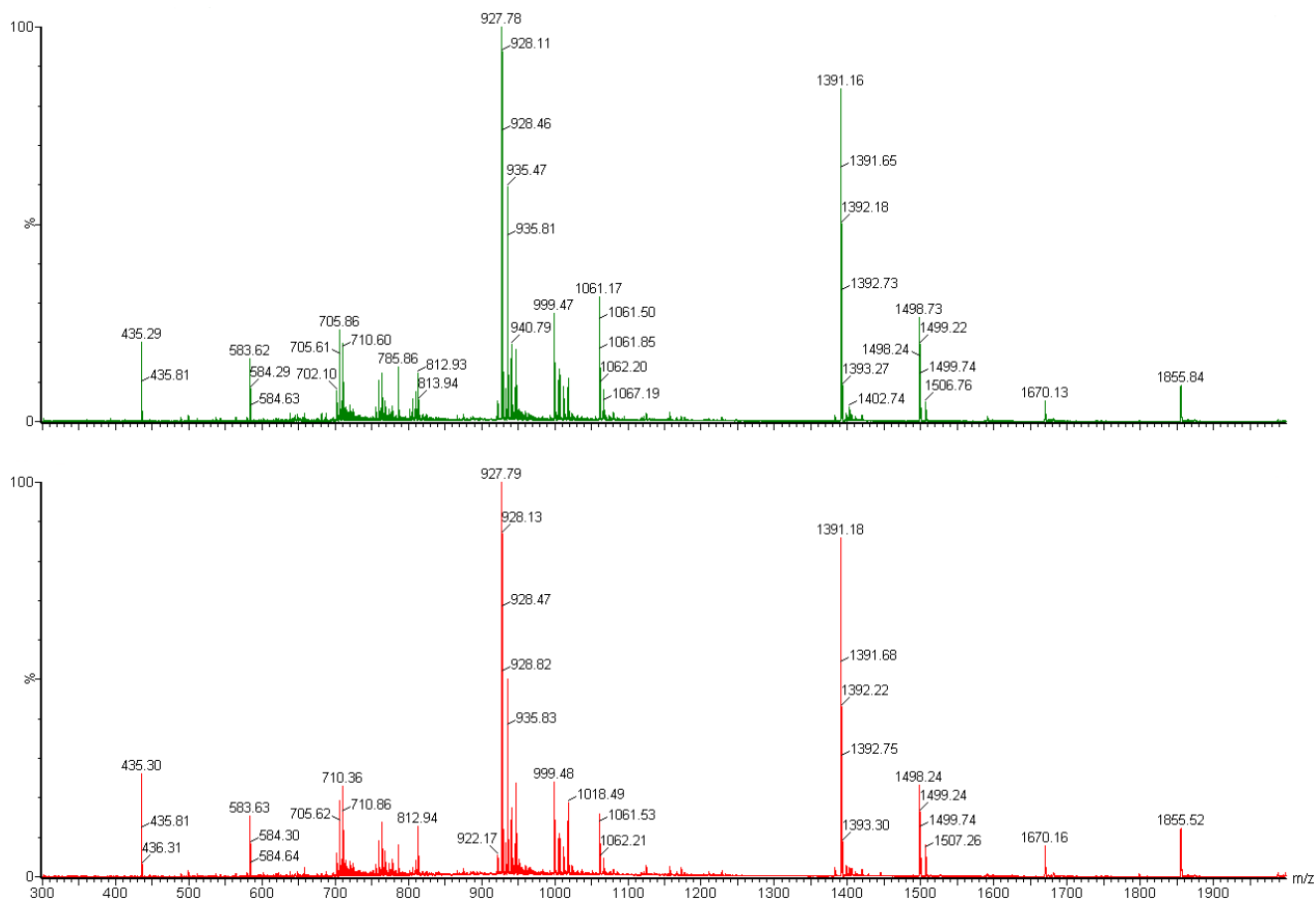
Appendix 6 Additional screen shots from the MS analysis (peptide mass fingerprints) of SP1 and SP2.



Screenshots from the MS analysis (peptide mass fingerprints) of SP1 and SP2 (5 min sections of the LC trace were combined and the MS spectra plotted). This screenshot was taken from 15-20 min retention time on the LC column run. Apart from small differences in intensity, the traces for SP1 and SP2 are super imposable and show no additional peptides.



Screenshots from the MS analysis (peptide mass fingerprints) of SP1 and SP2 (5 min sections of the LC trace were combined and the MS spectra plotted). This screenshot was taken from 20-25 min retention time on the LC column run. Apart from small differences in intensity, the traces for SP1 and SP2 are super imposable and show no additional peptides.



Screenshots from the MS analysis (peptide mass fingerprints) of SP1 and SP2 (5 min sections of the LC trace were combined and the MS spectra plotted). This screenshot was taken from 25-30 min retention time on the LC column run. Apart from small differences in intensity, the traces for SP1 and SP2 are super imposable and show no additional peptides.

Appendix 7 Bioaccumulation of metals by *Serratia* sp. biofilm (control showing the amount of metal biosorption by dead *Serratia* sp. biofilm).

Reactor systems were prepared, similar to those described in chapter 2 were exposed to Zr (1 mM) in the presence of citrate buffer (3 mM) pH 5, but in the absence of G2P. The biofilm used in this experiment was previously killed by autoclaving (20 min at 121°C). This reactor was used as a control to ascertain how much metal was accumulated by biosorption alone.

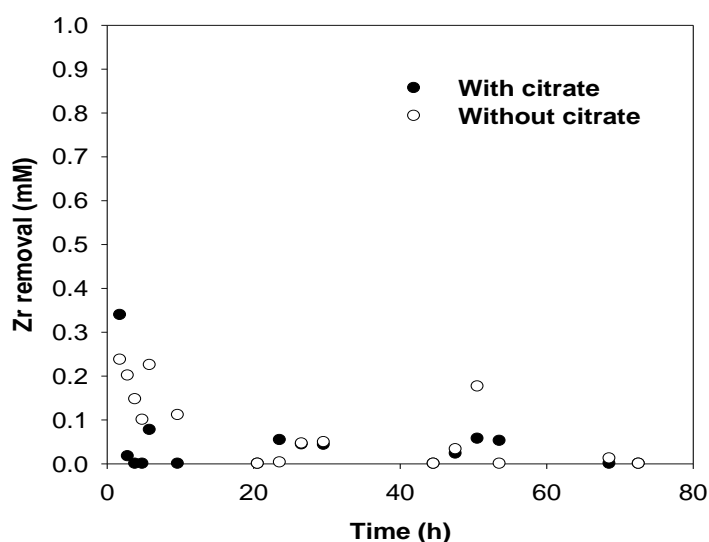


Fig . Zr removal (mM) by autoclaved *Serratia* biofilm in two control reactors, with and without citrate buffer. Metal removal is attributable to biosorption.

Appendix 8 MASCOT search results using peak list (pkl) files generated from mass spectrometry for SP1 and SP2 carried out at Warwick University by Susan Slade.

Results are shown below for searches within the NCBIInr database using the peak list files generated for SP1 and SP2 from analysis with mass spectrometry (Chapter 2, section 2.5.2 and 2.5.3). The database Swissprot was also searched using the same pkl files but returned no matching peptides for SP1 or SP2. NCBIInr returned one result for SP1 and two results for SP2, data shown are presented in a raw format directly from the search results observed from the MASCOT search engine (see below).

1. Search results for SP1 using the database; NCBIInr

1. Acid phosphatase [*Bacteroides vulgatus* ATCC 8482]

[gi|150003121](#) **Mass:** 29142 **Score:** 69 **Matches:** 2(0) **Sequences:** 2(0)

Nominal mass (M_r): **29142**; Calculated pI value: **6.47**

Taxonomy: *Bacteroides vulgatus* ATCC 8482

Matched peptides shown in **Bold Red**

```
1  MKTKFALLLV FCAISLNIFA QEKKIKDRRT NPELYYLEES EVANSLELLP
51 PPPEAGSILF LYDKARYDWG KLQRDTPRGE QAVSDARVNG DGVPFAPSEA
101 FGIEITRDKT PELYRLIINM REDAGDLATR HAKEYYMRVR PFSFFNEMTC
151 NPEQQEELST NGSYPGHTA IGWATALVLA EINPDRQNEI LKRGFEMGQS
201 RVICGYHFQS DVDAARIVAS AVVARLHAND AFVKQLNKAK DEFSKLQKAG
251 LIQSVSKK
```

2. Search results for SP2 using the database; NCBIInr

1. PhoN1 [candidate division TM7 single-cell isolate TM7a]

[gi|169839741](#) **Mass:** 14189 **Score:** 82 **Matches:** 2(0) **Sequences:** 2(0)

Nominal mass (M_r): **14189**; Calculated pI value: **9.39**

Taxonomy: candidate division TM7 single-cell isolate TM7a

Matched peptides shown in **Bold Red**

```
1 DAGDLATRSA KQTYMRIRPF AYFKESTCRP EDEATLSKNG SYPGHTSIG
51 WATALVLA EI NPARQSEIIK RGYEMGQSRV ICGYHWQSDV DAARVVASTV
101 VATLHSNSEF NAQLAKAKAE FQRISKRK
```

2. Acid phosphatase [*Bacteroides vulgatus* ATCC 8482]

[gi|150003121](#) **Mass:** 29142 **Score:** 54 **Matches:** 2(0) **Sequences:** 2(0)

Nominal mass (M_r): **29142**; Calculated pI value: **6.47**

Taxonomy: *Bacteroides vulgatus* ATCC 8482

Matched peptides shown in **Bold Red**

```
1 MKTKFALLLV FCAISLNIFA QEKKIKDRRT NPELYYLEES EVANSLELLP
51 PPPEAGSILF LYDKARYDWG KLQRDTPRGE QAVSDARVNG DGVPPFAFSEA
101 FGIEITRDKT PELYRLIINM REDAGDLATR HAKEYYMRVR PFSFFNEMTC
151 NPEQQEELST NGSYPGHTA IGWATALVLA EINPDRQNEI LKRGFEMGQS
201 RVICGYHFQS DVDAARIVAS AVVARLHAND AFVKQLNKAK DEFSKLQKAG
251 LIQSVSKK
```

NB pkl files for SP1 and SP2 were also used to search the database swissprot but returned no results.

Appendix 9 Additional publications

Removal of cobalt, strontium and cesium by biomineralization into biogenic metal phosphate matrices

L. E. Macaskie, M. Paterson-Beedle, C. Mennan, D. A. Graf von der Schulenburg, M. L. Johns, C., J. E. Readman, J. A. Hriljac

Geomicrobiology Journal (invited). To be submitted

NSAP class A acid phosphatase from a *Serratia* sp. atypical of *Enterobacteriaceae* contains no metal ions but shows homology to vanadium peroxidase and the phosphatase of pathogenic Enterobacterial species.

Claire Mennan¹, Susan E Slade², David Lee¹, Lynne E Macaskie^{1*} and Marion Paterson-Beedle¹.
Microbiology. To be submitted.

Conference Poster:

Migration: Chemistry and Migration Behaviour of Actinides and Fission Products in the Geosphere. June 2007. Munich, Germany.

Title: Accumulation of zirconium by *Serratia* sp.: a novel system for the removal of radionuclides from aqueous flows.

NSAP class A acid phosphatase from a *Serratia* sp. atypical of *Enterobacteriaceae* contains no metal ions but shows homology to vanadium peroxidase and the phosphatase of pathogenic *Enterobacterial* species.

This chapter comprises a paper to be submitted to the journal Microbiology. I prepared the manuscript and did the critical experimental work. Co-authors assisted by editing the manuscript. MS analysis was done by Susan Slade (University of Warwick). PIXE analysis was done at the Surrey Ion Beam Facility (University of Surrey).

Context

Chapter 4 detailed the purification of *Serratia* sp. phosphatases SP1 and SP2. The following chapter (to be submitted as a journal paper) shows the partial characterisation of SP2. At the time of this work, very low yields of SP1 meant that characterisation experiments could only be done with SP2. Later work (see chapter 6) shows the characterisation and comparison of SP1 and SP2.

NSAP class A acid phosphatase from a *Serratia* sp. atypical of *Enterobacteriaceae* contains no metal ions but shows homology to vanadium peroxidase and the phosphatase of pathogenic *Enterobacterial* species.

Claire Mennan¹, Susan E Slade², David Lee¹, Lynne E Macaskie^{1*} and Marion Paterson-Beedle¹.

¹*School of Biosciences, The University of Birmingham, Edgbaston, Birmingham, B15 2TT, UK*

²*Biological Mass Spectrometry and Proteomics Department, The University of Warwick, Coventry, UK CV4 7AL*

**Author for correspondence (Fax: +44-121-414-5925; E-mail: l.e.macaskie@bham.ac.uk)*

Abstract

NSAP class A acid phosphatase from a *Serratia* sp. was purified and partially characterised. Database interrogation using the Basic Local Allignment Search Tool (BLAST) with partial sequences of the phosphatase (obtained in earlier studies) confirmed homology with PhoN and also PhoC of several pathogenic enterobacterial species. Similarities were also found with the vanadium haloperoxidases which share a conserved sequence in the active site. However, analysis using highly sensitive Micro-Proton Induced X-ray Emission (PIXE) analysis failed to detect vanadium or any other metallic components. Tests probing the potentiating effect of the phosphatase with respect to free radical damage to deoxyribose in a Fenton type reaction showed that the phosphatase increased the radical damage significantly despite the absence of redox active components and a low cysteine content of the enzyme.

Introduction

A *Serratia* sp. atypical of *Enterobacteriaceae* has been extensively studied with respect to its potential for the bioremediation of heavy metals from aqueous solutions (Macaskie *et al.* 1992; 2000). Metals are deposited onto the bacterial cell surface as metal phosphates via the activity of a PhoN-type acid phosphatase, which exists both extracellularly and in the periplasm as shown by immunogold labelling (Jeong *et al.* 1997; Macaskie *et al.* 1994a; 2000). This phosphatase liberates inorganic phosphate ligand (HPO_4^{2-}) from a phosphate donor and deposits metal (M) as polycrystalline cell bound MHPO_4 (Macaskie *et al.* 1992; 2000).

The *Serratia* sp., isolated from metal contaminated soil (Macaskie & Dean., 1982), was initially identified commercially as a species of *Citrobacter* but more extensive molecular biological analysis (Pattanapitpaisal *et al.* 2002) re-assigned it as a *Serratia* sp. Unlike related pathogenic genera which express PhoN (e.g. *Salmonella*, *Morganella*, *Providencia*), *Citrobacter* and *Serratia* are not generally described as pathogenic, although some strains of *S.marcescens* are disease causing pathogens in plants and in a wide range of invertebrate and vertebrate hosts; in humans they are described as opportunistic pathogens (Kurz *et al.* 2003).

Although the *phoN* phosphatase is very well described historically (e.g. Kasahara *et al.* 1991; Groisman *et al.* 1992) a role for this enzyme has still not been assigned. An accepted role is that acid phosphatase acts as a scavenger of organic phosphate esters which are otherwise unable to pass through the cytoplasmic membrane (Uerkwitz & Beck, 1981). It has also been hypothesised that acid phosphatase functions as a phosphate retrieval system in pathogenic bacteria, activated upon phagosomal containment (Felts *et al.* 2006), as well as playing an integral role in survival of the pathogen within the host's phagocytic cells of the host (Aguirre-Garcia *et al.* 2000). Many of the intricacies of these survival mechanisms remain largely unknown. However, such mechanisms include: inhibition of the respiratory burst (Reilly *et al.* 1996), inhibition of phagolysosome fusion and survival and/or escape from within the phagolysosome (Fields *et al.* 1989). *Salmonella*

typhimurium is an intracellular pathogen which shows involvement of the *phoP* gene in its virulence and survival within the macrophage (Fields *et al.* 1989); the *phoP/phoQ* regulon which controls *S. typhimurium* virulence (Miller *et al.* 1989), also controls, amongst other factors, the production of PhoN (Kasahara *et al.* 1991).

Amino acid sequencing of peptide fragments of acid phosphatase from this *Serratia* sp. (from an earlier study, Macaskie *et al.* 2004a) revealed significant homology to the *phoN* product (acid phosphatase) of some pathogenic enterobacterial species of bacteria (Jeong, 1992; Macaskie *et al.* 1994a; Rossolini *et al.* 1998). In this *Serratia* sp. the phosphatase is localised within the periplasmic space and also exocellularly (Jeong, 1992; Macaskie *et al.* 2000), in association with extracellular materials, in accordance with the known export of phosphatase by a mechanism of extrusion within outer membrane vesicles (Kadurugamuwa & Beveridge, 1995). *Serratia* sp. does not normally contain PhoN. It is possible that this *Serratia* sp. obtained the gene (which fortuitously promotes deposition of heavy metal phosphates as a likely response to metal-stress) by natural gene transfer mechanisms, (Groisman *et al.* 1992; Macaskie *et al.* 2000). In support of this, Groisman *et al.* (1992) noted that the *phoN* DNA from *S. typhimurium* has a G+C ratio of 43 % which, is lower than the overall G+C content of the *S. typhimurium* chromosome which averages 52 %, while the G+C content of the third positions of codons in the *phoN* open reading frame is only 39 % (Groisman *et al.* 1992; Groisman, 2001). This suggests natural acquisition of a ‘foreign’ gene with a root in pathogenicity and its maintenance under selective pressure in a non-pathogenic environmental organism.

Regardless of the mechanism by which this *Serratia* sp. obtained *phoN*, the normal physiological role of the enzyme remains unclear. The aim of this study was to compare the *Serratia* PhoN acid phosphatase to related PhoN phosphatases from pathogenic strains using modern molecular methods and to investigate the presence of bound metals using highly sensitive micro-PIXE analysis. A previous study using EDTA concluded that the enzyme was not a

metalloenzyme since EDTA was not inhibitory (Jeong, 1992). However, this test is not definitive since various EDTA-resistant enzymes were later found to contain metal ions (Reynolds & Schlesinger, 1969).

Many phosphatases contain Zn(II) and also redox active metals such as Cu, Mn or Fe (Schenk *et al.* 2001). Anticipating a redox-active metalloenzyme component, the acid phosphatase was also tested for a role in promoting Fenton-type free radical reactions to test if the enzyme was capable of producing (or indeed scavenging) free radicals. This was prompted by the observations that the *phoN* DNA is ‘foreign’ in origin (Groisman *et al.* 1992), *phoN* expression is under the control of the *phoP/phoQ* transcription regulator which is associated with stress responses (Miller *et al.* 1989) and the phagolysosome host response involves both a lowering of local pH and a free radical burst. An exocellular ‘tethered’ location of the enzyme (see above) would accord with both defensive and aggressive functions.

Materials and methods

Microorganism and culture conditions

Serratia sp. (NCIMB 40259) was used under license from Isis Innovation, Oxford, UK. Following batch-scale tests, growth of *Serratia* sp was carried out at pilot-scale in lactose minimal medium (600 L) in a LSL Biolafitte fermenter (total volume of 800 L) as described previously by Macaskie *et al* (1995). The culture was chilled and harvested using a continuous centrifuge (Sharples) and stored as frozen pellets (0.5-1 kg) of wet biomass in 1-2 L blocks at -70 °C. Samples were chipped from the frozen blocks as required.

Purification of phosphatase and assay of phosphatase activity.

All procedures were at 4 °C unless otherwise stated. Portions of frozen *Serratia* biomass were thawed and weighed (100 g wet weight of *Serratia* cells were used in a typical purification). The cells were suspended in Tris-HCl buffer (20 mM, pH 8.0) and disrupted with two passages through a French pressure cell (SLMO AMINCO, SLM instruments Co.). The resulting cell lysate was subjected to centrifugation and ultracentrifugation followed by $(\text{NH}_4)_2 \text{SO}_4$ fractionation as previously described by Jeong (1992 and Jeong *et al.* 1998). Some of the chromatography materials previously used (Jeong *et al.* 1998) were not currently commercially available. Hence, the phosphatase was purified by a simplified method using anion exchange column chromatography and gel filtration on HiTrap Q (1 × 5 ml, GE Healthcare UK) followed by Superdex 200 (1.6 × 60 cm GE Healthcare UK). The phosphatase (suspended in Tris-HCl buffer, 20 mM, pH 8.0) was eluted as a single peak from HiTrap Q (flow rate of 2.5 ml min⁻¹) while contaminants remained bound to the column. The phosphatase was further purified on Superdex 200 (in Tris-HCl buffer, 20 mM, NaCl, 0.15 M, pH 8.0) (flow rate 1.0 ml min⁻¹) and it eluted before any of the contaminants at the 100 kDa mark (by comparison with molecular weight standards). De-salting and concentration of the enzyme between each step was achieved by use of vivaspin 20 centrifugal concentrators (Fisher Scientific, UK) with a molecular weight cut off of 10 kDa.

Phosphatase activity was assayed by the release of p-nitrophenol (pNP) from p-nitrophenyl phosphate (pNPP) (Jeong *et al.* 1999). One unit of activity is defined as that liberating 1 nmol product min⁻¹ mg bacterial protein⁻¹; protein was assayed by the method of Bradford (1976) using bovine serum albumin as the standard. The molar extinction coefficient for pNP was 9025 cm⁻¹ M⁻¹, measured under the conditions of assay at λ_{410} .

Elemental analysis of acid phosphatase by micro proton induced X-ray emission (PIXE) analysis

PIXE analysis is well suited to analysis of trace metals since it detects X-ray emissions from both inner and outer shell electrons under high energy proton bombardment and is both element-specific and highly sensitive (Grime & Watt, 1990).

The phosphatase was concentrated using vivaspin20 centrifugal concentrators (Fisher Scientific, UK) (molecular weight cut off of 10 kDa) and suspended in ultrapure water (20 mg ml⁻¹). For analysis, 1 µl of phosphatase was placed onto 4µm thick “Prolene” polypropylene film and allowed to dry. The resulting residues were analysed using micro-PIXE and Rutherford Backscattering Spectrometry (RBS) at the Surrey Micro Beam Facility (SMBF) at the University of Surrey, UK. Elemental maps were created by focussing the micro beam line (4x4µm beam, beam energy: 2.5 MeV; Ion: H⁺) on the dried protein sample using the sulphur component as a locator for the protein. Three points were analysed for each sample (data acquisition time 30 min each). Prior to sample analysis a Pb glass standard was used to determine the calibration parameters for the detector (distance and effective filter thickness). Assignment of X-ray emission energies to specific elements was made by reference to internal standards and elemental concentrations were calculated via the proprietary software of the SMBF taking into account sample thickness.

Polyacrylamide gel electrophoresis and MALDI-ToF of *Serratia* sp. phosphatase

All gels and chemicals were from Invitrogen (UK) unless otherwise stated. Sodium dodecyl sulphate-PAGE used pre-cast NuPAGE Novex Bis-Tris mini gels with MOPS SDS running buffer (pH 7.0) at 200 V for 50 minutes. The molecular weight of the phosphatase was estimated using NOVEX Mark12 unstained molecular weight standards; gels were stained with Coomassie blue (G-250). The purified phosphatase (single band on SDS-PAGE) was subjected to MALDI-ToF to

confirm its molecular weight, using a Bruker biflex IV mass spectrometer. The sample (approx 10-20 pmol) was embedded in a matrix of sinapinic acid (10 mg ml⁻¹ in 50:50 CH₃CN/0.1 % TFA) and irradiated at 337 nm utilising a nitrogen laser. Data acquisition and processing were performed using Bruker flexControl and flexAnalysis software.

Mass spectrometry for database searches

Serratia sp. phosphatase was loaded onto SDS-PAGE gel as above; approximately 200 µg of protein was separated on the gel. Phosphatase gel bands were excised using a sterile scalpel by cutting a section of gel no greater than 0.5 cm x 0.15 cm, which was then further sliced into five equally sized pieces. Further processing of the gel plugs was done by a MassPrep robotic protein handling system (Waters Micromass) using the manufacturer's protocol as described below. Gel plug(s) were destained twice using acetonitrile (50 % v/v) in ammonium bicarbonate (100 mM), rinsed with concentrated acetonitrile, allowed to dry in air (10 min) and reduced with dithiothreitol (10 mM) in ammonium bicarbonate (100 mM) for 30 minutes followed by alkylation with iodoacetamide (55 mM) in ammonium bicarbonate (100 mM). The gel plugs were then rinsed with acetonitrile and ammonium bicarbonate (mixture as above) followed by a further three washes with acetonitrile. An aliquot of trypsin (25 µl of 6 ng µl⁻¹) was added to each sample and the mixture was incubated at 37 °C (4.5 h). The resulting peptides were initially extracted using an aqueous solution (30 µl) containing 2 % acetonitrile (2 % v/v) and formic acid (1 % v/v). A second extraction using an aqueous solution (15 µl) containing acetonitrile (51 %) and formic acid (0.5 %) was then made and combined with the first extraction in a cooled 96-well plate and, if necessary, stored at -80 °C prior to analysis by mass spectrometry. The extracted tryptic peptides were resolved using an in-line NanoAcquity LC and autosampler system. The eluted peptides were analysed on a Waters Micromass Q-ToF Global Ultima mass spectrometer fitted with a nano-LC emitter (New Objective). The instrument was operated in data dependent acquisition

(DDA) mode over the mass/charge (m/z) range of 50-2000. A peak list file (pkl) was created for each sample and used for database interrogation.

Eluted peptides were also analysed in ESI-MS positive ion mode over the mass/charge (m/z) range, using a neutral loss driven acquisition (to allow detection of phosphorylated peptides). On alternate MS scans the energy applied to the collision cell was either 10 eV or a stepped up energy of 25 eV rising to 35 eV. Real time data selection was used to identify any H_3PO_4 neutral loss events during the analysis, which would then trigger an MS/MS acquisition.

Effects of various compounds on *Serratia* sp. phosphatase

Phosphatase activity was tested in the presence and absence of each of the indicated substances with the pH of the mixture checked before and after each effector addition. Enzyme activity was tested in the presence and absence of: L-(+)-Sodium tartrate, EDTA, H_2O_2 and β -mercaptoethanol (concentrations as shown in individual experiments). With the exception of EDTA, tests were incubated at 30 °C for 15 minutes with *Serratia* phosphatase (0.2 μ g in 40 mM MOPS-NaOH buffer, pH 7.0), prior to the addition of pNPP. EDTA was incubated with phosphatase for 24 h prior to the addition of pNPP to allow metal chelation to take place since prolonged incubation can be required to remove bound metals (Sugiura *et al.* 1981). The activity was expressed as a percentage of that observed without effector substance.

Deoxy ribose method for assessment of free radical damage

The assay was done according to the method of Halliwell *et al* (1987). All chemicals (unless otherwise stated) were from Sigma-Aldrich (UK) (AnalaR). The reaction mixture contained: phosphatase (variable concentration, 0-8 nM, MW = 100 kDa, 1 nmol enzyme = 0.1 mg protein), 2-deoxy-D-ribose (5 mM), phosphate buffer (20 mM, pH 7.4), FeCl₃ (100 µM), EDTA (104 µM), H₂O₂ (5 % w/w, 1 mM) and ascorbic acid (1 µM) in a final volume of 1 ml. The reaction mixture was incubated at 37 °C for 1 h and 2-thiobarbituric acid solution 1 ml (1 % w/v in 0.05 M NaOH) was added, followed immediately by 1 ml glacial acetic acid. The solution was heated at 100 °C for 10 mins, cooled and the absorbance measured at 532 nm. Controls used ethanol and heat denatured phosphatase. Ethanol is a known scavenger of free radicals and a rate constant has been calculated and published (Halliwell *et al.* 1987) as $1.4 \times 10^9 \text{ M}^{-1} \text{ S}^{-1}$. As a positive control, ethanol (0-20 mM) was used as above, replacing phosphatase in the reaction mixture. Phosphatase was denatured (negative control) by heating at 100 °C for 10 mins and the loss of activity was confirmed by the absence of release of p-nitrophenol from p-nitrophenyl phosphate (see above). The denatured enzyme was used at a variable concentration (0-8 nM) as above in place of the active enzyme. Calculation of the rate constant for a scavenger (or generator) of free radicals was calculated from the following equation (Halliwell & Gutteridge, 1987):

$$\frac{1}{A} = \frac{1}{A^0} \left(1 + \frac{K_p [S]}{K_{DR} [DR]} \right)$$

Where A = absorbance, A⁰ = absorbance in the absence of a scavenger, S = scavenger, [S] = concentration of scavenger, [DR] = 2-deoxy-D-ribose, K = rate. Concentration is in moles.

A plot of 1/A against [S] gives a straight line of slope $K_p / K_{DR} [DR] A^0$ with an intercept on the y-axis of $1/A^0$. The rate constant for reaction of S with free radicals is obtained from the slope of the

line. The results for purified phosphatase are presented in this way to enable direct comparison for other enzymes with scavenging ability cited in the literature with rate constants determined using the same test.

Results and Discussion

Comparison of *Serratia* NCIMB 40259 phosphatase with other PhoN enzymes

The phosphatase purification scheme and typical enzyme recoveries are shown in Table 1. The acid phosphatase was purified to homogeneity after two step chromatography on HiTrap Q and gel filtration on Superdex 200. Phosphatase was eluted in the flow through from HiTrap Q with active fractions identified using pNPP. The enzyme was eluted as a single peak of 100 kDa from Superdex 200, estimated by comparison with protein standards of known molecular weight analysed in parallel and eluted after the void volume. The enzyme subunits (4/mol; Jeong *et al.* 1998)) were visualised as a single band of 25 kDa using SDS-PAGE (Fig 1a). The subunit molecular mass was confirmed as 25 kDa by MALDI-ToF mass spectrometry (Fig 1b) and in accordance with the conclusion of Jeong (1992) the enzyme was concluded to be a homotetramer. Earlier work by Jeong (1992) that determined the holoenzyme mass did not use MS analysis but the mass was found to be around 100 kDa using a Superose Q-6 sizing column. An accurate mass determination in this study showing 25 kDa suggests a tetrameric protein whose mass should be concluded as ~100 kDa.

A previous study using limited amino acid sequencing of peptides compared against early databases suggested homology to the PhoN phosphatase of several other enterobacteria (Macaskie *et al.* 1994a). In comparison, the PhoN phosphatases of *Providencia stuartii*, *Shigella dysenteriae* and *Shigella flexneri* have a molecular weight of 27 kDa (four subunits), *Morganella morganii* has a 25 kDa subunit phosphatase (PhoC) also composed of four subunits in addition to a 25 kDa

monomeric phosphatase (Thaller *et al.* 1994 & 1995). *Klebsiella pneumoniae* and *Enterobacter aerogenes* have 25 kDa monomeric phosphatases, while *Salmonella typhi* and *S. typhimurium* have 27 kDa (tetrameric) and 28 kDa (monomeric) phosphatases, respectively (Thaller *et al.* 1994 & 1995). Based on work by Rossolini *et al.* (1998) on the classification of phosphatases, it was suggested that the PhoN phosphatase from this *Serratia* sp. fits into Class A (subclass A2) based on its resistance to EDTA, Mg^{2+} , Mn^{2+} , Zn^{2+} , sensitivity to fluoride and mercuric ions (Jeong, 1992) and its homotetrameric form.

The phosphatase from this *Serratia* has a maximum recorded specific activity of ~71000 units/mg (Jeong, 1992) and ~50000 units/mg (this study) (Table 1). A study characterising an acid phosphatase isolated from *Francisella tularensis* (involved in virulence) claimed that the activity of purified enzyme (13000-30000 units/mg) represents the highest specific activity ever reported for a bacterial or protozoan acid phosphatase (Reilly *et al.* 1996) i.e. ~two-fold less than the *Serratia* sp. enzyme. The activity of the *F.tularensis* phosphatase is reportedly ten times higher than the acid phosphatase of *Legionella micdaidei*, four times higher than that of *Coxiella burnettii* and twice that of the protozoan *Leishmania donovani* (Reilly *et al.* 1996). It is interesting to note that all of these organisms produce a phosphatase which is not only linked to virulence and survival in the phagosome (Reilly *et al.* 1996; Baca *et al.* 1993; Olivier *et al.* 2005), but they also have some of the highest phosphatase activities reported. In the metal contaminated soil from which this strain was isolated there would be strong selective pressure to retain the gene since metal phosphate precipitation is a likely method to precipitate toxic metals outside the cell (Macaskie *et al.* 1994b). Such selective pressure could help retain a pathogenicity related enzyme at a high level in an organism which is normally non-pathogenic.

Analysis of *Serratia* phosphatase by mass spectrometry and identification of the protein by database interrogation

Since the acid phosphatase of *Serratia* sp. appeared to be atypical (above) its relationship to other phosphatases was examined in more detail using modern methods. The phosphatase was subjected to tryptic digest and analysis by mass spectrometry as described in Materials and Methods. MS results showed that the enzyme is not phosphorylated. Phosphorylation is detectable by the neutral loss of H_3PO_4 during analysis, from a phosphorylated peptide (normally phosphorylated serine or threonine) and this mass loss was not detected. A pkl file was generated from the mass spectrometry results, which was used to interrogate the protein data bank for possible matches to this protein. Databases were interrogated through the MASCOT (MS/MS Ions) search engine. “NCBIInr” and “Swissprot” were searched and results showed no significant homology to any protein in the databases.

Database searches using partial amino acid sequences of the *Serratia* phosphatase as reported by Jeong (1992) returned several partial matches to; PhoN and PhoC of several microorganisms. The amino acid sequences of two peptide fragments of purified *Serratia* phosphatase obtained in early work by Macaskie *et al* (1994a) were compared in this study with known polypeptide sequences using the Basic Local Alignment Search Tool (BLAST) to find any regions of local similarity between sequences contained within the following six databases: Non redundant protein sequences, reference proteins, swissprot protein sequences, patented protein sequences, protein data bank protein and environmental samples. Sequence fragments used to search the databases were: Fragment 1 (F1) N-terminal sequence of *Serratia* acid phosphatase (Jeong, 1992) and Fragment 2 (F2) *Serratia* acid phosphatase (Macaskie *et al.* 1994a).

Results using fragment 1 for database interrogation showed matches to sequences from several members of the *enterobacteriaceae*, many of which are pathogenic (Table 2). Homology can be seen (amongst others) between the *Serratia* peptide fragments and *P.stuartii* and *M. morganii*

(PhoN and PhoC respectively), which were noted (see above) for their low G+C content and possible involvement in the horizontal transfer of *phoN* into *S.typhimurium* (Groisman *et al.* 1992; 1993; 2001). Results using fragment 2 (Table 2) showed a match for the active site conserved domain for PAP2 acid phosphatases and PAP2-like superfamily. The latter, are a super family of histidine phosphatases and vanadium haloperoxidases. The group includes glucose-6-phosphatase and bacterial acid phosphatase and also vanadium bromoperoxidases and vanadium chloroperoxidases (Hemrika *et al.* 1997).

The phosphatases of *M. morganii* (*phoC*), *P. stuartii* (*phoN*), *S. flexneri* and *S. typhimurium* (*phoN*), which all share sequence homology with *Serratia phoN* (and all fit into the Class A phosphatases (Rossolini *et al.* 1998)) also share sequence homology and active site conserved domain matches with vanadium peroxidases (Hemrika *et al.* 1997). It is not possible to compare *Serratia phoN* homology with vanadium peroxidase as the full sequence of the former is not yet known, however it has been shown that Class A phosphatases and vanadium haloperoxidases have a conserved active site (Tanaka *et al.* 2002). The vanadium-containing chloroperoxidase from *Curvularia inaequalis* was found to have phosphatase activity in addition to peroxidase activity, indicating that the active site of this enzyme is indeed similar to that of other acid phosphatases (Hemrika *et al.* 1997). The active site structure of acid phosphatase from *Escherichia blattae* has recently been determined; crystallisation studies show that sulfate cocrystallises with the active site of this acid phosphatase in the same way as vanadium in the active site of the vanadium chloroperoxidase (Tanaka *et al.* 2002). The similarity between the enzymes from the organisms noted above indicates that the vanadium-containing haloperoxidases and this group of phosphatases may have divergently evolved from a common ancestor (Hemrika *et al.* 1997). This is further corroborated by the fact that vanadate is a potent inhibitor of the phosphohydrolase activity of the above phosphatases (Tanaka *et al.* 2002) while that all these organisms show significant homology of their phosphatases with each other (see sequence homology, Table 1).

However an extensive search failed to show any vanadium component of the *Serratia* enzyme (see below); indeed, the activity of the enzyme was inhibited by vanadyl ion (Jeong, 1992).

Examination of transition metal associations with *Serrratia* phosphatase by micro PIXE analysis

A previous study Jeong *et al* (1998) suggested that this phosphatase was probably not a metalloenzyme since its activity was unaffected by EDTA. However other studies (e.g. Reynolds & Schlesinger, 1969) noted that extended incubation with EDTA may be necessary to chelate metal atoms that are sequestered within a protein. Accordingly, the phosphatase was treated with 10 mM EDTA for 24 h which, similarly, had no effect on its activity (Table 3). However even some EDTA resistant enzymes have been later shown to be metalloenzymes (Sugiura *et al.* 1981; Reilly *et al.* 1996 & Felts *et al.* 2006). Therefore, in an attempt to identify any bound metals (see above) the *Serratia* phosphatase was examined using PIXE which, being able to detect X-ray emissions from both outer and inner shell electrons under bombardment with a high energy proton beam enables highly sensitive, element-specific detection at very low levels against the background at a spatial resolution of a few microns (Grime & Watt, 1990) (Fig 2). Different areas of a specimen will have different metal contents according to thickness, therefore each metal was normalized against an internal standard, in this case chloride which was present in the suspension buffer. Only Zn (a common metal within phosphatases), Fe and Cu were found at levels above the background chloride, which was used as the reference to normalise the metal concentrations to overcome any heterogeneities in the sample points. Typically the atomic ratio of Ca above the Cl background was 3.68 ± 0.82 -fold (mean \pm SEM; four point determinations) and for Fe and Cu it was, similarly, 2.54 ± 0.45 -fold and 3.42 ± 0.73 -fold, respectively. Calcium was chosen as the reference metal against which to quantify transition metals, since it is not known to be a component of metalloenzymes and

since the ratio of Ca to Cl in the protein was identical (within error, see above) to that of the transition metals.

Metal analysis of the *Serratia* phosphatase is shown in Table 3.a, with individual results shown for three independent protein preparations (each datum is the mean from at least three replicate determinations) since inter-batch variations were seen. The literature reports that transition metals can be interchangeable in metalloenzymes (e.g. Beck *et al.* 1988; Schenk *et al.* 1999) and hence pooled data for Fe and Cu in each analytical spot were also calculated. Titanium was examined as a 'pathfinder' element for vanadium since it is detectable by PIXE at lower levels than V. Ti was present only at the detection limit (within experimental error), therefore it was concluded that vanadium was absent, PIXE shows all metals that are present; no selenium was found in any sample (Table 4). Cu and Fe were consistently present at more than 2-fold over the detection limits but at varying proportions. However the amounts (even pooled) were very small as compared to Ca and their presence was concluded to be not biologically significant and probably attributable to non specific binding of trace metal impurities to the protein. Zinc was found in two of the three preparations and was also concluded to be probably a spurious contaminant since, like Cu and Fe, the amount found varied, from a significant amount in preparation 1 (ratio of S:Zn was 23.1 ± 1.5 :1, i.e. ~ 1.5 Zn atoms per enzyme molecule, assuming 4 sulphur atoms per subunit; Jeong *et al.* 1998) to zero in preparation 3. Hence no firm conclusions about a role for zinc are possible but its presence seems unlikely since preparation II showed about 1 % of zinc as compared to calcium (Table 3.a).

Using sulphur as a reference (16 atoms per tetrameric holoenzyme: Jeong *et al.* 1998) the number of atoms of Cu and Fe per molecule was far too low to attribute any biological significance since the concentration was generally a few atoms per thousand sulphur atoms and, indeed, the transition metals were present at well below the levels of Si, a ubiquitous contaminant, and calcium, which is not known to have a biochemical role in the context of this study (Table 3.a). Hence from the

elemental analysis it can be concluded that the *Serratia* phosphatase is not a metalloenzyme and that the very low levels of transition metals detected rule out any role in enzyme structure or function, although it cannot be precluded that metals associated with the surface of the protein and loosely bound were not lost during the preparation.

Since PIXE provides a full elemental analysis the opportunity was taken to determine the P:S ratio. This was ~1:10 in preparation III, 1: 2 in preparation I (which included a hydroxyapatite preparation step and hence the high possibility of trace phosphate contamination) and zero in preparation II, Hence no firm conclusions are possible about phosphorylation of the purified protein from micro PIXE analysis but phosphorylation seems unlikely. In agreement with this, analysis using mass spectrometry concluded that the enzyme was not phosphorylated (see earlier). The collision energy on MS scans is elevated in this type of analysis to determine if the neutral loss of H_3PO_4 occurs from a phosphorylated peptide. None of the peptides in the protein sample showed neutral loss of H_3PO_4 .

Effect of various compounds on *Serratia* sp. phosphatase

Phosphatase activity was tested in the presence and absence of each of the indicated effectors/inhibitors as described in Materials and Methods. The phosphatase was tartrate sensitive, retaining only 48 % (Table 3) of the initial activity with 1mM L-(+)-sodium tartrate. EDTA had no effect on the enzyme activity, despite incubation for over 24 h. H_2O_2 had no effect on the activity suggesting an “immunity” to the free radical products of H_2O_2 decomposition in water and in accordance with the absence of “Fenton reagent” metals (Fe, Cu) in the protein (see above). A high resistance to free radicals derived from the ionising effects of gamma-irradiation of water was found (Jeong, 1992); this would be a benefit where this enzyme is to be used for the decontamination of radioactive species (Paterson-Beedle *et al.* unpublished).

The presence of β -mercaptoethanol increased the phosphatase activity by 30 %. Previous work on radiostability of the enzyme by Jeong (1992) showed that incorporation of mercaptoethanol into the enzyme buffer gave some protection from irradiation with ^{60}Co (gamma source); the enzyme retained ~45% residual activity with 10 mM 2-mercaptoethanol and had no activity without it after 12 h irradiation (Jeong, 1992), e.g. after a dose of 684 Gray (Gy) the relative activities with and without mercaptoethanol (a well known radioprotectant; Coggle, 1983) were 45 and ~7 % respectively (Jeong, 1992).

Due to the ancestral similarity of some phosphatases to vanadium peroxidases (above) the effect of vanadium was examined. The enzyme contains no vanadium component (above) and addition of vanadyl sulphate promoted 95 % inhibition by the enzyme. A possible role as a peroxidase, and indeed vanadium ion incorporation into the phosphohydrolase activity-inhibited enzyme were not tested and are forming the basis of current studies in conjunction with crystallographic analysis. A previous study examining the potential of whole cells to precipitate vanadyl ion as its phosphate showed a series of colour changes indicative of various valence changes of the vanadium in the presence of active enzyme (Macaskie, unpublished). Redox studies were not carried out but the possibility of generating vanadate ion (HVO_4^{2-}) at the expense of cystine reduction is a possibility with loss of disulphide bridges and location of HVO_4^{2-} to the active site both possible mechanisms of enzyme inhibition.

Phosphatase as a potentiator of free radical damage

Although a role as a vanadium peroxidase was not tested, the ability of the native enzyme (which contains negligible content of redox active metals-above) to generate free radicals from H_2O_2 breakdown was examined in the presence of added iron. Since the *Serratia* phosphatase showed a resistance to radical generating molecules such as H_2O_2 and also to free radicals generated by gamma irradiation (above) the possible involvement of the enzyme itself in free radical mediated reactions was tested using Fe(III) as an exogenous radical generator ($\text{Fe(III)} \rightarrow \text{Fe(II)} + \text{e}^-$) in the absence of any detectable Fe or Cu as enzyme components (above).

Free radical tests carried out by Halliwell & Gutteridge (1987) with superoxide dismutase gave a rate constant for radical scavenging ability using a simple test tube method, comparable to that observed with the more precise method of pulse radiolysis (Halliwell & Gutteridge, 1987). This method was used in this study with purified *Serratia* sp. acid phosphatase in comparison with ethanol (Fig 3). Ethanol is a known scavenger of free radicals and a rate constant of $1.0 \times 10^9 \text{ M}^{-1} \text{ S}^{-1}$ was obtained which agrees with the published rate constant (for ethanol) of $1.4 \times 10^9 \text{ M}^{-1} \text{ S}^{-1}$ (Halliwell *et al.* 1987) and was similar to that seen using superoxide dismutase ($1.8 \times 10^9 \text{ M}^{-1} \text{ S}^{-1}$; Rotilio *et al.* 1972). Halliwell & Gutteridge (1981) showed that superoxide dismutase (SOD) moderated free radical damage to deoxyribose by 96 %, but when the (SOD) enzyme was denatured, the same level of activity was observed, suggesting a largely chemical effect due to bound transition metal. The SOD used in the published study was a copper protein and it is likely that Cu^{2+} (released upon denaturation; Halliwell & Gutteridge, 1981) was responsible for this effect, since free Cu^{2+} and copper amino acid complexes can scavenge $\text{O}_2^{\cdot-}$ (Klug-Roth *et al.* 1976) and hence generate free radicals by the Fenton reaction. In contrast (and in accordance with the absence of Fe and Cu in the protein) denatured phosphatase (used as a control) shows no effect on the free radical damage to deoxyribose. The rate constant using active phosphatase enzyme (calculated from the slope of the line; $-1 \times 10^{15} \text{ M}^{-1} \text{ S}^{-1}$; Fig 3) showed the *Serratia* phosphatase to

be an effective potentiator of free radical damage; critically, this effect is enzymatic since the heat inactivated enzyme was ineffective. It could be argued that due to the structural homology with vanadium peroxidase (above) the enzyme might be expected to contain V. However the absence of V was confirmed by highly sensitive PIXE analysis (Table 3.a).

Peroxidases are usually associated with detoxification *in vivo* e.g. breaking down the H_2O_2 produced via oxic metabolism (Renirie *et al.* 2000). In the presence of Fe or Cu as a Fenton reagent, peroxidase activity is a powerful source of free radicals (single unpaired electrons) and from the effect on deoxyribose it can be concluded that the phosphatase in these tests was behaving as a metal-unsubstituted peroxidase. In confirmation examination of the enzyme using electron paramagnetic resonance in the laboratories of Bruker Biospin failed to detect any evidence of Fe or Cu (Paterson-Beedle & Hoefer, unpublished). However an association of (e.g.) Fe (III) with the enzyme during the free radical test (and *in vivo*) cannot be precluded.

The reasons for radical potentiation by active acid phosphatase are still unclear however it is possible that due to homology with PhoN and a possible root in pathogenicity (see earlier) that the radical production has a role as a defensive mechanism for the bacterial cell; indeed it may even function as an “attack enzyme”. The immune response is classically associated with a local fall in pH and with a free radical attack on invading bacteria by phagocytic cells i.e. neutrophils and macrophages which kill pathogens by oxygen dependent and oxygen independent mechanisms (Fields *et al.* 1989). It has been assumed that attack by free radicals happens *via* the host response; activated neutrophils for example engulf and kill the invading bacteria, each phagocytic event resulting in the formation of a phagosome into which reactive oxygen species and hydrolytic enzymes are secreted (Fields *et al.* 1989) along with a fall in the pH. The pH optimum of “acid” phosphatase is 5-7 and it is possible that the enzyme acts bifunctionally; first to provide localised phosphate buffer (upon phagosomal containment); (Felts *et al.* 2006) and secondly to redirect and amplify the free radical attack back at the host cell. The production of the phosphatase into the

exocellular matrix and its tethering via components of the extracellular polymer matrix (visualised by immunogold labelling; Jeong *et al.* 1997) is consistent with a defensive role. The possibility of ‘phosphatase’ as an enzyme of aggression seems not to have been considered before although fungal laccases (peroxidases) are considered to be responsible for radical generation in woody plants which have polymeric barriers capable of trapping and holding the radicals stably (Pearce *et al.* 1997) by their distribution around multiple aromatic rings (Thurston, 1994), as confirmed by electron paramagnetic imaging in situ (Pearce *et al.* 1997). A previous study (Allen *et al.* 2002) showed that under carbon-limited continuous culture not only very high levels of phosphatase but also numerous pili are produced. Pili are classically thought to be involved in adhesion to surfaces. However a watershed study showed that the pili of the Fe(III)-reducing organism *Geobacter metallireducens*, in addition to facilitating adhesion of the organism to Fe(III)-solid material surfaces, function also as extracellular conducting ‘nanowires’ to direct the electron flow onto the target, probably via associated extracellular cytochromes (Reguera *et al.* 2005). It is not unreasonable to speculate that a similar pilial function may apply in pathogenic bacteria that may direct an electron (free radical) flow aggressively instead of merely utilising exogenous solid electron acceptors. This area of study is currently controversial (Gorby *et al.* 2006) but the possibility warrants mention in the current context.

phoN is upregulated by the *phoP/phoQ* system as a stress response (Miller *et al.* 1989) and it is possible that this occurs in response to the low pH and radical burst that accompany the immune response (Fields *et al.* 1989); hence its presence would be expected in pathogenic species that elicit this response. It cannot be said that the PhoN from *Serratia* is linked with classical pathogenicity mechanisms but, from the above, rather that it may play an ancestral part in the survival of the pathogen within the host cell. The *phoP/phoQ* system in *Salmonella typhimurium* has been extensively studied; *phoP/phoQ* is the regulatory locus and *phoN* is the phosphatase structural gene, mutation in either of *phoP/phoQ* causes a 10³ fold reduction in

virulence (Miller *et al.* 1989). However *phoN* was not thought to have a role in *Salmonella* pathogenesis despite being under the transcriptional control of PhoP (Fields *et al.* 1989; Groisman *et al.* 1992), but it was postulated that the products of *phoP/phoQ* are able to “sense” starvation and low pH in the phagolysosome and act accordingly (Miller *et al.* 1989). It is likely that PhoN would be required to retrieve phosphatase (e.g. from phospholipids) for the bacterial cell trapped in the phagolysosome (a widely accepted theory for the role of phosphatases; Felts *et al.* 2006) whilst other components necessary in the bacterial escape (under the control of *phoP/phoQ*) or evasion of the immune response were also upregulated (Miller *et al.* 1989). This is also supported by the phosphatases broad substrate specificity, overexpression (Reilly *et al.* 2006), location in the periplasm and extracellularly (Macaskie *et al.* 2000) and its high activity (see earlier). A *phoN* gene encoding a non specific phosphatase has also been found on the large virulence plasmid of *Shigella flexneri* which (like *Salmonella phoN*, above) is also not responsible for virulence of the organism, however the phosphatase of *S. flexneri* shares significant homology with that of other *Enterbacteriaceae* such as *Providencia stuartii*, *Morganella morganii* and *Salmonella typhimurium* (Uchiya *et al.* 1996).

Certainly a pH optimum of 6 for the phosphatase (Jeong, 1992) adds credence to this hypothesis as the enzyme would remain active during phagosomal containment and during the resulting pH drop to pH 5-6 (Jenson, 1973) as a result of the immune response. The prevalence of phosphatases in many different species of bacteria had indicated that its role may vary between species, but a unified role seems not to have been noted previously. In *Salmonella typhimurium* the phosphatase was thought to act as a scavenger or phosphate for the pathogenic cell, while in *Francisella tularensis* the phosphatase has a direct role in pathogen survival in the host by preventing the respiratory burst of activated neutrophils (Felts *et al.* 2006). It is thought that the acid phosphatase of *F. tularensis* achieved this by the hydrolysis of neutrophil surface-exposed substrates involved in signal transduction pathways necessary to respiratory burst

activation (Reilly *et al.* 1996). A second function of the same enzyme following engulfment within the phagolysosome (via phosphohydrolytic and free radical dual functions) would suggest a multifunctional role in the host-pathogen interaction.

It cannot be said at this stage that PhoN phosphatase does or does not have a direct role in virulence or in the survival of the organism in a host, however the homology of *Serratia* PhoN with other PhoNs from known pathogens, the very high activity of the phosphatase and its presence in an organism which is not considered a pathogen suggests that the PhoN has been acquired from another (possibly pathogenic) member of the *Enterobacteriaceae* family or that this is a relic of divergent evolution. The homology between several pathogenic members of the *Enterobacteriaceae* in addition to the conserved active site of vanadium peroxidases suggests that PhoN has a common ancestor and has diversified depending on the species in which it resides. The question of free radical generation in the absence of bound transition metal suggests possible ‘recruitment’ from the solution matrix (or via enzyme cysteines) which is under the current study to determine comparative crystallographic structures.

Acknowledgements

The authors wish to thank the EPSRC for financial support (Grant no: EP/CS48809/1) and for a studentship to C Mennan. They also thank Dr M Bailey of the Surrey Ion Beam Facility and Mr P Ashton (School of Chemistry, University of Birmingham) for assistance with MALDI-ToF analysis. The study of EPR on the enzyme was in collaboration with Dr P Hoefer (Bruker Biospin, Karlsruhe, Germany) whom we thank for the use of facilities.

References

- Allan, V.J.M., Callow, M.E., Macaskie, L.E. & Paterson-Beedle, M. (2002). Effect of nutrient limitation on biofilm formation and phosphatase activity of a *Citrobacter* sp. *Microbiology* **148**, 277-288
- Aguirre-García, M. M., Cerbón, J. & Talamás-Rohana, P. (2000). Purification and properties of an acid phosphatase from *Entamoeba histolytica* HM-1:IMSS. *Int J Parasitol* **30**, 585–591.
- Baca, O. G., Roman, M. J., Glew, R. H., Christner, R. F., Buhler, J. E. & Aragon, A. S. (1993). Acid phosphatase activity in *Coxiella burnetii*: a possible virulence factor. *Infect Immun* **61**, 4232-4239.
- Beck, J. L., McArthur, M. J., De Jersey, J. & Zerner, B. (1988). Derivatives of the purple phosphatase from red kidney bean: Replacement of zinc with other divalent metal ions. *Inorg Chim Acta* **153**, 39-44.
- Bradford, M. M. (1976). A rapid and sensitive method for quantitation of microgram quantities of protein utilizing the principle of protein-dye-binding. *Anal. Biochem*, **72**, 248-254.
- Coggle, J. E. (1983). Biological Effects of Radiation. Taylor and Francis Ltd. London.
- Felts, R. L., Reilly, T. J. & Tanner, J. J. (2006). Structure of *Francisella tularensis* AcpA. Prototype of a unique superfamily of acid phosphatases and phospholipases C. *J Biol Chem* **281**, 30289-30298.
- Fields, P. I., Groisman, E. A. & Hefron, F. (1989). A *Salmonella* locus that controls resistance to microbicidal proteins from phagocytic cells. *Science*. **243**, 1059-1062.
- Gorby, Y. A., Yanina, S., McLean, J. S., Rosso, K. M., Moyles, D., Dohnalkova, A., Beveridge, T. J., Chang, I. S., Kim, B. & others. (2006). Electrically conductive bacterial nanowires produced by *Shewanella oneidensis* strain MR-1 and other microorganisms. *PNAS* **103**, 11358–11363.
- Grime, G. W. & Watt, F. (1990). Nuclear microscopy & elemental mapping using high-energy ion beam techniques. *Nucl Instr Methods* **50**, 197-207.
- Groisman, E. A., Saier, J., M. H. & Ochman, H. (1992). Horizontal transfer of a phosphatase gene as evidence for mosaic structure of the *Salmonella* genome. *EMBO J* **11**, 1309-1316.
- Groisman, E. A., Sturmoski, M. A., Solomon, F. R., Lin, R. & Ochman, H. (1993). Molecular, functional and evolutionary analysis of sequences specific to *Salmonella*. *PNAS* **9**, 1033-1037.
- Groisman, E. A. (2001). The pleiotropic two-component regulatory system PhoP-PhoQ. *J Bacteriology* **183**, 1835-1842.
- Halliwell, B & Gutteridge, J. M. C. (1981). Formation of a thiobarbituric acid reactive substance from deoxyribose in the presence of iron salts. The role of superoxide and hydroxyl radicals. *FEBS Letters* **128**, 347-351.

- Halliwell, B., Gutteridge, J. M. C. & Aruoma, O. I. (1987).** The Deoxyribose Method: A simple “test-tube” assay for determination of rate constants for reactions of hydroxyl radicals. *Anal Biochem* **165**, 215-219.
- Hemrika, W., Ranirie, R., Dekker, H., Barnett, P. & Wever, R. (1997).** From phosphatases to vanadium peroxidases: A similar architecture of the active site. *Biochemistry* **94**, 2145-2149.
- Jensen, M. S. & Bainton, D. F. (1973).** Temporal changes in pH within the phagocytic vacuole of the polymorphonuclear neutrophilic leukocyte. *J Cell Biol* **56**, 379-388.
- Jeong, B. C. (1992).** Studies on the atypical phosphatase of a metal-accumulating *Citrobacter* sp. *PhD thesis*, University of Oxford, UK.
- Jeong, B. C., Hawes, C., Bonthorne, K. M. & Macaskie, L. E. (1997).** Localisation of enzymically enhanced heavy metal accumulation by *Citrobacter* sp. and metal accumulation *in vitro* by liposomes containing entrapped enzyme. *Microbiology* **143**, 2497-2507.
- Jeong, B. C., Poole, P. S., Willis, A. & Macaskie, L.E. (1998).** Purification and characterization of acid-type phosphatases of a *Citrobacter* sp. *Arch Microbiol* **169**, 166-173.
- Jeong, B. C. & Macaskie, L. E. (1999).** Production of two phosphatases by a *Citrobacter* sp. grown in batch and continuous culture. *Enzyme Microb Technol* **24**, 218-224.
- Kadurugamuwa, J. L. & Beveridge, T. J. (1995).** Virulence factors are released from *Pseudomonas aeruginosa* in association with membrane vesicles during normal growth and exposure to gentamicin: a novel mechanism of enzyme secretion. *J Bacteriol* **177**, 3998-4008.
- Kasahara, M., Nakata, A. & Shinagawa, H. (1991).** Molecular analysis of the *Salmonella typhimurium* *phoN* gene which encodes a nonspecific acid phosphatase. *J Bacteriol* **173**, 6760-6765.
- Klug-Roth, D. & Rabani, J. (1976).** Pulse radiolytic studies on reaction of aqueous superoxide radicals with copper (II) complexes. *J Phys Chem* **80**, 558-591.
- Kurz, C. L, Chauvet, S., Andrès, E., Aurouze, M., Vallet, I., Michel, G. P. F., Uh, M., Celli, J., Filloux, A. & others. (2003).** Virulence factors of the human opportunistic pathogen *Serratia marcescens* identified by *in vivo* screening. *EMBO J* **22**, 1451-1460.
- Macaskie, L. E. & Dean, A. C. R. (1982).** Cadmium accumulation by micro-organisms. *Environ Technol Lett* **3**, 49-56.
- Macaskie, L. E., Empson, R. M., Cheetham, A. K., Grey, C. P. & Skarnulis, A. J. (1992).** Uranium bioaccumulation by a *Citrobacter* sp. as a result of enzymically-mediated growth of polycrystalline $\text{H}_2\text{UO}_2\text{PO}_4$. *Science* **257**, 782-784.
- Macaskie, L. E., Bonthorne, K. A. & Rouch, D.A. (1994).** Phosphatase-mediated heavy metal accumulation by a *Citrobacter* sp. and related enterobacteria. *FEMS Microbiol. Lett* **121**, 141-146.

Macaskie, L. E., Jeong, B. C. & Tolley, M. R. (1994). Enzymically accelerated biomineralization of heavy metals: application to the removal of americium and plutonium from aqueous flows. *FEMS Microbiol Rev* **14**, 351-368.

Macaskie, L. E., Hewitt, C. J., Shearer, J. A. & Kent, C. A. (1995). Biomass production for the removal of heavy metals from aqueous solution at low pH using growth-decoupled cells of a *Citrobacter* sp. *Int Biodeterior Biodegrad* **35**, 73-92.

Macaskie, L. E., Bonthron, K. M., Yong, P. & Goddard, D.T. (2000). Enzymically mediated bioprecipitation of uranium by a *Citrobacter* sp.: a concerted role for exocellular lipopolysaccharide and associated phosphatase in biomineral formation. *Microbiology* **146**, 1855-1867.

Miller, S. I., Kukral, A. M. & Mekalanos, J. J. (1989). A two component regulatory system (*phoP phoQ*) controls *Salmonella typhimurium* virulence. *Genetics* **86**, 5054-5058.

Olivier, M., Gregory, D. J. & Forget, G. (2005). Subversion mechanisms by which *Leishmania* parasites can escape the host immune response: a signalling point of view. *Clin Microbiol Rev* **18**, 293-305.

Pattanapitpaisal, P., Mabbett, A. N., Finlay, J. A., Beswick, A. J., Paterson-Beedle, M., Essa, A., Wright, J., Tolley, M. R., Badar, U. & others. (2002). Reduction of Cr(VI) and bioaccumulation of chromium by gram positive and gram negative microorganisms not previously exposed to Cr-stress. *Environ Technol* **23**, 731-45

Pearce, R. B., Edwards, P. P., Green, T. L., Anderson, P. A., Fisher, B. J., Carpenter, T. A. & Hall, L. D. (1997). Immobilized long-lived free radicals at the host-pathogen interface in sycamore (*Acer pseudoplatanus* L). *Phys Mol Plant Pathol* **50**, 371-390.

Reilly, T. J., Baron, G. S., Nano, F. E. & Kuhlenschmidt, M. S. (1996). Characterisation and sequencing of a respiratory burst-inhibiting acid phosphatase from *Francisella tularensis*. *J Biol Chem* **271**, 10973-10983.

Renirie, R., Hemrika, W. & Wever, R. (2000). Peroxidase and phosphatase activity of active site mutants of vanadium chloroperoxidase from the fungus *Curvularia inaequalis*. *J Biol Chem* **275**, 11650-11657.

Reynolds, A. & Schlesinger, M. J. (1969). Alterations in the structure and function of *Escherichia coli* alkaline phosphatase due to Zn^{2+} binding. *Biochemistry* **8**, 588-593.

Rossolini, G. M., Schippa, S., Riccio, M. L., Berlutti, F., Macaskie, L. E. & Thaller, M. C. (1998). Bacterial nonspecific acid phosphohydrolases: physiology, evolution and use as tools in microbial biotechnology. *CMLS* **54**, 833-850.

Rotilio, G., Bray, R. C. & Fielden, E. M. (1972). A pulse radiolysis study of superoxide dismutase. *Biochim Biophys Act* **268**, 605-609.

Ruguera, G., McCarthy, K.D., Mehta, T., Nicoll, J.S., Tuominen, M.T & Lovley, D.R. (2005). Extracellular electron transfer via microbial nanowires. *Nature*. **435**: 1098-1101.

Schenk, G., Ge, Y., Carrington, L. E., Wynne, C. J., Searle, I. R., Carroll, B. J., Hamilton, S. & de Jersey, J. (1999). Binuclear metal centers in plant purple acid phosphatases: Fe±Mn in Sweet Potato and Fe±Zn in Soybean. *Arch Biochem Biophys* **370**, 183–189.

Schenk, G., Boutchard, C. L., Carrington, L. E., Noble, C. J., Moubaraki, B., Murray, K. S., de Jersey, J., Hanson, G. R. & Hamilton, S. (2001). A purple acid phosphatase from sweet potato contains an antiferromagnetically coupled binuclear Fe-Mn Center. *J Biol Chem* **276**, 19084-19088.

Sugiura, Y., Kawabe, H., Tanaka, H., Fujimoto, S. & Ohara, A. (1981). Purification, enzymatic properties and active site environment of a novel manganese (III)-containing acid phosphatase. *J Biol Chem* **256**, 10664-10670.

Tanaka, N., Dumay, V., Liao, Q., Lange, A. J. & Wever, R. (2002). Bromoperoxidase activity of vanadate-substituted acid phosphatases from *Shigella flexneri* and *Salmonella enterica* ser. typhimurium. *Eur J Biochem* **269**, 2162–2167.

Thaller, M. C., Berlutti, F., Schippa, S., Lombardi, G. & Rossolini, G. M. (1994). Characterization and sequence of PhoC, the principal phosphate-irrepressible acid phosphatase of *Morganella morganii*. *Microbiology* **140**, 1341-1350.

Thaller, M. C., Lombardi, G., Berlutti, F., Schippa, S. & Rossolini, G. M. (1995). Cloning and characterization of the NapA acid phosphatase/phosphotransferase of *Morganella morganii*: identification of a new family of bacterial acid-phosphatase-encoding genes. *Microbiology* **141**, 147-154.

Thurston, C. F. (1994). The structure and function of fungal laccases. *Microbiology* **140**, 19-26.

Uchiya, K. I., Tohsuji, M., Nikai, T., Sugihara, H. & Sasakawa, C. (1996). Identification and characterization of *phoN-Sf*, a gene on the large plasmid of *Shigella flexneri* 2a encoding a nonspecific phosphatase. *J Bacteriol* **178**, 4548–4554.

Uerkvitz, W & Beck, C. F. (1981). Periplasmic phosphatases in *Salmonella typhimurium* LT2. A biochemical, physiological, and partial genetic analysis of three nucleoside monophosphate dephosphorylating enzymes. *J Biol Chem* **256**, 382-389.

Table 1. Purification of acid phosphatase from *Serratia* sp.

Purification step	Total activity (Units)	Total protein (mg)	Specific activity (Units/mg)	Purification (Fold)	Yield (%)
Cell lysate	3150000	2100	1500	1	100
Ammonium sulphate fractionation	567000	270	2100	1.4	18
HiTrap Q	3098428.2	78.75	39345.12	26.23	98
Superdex 200	605163.72	12.12	49931	33.28	19

Data are shown for a typical purification.

Table 2. A new database search (using BLAST) for homology to the amino acid sequences of two peptide fragments of *Serratia* phosphatase which were obtained in an earlier study (Jeong, 1992; Macaskie *et al.* 1994a).

Fragment 1:

<i>Serratia</i> phosphatase	ARDVTTTTPDFYYLKEAQSIDSLSLLPPPPAVDSIDFLND
<i>Klebsiella pneumoniae</i>	GNDVTTTKPDLYYLTNAOAIDSLALLPPPPAVGSI AFLND
<i>Providencia stuartii</i>	GNDVTTTKPDLYYLNKNSQAIDSLALLPPPPPEVGSILFLND
<i>Morganella morganii</i> (PhoC)	DATTKPDLYYLNKNEQAIDSLKLLPPPPPEVGSIQFLND
<i>Shigella dysenteriae</i> (Periplasmic NSAP)	DVTTTKPDLYYLTNDNAIDSLALLPPPPQIGSIAFLND
<i>Shigella flexneri</i> (Periplasmic NSAP PhoN1)	DVTTTKPDLYYLTNDNAIDSLALLPPPPQIGSIAFLND
<i>Escherichia blattae</i>	DTTTKPDLYYLNKSEAINSLALLPPPPAVGSI AFLND

†Consensus **D-TT-PD-YYL-----IDSL-LLPPPP---SI-FLND**

* *Francisella novicida*/*F.tularensis*

NSLALLPPPPATDSIAFMND

†Consensus **-----SL-LLPPPP---SI-F-ND**

* Hypothetical protein of *Francisella novicida* similar to membrane associated phospholipid phosphatase of *Francisella tularensis* sub species *novicida*.

Fragment 2:

<i>Serratia</i> phosphatase	VICGYHNQSDVTAG
<i>Klebsiella pneumoniae</i>	VICGYHWQSDVDA
*(PAP2 family protein PhoN1)	
<i>Klebsiella pneumoniae</i> (PhoC)	VICGYHWQSDVDA
<i>Rahnella sp</i> (NSAP)	VICGYHWQSDVDA
<i>Shigella dysenteriae</i> (PhoN1)	VICGYHWQSDVDA
<i>Shigella flexneri</i> (PhoN1 NSAP)	VICGYHWQSDVDA
*PhoN (NSAP)	VICGYHWQSDVDA
<i>Salmonella typhimurium</i> (PhoN)	VICGAHWQSDVDAG
<i>Escherichia blattae</i>	VICGYHWQSDVDA

†Consensus **VICG-H-QSDV-A-**

* PAP2 (Purple Acid Phosphatase). NSAP: Nonspecific acid phosphatase.

†Consensus : sequences found in six other enterobacterial phosphatases.

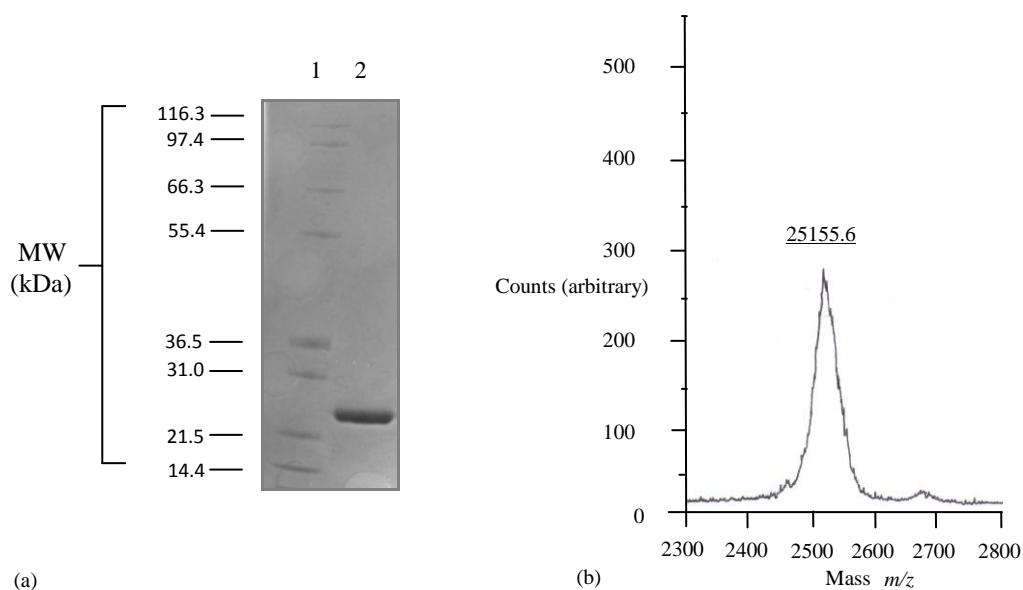


Figure 1(a) SDS-Page analysis of acid phosphatase from *Serratia* sp. after purification. Lane 1 Novex Mark12 molecular weight standards. Lane 2 phosphatase (10 μ g) stained with Coomassie blue (R-250). The molecular weight of 25 kDa was obtained from a log plot of distance versus relative molecular mass and also from MALDI-ToF MS. (b) Confirmation of the sub-unit molecular mass as 25,155.6 kDa using MALDI-ToF MS.

Table 3. Effect of various compounds on *Serratia* sp. phosphatase

Effector substance	Effector concentration (mM)	Enzyme specific activity (%) of control
Control	0	100 \pm 2
L-(+)-Sodium tartrate	1	48 \pm 5
*EDTA	10	100 \pm 3
β -Mercaptoethanol	30	130 \pm 7
H ₂ O ₂	50	100 \pm 2
^a Vanadyl sulphate	0.5	5 \pm 3

* In the case of EDTA mixtures were left for 24 h before testing with the result as shown.

^a Vanadium data taken from Jeong (1992). The effect of vanadate was not tested not the possibility of a redox couple between enzyme cystines and vanadyl (VO²⁺).

The activity was determined in 40 mM MOPS-NaOH, pH 7.0. The activity was expressed as a percentage of that observed without effector substance. Data are mean \pm sem of 3 experiments.

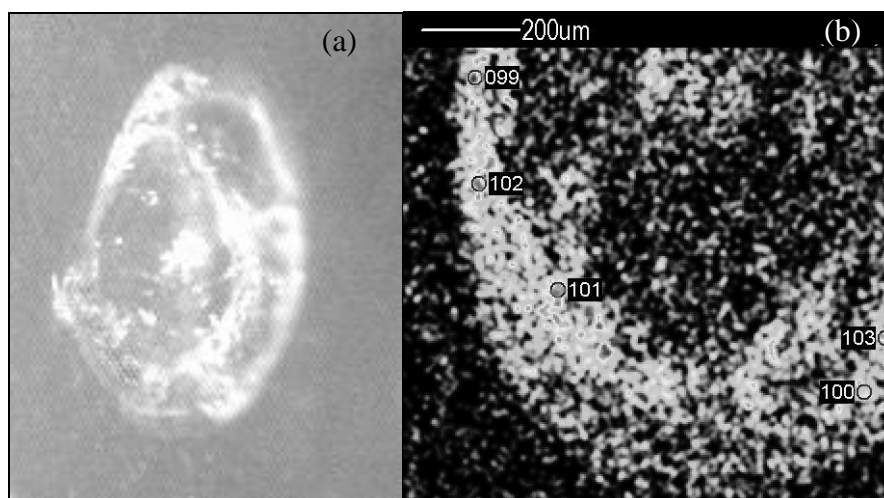


Fig 2(a) The protein drying ring on the target prior to PIXE analysis. (b) The PIXE map of the protein with numbered circles indicating points selected for analysis of elemental composition. Pale areas show localisations of high sulphur content; numbers indicate sampling points. Analyses were compared to points outside the protein ring (buffer background).

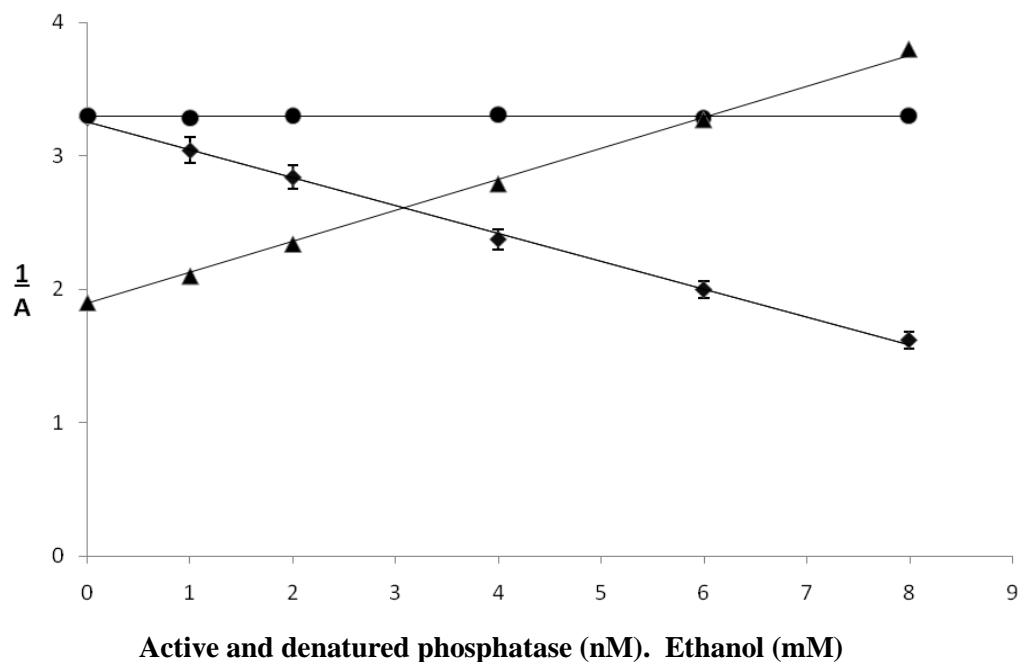


Figure 3. The effect of phosphatase, denatured phosphatase and ethanol on the free radical damage to deoxyribose. For phosphatase data are means \pm SEM from three experiments; where no error bars are shown, these were within the symbol dimensions. Data using denatured phosphatase and ethanol were each calculated from two separate experiments where errors were less than 5%, the means are displayed. The rate constant was determined from the slope of the line ($k = \text{slope} \times K_{\text{DR}} \times [\text{DR}] \times A^0$) as described in the text, giving a value of $-1 \times 10^{15} \text{ M}^{-1} \text{ S}^{-1}$. A is absorbance at 532 nm. Phosphatase (♦), Denatured phosphatase (●) and Ethanol (▲).

Table 3 (a) Trace metal content of *Serratia* phosphatase (atomic ratios of metal to Ca)

Prep. No	Metal concentration (atomic ratio to Ca)					
	Ca	Zn:Ca	Fe:Ca	Cu:Ca	[Cu + Fe]:Ca	Ti:Ca
I	1.0	0.315 ± 0.052	0.0135 ± 0.002	0.066 ± 0.14	0.094 ± 0.010	NR
II	1.0	0.092 ± 0.003	0.111 ± 0.015	0.060 ± 0.01	0.172 ± 0.052	0.020 ± 0.003
III	1.0	0	0.179 ± NR	0.018 ± NR	0.196 ± NR	0.029 ± NR

(b) Metal concentration (ppm) over its detection limit (ppm, in bold) at that point for the lowest concentration found in each test

Prep.	Ca	Zn	Fe	Cu	Ti	Si
I	1180/ 13	436/ 22	18/ 6	67/ 17	NR	NR
II	394/ 7	62/ 1	48/ 1	37/ 1	23/ 15	627/ 21
III	Not calculated					

(a) Trace metals were referenced to calcium since this is a background ubiquitous contaminant. The concentrations of Ti are also shown since this is not known to be enzyme components or cofactors.

(b) Detection limits (ppm) are shown for each element in each particular spot; this has to be determined for each point individually since it depends on the sample thickness, which is not homogeneous (see the ‘drying ring’ in Fig 2 (b) using sulphur as the enzyme locator). Data in (b) are the lowest concentration in each point (ppm) from several replicates compared to its detection limit (ppm) at that point (bold). PIXE analysis gives the total metal composition; metals not shown were not present. The detection limits and PIXE technique are described by (Grime & Watt, 1990). The emission intensity for vanadium (see text) is such that an analysis detecting Ti will also detect V, since the limits of these are similar. Data are means ± SEM for three of four determinations from random points within the protein spot. NR: data not recorded. All metals found were recorded therefore the enzyme does not contain selenium or vanadium.

Data from three independent preparations are shown (I, II and III): Preparation I was taken from an earlier study (M. Paterson-Beedle & L.E. Macaskie, unpublished), which used a different purification protocol which was taken from Jeong (1992) and involved the use of a hydroxyapatite column. The PIXE analysis of the earlier preparation (M. Paterson-Beedle et al, unpublished) were compared with the PIXE results in this study (II and III).

NR: Data not recorded.

ACCUMULATION OF ZIRCONIUM BY *SERRATIA* SP.: A NOVEL SYSTEM FOR THE REMOVAL OF RADIONUCLIDES FROM AQUEOUS FLOWS

C. Mennan¹⁾, M. Paterson-Beedle¹⁾, J.E. Readman²⁾, J.A. Hriljac²⁾, E. Valsami-Jones³⁾ and L.E. Macaskie¹⁾

¹⁾School of Biosciences, The University of Birmingham, Edgbaston, Birmingham, B155 2TT, UK. Email: L.E.Macaskie@bham.ac.uk

²⁾School of Chemistry, The University of Birmingham, Edgbaston, Birmingham, B155 2TT, UK

³⁾Department of Mineralogy, The Natural History Museum, Cromwell Road, London, SW7 5BD

Introduction

Serratia sp. biofilm immobilised onto polyurethane foam accumulates heavy metal (Fig.1) as polycrystalline metal phosphate (MHPO₄) using enzymatically (acid phosphatase) generated inorganic phosphate (HPO₄²⁻) from a phosphate donor, in this case glycerol-2-phosphate (G2P) [1].

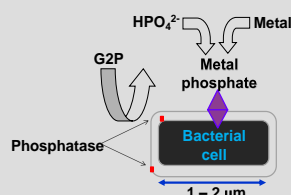


Fig. 1. Metal phosphate accumulation by the action of acid phosphatase, e.g. UO₂²⁺ as HUO₂PO₄.

Serratia sp. accumulates uranyl ion (UO₂²⁺) as crystalline HUO₂PO₄ (hydrogen uranyl phosphate, HUP). HUP-coated *Serratia* sp. biofilm, immobilised onto polyurethane foam, in packed bed reactors, removed 100% of Co²⁺, Sr²⁺ and Cs⁺ (and their radioisotopes) from aqueous solutions until the reactors reached saturation [2]. Zirconium phosphates offer an alternative to the use of HUP, where a non toxic, non radioactive metal is a pre-requisite, e.g. a remediation process for potable water.

Objective

To develop the science and technology necessary to produce a portable, highly effective system for removal of radionuclides from aqueous flows.

Methods and Results

Biominingalisation of zirconium by *Serratia* sp.

Continuous process

A system similar to that used for production of HUP [2] was tested for the biominingalisation of Zr. Packed-bed reactors containing *Serratia* sp. biofilm immobilised onto polyurethane foam (cubes, 125 mm³, or cylinders, 1.6 cm³) were set up as seen in Fig. 2.

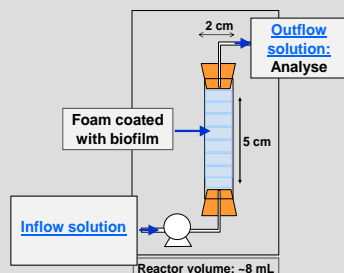


Fig. 2. Biominingalisation of Zr by *Serratia* sp. biofilm.

Inflow solutions used in Fig. 2:

- ZrOCl₂·8H₂O (1 mM), G2P (5 mM) and citrate (3 mM), pH 5, 10 mL/h, for 3 days.
- ZrOCl₂·8H₂O (1 mM) and G2P (5 mM), pH 5, 10 mL/h, for 3 days.
- ZrOCl₂·8H₂O (1 mM), G2P (5 mM) and ethanol (5 M), pH 5, intermittent flow for 9 days.

Continuous process (continued)

The ZrP product formed in the reactor containing ethanol was observed as a loosely bound white precipitate around the biofilm surface (Fig. 3). The Zr removal and molar ratios of Zr:P for all inflow conditions can be seen in Table 1. Fig. 4 shows environmental scanning electron microscopy (ESEM) of dried ZrP.



Fig. 3. Formation of white ZrP precipitate on the biofilm.

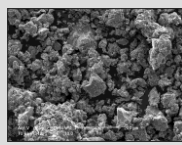


Fig. 4. ESEM under vacuum of carbon coated, dried biominingalised ZrP produced using ethanol.

Table 1. Removal of Zr from solution by several different bio-systems.

Inflow	Process	Zr removed (%)	Molar ratio Zr:P
Zr+G2P+citrate	Continuous	30	1:1.7
Zr+G2P	Continuous	65	1:1.2
Zr+G2P+ethanol	Continuous	>95	1:2.8
Zr+G2P+ethanol	Batch	~100	1:3.4

Batch process

Biofilm-coated polyurethane foam (8 cylinders) were transferred to a flask containing ethanol (5 M). Cells were dosed daily, over 11 days, with G2P and ZrOCl₂·8H₂O in ethanol to give a concentration of 5 mM and 1 mM respectively (pH 6). The moisture content of the material was 95%. The uptake of Zr is shown in Table 1 and the ZrP material obtained was 7.8 g ZrP (dry weight)/g dry biofilm.

Chemical production of α-Zr(HPO₄)₂

Zirconium phosphate was produced chemically as described by Trobaj [3], using a hydrothermal bomb (Fig. 5). Fig. 6 shows ESEM of α-Zr(HPO₄)₂ identity was confirmed by XRD (Fig. 7).



Fig. 5. Hydrothermal bomb.

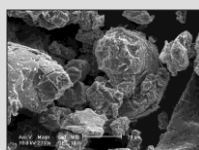


Fig. 6. ESEM under vacuum of carbon coated, dried chemically synthesized ZrP.

X-Ray diffraction analysis

Biogenic ZrP materials were analysed with and without H₃PO₄ (0.3 M) washing. Samples washed with H₃PO₄ showed some crystalline phases present in small quantities; however, these were absent in samples without acid washing (Fig. 7).

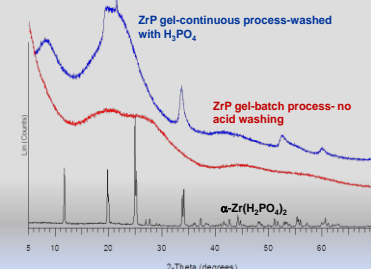


Fig. 7. XRD patterns of ZrP materials produced by *Serratia* and α-Zr(H₂PO₄)₂.

Removal of cobalt and strontium from aqueous flows

Continuous process

Reactors containing ZrP supported on biofilm-cylinders removed 100% of the metals (Fig. 8) until reactor saturation.

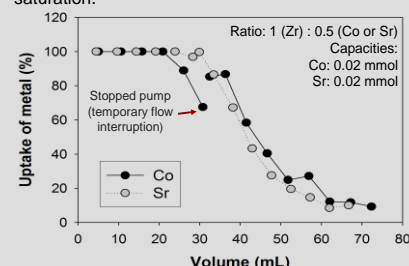


Fig. 8. Removal of Sr²⁺ and Co²⁺ using a reactor containing ZrP (~4 mg Zr) supported on *Serratia* sp. biofilm immobilised onto polyurethane foam and exposed to: Co(NO₃)₂·6H₂O (0.5 mM, pH 5) and Sr(NO₃)₂ (0.5 mM, pH 5). Flow-rate: 4.7 mL/h.

Batch process

The gel-like material (~1 g wet weight) and α-Zr(H₂PO₄)₂ (~70 mg) were transferred to universal bottles and exposed separately to Co(NO₃)₂·6H₂O (50 mM, 4 mL), Sr(NO₃)₂ (100 mM, 3 mL) and Sr(OH)₂·8H₂O (23 mM, 10 mL) for 24 h. Fig. 9 shows the materials obtained after exposure to Co²⁺.



Fig. 9. (A) α-Zr(HPO₄)₂ and (B) ZrP gel-like material treated with Co(NO₃)₂·6H₂O.

According to Clearfield [5] the ion exchange capacity of Zr(HPO₄)₂·H₂O is 6.64 mequiv/g. A comparison of the capacities of the ZrP gel-like material and α-Zr(HPO₄)₂ are shown in Table 2.

Table 2. Capacities of ZrP gel-like material and α-Zr(HPO₄)₂ treated with Sr(OH)₂·8H₂O, Sr(NO₃)₂·6H₂O or Co(NO₃)₂·6H₂O.

Sample	Solution	Initial pH	Capacity
ZrP gel	Sr(OH) ₂ ·8H ₂ O	12.0	8.4 mequiv Sr ²⁺ /g
α-Zr(HPO ₄) ₂	Sr(OH) ₂ ·8H ₂ O	13.0	7.4 mequiv Sr ²⁺ /g
ZrP gel	Sr(NO ₃) ₂	7.1	3.9 mequiv Sr ²⁺ /g
α-Zr(HPO ₄) ₂	Sr(NO ₃) ₂	7.0	3.1 mequiv Sr ²⁺ /g
ZrP gel	Co(NO ₃) ₂ ·6H ₂ O	5.2	3.5 mequiv Co ²⁺ /g
α-Zr(HPO ₄) ₂	Co(NO ₃) ₂ ·6H ₂ O	5.2	0.5 mequiv Co ²⁺ /g

Conclusions

ZrP gel-like material, produced using *Serratia* sp., removed 100% of Co²⁺ or Sr²⁺ from aqueous solutions, in a continuous process, until saturation of reactor. Also, the metal capacity of the gel-like material, from *Serratia* sp., was comparable to that obtained with α-Zr(HPO₄)₂.

Acknowledgments

This work was supported by EPSRC. The authors thank Recticel (Belgium) for the biofilm support (Filtren TM30).

References

- [1] Macaskie, L.E. *et al.* Science, 257, 782-784 (1992).
- [2] Paterson-Beedle, M. *et al.* Hydrometallurgy 83, 141-145 (2006).
- [3] Trobaj, C. *et al.* Chem Mater 12, 1789 (2000).
- [4] Paterson-Beedle, M. *et al.*, in: Tzesos, M. *et al.* (eds) Proceedings of the 15th International Biohydrometallurgy Symposium, Athens, 1155-1161 (2004).
- [5] Clearfield, A. *et al.* Chem Rev, 88, 125-148 (1988).